BINDING SERVICES
Tel +44 (0)29 2087 4949
Fax +44 (0)29 20371921
e-mail bindery@cardiff.ac.uk

TOXICOLOGICAL, HISTOPATHOLOGICAL AND PROTEOMIC ANALYSIS OF A POLYMER-INDUCED LUNG INJURY MODEL

Martina Hicks

A thesis presented for the degree of Doctor of Philosophy

at

Cardiff University

June 2006

Cardiff School of Biosciences
Cardiff University
Museum Avenue
CARDIFF
CF10 3US

ProQuest LLC
789 East Eisenhower Parkway
P.O. Box 1346
Ann Arbor, MI 48106-1346

CONTENTS

ACKNOWLEDGEMENTS

Firstly I would like to thank Unilever and BBSRC for funding my PhD research. In particular I would like to thank Samantha Fletcher at Unilever for all her help and guidance with proteomics.

Thank you to my two main supervisors, Prof. Roy Richard for setting up the project and Dr. Kelly BéruBé for supporting me through the second half of my PhD. Thank you both for all the time and energy you have spent on me and my work, I couldn't have done it without you both. I am also grateful for the opportunities to attend an international conference in Auckland, New Zealand and to take part in a research exchange to Beijing, China. Both of which leave me with fond memories and fantastic photograph albums.

Thanks to everyone in W2.01 in particular all the past members of the RJR group and the present members of the KAB group who all made my PhD a lot of fun. I would like to especially thank Keith, who without his vast knowledge about science and everything else in the world that you need to know, I don't think I would have survived. Also special thanks to Dominique who was not only a fantastic travel buddy but also a great support on a day to day basis. Thank you both for all the cups of tea and for always being there when I needed help. I have not only learnt a lot from my PhD but I have also made some lifelong friends. Thanks to Matt for his continuous support during my writing up. Thank you for being my rock especially through the final stages of my PhD. You made me smile instead of cry!!

Finally I would like to thank my family for all their support, Mum and Dad for putting a roof over my head and feeding me, and Kerstin for her daily phone calls from New York to check that I was surviving the writing up period.

Without all your support I wouldn't have been able to "push back the boundaries of science"!!

Thank you!

PUBLICATIONS

BéruBé KA, Jones TP, Moreno T, Sexton K, Balharry D, Hicks M, Merolla L, Mossman BT. (2006) "Characterisation of airborne particulate matter and related mechanisms of toxicity." In: *Air Pollution Reviews*, Vol. 3. Ayres J, Maynard R, Richards R (Editors). Imperial College Press, London, *in press*.

PUBLICATIONS (IN PREPARATION)

Hicks M., Balharry D. and BéruBé K. "Immunohistochemical analysis of two potential marker proteins for polymer-induced lung injury" *European Journal of Immunology*

Hicks M., Sexton K., Balharry D. and BéruBé K. "Toxicological, histopathological and proteomic analysis of a polymer-induced lung injury model" *Occupational Environmental Medicine*

PUBLISHED ABSTRACTS

Hicks, M., Fletcher, S., Carthew, P., Richards R. and Berube, KA. (2006) Study of Polymer Induced Lung Injury by Proteomic Analysis. *Abstracts of the British Association for Lung Research, Summer Meeting, 2005, Edinburgh, UK*, Experimental Lung Research (In Press)

Hicks, M., Fletcher, S., Carthew, P., Caswell, R. and Richards R. (2005) Proteomic Analysis of Lung Injury Induced by Low Molecular Weight Polymer. *Abstracts of the British Association for Lung Research, Summer Meeting, 2004, Leicester, UK.* Experimental Lung Research **31(6)**, 623-649

Hicks, M., Fletcher, S., Carthew, P., Caswell, R. and Richards R. (2004) Modelling Pulmonary Oedema in Lungs for Proteomic Analysis. *Abstracts of the British Association for Lung Research, Summer Meeting, 2003, Brighton, UK.* Experimental Lung Research **30(6)**, 503-534

COMMUNICATIONS

Proteomic Analysis for Geo-biologists. *Cardiff-Beijing Scientific Exchange, Chinese University of Mining and Technology, Beijing, China,* **2006**

Proteomic Analysis of Lung Injury. *Unilever Inhalation Toxicology Meeting, Colworth House, Bedfordshire, UK*, **2006**

Study of Polymer Induced Lung Injury by Proteomic Analysis. *British Association for Lung Research, Summer Meeting, Edinburgh, UK*, **2005**

Using 2D SDS PAGE to Analyse Lung Injury and Repair. The *Genomic Approaches to Health and Disease & the Cancer Interdisciplinary Research Group, Cardiff, UK*, **2005**

Using 2D SDS PAGE to Analyse Lung Injury and Repair *Unilever Inhalation Toxicology Meeting, Colworth House, Bedfordshire, UK*, **2005**

Proteomic Analysis of Lung Injury. *3rd Annual International Conference on Bioinformatics, Auckland, NZ,* **2004**

Proteomic Analysis of Lung Injury Induced by Low Molecular Weight Polymer. *British Association for Lung Research, Summer Meeting, Leicester, UK,* **2004**

Pulmonary Oedema in Lungs for Proteomic Analysis. *British Association for Lung Research, Summer Meeting, Brighton, UK*, **2003**

ABBREVIATIONS

2D	Two dimensional
2D SDS PAGE	Two-dimensional Sodium Dodecyl Sulphate Polyacrylamide Gel Electrophoresis
2D-DIGE	Two dimensional Fluorescence Difference Gel Electrophoresis
AL	Alveolar lipoproteinosis
AMs	Alveolar Macrophages
APS	Ammonium persulphate
ARDS	Acute Respiratory Distress Syndrome
BAL	Broncho-alveolar lavage
BM	Basement Membrane
BSA	Bovine Serum Albumin
CB	Carbon Black
CC	Cocoacrisp
CHAPS	3[(3-Cholamidopropyl) dimethylammonio]-propanesulfonic acid
CO_2	Carbon dioxide
CRISP	Cysteine rich secretory protein
DCC	Differential cell count
dd-H_2O	Double distilled water
DEP	Diesel exhaust particles
DTT	Dithiothreitol
ECM	Extracellular matrix
EDTA	Ethylenediaminetetracetic acid
ELISA	Enzyme-linked immunosorbant assay
ESI	Electrospray ionisation
H&E	Haematoxylin and eosin
HCl	Hydrogen chloride
HSA	Human Serum Albumin
IA	Image Analysis
IEF	Isoelectric focusing
IL	Interleukin

IgA	Immunoglobulin A
IgG	Immunoglobulin G
IPG	Immobilised pH gradient
KeV	Kilo electron-volts
kDa	Kilo daltons
LB	Lamellae bodies
LCCL	Domain-family first discovered in Limulus factor C, Coch-5b2 and Lgl1
LFC	Lavage free cells
LgL1	Late gestation lung protein
LM	Light microscopy
MALDI-ToF	Matrix assisted laser desorption ionization time of flight
MMP-1	Matrix metalloproteinase-1
MRPs	Myeloid related proteins
MS	Mass spectrometry
MS/MS	Tandem mass spectrometry
MW	Molecular weight
MWCO	Molecular weight cut off
n	Number of replicates
Na	Sodium
NaCl	Sodium chloride
NCBInr	Non-identical protein sequence database
NL	Nasal lavage
O_2	Oxygen
pI	Isoelectric point
PMNs	Polymorphonuclear Cells
PSPs	Poorly soluble particles
RBC	Red blood cells
RS	Respiratory system
RT	Respiratory tract
SALIPs	Saposin-like protein
SDS	Sodium dodecyl sulphate
SP-A	Surfactant protein A

SP-B	Surfactant protein B
SP-C	Surfactant protein C
SP-D	Surfactant protein D
TBS	Tris buffered saline
TCA	Trichloroacetic Acid
TEM	Transmission electron microscopy
TEMED	Tetramethylethylene Diamine
TIFF	Tag image file format
TiO_2	Titanium oxide
TNF-α	Tumour necrosis factor
v/v	Volume to volume
w/v	Weight to volume
wt	Weight

ABSTRACT

The inhalation of poorly soluble particles such as synthetic resin polymers is characterised by a series of biochemical and histopathological responses in the lung. These responses can be characterised as acute and chronic pathologies that include pulmonary oedema, inflammation and fibrosis. The ability correctly to identify patients that manifest early signs of lung injury could significantly reduce the morbidity from these types of pathologies. Consequently, this study was undertaken to identify protein markers of early oedema and inflammation.

Models of pulmonary injury were induced in the rat lung via intratracheal instillation of a synthetic resin polymer. Conventional quantitative analysis of broncho-alveolar lavage (BAL) fluid was used to indicate the severity of the oedematous response, whilst morphological changes were identified by histological examination. Two dimensional sodium dodecyl sulphate polyacrylamide gel electrophoresis (2D SDS PAGE) was then employed to separate the proteins in the BAL fluid collected from the mild and persistent models of lung injury.

The complete toxicological and histological characterisation of the polymer-induced model of pulmonary injury successfully identified specific endpoints of injury. This model was used to study the protein profiles in response to polymer-induced lung injury. 2D SDS PAGE was optimised for use with BAL fluid and identified two interesting proteins, prosaposin and calgranulin A, which have the potential to act as biomarkers for lung injury.

Furthermore, immunohistochemistry can provide an insight into co-localization and quantitative analysis of proteins identified by proteomics with cellular organisation/structure, which in turn, may be reflective of their function. This was demonstrated using two proteins, cocoacrisp and surfactant protein A that were found to have elevated levels in tissue sections from the polymer treated lungs. Finally, in addition to all these proteins being potential biomarkers of lung injury, they are also prospective targets for clinical treatment.

CHAPTER 1

GENERAL INTRODUCTION

1.1 THE RESPIRATORY SYSTEM

1.1.1 GENERAL ARCHITECTURE

The lungs are a complex organ that have to contend with numerous inhaled and ingested xenobiotics on a daily basis. The primary function of the lungs is gaseous exchange, whereby oxygen (O_2) from the atmosphere is transported to the respiratory tissues and carbon dioxide (CO_2) made by all tissues is expelled to the atmosphere. Due to the importance of this process, the lungs require a defence system to prevent damage. Lung damage can result in a multitude of lung conditions such as pulmonary oedema, fibrosis and tumour formation.

1.1.1.1 Anatomic Distinction

The respiratory system (RS) consists of two lungs that are situated in the chest. Each lung can be divided into the upper, lower and distal respiratory tracts (RT) (Figure 1.1). The upper RT includes the airways that begin at the nose and mouth and end with the larynx. The lower RT begins at the trachea and includes the bronchi and the lungs. The distal RT comprises of the gaseous exchange region of the lungs (respiratory bronchioles and alveoli).

1.1.1.2 Functional Distinction

Alternatively, the RS can be divided into the conducting and respiratory portions. The conducting zone allows the movement of air into and out of the RS, whereas the respiratory zone allows gaseous exchange of O_2 and CO_2.

1.1.2 CONDUCTING ZONE

When we inhale, air enters through our nasal cavity or buccal cavity and passes over the pharynx and through the trachea. The trachea branches into two bronchi each of which supplies air to one of the lungs. Branching of the airways produces subsequent generations of smaller airways (Table 1.1). The first 15 generations of the airways are the conducting zone. Within the lungs,

each bronchus divides into smaller bronchioles that eventually divide into the terminal bronchioles, the smallest of the conducting airways.

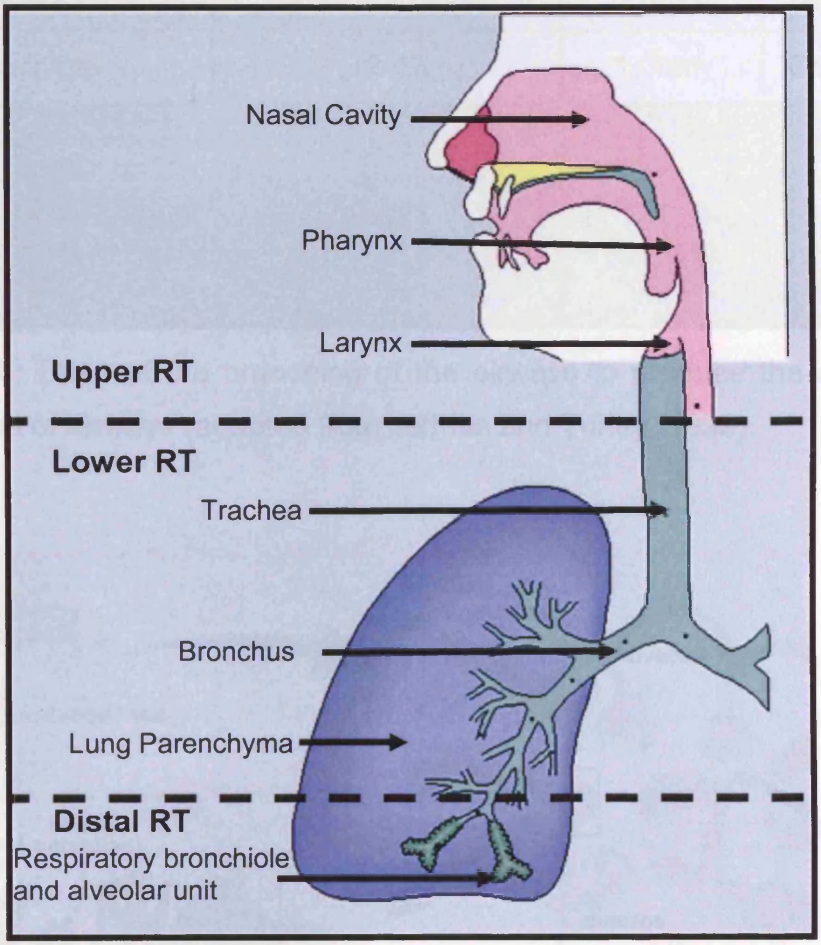

Figure 1.1: Cartoon of the general plan of the respiratory system indicating the different respiratory tracts (reproduced with permission of Dr. K BéruBé)

1.1.3 Respiratory Zone

The respiratory zone begins when the terminal bronchioles become respiratory bronchioles. Their primary role is to supply gas to the alveoli but alveoli are also present in their walls. Tiny airways, called alveolar ducts branch from each respiratory bronchiole. Alveolar ducts end in a cluster of alveoli called an alveolar sac. Each alveolar sac opens into approximately 10 to 16 alveoli (Figure 1.2).

Airways	Generation Number	Diameter	Zone
Trachea	0	25mm	Conducting
Bronchus	1-11	1-10mm	Conducting
Bronchiole	12-16	1.0mm	Conducting
Respiratory Bronchiole	18+	0.5mm	Respiratory
Alveolar Duct	20-23	0.5mm	Respiratory
Alveolus	24	0.2-0.5mm	Respiratory

Table 1.1: Table of the branching of the airways to produce the different generation of airways (adapted from Jeffries and Turley, 1999).

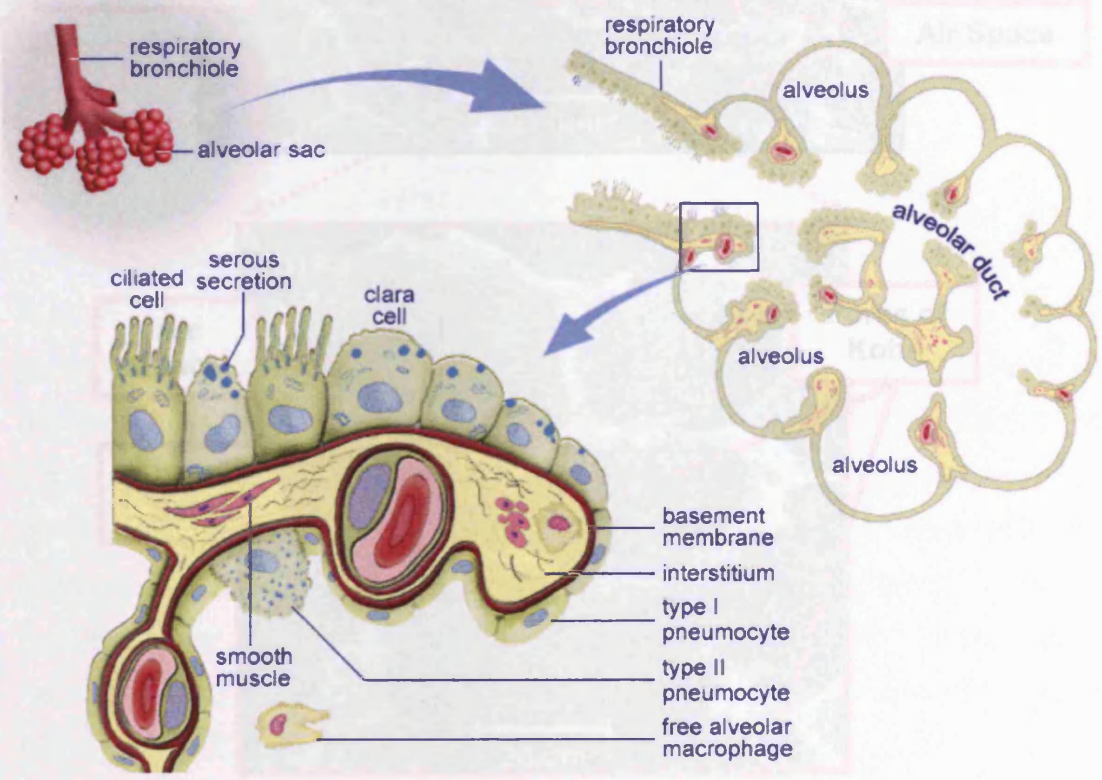

Figure 1.2: Anatomy of the respiratory bronchioles and alveolar subunit in the human lung (Jeffries and Turley, 1999).

1.1.4 ALVEOLAR UNIT

Gaseous exchange occurs in the alveoli (Figure 1.3). They require a rich supply of blood, which is provided by a network of capillaries. The walls of the alveoli are shared with surrounding alveoli. The major cell types present within the alveolar units are: type I and II pneumocytes, endothelial cells, fibroblasts and alveolar macrophages (AMs).

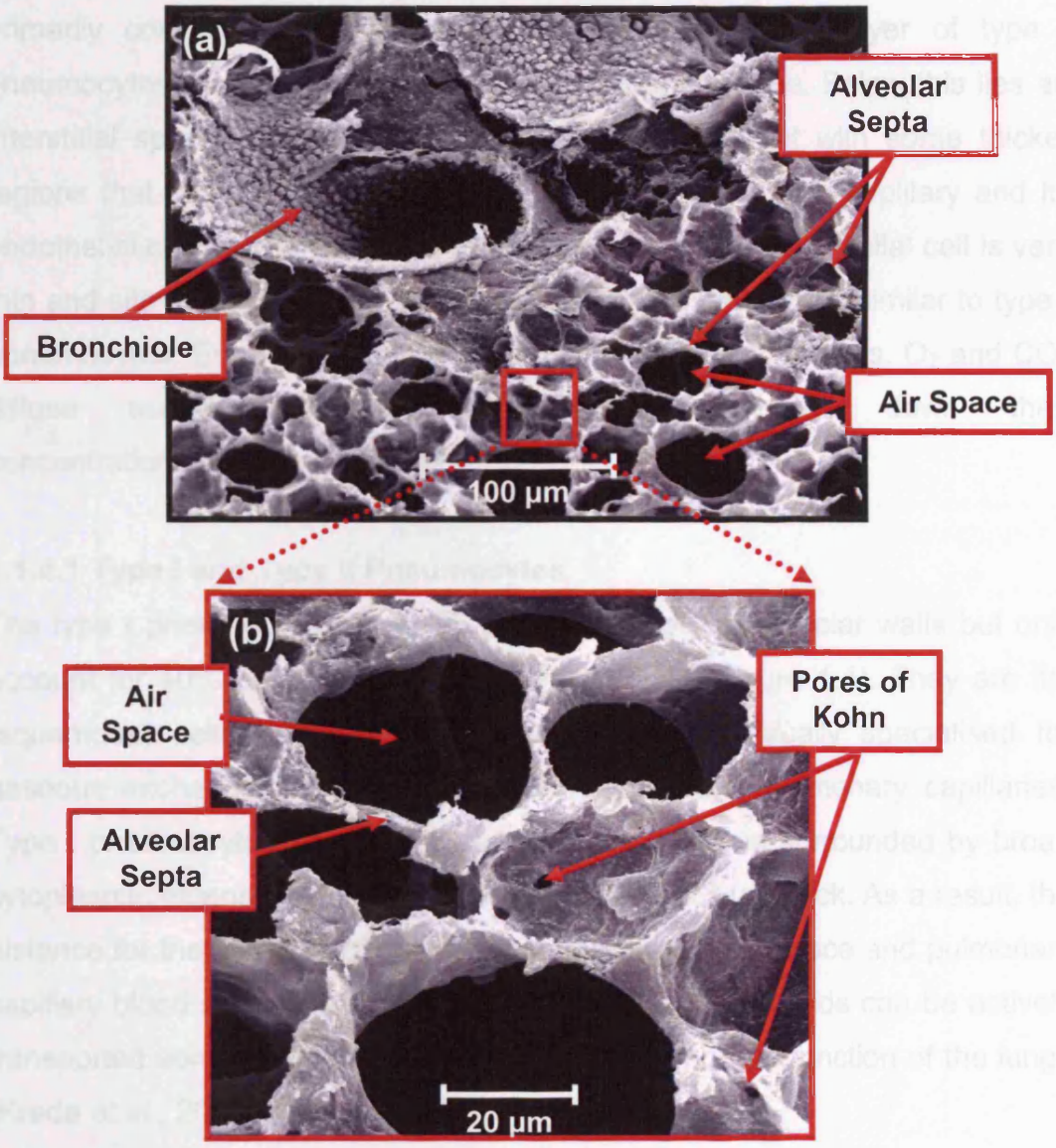

Figure 1.3: Scanning electron micrograph of (a) the distal RT and (b) close up of alveoli (rat lung samples donated by Dr K. BéruBé, images taken by Dr D. Balharry and M. Hicks, 2004).

The pulmonary capillaries are contained in the interstitial space within the septum. Pores of Kohn are small openings located in the alveolar septa (Figure 1.3), which allows the movement of AMs (Section 1.1.5.2) to transfer from one alveolus to another.

The alveolar capillary membrane has a total surface area of more than 70 m^2 but is only 1 to 2 µm thick. The outermost layer comprises of a thin film of fluid primarily consisting of surfactant. Underneath is a thin layer of type I pneumocytes that sits on top of the basement membrane. Below this lies an interstitial space, which is very thin in most areas, but with some thicker regions that contain connective tissue and other cells. The capillary and its endothelial cell wall lie within the interstitial space. The endothelial cell is very thin and sits on the opposite side to the basement membrane similar to type I pneumocytes. Endothelial cells contain plasma and erythrocytes. O_2 and CO_2 diffuse across the alveolar capillary membrane down their concentration/pressure gradients.

1.1.4.1 Type I and Type II Pneumocytes

The type I pneumocytes cover 95 percent (%) of the alveolar walls but only account for 40% of the number of epithelial cells (Figure 1.4). They are flat (squamous) cells that are metabolically and anatomically specialised for gaseous exchange between the alveolar space and pulmonary capillaries. Type I pneumocytes have a flat central nucleus that is surrounded by broad cytoplasmic extensions that are between 0.1 and 0.3 µm thick. As a result, the distance for the diffusion of gas between the alveolar airspace and pulmonary capillary blood is minimised (Figure 1.4b). Proteins and fluids can be actively transported across the epithelium to maintain the normal function of the lungs (Kreda *et al.,* 2001; Johnson *et al.,* 2002).

Interspersed with type I pneumocytes are type II pneumocytes (about 5% cover). These are more metabolically active than type I pneumocytes and carry out 4 important functions:

(1) Pulmonary surfactant synthesis, secretion and recycling (See Section 1.1.5.4)

(2) Xenobiotic metabolism

(3) Transepithelial movement of water

(4) Proliferation and differentiation in response to lung injury to restore normal alveolar architecture.

Type II pneumocytes are rich in mitochondria and have microvilli protruding from their surface. The microvilli aid in the distribution of surfactant and antioxidants (Figure 1.5).

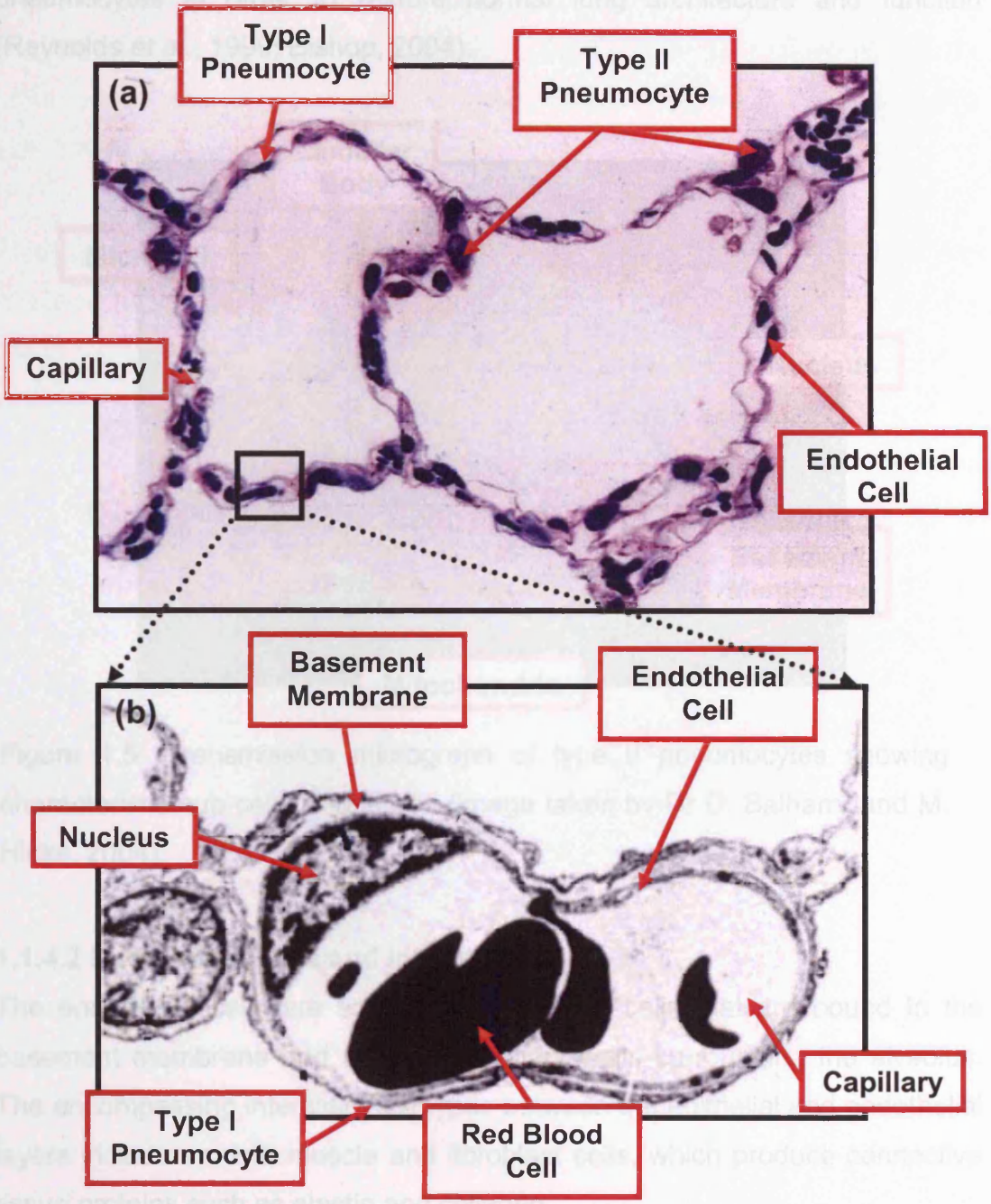

Figure 1.4: (a) Light micrograph (image from Dr. K. BéruBé) and (b) transmission electron micrograph of an alveolar unit (image from West, 1992).

The attenuated cytoplasm of type I pneumocytes and the fact they cover the majority of the surface area of the epithelia make them a ubiquitous target for damage by xenobiotics, hence making them more susceptible to injury. Upon damage, it is commonly hypothesised that type I pneumocytes cannot regenerate as they have no mitotic potential. However, type II pneumocytes (or precursor cells within this population) are known to replicate and differentiate into either normal type II pneumocytes or squamous type I pneumocytes in order to restore normal lung architecture and function (Reynolds *et al.*, 1999; Bishop, 2004).

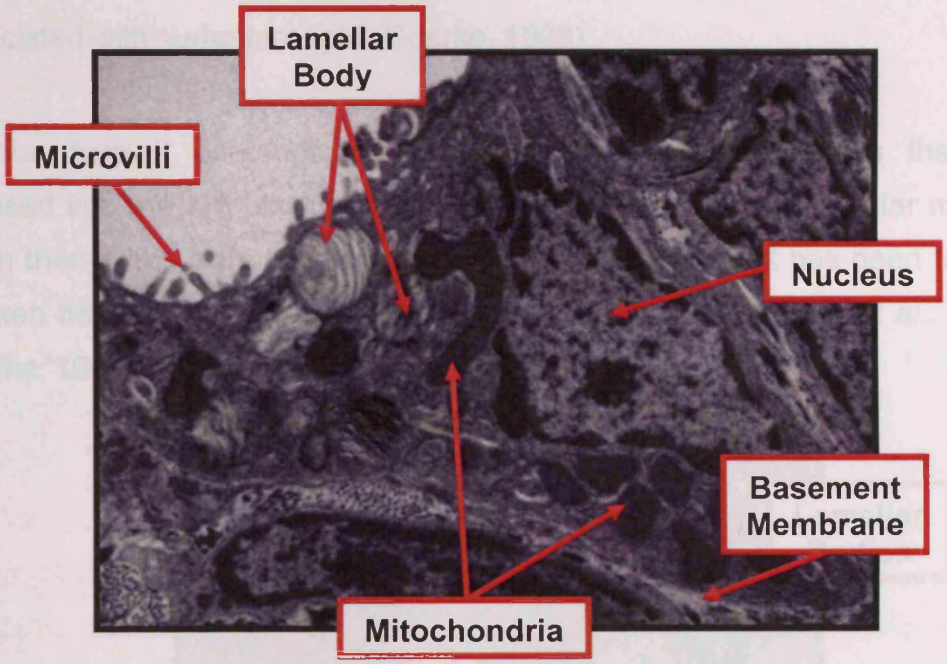

Figure 1.5: Transmission micrograph of type II pneumocytes showing characteristic sub-cellular features (image taken by Dr D. Balharry and M. Hicks, 2004).

1.1.4.2 Endothelial Cells and Interstitial Cells

The endothelial cells are squamous (flattened) cells that are bound to the basement membrane and form the capillary walls surrounding the alveolus. The encompassing interstitial cell types between the epithelial and endothelial layers include smooth muscle and fibroblast cells, which produce connective tissue proteins such as elastin and collagen.

1.1.4.3 Surfactant

Alveolar type II pneumocytes produce surfactant in the lungs. Surfactant provides a fluid film, which lowers surface tension and prevents alveolar collapse at the end of expiration. It also has a role in protecting lungs from injuries and infection brought on by inhaled xenobiotics (Goerke, 1998). Surfactant is comprised of 90% lipid and 10% protein (Lynn *et al.*, 1974). The dominant lipid is phosphatidylcholine of which dipalmitoylphosphatidylcholine predominates (Johansson and Curstedt, 1997). There are several surfactant-specific proteins, e.g. surfactant protein A (SP-A), surfactant protein B (SP-B), surfactant protein C (SP-C) and surfactant protein D (SP-D), that are closely associated with surfactant lipid (Goerke, 1998).

Alveolar type II pneumocytes store surfactant lamellar bodies that are released into the alveolar fluid. Surfactant is transformed into tubular myelin, which then forms a monolayer (Figure 1.6). After surfactant has been used it is taken back up by type II pneumocytes and reused (Creuwels *et al.*, 1997, Goerke, 1998).

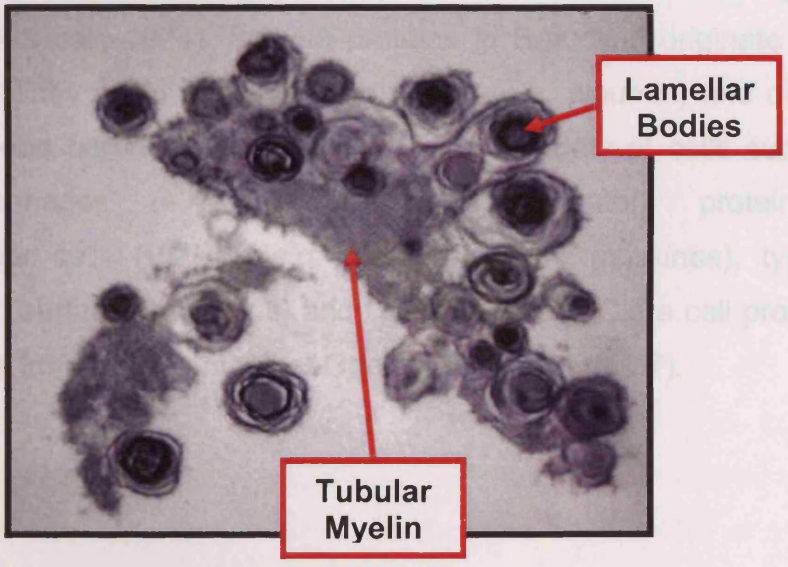

Figure 1.6: Transmission electron micrograph showing lamellar bodies unravelling to form tubular myelin in rat lung (image taken by Dr D. Balharry and M. Hicks, 2004).

Surfactant may alter during lung disease. Its dysfunction can play a major role in acute respiratory distress syndrome (ARDS). SP-A has been found to be elevated in patients with alveolar lipoproteinosis (AL) (Alberti *et al.,* 1996; Doyle *et al.,* 1998). Animal models of alveolar proteinosis provided evidence that the AL was related to an imbalance between surfactant biosynthesis, secretion and clearance possibly explaining the elevated levels of SP-A found in broncho-alveolar lavage (BAL) fluid (Hook, 1991). BAL fluid collected from cystic fibrosis patients shows a SP-A concentration that is lower than in normal subjects (Creuwels *et al.,* 1997, Goerke, 1998). Fragments of SP-A were also identified using proteomics suggesting proteolytic damage of SP-A in CF patients as a possible explanation for the reduced levels in BAL fluid (von Bredow *et al.,* 2001).

1.1.4.4 Broncho-alveolar Lavage (BAL) fluid

BAL fluid is used to obtain epithelial lining fluid samples (Pison *et al.*, 1996). It is an important component of a dynamic biological compartment that is modulated in a variety of medical conditions (Plymoth *et al.*, 2003). BAL has been performed as a research and clinical procedure for more than 30 years (Reynolds and Newball, 1974). Soluble proteins in BAL fluid originate from diverse sources. They could originate from serum (e.g. albumin) and diffuse across the air-blood barrier or be produced from a variety of cells such as alveolar macrophages (e.g. macrophage inflammatory proteins-2), polymorphonuclear cells (PMNs) (e.g. proinflammatory cytokines), type II pneumocyte (e.g. surfactant proteins) and Clara cells (e.g. Clara cell protein). Another source is from surfactant (Noel-Georis, 2002; Figure 1.7).

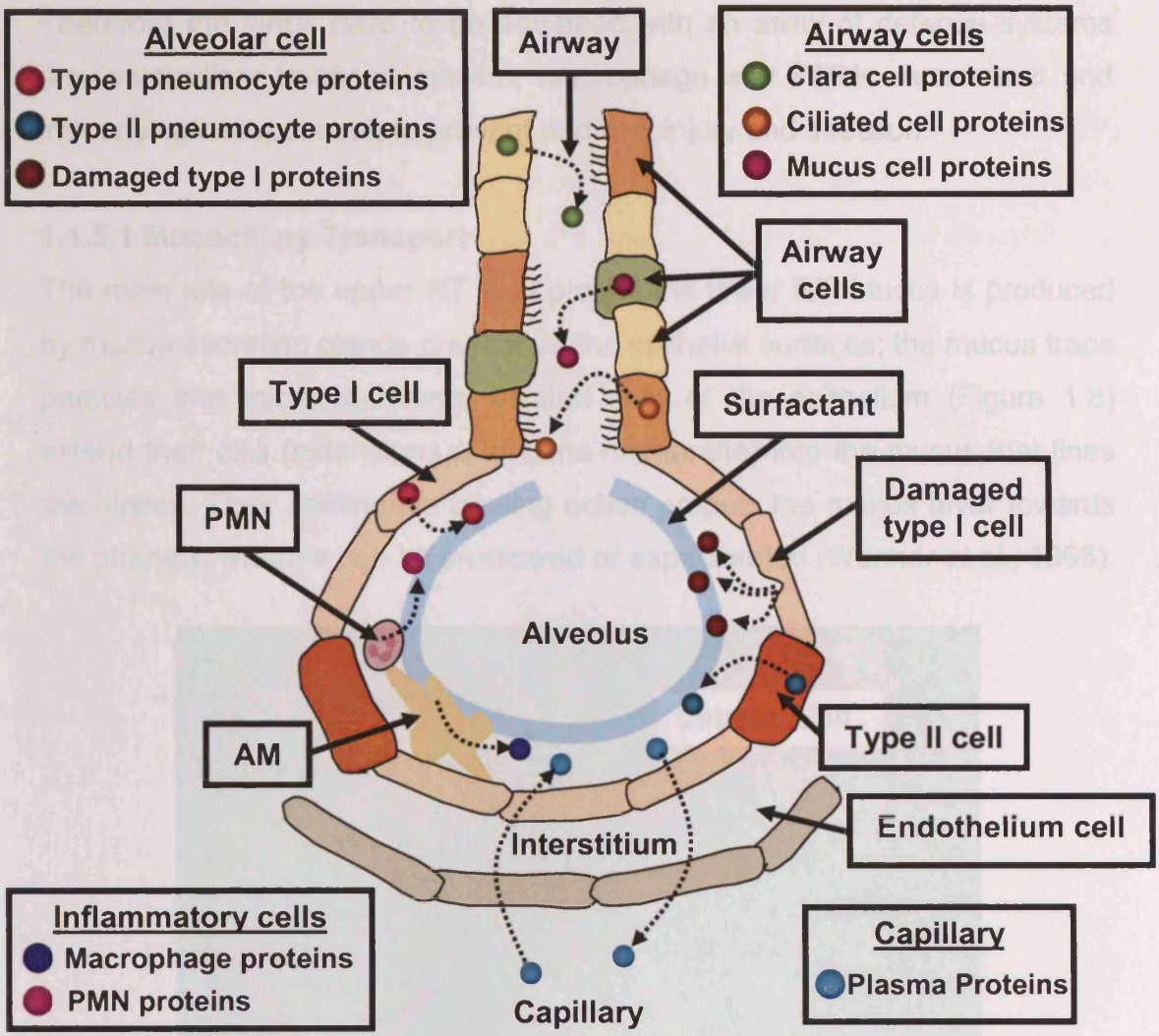

Figure 1.7: Origins of proteins in BAL fluid. Proteins are represented as coloured circles (adapted from Wattiez and Falmagne, 2005).

1.1.5 Lung Defence

The primary function of the pulmonary defensive response to inhaled xenobiotics is to keep the respiratory surface of the alveoli clean and available for respiration. The average human lungs are exposed to 10,000 litres of air a day, this air can contain:

1. Infectious microorganisms
2. Toxic particles
3. Hazardous chemicals.

Therefore the lungs have to be equipped with an array of defence systems (i.e. mucociliary transport system, macrophage and PMNs recruitment and immunologic responses), to prevent and limit injury and infection.

1.1.5.1 Mucociliary Transport

The main role of the upper RT is to protect the lower RT. Mucus is produced by mucus-secreting glands present on the epithelial surfaces; the mucus traps particles and microorganisms. Ciliated cells of the epithelium (Figure 1.8) extend their cilia (extensions of plasma membrane) into the mucus that lines the airway. Their continuous beating action propels the mucus layer towards the pharynx, where it can be swallowed or expectorated (Wanner *et al.*, 1996).

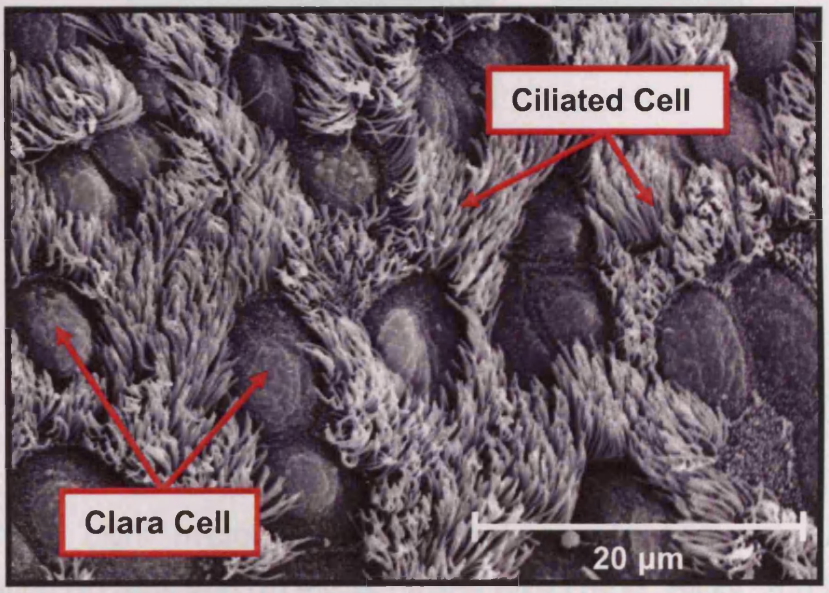

Figure 1.8: Scanning electron micrograph of the Ciliated cells and Clara cells present in the bronchioles of a rat lung (image taken by Dr D. Balharry and M. Hicks, 2004).

1.1.5.2 Alveolar Macrophages

AMs are resident lung phagocytes, found on the surface of the alveolar lining cells and in the supporting tissue of the alveolar septa. There is usually one AM per alveolus and they can migrate via the pores of Kohn (Gordon and Read, 2002). They form part of the mononuclear phagocyte system that originates from the bone marrow and are transported in the blood as

monocytes, differentiating into AMs within the airspace after recruitment to the lungs. AMs are large cells with a diameter of 10-12 µm (Telford and Bridgman, 1995; Figure 1.9). When viewed under transmission electron microscopy (TEM), they are usually recognisable by their numerous pseudopodia (Figure 1.10) that are used for movement, as well as phagocytosis.

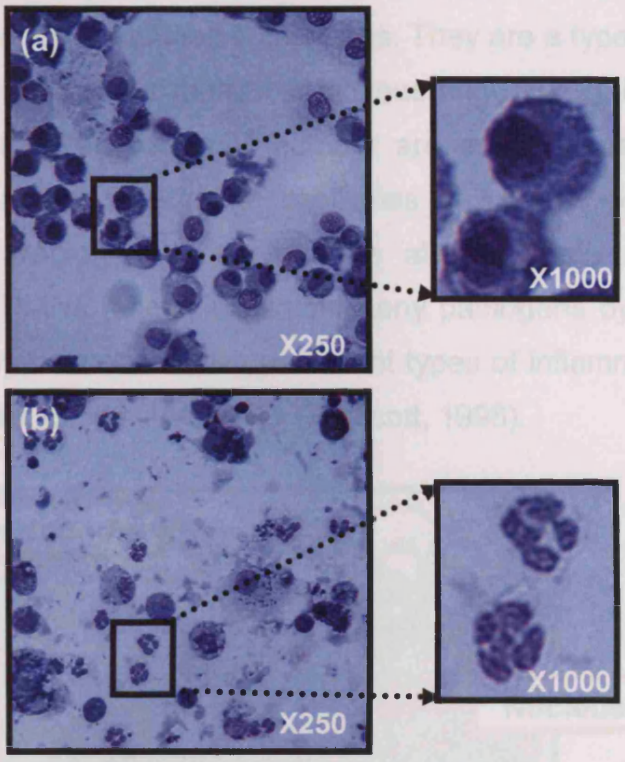

Figure 1.9: Light micrograph depicting free cells from rat BAL Fluid highlighting (a) AMs and (b) PMNs (image taken by M. Hicks, 2003).

AMs are the first line of cellular defence in the lower respiratory tract and play an important role in the defence against xenobiotic particles (Berg *et al.,* 1993). AMs engulf and digest any foreign material and bacteria in a process known as phagocytosis. Following phagocytosis, macrophages migrate to the small airways and are expelled via the mucociliary transport. Alternatively, they exit the lungs via the blood or in the lymphatic vessels, often accumulating in the lymph nodes (Lehnert *et al.*, 1986). During phagocytosis, macrophages are activated and release mediators including cytokines and chemotactic factors. The cytokines recruit PMNs (polymorphonuclear cells)

(Section 1.1.5.2.2) and the chemokines interact with the T-lymphocytes that are involved in a cell-mediated immune response (Lohmann-Matthes *et al.*, 1994). This response may lead to a complex cascade of events leading to inflammation and tissue injury (Moore *et al.*, 1992; van Eeden *et al.*, 2001).

1.1.5.3 Polymorphonuclear Cells

PMNs are inflammatory cells which are normally recruited when more persistent inflammation is induced in the lungs. They are a type of granulocyte and are recognisable by their multilobar nucleus (Figure 1.9). PMNs normally circulate in the blood and a small number are endogenous to the lungs. However, PMNs accumulate in the capillaries at the site of inflammation, where they then rapidly migrate into the alveoli. Once at the site of inflammation, the PMNs quickly eliminate many pathogens by phagocytosis. PMNs are normally associated with persistent types of inflammation because their influx generally follows AMs influx (Prescott, 1998).

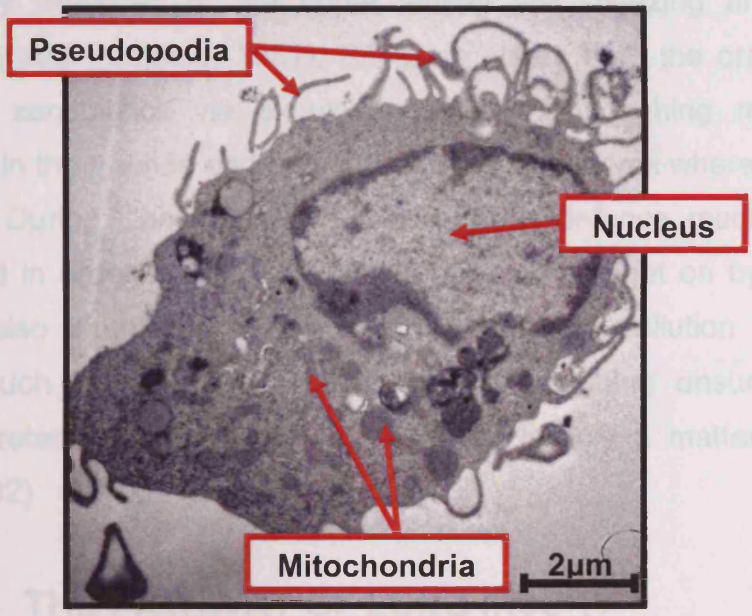

Figure 1.10: Transmission electron micrograph of an alveolar macrophage showing its distinguishable pseudopodia (image taken by Dr D. Balharry and M. Hicks, 2004).

1.1.5.4 Immunological response

Protective immune responses to inflammation and its regulation are endogenous to the lungs. A pro-inflammatory response is regulated by cytokines (accelerate inflammation) including interleukins (IL)-1, -6, and tumour necrosis factor (TNF)-α, which are responsible for acute phase effects, while IL-8 and interferon-γ are also implicated in phagocyte activation. There are also cytokines such as IL-10 that play a role in anti-inflammatory responses by inhibiting pro-inflammatory cytokine release. The net effect of an inflammatory response is determined by the balance between pro-inflammatory and anti-inflammatory cytokines (Fiorentino *et al.,* 1991). Prolonged inflammation can result in tissue damage and possibly the onset of certain types of lung disease (e.g. bronchitis, emphysema and asthma). It is therefore important for lung inflammation to be regulated.

1.1.5.5 Non Cellular

The primary defences of the upper airway are sneezing and coughing (Richardson and Peatfield, 1981). Sneezing clears both the oral and nasal cavities of xenobiotics via expulsion, while the coughing reflex moves xenobiotics in the trachea and pharynx into the oropharynx where they can be swallowed. During illness (e.g. cold, flu), these defence mechanisms are exacerbated in order to clear the mucus build up brought on by the illness. They are also intensified by high concentration of pollution and allergic reactions such as hay fever. Sneezing and coughing ensures that the particulate retention time in the upper airway is only a matter of minutes (Foster, 2002)

1.2 THE PATHWAY OF LUNG INJURY

As previously mentioned, the RS is one of the first lines of defence following exposure to inhaled xenobiotics. This exposure can lead to lung injury that typically elicits a sequential pattern of responses (Figure 1.11). The alveolar surface is the site of the first response. This may be altered by abnormal leakage of fluid into the alveoli (oedema) or by a failure of the clearance

mechanisms designed to remove the debris from the alveoli (Lewis *et al.*, 1987). Mild inflammatory responses may follow, leading to microscopic changes in vascular calibre and blood flow. Chronic inflammation may lead to excessive or abnormal tissue remodelling (hyperplasia, metaplasia). If the toxicant is persistent and bioreactive in the lungs, a common response is the formation of excess collagenous material on the interstitial tissue (pulmonary fibrosis) or a loss in the redistribution of tissue elements (emphysema).

1.2.1 INFLAMMATION IN THE LUNGS

Inflammatory responses are usually protective and beneficial but also have the potential to cause injury to the lungs (Larsen and Holt, 2000). The purpose of an inflammatory response is to repair, restore and if necessary, remodel the injured tissue. Inflammation resulting from an internal/external stimulus is associated with local vessel dilation, capillaries becoming leaky and airway smooth muscle constriction. While this occurs, fluid, proteins and phagocytic cells move into the injured region. The inflammatory response triggers the migration and activation of both resident and circulating inflammatory cells, as well as the production of cytokines and growth factors. This initial recruitment of inflammatory cells into the alveolar spaces is brought about by chemoattractant agents derived from the injured lung tissue.

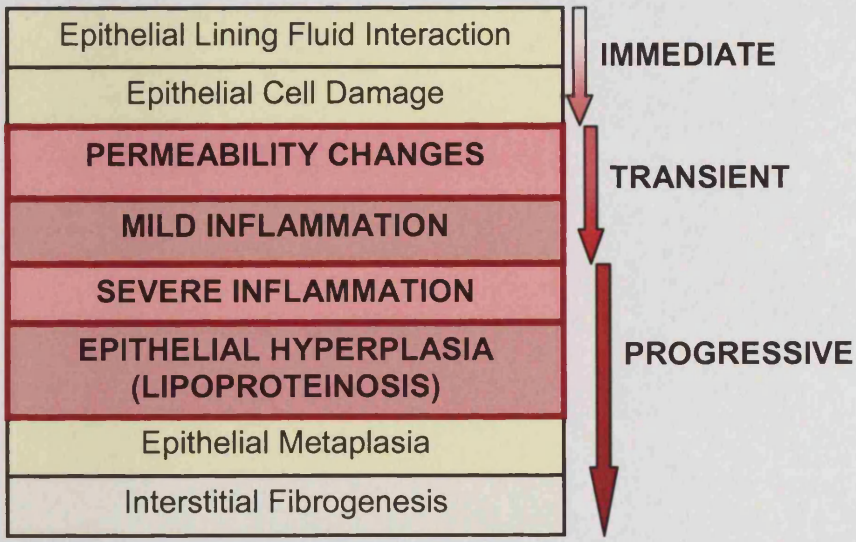

Figure 1.11: Responses to respiratory tissue injury. Sections highlighted in red are the areas investigated in the present study (adapted from Balharry, 2005).

If the damage is acute, the inflammatory cell infiltrate is predominantly made up of PMNs (Grattendick *et al.,* 2002). Initially, the blood flow is high but then it almost stops due to increased viscosity following water loss from the capillaries and the formation of clots. This response dilutes and minimises the spread of toxins, facilitates the clearance of cellular debris and helps to enable tissue healing. One consequence of the inflammatory response is localised regions of swelling of lung tissue that can reduce the gaseous exchange capability (Hicks, 2000). The duration of the acute phase response to injury is short, leading to resolution, healing and repair.

In contrast to acute inflammation, chronic inflammation results from repeated exposure to toxic agents. Vascular remodelling and sustained leukocyte influx are the most prominent features of chronic inflammatory diseases (Ezaki *et al.*, 2001). There is a replacement of the PMNs response with a predominantly lymphocytic response (Izbicki *et al.*, 2002). There is an increase in epithelial and endothelial permeability that results in the movement of plasma proteins. Ultimately, a fibrin clot may form in the alveoli. The degradation products of this fibrin can act as chemoattractants for leukocytes, augmenting the inflammatory response by the recruitment of new inflammatory cells (Richardson *et al.*, 1976).

The adherence of the recruited lymphocytes to the endothelium can lead to further induction of cytokines that may increase leukocyte traffic and recruitment of phagocytic cells during inflammation (Berman *et al.*, 1990). PMNs, AMs and lymphocytes are sources of endothelial cell mitogens (Ezaki *et al.*, 2001). The increased number of these cells could lead to endothelial cell proliferation, resulting in enlargement of the airway vasculature. These changes to the cell structure could be a further stimulus leading to the sustained influx of leukocytes that initiates tissue remodelling (Murphy *et al.*, 1999). This may then lead to an abnormal tissue restoration (hyperplasia, metaplasia), resulting in altered function or failure to function normally, as in fibrosis or emphysema (Jeffery, 2000).

1.2.2 PULMONARY OEDEMA

Pulmonary oedema is a life threatening condition that frequently leads to acute respiratory failure (Sartori and Matthay, 2002). It is the abnormal accumulation of excess interstitial fluid in the interstitial spaces (Hicks, 2000; West, 2003; Jeffries and Turley, 1999). This develops from either an increase in lung vascular permeability or an increase in lung vascular hydrostatic pressure.

There are two stages of pulmonary oedema, firstly, interstitial oedema that is characterised by the engorgement of interstitial tissue (Hansen-Flaschen, 1995; West, 2003). The lymphatics widen and there is an increase in lymph flow. There is also a widening of interstitium of alveoli wall. Interstitial oedema has little effect on pulmonary function. The second stage is alveolar oedema, which involves interstitial fluid moving across into alveoli and occluding them. The affected alveoli shrink due to surface tension (West, 2003). Alveolar oedema affects ventilation and induces hypoxemia (i.e. insufficient oxygenation of the blood) (Hansen-Flaschen, 1995; Dehler *et al.,* 2006). Oedematous fluid may move into the airways and is then coughed-up as frothy sputum: this is sometimes pink due to the presence of red blood cells (West, 2003).

The transition between the two stages is not well understood but may be due to a lymphatic overload, where the pressure in the interstitial space increases, causing it to spill into the alveoli. The epithelium is most likely damaged, resulting in an increase in its permeability. This would explain the presence of protein and red blood cells in the alveolar fluid (West, 2003).

The mechanisms through which pulmonary oedema occur can be split into four categories. The first category involves increased capillary hydrostatic pressure, caused by a rise in left atrial pressure (Hansen-Flaschen, 1995; Sartori and Matthay, 2002). A gradual increase over several years, as in mitral stenosis, shows no clinical evidence of oedema. However, there is often a marked interstitial oedema. A sudden rise in pressure, as in myocardial

infarction, may cause oedema. Another cause of increased capillary pressure can follow excessive infusion of saline, plasma or blood (West, 2003).

For many years it was thought that Starling forces (hydrostatic and protein osmotic pressures), were responsible for keeping the alveolar space free from fluid. There is now strong evidence that active ion transport across the epithelium creates an osmotic gradient leading to reabsorption of water (Sartori and Matthay, 2002; West, 2003)

The second category is represented by increased capillary permeability, caused by inhaled or circulated toxins. Many chemical agents can disrupt the endothelial barrier by disrupting tight junctions and making membrane barriers extremely permeable (Lum and Malik, 1994). Oedema ensues because of the increased movement of fluids and proteins through the damaged membrane (Jones and McAteer, 1990; Sartori and Matthay, 2002). The last two categories include, reduced lymph drainage and decreased colloid osmotic pressure, but are rarely responsible for causing oedema on their own, and normally exaggerate oedema if another cause is present (West, 2003).

Clinical features of pulmonary oedema include prominent dyspnea, i.e. shallow and rapid breathing. Coughing is dry at the early stages but in more severe oedema patients, large quantities of pink foamy sputum can be found in the expectorate. In mild oedema, patients exhibit symptoms on exertion (Hansen-Flaschen, 1995; West, 2003).

1.2.3 ALVEOLAR LIPOPROTEINOSIS (AL)

Rosen *et al.* first described the rare lung disease AL in 1958 (Rosen *et al.*, 1958). AL is also known as pulmonary alveolar proteinosis, pulmonary alveolar phospholipoproteinosis and alveolar phospholipidosis. It is characterised by the accumulation in the lungs of large amounts of insoluble material rich in lipids and proteins (Hook, 1991; Shah *et al.,* 2000). These accumulations can occur intracellularly and extracellularly. Intracellular accumulations interfere with cellular functions. For example, accumulation of

lipid in the cytoplasm of AMs impairs their phagocytic function, causing a decrease in the lungs' defence against infection. Accumulation extracellularly in the alveoli causes interference in gas exchange (Hook, 1991). The most common clinical feature of AL is dyspnoea. Coughing, weight loss and fever are also commonly associated with alveolar lipoproteinosis. Raised serum levels of SP-A, SP-B and SP-D have been observed in AL patients (Shah *et al.,* 2000; Seymour and Presneill, 2002).

AL has an unknown origin, but the characteristic accumulation of insoluble material rich in lipids and proteins contains abnormal tubular myelin (Hook, 1991). BAL fluid of affected lungs is usually a milky fluid, the major constituent is phospholipids, but it also contains serum proteins and surfactant proteins (Hook, 1991; Shah *et al.*, 2000).

Presently most clinical tests for lung injury are based on changes in pulmonary function (Jones and McAteer, 1990). Chest radiographs and blood gas monitoring will only describe the situation relatively late after the initial cellular disturbance (Jones and McAteer, 1990; Hansen-Flaschen, 1995). Hence, there is now considerable interest in detecting early phases of lung injury to aid in diagnoses and treatment.

1.3 PARTICLES AND THE LUNGS

1.3.1 TOXICOLOGICAL PROFILE OF AIRBORNE PARTICLES

The biological activity and toxicity of airborne particles are defined initially by their size shape and chemistry. Even the most toxic particles can have low biological activity if their aerodynamic properties prevent them from reaching the most susceptible part of the lungs. Equally, particles that exhibit the ideal morphology to deposit into the alveoli and mesothelium may have very low biological activity.

There is growing evidence that inhalation of particles in the ambient air have potential health effects for susceptible people (e.g. asthmatics) (Frampton,

2001). In today's environment there are numerous natural and man-made (anthropogenic) airborne particles. The source of natural particles include erosion-derived particles, such as soil particles, mineral particles, volcanic ash and sea salt. Anthropogenic particles are derived from emissions from motor vehicles and jet planes (e.g. diesel exhaust particles) or industrial operations (e.g. carbon black, titanium dioxide (TiO_2) and synthetic polymers). The lungs have to contend with being bombarded with a number of these particles on a daily basis (Figure 1.12). A number of synthetic particles have proved to be toxic to the lung (Kim *et al.,* 2001; Kagawa, 2002). Therefore, more information is required about the typical damage caused by their inhalation.

Airborne particles fall into 3 main size categories that may be classified into the following site ranges: ultrafine, fine and course,

1) Ultrafine – aerodynamic diameter (the diameter of a spherical particle with unit density and its mass is equal to the mass of the particle of interest) of less than 0.1 μm
2) Fine – aerodynamic diameter of 2.5-0.1 μm
3) Coarse – mean aerodynamic diameter between 10-2.5 μm

(Cullen *et al.*, 2000; Tran *et al.*, 2000).

Particle deposition does not occur evenly throughout the lungs. Focal areas such as nasal vibrissae, mucous, cilia, bifurcation (branch) in bronchi and alveolar septa are specialised regions of the RS that trap (impede) inhaled material. Some particles also aggregate (e.g. CB, DEP), which reduces their translocation and deposition in the RS (Murphy *et al.,* 1998).

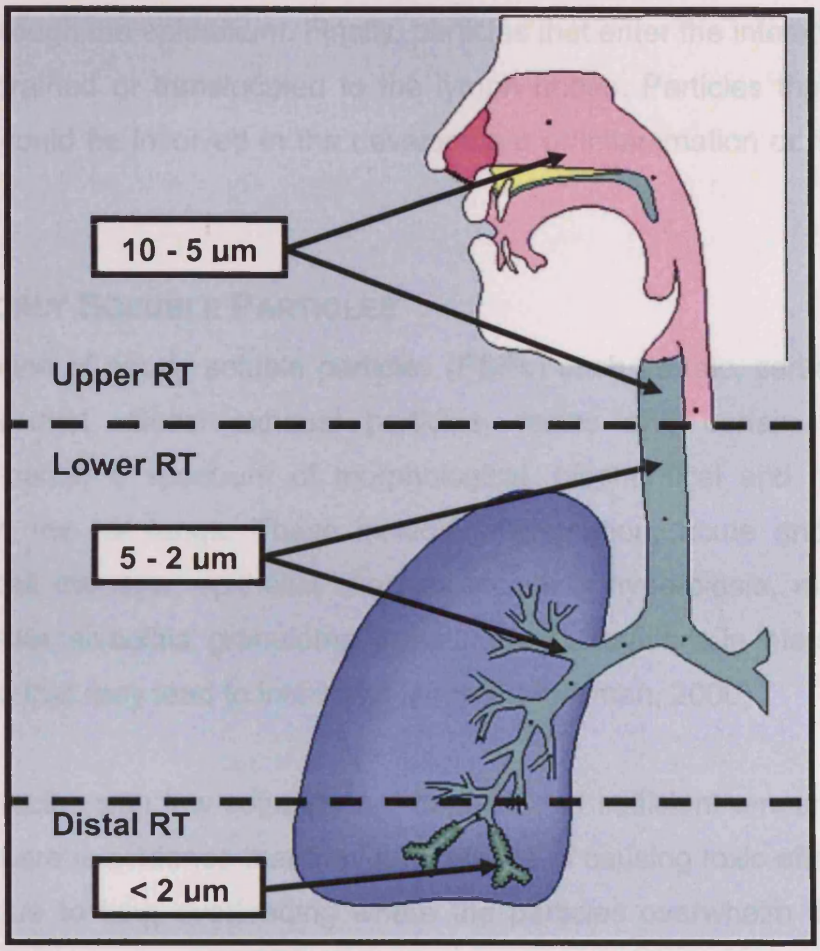

Figure 1.12: Cartoon of the general plan of the respiratory system indicating particle deposition in the lungs (adapted with permission of Dr. K BéruBé).

1.3.2 PARTICLE CLEARANCE

Particles instilled into the lungs are translocated by AMs to the thoracic lymph nodes (Adamson and Prieditis, 1998; Friedetzky *et al.*, 1998; Seaton and Cherrie, 1998; Davies *et al.*, 2001) and once deposited can cause lymph nodes to increase in size or form granulomas (Lee and Richards, 2002). There are thought to be three mechanisms for particle clearance (Kuempel *et al.*, 2001). Firstly, particles can be cleared from the alveolar region by phagocytosis by AMs, which can transport the particles via the mucociliary clearance to the tracheobronchi. These particles can then either be cleared by coughing or swallowed. The second mechanism of particle removal involves

translocation in the alveolar region, whereby particles enter the interstitium of the lung through the epithelium. Finally, particles that enter the interstitium can either be drained or translocated to the lymph nodes. Particles that escape clearance could be involved in the development of inflammation or fibrosis in the lung.

1.3.3 POORLY SOLUBLE PARTICLES

The inhalation of poorly soluble particles (PSPs) such as talc, carbon black, TiO_2, coal dust, diesel exhaust particles, resins and certain synthetic polymers, cause a spectrum of morphological, biochemical and molecular changes in the rat lungs. These include inflammation, acute and chronic epithelial cell damage, epithelial changes including hyperplasia, metaplasia and neoplasia, alveolitis, granuloma formation and alterations in interstitial cell populations that may lead to interstitial fibrosis (Mossman, 2000).

If dusts/particles with low solubility are deposited in sufficient amounts within the lungs there is evidence that they are capable of causing toxic effects. This could be due to lung overloading where the particles overwhelm the lungs' normal particle clearance mechanism (Cullen *et al.*, 2000; Borm *et al.,* 2004). Clearance of inhaled respirable dusts from the alveolar surface of the lung is executed by AMs that phagocytose and remove particles by migrating to the mucociliary escalator (Chilvers and O'Callaghan, 2000). Chronic inhalation studies in rats using the PSPs CB or DEP show evidence of particle overload in the lung (Oberdorster, 2002; Borm *et al.,* 2004; Elder *et al.,* 2005). Overload can be characterised by:

(1) Retardation of alveolar clearance of particles
(2) Increase translocation of particles into the interstitial space
(3) Increase particle burden in the lymph nodes
(4) Persistent inflammation
(5) Increase in epithelial cell proliferation

(Cullen *et al.*, 2000).

1.3.3.1 Synthetic Polymers – Test Particles

S2218600 (herein referred to as polymer A) and S2219200 (polymer B) are synthetically made polymers of different sizes for the potential use in commercial aerosol preparations. Polymer A has a molecular weight of approximately 70kDa (Figure 1.13). Polymer B is a mixture of three different subunits (Figure 1.14) and has an average molecular weight of 700kDa (ranging from 600,000-1000,000).

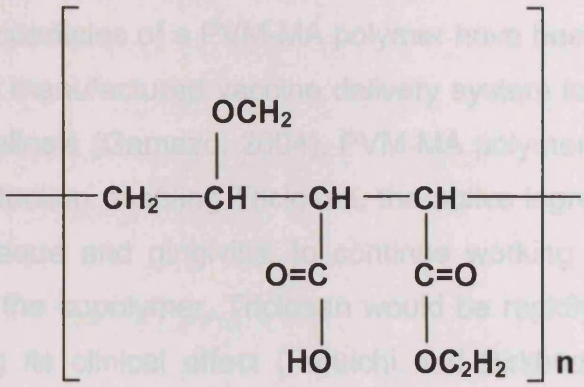

Figure 1.13: Chemical structure of polymer A

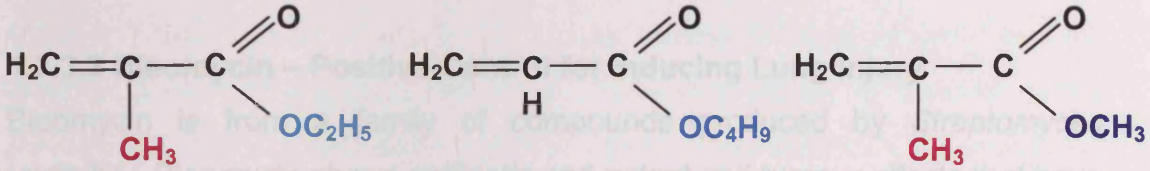

Figure 1.14: Chemical structures of polymer B subunits.

The relatively high molecular weight and poor aqueous solubility of these polymers can potentially lead to bio-persistence in the lungs and cause lung overload. Similar polymers have been used to induce pulmonary injury in rats (Carthew *et al.*, 2002; Carthew *et al.*, 2006). Chronic inflammation, AL, fibrosis and granuloma formation are commonly associated with similar polymer families (Carthew *et al.*, 2006). Activated and hypertrophic AMs with foamy cytoplasms were recorded. Some of the AMs were degenerated or necrotic and tended to form aggregates. Focal changes within the interstitium were

observed and hypertrophy and hyperplasia was evident in the type II cells (Carthew *et al.*, 2006).

Similar polymers to polymer A and B are available and being used for diverse commercial applications. The different polymers, such as poly(methyl vinyl ether-co-maleic anhydride) (PVM-MA), are widely employed for pharmaceutical applications such as denture adhesives, thickening and suspending agents and as drug delivery systems (Gamazo, 2004; Irache *et al.,* 2005). Nanoparticles of a PVM-MA polymer have been shown to provide a safe and easily manufactured vaccine delivery system to prevent human and poultry salmonellosis (Gamazo, 2004). PVM-MA polymers have been used in toothpaste production enabling Triclosan, the active ingredient that is used to help reduce plaque and gingivitis, to continue working in the mouth for 12 hours. Without the copolymer, Triclosan would be rapidly lost from teeth and gums, reducing its clinical effect (Furuichi and Birkhed, 1999). Due to the potential commercial usage of such polymers, the exposure risk must be investigated.

1.3.3.2 Bleomycin – Positive Control for Inducing Lung Injury

Bleomycin is from a family of compounds produced by *Streptomyces verticillis*. Bleomycin shows antibiotic and potent anti-tumour effects that have earned it an important place in cancer chemotherapy. Unfortunately, the use of bleomycin in the treatment of diseases is limited by its toxic effects; the most serious being pulmonary injury (Lazo and Humphreys, 1983). The pathological changes in the lungs following intratracheal instillation of bleomycin include cellular infiltration, pulmonary oedema, changes to type II pneumocytes and interstitial fibrosis (Brown *et al.,* 1988).

The initial morphological damage seen in the first 48 hours after treatment with bleomycin appears as damage in the pulmonary endothelial cells, i.e. cell swelling and blebbing (Aso *et al.*, 1976). Subsequently, there is loss of the type I epithelium resulting in the air-blood barrier being broken down, and thus, allowing oedematous fluid access to the interstitium. The permeability of the vascular endothelium is then altered (Adamson, 1984). There is also an

inflammatory cell infiltrate in the alveolar spaces, including the infiltration of macrophages, monocytes, lymphocytes and PMNs (Hay *et al.,* 1991).

Bleomycin was chosen as a positive control, as it is a well-documented, *in vivo* model of lung injury in rats (Thrall *et al.*, 1979; Balharry *et al.*, 2005), rabbits (Catravas *et al.*, 1983), hamsters (Starcher *et al.*, 1978) and mice (Aso *et al.*, 1976). When the instillation dosing regime is correctly chosen in rats then the type of inflammatory response and the extent of oedema and recovery can be regulated (Balharry, 2005). This opens up the possibility of investigating genomic changes associated with oedema (Balharry *et al.,* 2005) and importantly for the present study the opportunity to investigate proteomic changes at the surface of the lung.

1.4 PROTEOMICS

Proteomics is used to separate and identify proteins in a complex mixture for the purpose of quantitative and functional analyses of all the proteins present (Abbott, 1999, Hunter *et al.,* 2002). It has proven to be a powerful tool for identifying early changes at the protein level in a variety of disease states (Kvasnicka, 2003). It can also provide a non-invasive technique for evaluating body fluids in the search for pertinent or specific biomarkers of toxicity (Kennedy, 2001).

Genomics is the study of genes, their DNA sequence and variations of that sequence, their expression patterns in normal and diseased tissues, and their function in the organism. Every cell within a given organism contains all the genetic information necessary to make an exact copy of itself. That is, each cell contains a complete 'genome', however, not all the genes are expressed at the same time. Genomics offers a snapshot of expression of some or all of the genes in a given cell/tissue, but the level of mRNA does not necessarily predict the levels of the corresponding proteins in the cell, due to differing:

1. Stability of mRNA
2. Efficiencies in translation

3. Stability and turnover rates
4. Post-translational modifications

(Liebler, 2002).

Unlike the genome, that is a constant feature of the organism, the proteome is constantly changing depending on the conditions such as health, disease, growth rate and drug treatment. The Human Proteome Organisation has a goal to catalogue every distinct human protein, all protein-protein interactions and levels of proteins in different cells and tissues (www.hupo.org).

1.4.1 TWO-DIMENSIONAL SODIUM DODECYL SULPHATE POLYACRYLAMIDE GEL ELECTROPHORESIS

Two-dimensional Sodium Dodecyl Sulphate Polyacrylamide Gel Electrophoresis (2D SDS PAGE) is the most widely used method for analysing proteins in a complex mixture (Berkelman, 1998). Proteomic analysis is challenging due to the number of different proteins expressed at any given time under defined biological conditions (Görg *et al.*, 2004). 2D SDS PAGE has the capacity to separate thousands of proteins on a single gel. O'Farrell and Klose first introduced the method in 1975. 2D SDS PAGE is the combination of two separation techniques. The first dimension step is isoelectric focusing (IEF), where proteins are separated according to their isoelectric point (pI). This is performed in a pH gradient created by immobilized ampholytes. Each protein migrates to the pH that is equivalent to its pI where their net charge is zero. Focused proteins are then equilibrated and labelled with SDS-containing buffer before they are run on the second dimension which is the SDS-PAGE, where proteins are separated according to their molecular weight. The resulting protein pattern can be revealed by Coomassie blue, silver or fluorescent staining. Thousands of different proteins can be separated with each spot on the 2D gel corresponding to a single protein species in the sample. The gels can be used to gain information such as isoelectric point, apparent molecular weight and the amount of protein obtained.

Using this technique O'Farrell (1975), was able to resolve 1100 different components from *Escherichia coli,* and Klose (1975), used mouse tissue to resolve 275 spots from fetal liver, with approximately 230 from whole embryos and approximately 100 for serum. Since this technique was introduced in 1975, it has been used to investigate a wide variety of samples such as normal versus disease samples, disease versus treated samples and molecular markers in body fluids (Westermeier and Naven, 2002).

1.4.2 MASS SPECTROMETRY

2D SDS PAGE combined with mass spectrometry (MS) produces a powerful tool for the separation and identification of proteins from a sample. Once protein gels have been stained and spots of interest have been located, MS analysis is used to identify the proteins. There are three essential components of a MS machine: (1) the source which produces ions from sample, (2) the mass analyzer that resolves ions based on their mass/charge (m/z) ratio and, (3) the detector which detects the ions resolved by mass analyzer (Liebler, 2002).

There are two types of mass spectrometers that are used in proteomics, matrix assisted laser desorption ionization time of flight (MALDI-ToF) and Tandom mass spectrometer (MS/MS). In the present study MS/MS was employed as it has been found to be more accurate than MALDI instruments, however a limitation of MS/MS is that it is more susceptible to contamination (Beranova-Giorgianni, 2003). Once the MS data has been collected, a database search can be used to try and identify the protein (Liebler, 2002).

1.4.3 PROTEOMICS ON BRONCHOALVEOLAR LAVAGE FLUID

Proteomic analysis of BAL fluid was first performed in 1979 by Bell and Hook. They used the 2D SDS PAGE technique to compile a comprehensive map of the major proteins that were present in patients suffering from pulmonary alveolar proteinosis (Bell and Hook, 1979). Soluble proteins in BAL fluid may have originated from a broad range of sources, for example, diffusion from

blood across the air-blood barrier or as products from different cell types present in the lungs (Wattiez and Falmagne, 2005). A comparison between serum and BAL fluid 2D protein maps revealed that a certain number of the proteins are present at a higher concentration in the BAL fluid than in the serum, therefore suggesting that they are specifically produced in the lungs. Hence, these proteins are good candidates for lung specific biomarkers. They also found that these lung specific proteins could be detected in plasma using specific antibodies (Hermans *et al.*, 2003; Wattiez and Falmagne, 2005).

Since 1979 the 2D SDS PAGE technique has been employed by a number of research groups to investigate the changes in BAL fluid proteins during different disease states. Lenz and co-workers compared healthy volunteers with patients suffering from idiopathic pulmonary fibrosis, sarcoidosis, and asbestosis. They observed marked changes in protein spots. In particular, they found the number and intensity of low molecular weight proteins were increased in diseased samples (Lenz *et al.*, 1993).

A number of research groups have been developing master gels of BAL fluid proteins. Noel-Georis *et al.* (2002), have comprised a database of BAL fluid proteins in which they observed 1200 silver stain spots of which they could identify 900 spots as 78 different protein species. A profile of BAL fluid proteins of patients suffering from sarcoidosis has been investigated by Sabounchi-Schutt *et al.* (2003), using proteomics. In this study, they found alterations of 21 silver stained spots, of which 17 were identified and 12 of these were found to be significantly reduced (Sabounchi-Schutt *et al.,* 2003).

Other studies involving BAL fluid include;
BAL fluid and nasal lavage (NL) fluid – Lindahl *et al.* (1995), established 65% spot pattern homology. Immunoglobulin A (IgA) and immunoglobulin G (IgG) were found to be significantly higher in NL fluid possibly due to higher exposure to foreign antigens in the upper RT compared to the lower RT.

Smokers and non-smokers – Lindahl *et al.* (1998), observed levels of IgA, ceruloplasmin and the pro form of apolipoprotein A-1 to be lower in smokers BAL fluid than in non-smokers.

Cystic fibrosis – von Bredow *et al.* (2001), reported reduced amounts of SP-A in the BAL fluid of cystic fibrosis. This could be due to reduced synthesis or excessive proteolytic degradation.

Interstitial lung disease – Wattiez *et al.* (2000), determined accumulation of SP-A in patients suffering from idiopathic pulmonary fibrosis. This may have been due to alterations in synthesis or release following type II cell damage. They also found an increase in acidic low molecular weight proteins in patients suffering from idiopathic pulmonary fibrosis and hypersensitive pneumonitis. The proteins identified were involved in cellular processing relating to proliferation.

Diesel exhaust particles – Wang *et al.* (2005), revealed induction of the phosphorylation of several phosphoproteins belonging to a number of signal and oxidative stress pathways following exposure to DEP.

2D SDS PAGE was employed in the present study due to its extensive use for proteomic separation of BAL fluid proteins on a gel by other researchers, enabling possible comparisons to be made between different studies. In terms of equipment and personnel, the 2D based technology was well suited to the academic setting. The basic experimental design for the investigation into protein changes in BAL fluid following administration of polymers is shown in Figure 1.15. Proteomic analysis was used to produce a list of proteins that could potentially be used for early clinical diagnosis of lung injury replacing the current clinical tests such as chest radiographs and blood gas monitoring. These tests only describe the situation relatively late after the initial cellular disturbance so there is a considerable interest in detecting early phases of lung injury.

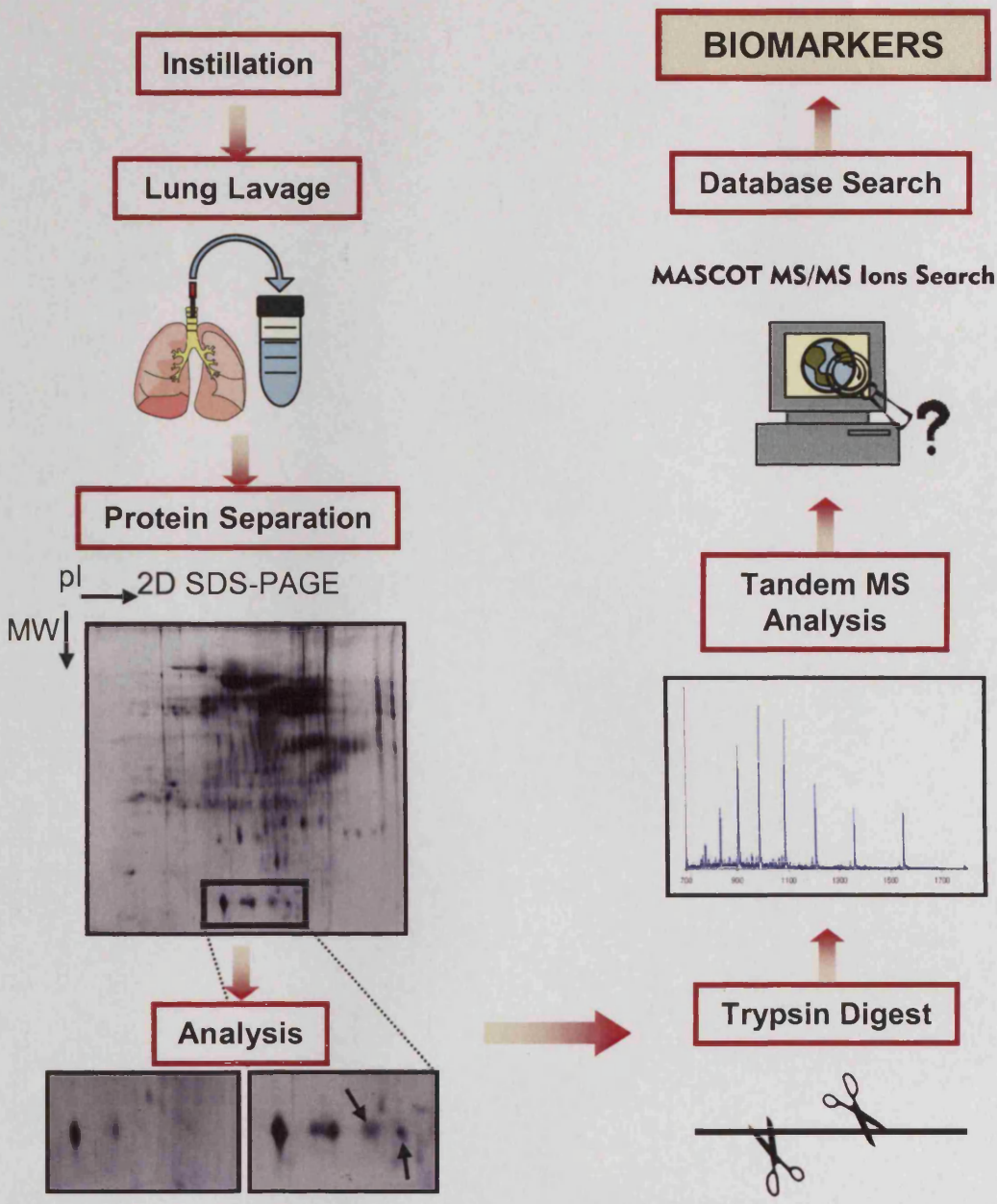

Figure 1.15: Flowchart of the proteomic process involve in investigating potential biomarkers in BAL fluid

1.5 AIMS AND OBJECTIVES OF THE STUDY

1.5.1 THE HYPOTHESIS

1. Polymer induced lung injury follows the same mechanism of damage as bleomycin induced lung injury.
2. Polymer and bleomycin induced lung injury causes protein changes in BAL fluid which can be identified using proteomic techniques.

1.5.2 PROJECT AIMS AND OBJECTIVES

The aim of this study was to develop a better understanding of the proteomic profile of chemical-induced lung injury, and specifically to identify protein biomarkers for inflammation, pulmonary oedema and repair. To accomplish this, animal models of polymer-induced (and bleomycin-induced) injury were employed.

Conventional toxicology and histology techniques were used to characterise the models and identify different endpoints of injury. Once these models had been established the proteomic techniques 2D SDS PAGE was utilized to evaluate protein profiles of the various stages of pulmonary damage and repair.

In detail, the sequential steps of this study were as follows:

1. To identify of pulmonary oedema/inflammation and repair in polymer induced models using broncho-alveolar lavage techniques, cellular counting methods and assays for alveolar surface protein (Chapter 2).

2. To confirm the morphological changes occurring during pulmonary oedema, inflammation and cellular repair following polymer-induced damage using histological analysis and to compare the polymer-induce model with the well-characterised bleomycin-induced model (Chapter 3).

3. To characterise the progressive severity of the polymer-induced model of pulmonary injury using the toxicology and histology information (Chapter 2 and 3).

4. To optimise the sample preparation and 2D SDS PAGE technique for broncho-alveolar lavage fluid samples (Chapter 4).

5. To profile proteins from broncho-alveolar lavage fluid samples collected from saline and polymer-instilled models (Chapter 5).

6. To analyse difference in protein profiles from saline and polymer-instilled models (Chapter 5).

7. To identify the potential protein markers using mass spectrometry for different severities of lung injury and repair (Chapter 5).

8. To evaluate the potential of novel lung proteins to act as biomarkers for pulmonary oedema using immunohistochemistry (Chapter 6).

CHAPTER 2:

MODELLING OF LUNG INJURY USING POLYMERS

2.1 INTRODUCTION

Synthetic particles, like polymer A and B are known to cause pulmonary toxicity (Bracco and Favre, 1998). In a recent study, Carthew *et al.* (2006) used polymer A as a positive control substance. Chronic inflammation and granuloma formation were associated with this 13 week polymer instillation study carried out in male rats (Carthew *et al.,* 2006). In this present study, the models were used to obtain proteomic profiles of peak inflammation/oedema and the subsequent repair. To date, no studies have been done using polymer B.

There are two experimental routes by which animals lungs can be exposed to a synthetic polymer, either inhalation or intratracheal instillation. Inhalation gives the most authentic exposure when compared to actual real life exposures and is the natural route of entry for xenobiotics into the lung. Nevertheless, instillation has certain advantages over inhalation:

- Exact dose can be delivered to the lungs
- Technical procedure is simpler
- Large range of doses can be delivered in a short period of time
- Specific lobe exposure can be carried out
- Auto-controlled studies with a non-dosed lobe from the same lung can be used as a control
- Comparatively inexpensive

(Driscoll *et al.,* 2000).

However, there are also aspects requiring consideration when utilising instillation technique;

- Distribution differs from inhaled particles - although non-invasive instillation studies over 20 years have indicated that both short and long term endpoints (inflammation, epithelial repair and fibrosis) are identical to those found in inhalation models (Richards and Curtis 1984). These endpoints tend to be achieved more rapidly with instillation models

- Upper respiratory tract (RT) is by-passed - although in the rat model chosen in the present study the upper RT is quite different from that of human subjects
- Instillation vehicle could alter the physicochemical properties of the test material or can induces its own effects
- Effect of the anaesthesia on the lungs - although with the technique employed in the present studies (approximately 2 mins exposure) minimal changes are expected and sham-treated control animals receive identical anaesthesia

(Driscoll *et al.,* 2000).

Despite the potential variations associated with intratracheal instillation, it was chosen as the method of exposure in this study, since the administration of exact doses was important, as well as the ability to assess toxicity at acute time points.

Conventional toxicological parameters (Richards and Curtis, 1984, Richards *et al.,* 1991, Murphy *et al.,* 1998), were used to assess the status of the lung (e.g. healthy verses injured) (Table 2.1).

To characterise and compare the polymer models further, a bleomycin model was used as a positive control (Balharry, 2005). The intratracheal instillation of bleomycin produces a well-characterised model, which initially induces lung inflammation that is followed by oedema and the progressive destruction of normal lung architecture (Starcher *et al.*, 1978; Thrall *et al.*, 1979; Catravas *et al.*, 1983; Balazs *et al.*, 1994; Kaminski *et al.*, 2000).

The objective of the present study was to test the hypothesis that single and double instillations of test polymers will induce different pulmonary responses and benchmark against a bleomycin control model of oedema and inflammation.

Parameter	Injured Lung Status	References
Lung to body weight ratio	Assesses the health status of the lung: an early increase above control is indicative of increased lung permeability. A later increase denotes chronic lung remodelling.	(Reynolds and Richards, 2001; Housley *et al.*, 2002; Balharry *et al.*, 2005).
Surface protein concentration	An increase in the amount of acellular protein from the lavage fluid was taken as a sensitive marker for oedema, resulting from epithelial or endothelial cell damage.	(Richards and Curtis, 1984; Murphy *et al.*, 1998; Reynolds and Richards, 2001; Bermudez *et al.*, 2002).
Lavage free cell count (LFC)	An increase in the number of macrophages and PMNs represents an inflammatory response.	(Reynolds *et al.*, 1977; Bermudez *et al.*, 2002).
Differential cell count (DCC)	Assesses the severity of the inflammation: an increase in macrophage number alone is suggestive of mild inflammation whereas, increases in PMNs are associated with more severe inflammation.	(Reynolds *et al.*, 1977; Grattendick *et al.*, 2002; MacNee and Donaldson, 2003).

Table 2.1 Parameters in conventional toxicology (PMNs – polymorphonuclear cells).

2.2 MATERIALS AND STOCK SOLUTIONS

2.2.1 MATERIALS

Centurion, UK.

Cytospin

Harlan, UK.

Male (200-250 g) *Wistar* Rats (pathogen free)

Raymond A Lamb Limited, East Sussex, UK.

Lamb Stain-Quick Staining Kit (LAMB/600-K)

Rhone Merieux, Harlow, Essex, UK.

Euthatal

Halothane

Sigma Aldrich, UK.

Bradford reagent (B6916)

Bovine Serum Albumin (P0834)

Unilever, Bedfordshire, UK.

S2218600 (Polymer A)

S2219200 (Polymer B)

2.2.2 STOCK SOLUTIONS

Saline NaCl (0.09 % 0.15M)

2.3 METHODS

2.3.1 ADMINISTRATION OF POLYMERS

Aside from the very recent work by Carthew *et al.* (2006) there have been no previous instillation experiments using Polymer A and B to induce lung injury. Therefore, a time point of 3 days post-instillation was initially used to assess lung injury during the preliminary experiments reported here. This time point has previously been shown to represent the peak of lung injury following instillation of bleomycin (Hay *et al.,* 1991; Adamson and Bakowska, 1999; Balharry *et al.,* 2005,) and zinc chloride (Richards *et al.,* 1989).

Three preliminary experiments were carried out to optimise the model of lung injury and repair using the polymers:

1. **Concentration Experiment:** Previous inhalation studies have shown the maximum bronchial exposure concentration in rats is 45mg/m^3. This is equivalent to a 4.5 mg/ml instillate concentration, as the deposition of the polymer at 1 mg/m^3 in the rat is 10% (Dr. P. Carthew, Personal Communication). The polymers come as a 4% solution (96% carrier vehicle). The polymers were resuspended in saline to give a final concentration of 12 mg/ml. At the time these experiments were set up there were no previous studies using either polymer, therefore, to induce lung injury, a range of doses (6, 9 or 12 mg/ml) were instilled.
2. **Control Experiment:** The polymers were not water-soluble and were suspended in carrier solutions, thus necessitating a second experiment to determine whether any damage observed was due to the polymers themselves or their carrier solutions. The carrier solutions were instilled at equivalent concentrations to 9 mg/ml of polymers. Polymer A carrier solution contained methyl aminopropanol and diisopropanolamine in aqueous ethanol and polymer B carrier solution contained methyl aminopropanol.
3. **12 week study:** A single instillation of 9 mg/ml of polymer A was used to determine time points for peak oedema/inflammation and resolution. In a previous study using a different polymer, Resin 6965,

lipoproteinosis material was observed after 13 weeks inhalation exposure (Carthew, 2002).

In the present study, models for short and longer term effects were required, consequently, single and double doses of polymer A (9 mg/ml) were initially used in an attempt to produce those endpoints. Data from the 12 week study was utilised to determine the time points required to induce these acute and chronic models of lung injury.

For the double instillation, the second instillation took place seven days after the first instillation, as this was the time point at which lung injury peaked. Thus the polymer would be administered to a lung that was already compromised and probably undergoing some epithelial repair (Brown et al., 1988).

Prior to treatment, rats were lightly anaesthetised with Halothane. The administration of the doses was via non-invasive intra-tracheal instillation (Reynolds and Richards, 2001), which ensured every animal received the same quantity of instillate directly to the target tissue. For each experiment, the recovery time of rats was monitored every 2 hours for the first 6 hours and twice a day thereafter, using a post-procedure pain and distress scoring sheet and weight gain measurements (e.g. shortness of breath, hunched appearance, 20% body weight loss) (Wolfensohn and Lloyd, 1998).

2.3.2 SACRIFICING RATS

Saline and polymer treated rats (200-250 g) were anaesthetised with Halothane and then administered a lethal intraperitoneal injection (150 mg/kg) of Euthatal. The rats were weighed and cardio-respiratory death confirmed by checking if pulse/breathing had ceased and by squeezing the foot pad, prior to dissection.

2.3.3 DISSECTION OF THE RAT

The dissection of the rat to obtain the pulmonary tissue involved the following procedures. Ethanol (70% v/v) was applied to the rat abdomen and thorax in order to reduce airborne particles before the ventral surface skin was removed. The peritoneal cavity was opened by midline incision and blood (5 ml) was removed from the major aorta before they were cut. A tracheotomy was performed and a Luer cannula, attached to a 20 ml syringe, was securely tied into place in the trachea. The diaphragm was then opened and the ventral portion of the rib cage and thymus removed.

A Luer cannula attached to a gravity feed of sterile saline was then fed into the pulmonary artery and the right atrium was cut upon expansion to allow fluid to exit. The lungs were perfused via artificial ventilation with 8-10 ml of air by means of the syringe attached to the Luer cannula of the trachea. Ventilations (usually 8-10) were continued until the pulmonary circulation was clear of all blood to produce white parenchymal lung tissue.

The heart was removed and the lungs and trachea dissected free from the carcass. The oesophagus and any fatty tissue were dissected from the lungs and trachea. Any mucoidal material or blood clots on the exterior of the tissue were removed by means of absorbent tissue. The lung parenchyma was weighed to calculate the lung to body weight ratio.

2.3.4 BRONCHO-ALVEOLAR LAVAGE (BAL) FLUID

The lungs were lavaged (6 times) with 6-8 ml of 0.15 M saline (Figure 2.1). The BAL fluid was pooled into sterile Falcon plastic tubes, cells were removed by centrifugation (at 300 x *g*) and the supernatant stored for use in later experiments. After lavaging, the five lung lobes were separated, cut and immediately placed in labelled bags into liquid nitrogen before being stored at -80 °C (Lee and Richards, 2004).

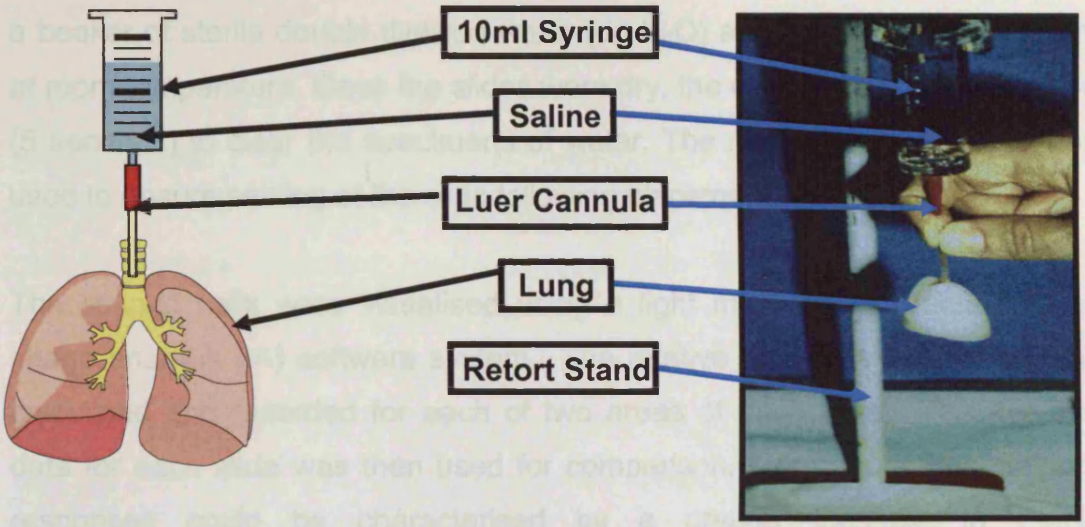

Figure 2.1: A diagrammatic representation of the instillation procedure.

2.3.5 FREE CELL COUNTS

The cell pellet was resuspended in saline (3 ml 0.15 M) and a standard haemocytometer was used to calculate the number of large free cell alveolar macrophages (AMs) and PMNs in each lavage pool. Any residual red blood cells, damaged cells and debris were not included in the cell count. The residual free cells were re-suspended to a concentration of 200,000 cells per ml in saline.

2.3.6 CYTOSPINS AND DIFFERENTIAL CELL COUNTS

Standard light microscopy slides and filters were sealed into cytospin chambers and the diluted lavage free cells (LFC) suspension (0.5 ml) was transferred into the chamber. Duplicate pools of each cellular suspension underwent cytospin centrifugation at 13 000 x for 6 minutes. The resulting slides with the LFC adhered to the surface were stored at 0-4 °C until further analysis.

The cytospin slides were stained using the Quick Stain system. This system consisted of a fixative, an acidic dye and a basic dye. Each slide was placed in the fixative for 5 seconds to stop metabolic processes. Then into the first

dye which had an affinity for basic cell components and finally into the second dye which had an affinity for acidic cell components. The slides were rinsed in a beaker of sterile double distilled water (dd-H_2O) and then allowed to air dry at room temperature. Once the slides were dry, the cells were rinsed in xylene (5 seconds) to clear the specimens of water. The mounting media DPX was used to ensure sealing of the cells following placement of the coverslip.

The stained cells were visualised using a light microscope attached to an image analysis (IA) software system. The relative ratio of AMs to PMN was calculated and recorded for each of two areas of each slide. The average data for each slide was then used for comparison. More acute inflammatory responses could be characterised by a greater increase in PMNs concentration. Macrophages were identified on the basis of cellular size (i.e. large) and by the shape of their nuclei; PMNs have a multi-lobar shaped nucleus (Chapter 1; Figure 1.9).

2.3.7 LAVAGE PROTEIN CONCENTRATION–THE BRADFORD ASSAY

An increase in the amount of acellular protein from the lavage fluid is taken as a sensitive marker for oedema, resulting from epithelial or endothelial cell damage (Richards and Curtis, 1984; Murphy *et al.*, 1998) The concentration of proteins in lavage was determined by the Bradford assay (Bradford, 1976). Briefly, sets of standards were made up using bovine serum albumin (BSA) (0 to 20 µg/ml). BAL fluid was diluted 10-fold in 0.15 M saline and 200 µl of sample was added to each well in a 96 well plate. Bradford reagent (50 µl) was added to each sample and the absorbance was read at 590 nm using a plate reader. Assays were performed in triplicate for each animal and the mean value recorded.

2.3.8 POSITIVE CONTROL MODEL

The polymer models were compared with a bleomycin model that is a well established model for oedema and inflammation (Aso *et al.*, 1976, Starcher *et al.*, 1978, Thrall *et al.*, 1979, Catravas *et al.*, 1983, Balharry, 2005). This

model used either single or double instillations of bleomycin (0.5 units). Toxicological data were collected as described in Sections 2.3.4 – 2.3.6.

2.3.9 STATISTICAL ANALYSIS

All data handling and graphical representation of results were performed in Microsoft Excel '97. Statistical analyses included Andersson-Darling normality test, two-sample t-test and non-parametric Mann-Whitney test. A two-sample t-test was chosen as an appropriate test due to the data being derived from two independent random samples. This test was used if the data were normally distributed and the variances were equal within each group. If this was not the case, a non-parametric Mann-Whitney test was used. All analyses were performed in Microsoft Minitab 13. Significance was assumed at $p \leq 0.05$.

2.4 RESULTS

2.4.1 PRELIMINARY EXPERIMENTS

2.4.1.1 Concentration Experiment

Test rats were instilled with 6, 9 or 12 mg/ml of either polymer A or polymer B alongside control animals dosed with saline. The instillation of 12 mg/ml of polymer B caused animals in the group to exhibit signs of distress, including shortness of breath, hunched appearance and erected hairs. The group also failed to increase in body weight over the first 48 hours. Therefore, this dose proved too toxic and the rats had to be culled in concordance with Home Office guidelines. The lung to body weight ratios in rats instilled with either polymer were found to increase (Figure 2.2a). However, only the rats instilled with polymer A demonstrated significant increase in lung weight compared to the saline treated controls ($p \leq 0.05$) (n=3).

Instillation with either polymer A or polymer B at 9 mg/ml resulted in a significant increase in lavage fluid protein compared to saline instilled rats ($p=0.003$ and $p=0.015$, respectively). Rats exposed to polymer A or B exhibited a 2.6 and 2.7-fold increase, respectively (Figure 2.2b).

In order to assess cellular infiltration into the alveolar space post-instillation, the total and differential cell counts were determined. Rats instilled with polymer A at all three doses showed a similar increase in free cells counts (4.3, 4.4 and 4.4-fold increase, respectively). Polymer B instilled rats, at the lowest dose, showed little increase in free cells compared to saline instilled rats (1.3-fold), whereas the medium concentration had the largest fold increase (9.2-fold) (Figure 2.2c).

The differential cell counts revealed that in the saline-treated lungs, the PMNs were approximately 3 % (± 2 %). There were considerable increases in the percentage of PMNs after instillation of both polymers (Figure 2.2d). Rats instilled with polymer A, at all doses, showed an increase from 3 % (± 2 %) to 50, 54 and 60% of PMNs when compared with the saline-instilled rats. While

rats instilled with polymer B exhibited an increase from 3 % (± 2 %) to 27 and 65% in PMNs, respectively.

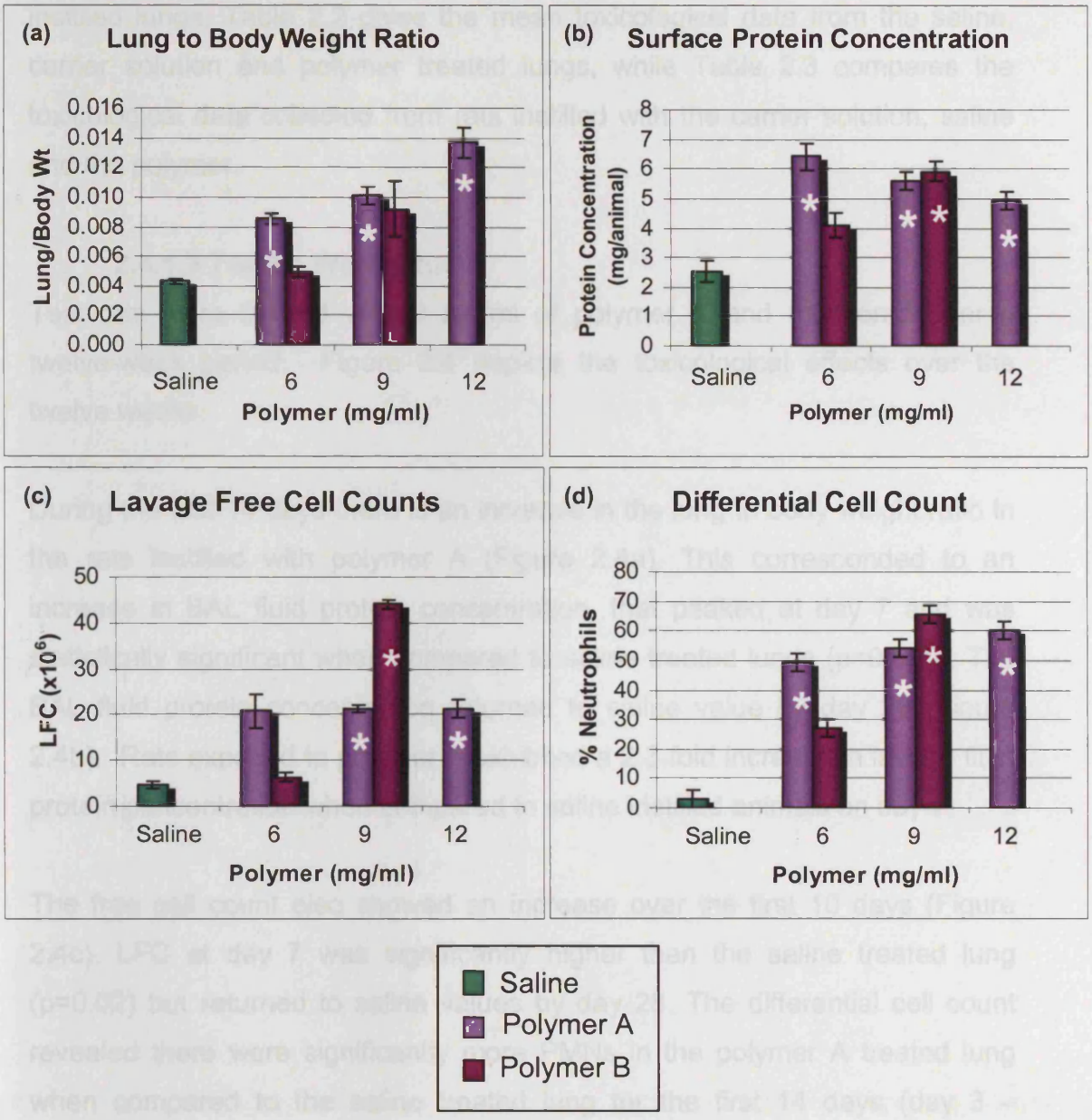

Figure 2.2: The conventional toxicological data collected after 3 days instillation from the preliminary concentration experiment; Lung to body weight ratio (a); surface protein concentration (b); lavage free cell counts (c) and differential cell counts (d) (mean±SEM; * = significantly different from saline instilled rats (Andersson-Darling normality test Student two-sample t-test)) (n=3).

2.4.1.2 Carrier Solution Experiment

The toxicological data were recorded in the same manner as the preliminary concentration experiment (Figure 2.3 a-d). The data collected for the carrier solution instilled lungs showed no significant difference from that of the saline-instilled lungs. Table 2.2 gives the mean toxicological data from the saline, carrier solution and polymer treated lungs, while Table 2.3 compares the toxicological data collected from rats instilled with the carrier solution, saline and the polymer.

2.4.1.3 Twelve Week Study

Test rats were treated with 9 mg/ml of polymer A and monitored over a twelve-week period. Figure 2.4 depicts the toxicological effects over the twelve weeks.

During the first 14 days there is an increase in the lung to body weight ratio in the rats instilled with polymer A (Figure 2.4a). This corresponded to an increase in BAL fluid protein concentration, that peaked at day 7 and was statistically significant when compared to saline treated lungs ($p=0.006$). The BAL fluid protein concentration returned to saline value by day 28 (Figure 2.4b). Rats exposed to polymer A exhibited a 2.3-fold increase in lavage fluid protein concentration when compared to saline instilled animals on day 7.

The free cell count also showed an increase over the first 10 days (Figure 2.4c). LFC at day 7 was significantly higher than the saline treated lung ($p=0.02$) but returned to saline values by day 28. The differential cell count revealed there were significantly more PMNs in the polymer A treated lung when compared to the saline treated lung for the first 14 days (day 3 – $p=9.22\times10^{-4}$, day 7 – $p=0.007$, day 10 – $p=2.56\times10^{-4}$ and day 14 – $p=0.005$). However, values returned to the normal control values by day 28 ($p=0.113$) (Figure 2.4d). There was a significant increase in PMNs at day 42 ($p=2.44\times10^{-4}$) but by day 56 there was no significant difference between the treatment and the saline values ($p=0.102$).

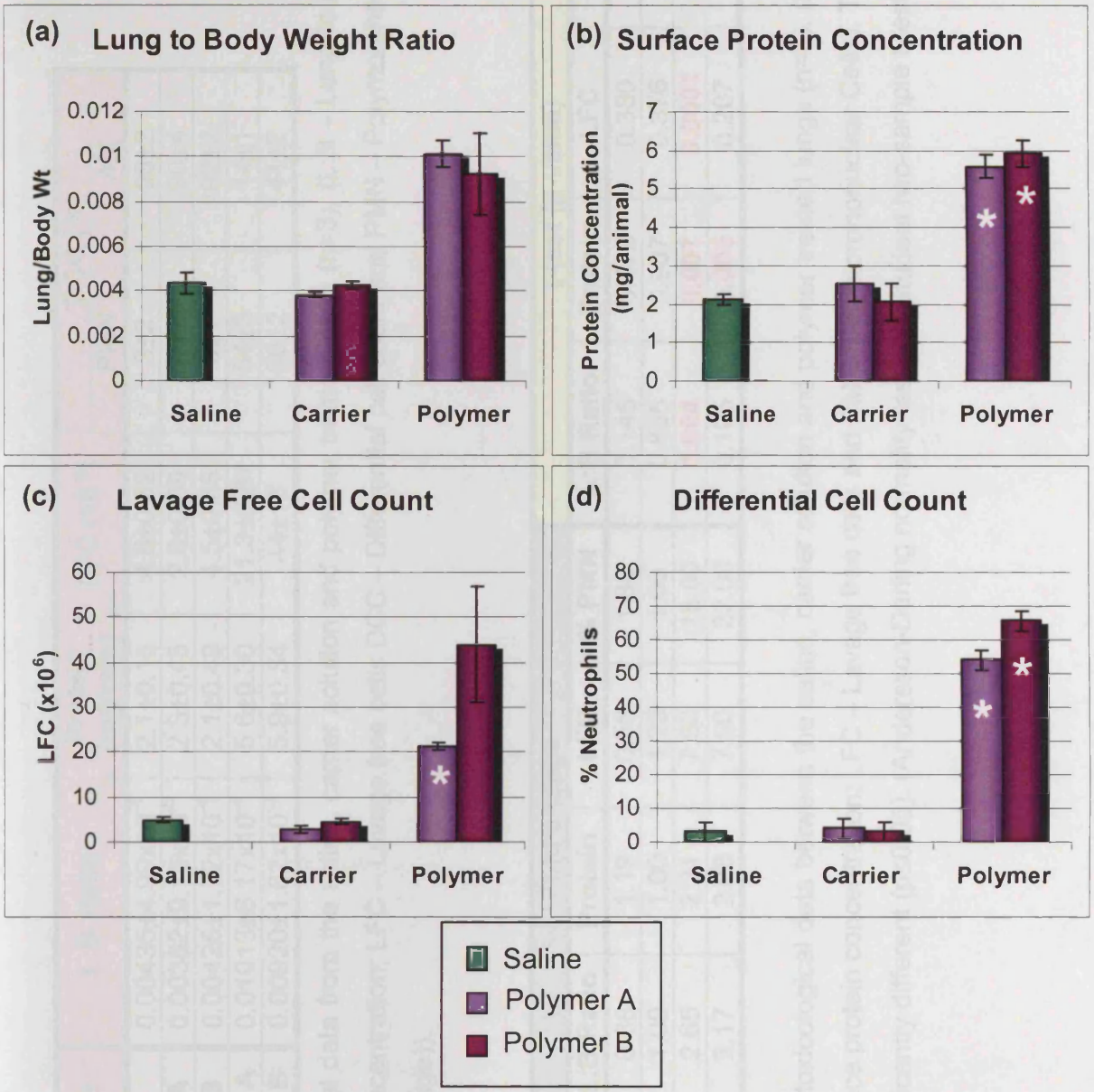

Figure 2.3: The toxicological data collected after 3 days instillation from the carrier solution experiment: Lung to body weight ratio (a); surface protein concentration (b); lavage free cell counts (c) and; differential cell counts (d). (mean±SEM; * = significantly different from saline instilled rats $p \leq 0.05$ (Andersson-Darling normality test and Student two-sample t-test)) (n=3). Polymer concentration 9mg/ml and carrier solution equivalent to 9mg/ml.

Instillate	L:B Ratio	Protein (mg/rats)	LFC (10^{-6})	DCC (%)	
				PMN	AM
Saline	$0.00435\pm4.99\times10^{-4}$	2.1±0.15	4.8±0.62	3±2	98±2
Carrier A	$0.00382\pm9.13\times10^{-5}$	2.5±0.45	2.8±0.69	4±2	90±4
Carrier B	$0.00425\pm1.72\times10^{-4}$	2.1±0.49	4.5±0.68	3±1	92±2
Polymer A	$0.01013\pm6.17\times10^{-4}$	5.6±0.30	21.3±0.87	54±3	44±1
Polymer B	$0.00920\pm1.82\times10^{-3}$	5.9±0.34	44±13	66±2	41±2

Table 2.2: Mean toxicological data from the saline, carrier solution and polymer treated lungs (n=3). (L:B – Lung to body weight; Protein – surface protein concentration; LFC – Lavage free cells DCC – Differential cell count and PMN – Polymorphonuclear cells and AM – Alveolar macrophage)).

	Fold change				t-test (p-value)			
	L:B Ratio	Protein	LFC	% PMN	L:B Ratio	Protein	LFC	% PMN
Saline v Carrier A	0.88	1.19	0.58	1.33	0.145	0.476	0.380	0.422
Saline v Carrier B	1.00	1.00	1.23	1.00	0.835	0.907	0.376	0.686
Polymer A v Carrier A	2.65	2.21	7.50	18.00	**0.004**	**0.007**	**0.0001**	**0.004**
Polymer B v Carrier B	2.17	2.88	7.00	22.00	0.105	**0.005**	0.207	**0.001**

Table 2.3: Comparison of the toxicological data between the saline, carrier solution and polymer treated lungs (n=3). (L:B – Lung to body weight; Protein – surface protein concentration; LFC – Lavage free cells and PMN- Polymorphonuclear Cells). The red text indicates data which are significantly different ($p \leq 0.05$). (Andersson-Darling normality test and Student two-sample t-test).

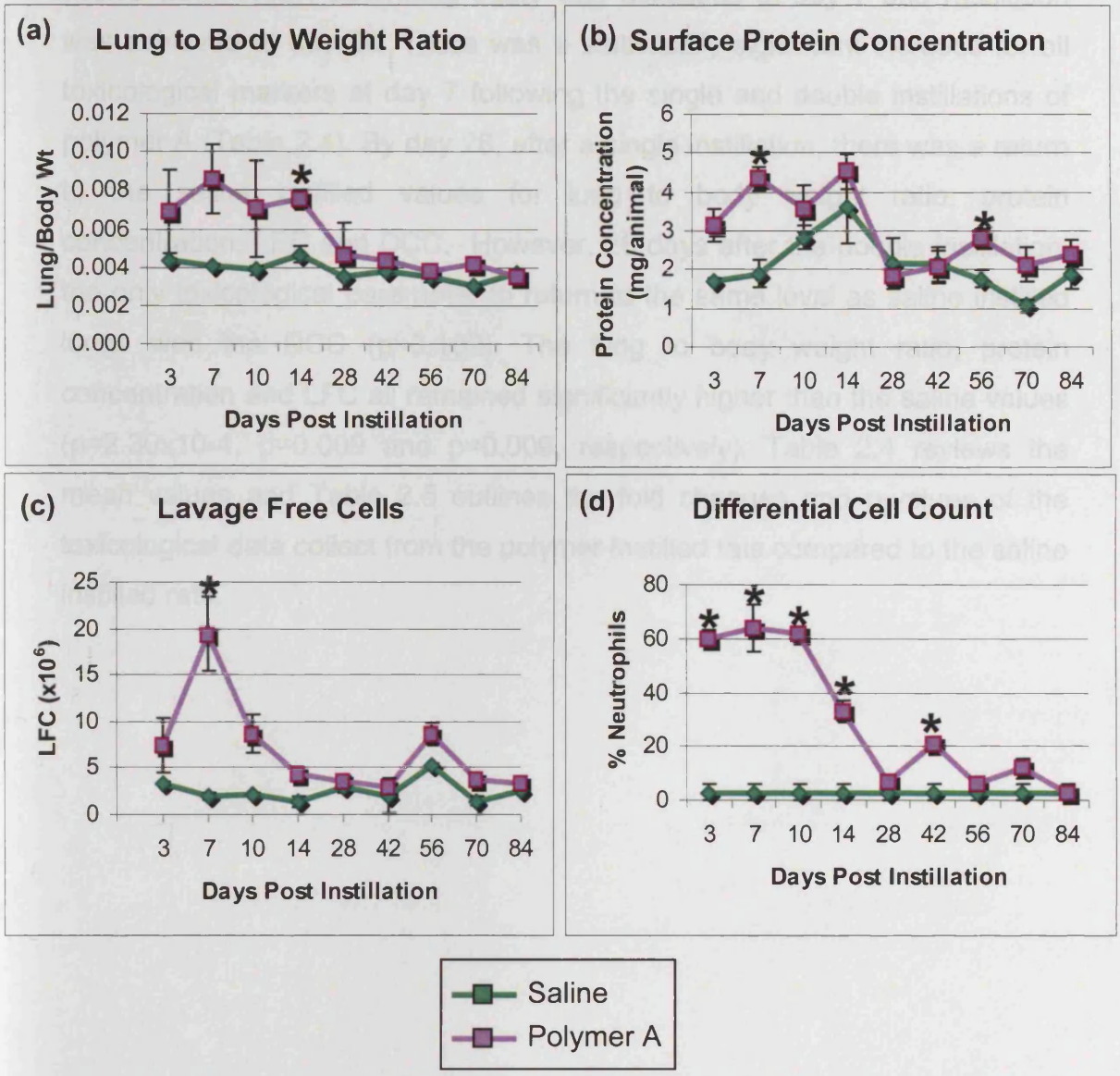

Figure 2.4: Twelve week time point study was used to find the time points for peak oedema and resolution. Animals were instilled with polymer A (9 mg/ml) and compared with saline instilled animals. Lung to body weight (a) and surface protein concentration (b), lavage free cell count (c) and differential cell count (d) (mean±SEM; *= significantly different from saline instilled rats $p \leq 0.05$ (Andersson-Darling normality test and Student two-sample t-test)) (n =3).

2.4.2 SINGLE AND DOUBLE INSTILLATIONS OF POLYMER A

Rats were instilled with either a single or a double dose of polymer A and the toxicological effects were monitored (Figures 2.5a-d and 2.6a-d). From the twelve week study, peak lung injury was assessed at day 7 and resolution was achieved at day 28. There was a statistically significant increase for all toxicological markers at day 7 following the single and double instillations of polymer A (Table 2.4). By day 28, after a single instillation, there was a return to the saline instilled values for lung to body weight ratio, protein concentration, LFC and DCC. However, 28 days after the double instillation, the only toxicological parameter to return to the same level as saline instilled lungs was the DCC ($p=0.102$). The lung to body weight ratio, protein concentration and LFC all remained significantly higher than the saline values ($p=2.30x10\text{-}4$, $p=0.009$ and $p=0.009$, respectively). Table 2.4 reviews the mean values and Table 2.5 outlines the fold changes and p-values of the toxicological data collect from the polymer-instilled rats compared to the saline instilled rats.

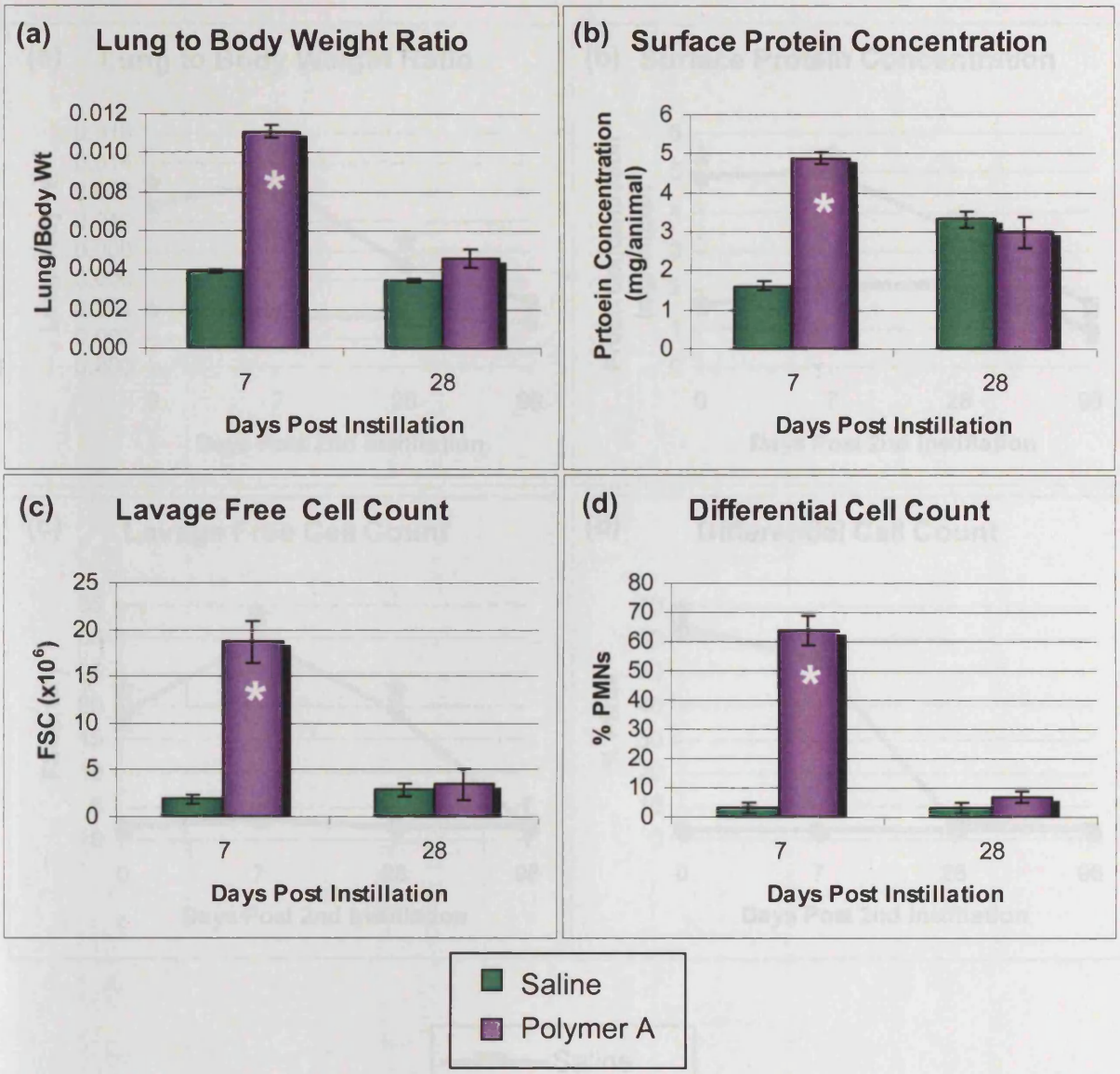

Figure 2.5: Animals were instilled with a single dose of polymer A (9 mg/ml) and compared with saline instilled animals. Lung to body weight (a), surface protein concentration (b), lavage free cell count (c) and differential cell count (d) (mean±SEM, * = significantly different from saline instilled rats p≤ 0.05 (Andersson-Darling normality test and Student two-sample t-test)) (n =6).

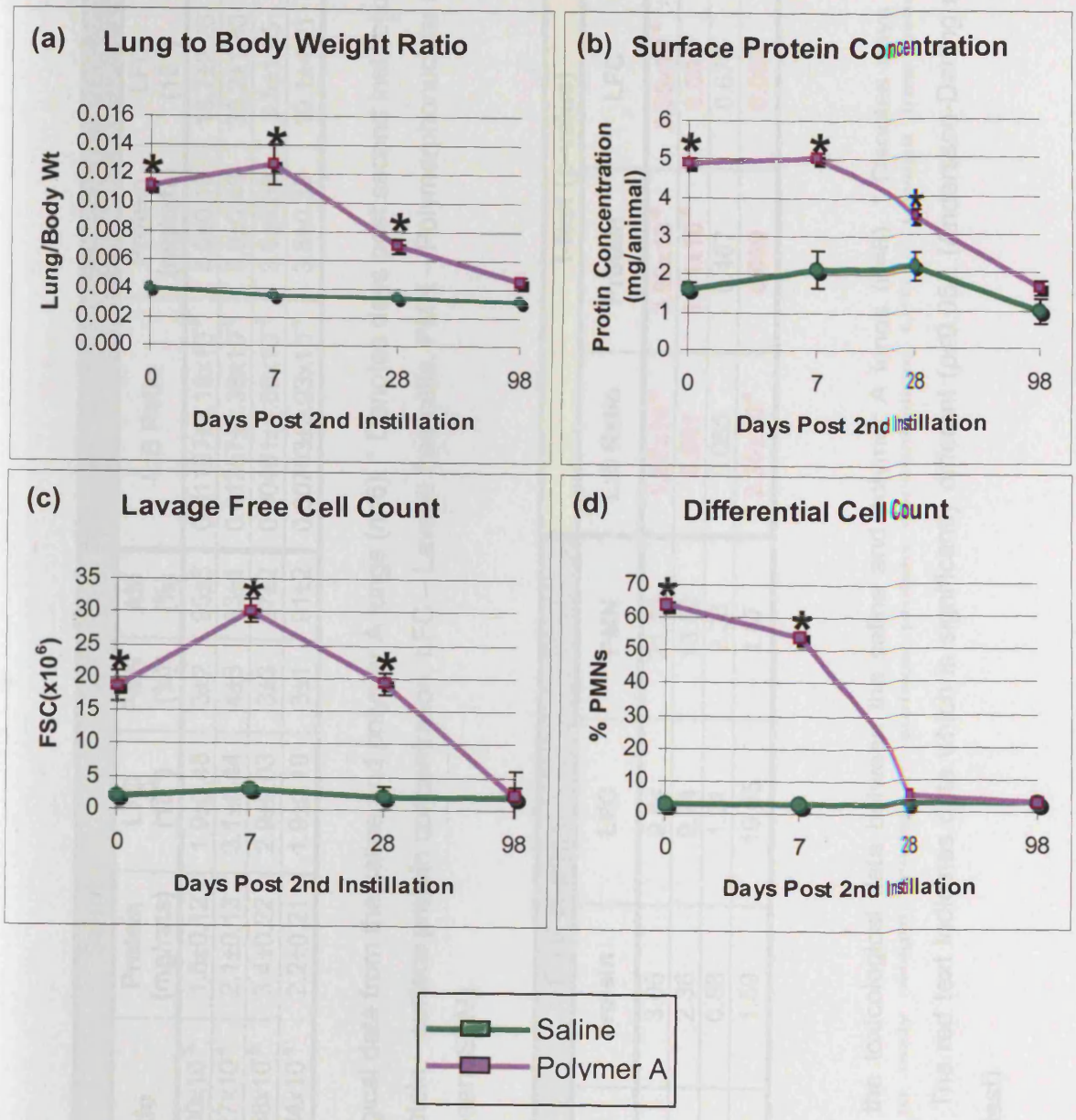

Figure 2.6: Animals were instilled with a double dose of polymer A (9 mg/ml) and compared with saline instilled animals. Lung to body weight (a), surface protein concentration (b), lavage free cell count (c) and differential cell count (d) (mean±SEM, * = significantly different from saline instilled rats $p \leq 0.05$ (Andersson-Darling normality test and Student two-sample t-test)) (n =6). (Day 0 data before second instillation).

Days Post Instillation	Saline					Polymer				
	L:B Ratio	Protein (mg/rats)	LFC (10^{-6})	PMN (%)	AM (%)	L:B Ratio	Protein (mg/rats)	LFC (10^{-6})	PMN (%)	AM (%)
7	$0.00394\pm6.00\times10^{-5}$	1.6±0.12	1.9±0.48	3±2	95±3	$0.01107\pm3.19\times10^{-4}$	4.9±0.16	18.7±2.26	64±3	42±1
14 (*7)	$0.00356\pm1.27\times10^{-4}$	2.1±0.13	3.1±0.44	4±3	93±1	$0.01257\pm1.38\times10^{-3}$	5.0±0.49	30.2±1.80	54±4	50±3
28	$0.00347\pm6.68\times10^{-5}$	3.4±0.22	2.9±0.03	3±3	97±2	$0.00461\pm4.86\times10^{-4}$	3.0±0.39	3.5±1.65	7±3	97±3
35 (*28)	$0.00343\pm4.84\times10^{-5}$	2.2±0.21	1.9±0.19	3±1	91±2	$0.00703\pm3.93\times10^{-4}$	3.5±0.32	19.1±4.21	5±2	96±2

Table 2.4: Mean toxicological data from the saline and polymer A lungs (n=6). * Denotes days post second instillation. (L:B – Lung to body Mean weight; Protein – surface protein concentration; LFC – Lavage free cells, PMN – Polymorphonuclear cells and AM – Alveolar macrophage) (mean±SEM).

Days Post Instillation	Fold change				t-test (p-value)			
	L:B Ratio	Protein	LFC	PMN	L:B Ratio	Protein	LFC	PMN
7	2.81	3.06	9.84	21.33	**1.87×10^{-6}**	**3.99×10^{-8}**	**5.35×10^{-4}**	**0.001**
14 (*7)	3.53	2.38	9.74	13.50	**0.001**	**1.11×10^{-5}**	**0.001**	**2.95×10^{-4}**
28	1.33	0.88	1.21	2.33	0.065	0.467	0.670	**0.009**
35 (*28)	2.05	1.59	10.05	1.67	**2.30×10^{-4}**	**0.009**	**0.009**	0.120

Table 2.5: Comparison of the toxicological data between the saline and polymer A lungs (n=6). * Denotes days post second instillation. (L:B – Lung to body weight; Protein – surface protein concentration; LFC – Lavage free cells and PMN- Polymorphonuclear Cells). The red text indicates data which is significantly different ($p\leq0.05$). (Andersson-Darling normality test and Student two-sample t-test)

2.4.3 COMPARISON BETWEEN THE POLYMER A AND BLEOMYCIN MODEL

At all time points measured, for all toxicological markers of injury, the polymer treated lungs were significantly different ($p \leq 0.05$) from the bleomycin treated lungs (Figure 2.7 a-c and Table 2.6 and 2.7). Lung to body weight and LFC for all time points were significantly higher than in the bleomycin model, although the surface protein concentration was found to be significantly lower. There was a 2.7-fold increase in protein concentration at day 7 following single and double instillation of bleomycin and a 2.3-fold change after 22 days following a double instillation.

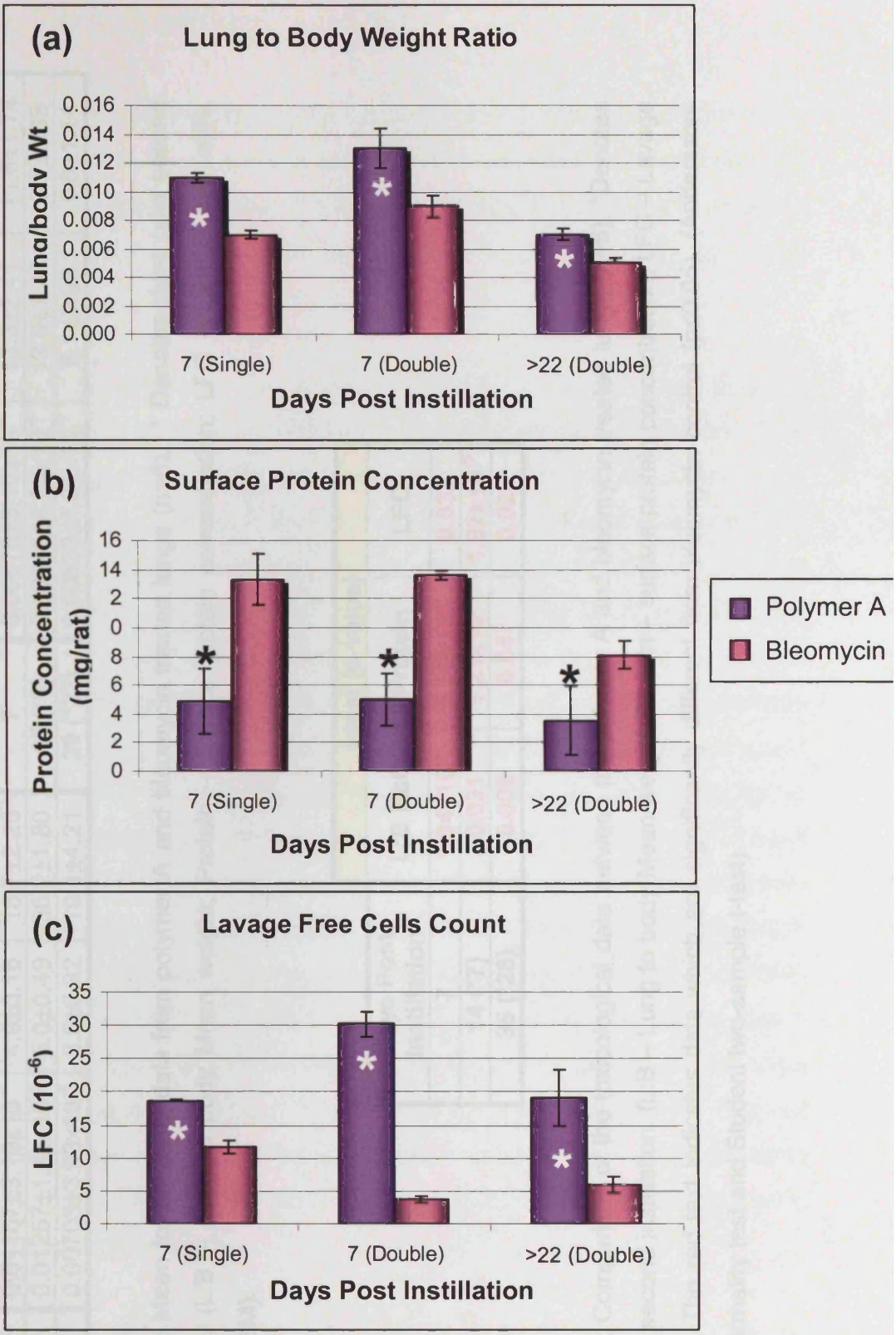

Figure 2.7: Comparison of animals instilled with polymer A (9 mg/ml) versus bleomycin instilled (1 unit) animals. Lung to body weight (a), surface protein concentration (b) and lavage free cell count (c) (* = significantly different from positive control $p \leq 0.05$) (n =6).

	Polymer				Bleomycin		
Days Post Instillation	L:B Ratio	Protein (mg/rats)	LFC (10^{-6})	Days Post Instillation	L:B Ratio	Protein (mg/rats)	LFC (10^{-6})
7	$0.01107\pm3.19\times10^{-4}$	4.9±0.16	18.7±2.26	7	$0.00676\pm3.10\times10^{-4}$	13.3±2.41	11.6±1.74
14 (*7)	$0.01257\pm1.38\times10^{-3}$	5.0±0.49	30.2±1.80	15 (*8)	$0.00845\pm8.29\times10^{-4}$	13.6±1.38	3.7±0.33
35 (*28)	$0.00703\pm3.93\times10^{-4}$	3.5±0.32	19.1±4.21	29 (*22)	$0.00533\pm4.01\times10^{-4}$	8.1±2.96	6.0±1.14

Table 2.6: Mean toxicological data from polymer A and bleomycin treated lungs (n=6). * Denotes days post second instillation. (L:B – Lung to body Mean weight; Protein – surface protein concentration; LFC – Lavage free cells, (mean±SEM).

	t-test (p-value)		
Days Post Instillation	L:B Ratio	Protein	LFC
7	1.94×10^{-6}	3.00×10^{-4}	0.032
14 (*7)	0.031	1.21×10^{-4}	1.97×10^{-5}
35 (*28)	0.009	0.047	0.026

Table 2.7: Comparison of the toxicological data between the polymer A and bleomycin treated lungs (n=6). *Denotes days post second instillation. (L:B – Lung to body Mean weight; Protein – surface protein concentration; LFC – Lavage free cells. The red text indicates data which are significantly different from bleomycin control ($p\leq0.05$). (Andersson-Darling normality test and Student two-sample t-test).

2.5 DISCUSSION

The primary aspect of this study used conventional toxicological approaches to assess lung injury and repair in rats that had been instilled with synthetic particles represented by polymer A or polymer B. The investigation focused on two early biological endpoints in the lungs; inflammation and pulmonary oedema.

There were differences in the toxicological data collected from polymer instilled lungs versus saline instilled lungs. The polymer carrier solutions were shown to be non-toxic after three days at a concentration equivalent to 9 mg/ml of polymer and, as such, the observed toxicological responses could be attributed to exposure to the synthetic particles/polymers under these experimental conditions. However, further polymer carrier solution instillations would have been beneficial at all experimental time points, especially double instillations, to ensure that there was no longer term damage. In the absence of such vehicle control experiments, it is impossible to rule out a contribution of the carrier to the toxicological profile of the polymer at concentrations >9 mg/ml and for experimental periods > 3 days. The carrier solution could have some protective effect on the lung, masking the full toxicity of the polymer. Alternatively at higher doses or over a longer time period the carrier solution itself could become toxic to the lung. Toxicological changes may not have been apparent in the lung at the time point (i.e. 3 days) and concentration (equivalent to 9 mg/ml of polymer) chosen for the carrier control experiments as the peak of injury may have been earlier or this concentration may not have an immediate effect in the lungs. There have been no other experiments carried out, to date using the carrier solution apart from the ones that were undertaken during this study.

Conventional toxicology methods were successfully used to determine the extent of lung injury. The concentration experiment using 6, 9 and 12 mg/ml showed a dose-dependent response. In a recent 13 week study, a total of 7 mg/ml of polymer A was instilled in three doses and used as a positive control (Carthew *et al.,* 2006). There was no evidence of oedema after 13 weeks,

which correlates with the results seen in the 12 week single instillation study. There were, however, inflammatory changes observed by Carthew *et al.* unlike the 12 week single instillation carried out in this study. No further comparisons can be made between these two studies since Carthew and co-workers used a triple instillation and had no data for the earlier time points.

There was a significant increase in the oedema indicators (lung to body weight ratio and protein concentration) following the administration of a single or double dose of polymer A. These both reflect an increase in lung permeability (Bermudez *et al.,* 2002; Housley *et al.,* 2002). Thus, the results suggest mild oedema in both models at day 7. Unlike the single dose model, which returned to normal by day 28, the oedema markers were still significantly elevated 28 days after the double instillation, suggesting oedema was still present.

A peak in LFC at day 7 in the lungs of rats that had been treated with both single and double doses of polymer A, indicated a peak of inflammation in the lungs. The proportion of PMNs in a healthy lung is approximately 3-5%. In order to confirm the extent of inflammation DCC were used to distinguish between the macrophages and the PMNs. An increase in the macrophage population alone indicates mild inflammation while an increase in PMNs is associated with more severe inflammatory response (Prescott, 1998). Thus, the results suggest severe inflammation in both models at day 7. Being highly motile, PMNs quickly congregate at the site of inflammation, attracted by cytokines expressed by activated endothelium, mast cells and macrophages. Due to their high motility and abundance they are normally the first phagocyte a pathogen is likely to encounter. PMNs are active phagocytes, capable of ingesting microorganisms or particles. However, they can only execute one phagocytic event, expending all of their glucose reserves in an extremely vigorous "respiratory burst". (Sendo *et al,.*1996).

By day 28 the cell counts return to baseline value, following a single instillation, implying the resolution of inflammation in the lungs. However, following a double instillation, there were still an elevation in the number of

macrophages that is indicative of mild inflammation, hence although the PMN-driven inflammation had resolved, a degree of inflammation remained. PMNs only survive for 1–2 days at the site of inflammation before undergoing spontaneous apoptosis and are eventually engulfment by macrophages. Unlike short-lived PMNs, macrophages arrive earlier to sites of infection and their life span can ranges from months to years, as opposed to just a few days (Savill *et al.,* 1989). The presence of macrophage at day 28 after a double instillation may be due to them not only engulfing any remain polymer particles but also removing the remaining PMN debris. PMNs antimicrobial products can damage host tissues, therefore one reason for their short life span is limiting the damage to the host during inflammation (Savill *et al.,* 1989). All markers of inflammation had returned to baseline values by 98 days.

BAL fluid collected from lipoproteinosis patients has an opaque and milky appearance. The major constituent is phospholipid but it also comprises of serum proteins and surfactant proteins. The BAL fluid also contains large and foamy AMs and increased numbers of lymphocytes (Hook, 1991; Shah *et al.*, 2000; Trapnell *et al.*, 2003). Over the twelve week study there was no indication of lipoproteinosis (e.g. the BAL fluid was clean) and the toxicological parameters appeared to have returned to normal baseline values. Therefore the damage caused following the instillation of a single dose of polymer A appeared to be reversible.

Polymer B, at 12 mg/ml, proved to be too toxic to the lung resulting in the culling of the animals in that group. Polymer B has a higher molecular weight than polymer A (700 kDa compared to 70 kDa, respectively). This size difference may affect the repair and defence mechanism in the lungs. At lower doses polymer A appears to induce more severe toxicological response than polymer B, suggesting that it causes more damage. Its size may allow it to penetrate the lung faster and more effectively. At the higher dose of polymer B the observed toxicity may be explained by lung overload. The hallmark of the particle-overloaded lungs are an impairment of AM-mediated lung clearance

that eventually leads to accumulation of excessive particles and AMs in the lungs (Cullen *et al.*, 2000).

Studies on rats by previous workers have also indicated that inert particles can induce serious adverse pulmonary effects if inhaled at high concentrations (Oberdörster, 1995). At high particle concentrations, the upper limit of the clearance systems can be reached, possibly leading to lung fibrosis or lung tumours (Ferin, 1994). Particles of ~10 μm in diameter can overload rat AM resulting in no clearance of these particles (Oberdörster *et al.*, 1992). Lymph nodes could also be overloaded, further preventing clearance of the polymer from the lung tissue. This could explain the adverse affects of polymer B, at the highest concentration, as well as some of the toxic effects of polymer A.

Intratracheal instillation is a widely used procedure to deliver materials to the lungs. The reasons for employing it in the present study rather then the more physiological inhalation procedure include its simplicity, its relative low cost and its ability to allow delivery of exact doses. A key difference between instillation and inhalation studies is the dose rate, with intractracheal instillation the administration of the dose is within a few seconds compared to minutes, hours, days or weeks with inhalation studies. The speed of delivery with instillation studies poses a risk of overwhelming the lungs defence systems resulting in effects not seen in inhalation studies (Driscoll *et al.,* 2000). Henderson *et al.* (1995) compared intratracheal instillation with inhalation of quartz and titanium oxide, both classed as poorly soluble particles. The results from the study indicated that the degree of lung inflammation and tissue injury characterised by BAL fluid analysis and histopathology was similar after both methods of exposure.

A bleomycin-induced oedema and inflammation model was used as a positive control comparison to the polymer model. For the three conventional toxicology methods compared (lung to body weight, surface protein concentration and LFC), significant differences were observed. Unfortunately, there was no DCC data available for the bleomycin model, and no distinction

could be made with regard to the type of inflammation, i.e. mild or severe. It is well documented that bleomycin instillation initially induces lung inflammation (Kaminski *et al.*, 2000; Balharry *et al.*, 2005), however, there were significantly more free cells collected in lavage from the polymer model, inferring a more severe form of inflammation at this stage in the injury. Alternatively, the bleomycin peak in inflammation may occur at an earlier time point.

Lung inflammation is followed by oedema and the progressive destruction of normal lung architecture in bleomycin instilled models (Kaminski *et al.*, 2000; Balharry *et al.*, 2005). The significant difference in surface protein suggests the bleomycin model induces a more severe oedema when compared to the polymer model at the time points studied. This is probably due to there being a different mechanism involved. The bleomycin model may have caused a greater degree of alveolar wall damage, therefore, allowing more protein to leak on to the surface of the lung and subsequently be collected in the BAL fluid. Alternatively, the collection of BAL fluid may have been restricted in the polymer model due to the airways collapsing, loss of epithelial elasticity or plugging with mucus/debris; all these responses would render it difficult to lavage.

2.6 CONCLUSION

The instillation of polymer A caused significant alterations in the toxicological data collected from the lungs. It was determined that the polymer was causing the effect not the carrier solution it is suspended in. A distinction, at both the morphological and biochemical levels, between the single and double models was successfully achieved. A single dose of polymer A produced a model for mild oedema/inflammation, whereas the double instillation created a model that was more persistent.

Lung samples from parallel experiments to those reported in this chapter were processed for histological analysis (Chapter 3), before proceeding with proteomic analysis of the BAL fluid (Chapter 4).

CHAPTER 3:

HISTOLOGICAL INVESTIGATION OF POLYMER INDUCED LUNG INJURY

3.1 INTRODUCTION

From the cellular and biochemical investigations (Chapter 2), polymer A was found to be bioreactive in the lungs. The investigations described so far have centred on the use of broncho-alveolar lavage (BAL) fluid. The collection of BAL fluid is a useful technique but drawbacks occur if the airways collapse, there is a loss of epithelial elasticity or plugging occurs with mucus/debris, all of which may result in difficulties with washing the BAL fluid out of the alveoli. Also, BAL fluid provides little morphological information on the cellular or the interstitial changes that may accompany lung damage. Therefore, in order to compliment the BAL fluid studies and to obtain further information on the health status of the lungs following challenge by polymer A, a histopathology study was performed.

In a recent study (Carthew *et al.*, 2006), polymer A was used as a positive control to produce lung damage. Chronic inflammation and granuloma formation were associated with this 13 week polymer instillation study carried out in male rats. Activated and hypertrophic alveolar macrophages (AMs) with foamy cytoplasms were recorded. Some of the AMs were degenerated or necrotic and tended to form aggregates. Focal changes within the interstium were observed and hypertrophy and hyperplasia was evident in the type II cells. Interstitial fibrosis and focal alveolitis was also seen (Carthew *et al.,* 2006). In Chapter 2, it was established that polymer A induced a peak in lung inflammation and oedema 7 days after instillation, as determined by BAL fluid studies. The study conducted by Carthew *et al.* (2006) only investigated these parameters 13 weeks post-instillation, therefore, histological data were required for the time points being investigated in the present study.

The classical bleomycin-induced model of lung injury was used as a positive control to compare with the observations seen with polymer A. Bleomycin has been used to induce pulmonary injury and ultimately fibrosis in rats (Thrall *et al.,* 1979). It initially induces pulmonary oedema and inflammation followed by progressive destruction of normal lung architecture (Shen *et al.,* 1988). The bleomycin model was used as a comparison as it was already an established

model for pulmonary injury to examine genomic changes during inflammation and repair (Balharry *et al.,* 2005).

Damage to the lungs results in a characterised cellular response, regardless of the toxic agent. The typical morphological changes that occur in the respiratory epithelia due to injury can be classified into six discrete steps:

(1) Membrane blebbing of type I pneumocytes
(2) Blebs full of intercellular fluid
(3) Caveolae in type I pneumocytes and endothelial cell
(4) Accumulation of fibrin
(5) Influx of monocytes, polymorphonuclear cells (PMNs) and eosinophils
(6) Disorganised cellular tissue architecture

(Richards and Curtis, 1984; Richards *et al.,* 1991).

Steps 1-4 are the typical changes seen due to an increase in lung permeability and the rapid transfer of plasma and fluid to the alveolar surface, where it accumulates as intra-alveolar oedema or becomes deposited as fibrin. Futhermore, there are clear links between these processes and an increase in size of tracheobronchial lymph nodes (Lee and Richards, 2004). Both particulate matter and cellular debris undergo lymphatic drainage as part of lung clearance processes. Steps 5 and 6 are related to the activation of dying cells releasing inflammatory mediators that cause the recruitment of monocytes, PMNs and eosinophils.

However, if damage is persistent, the lungs may take on a different architectural organisation. At focal points, the normally thin epithelium may become thick due to the introduction of type II pneumocyte hyperplasia. The alveolar spaces may fill up with cellular debris (e.g. cell membrane, plasma products and AMs) and this may result in lipoproteinosis. Fibrosis is the last stage of repair, where the tissue attempts to isolate the damaged area, unfortunately this is irreversible (Richards *et al.,* 1991).

The aims of this study were (1) to investigate the changes in the gross and ultrastructural morphology of the lungs and the lymph nodes from lungs instilled with either a single or double dose of polymer A, thereby validating the generation of an accurate model of polymer-induced lung injury compared to existing data; (2) to compare the pathological profile of polymer-induced lung damage to that of a well-characterised bleomycin model; and (3) to provide comparative histopathological assessment of possible sources of observed toxicology effects reported in Chapter 2.

3.2 MATERIALS AND STOCK SOLUTIONS

3.2.1 MATERIALS

Agar Scientific, Stansted, UK.

200-mesh 3.05mm Copper Grid (G246)

Araldite CY212 (R1040)

Glutaraldehyde (25 %) (R1010)

Osmium Tetroxide (R1015)

Propylene Oxide (R1080)

Reynolds Lead Citrate (R1210)

Sodium Cacodylate (R1102)

Uranyl Acetate (2%) (R1260)

Fisher, UK.

Toluidine Blue (34860-0050)

Harlan, UK.

Male (200-250g) *Wistar* Rats (pathogen free)

Kyowa Hakko (UK) Ltd., Slough, UK.

Bleomycin (12196/0005)

Leica Micro System Imaging Solution Ltd., UK.

Leica Q550IW Image Analysis System

Leica RM2135 Microtome

Leica EG1140 Embedding Centre

Vacuum Tissue Processor

R A Lamb, Sussex, UK.

Aqueous Eosin (1%) (LAMB/100-D)

Sigma-Aldrich, Dorset, UK.

Mayers Hematoxylin (S1275)

Unilever, Bedfordshire, UK.

S2218600 (Polymer A)

3.3 METHOD

3.3.1 PROCESSING LUNG TISSUES FOR LIGHT MICROSCOPY

3.3.1.1 Instillation

Animals were instilled using the same method as described previously in Chapter 2 (Section 2.3.1). Test animals received either a single or double dose of 9 mg of S2218600 (polymer A). Animals instilled with a single dose of polymer A were sacrificed at day 7 or day 28 post-instillation while animals instilled with a double dose were sacrificed at day 7 or day 28 after the second instillation. A double instillation of bleomycin (0.5 units) was used as a positive control for inducing lung injury. Animals were sacrificed at day 7 and day 22 as these were the time points for peak injury and resolution (Balharry, 2005).

3.3.1.2 Lung Tissue and Lymph Nodes

The gross morphology of the whole of the lungs was compared, changes in appearance such as discolouration were noted. Digital images were generated to record the gross morphology of the lymph nodes. Comparative analysis of the size of the lymph nodes from saline and polymer A-instilled animals was performed using the Leica Qwin image analysis (IA) system.

3.3.1.3 Fixing the Lung Tissue

The lungs were excised as detailed in Chapter 2 (Section 2.3.3). The intact lungs were filled with 10% neutral buffered formalin via a syringe and cannula. The inflated lungs were then immersed in 10% neutral buffered formalin at 4°C for 24 hours in preparation for paraffin embedding and sectioning.

Tissue processing, i.e. paraffin embedding, sectioning and staining, was carried out by a histotechnologist, Mr Derek Scarborough, at the School of Biosciences, Cardiff University. A brief overview of these procedures has been outlined below in Sections 3.3.1.4 to 3.3.1.6.

3.3.1.4 Tissue Processing

Once the tissue has been fixed (Section 3.3.1.3), it must be processed into a form in which it can be made into thin microscope sections. This is achieved by embedding tissues in paraffin, that is similar in density to tissue and can be sectioned at anywhere from 3 to 10 microns. The main steps in this process when dealing with wet-fixed tissue are "dehydration", "clearing" and "paraffin infiltration".

Wet-fixed tissues, such as the lung samples from this study, cannot be directly infiltrated with paraffin. The water from the tissues must be removed by "dehydration" via a series of alcohols (e.g. 70% to 95% to 100%). Following dehydration, the next step was "clearing" and consisted of replacement of the dehydrant, i.e. alcohol, with a substance that would be miscible with the paraffin. The common clearing agent was xylene and the tissues were processed through several changes of xylene. The final step in processing was to infiltrate the tissue with molten paraffin wax at 60°C; several changes of wax were used. Tissues were placed in plastic processing cassettes prior to loading on the automatic processing machine. All the above processes were automated using a fully enclosed Vacuum Tissue Processor.

3.3.1.5 Paraffin Embedding

It was important for the tissue to be fully supported by paraffin wax to prevent the tissue shredding during sectioning. This was achieved by placing the "cleared" tissue into a vacuum to remove all air pockets. The lung tissue was then placed into a plastic "embedding mould", and a Leica EG1140 Embedding Centre was used to embed the tissue in warm paraffin wax. After allowing the wax to set (30 minutes on a cold plate), the tissue was removed from the embedding mould and the sample was ready for sectioning.

3.3.1.6 Sectioning

Following tissue processing and paraffin embedding, the lung tissue had to be cut into sections that could be placed on a glass slide for the purpose of LM. Sectioning was achieved using a Leica RM2135 microtome (i.e. a knife with a mechanism for advancing a paraffin block standard distances across it). The

embedded lung tissue samples were placed on ice to ensure uniform sections were obtained. The ice hardens the wax and softens the tissue so the entire sample is of the same consistency for sectioning. The tissue was then cut into 5μm sections via the microtome.

Once the sections were cut, they were floated on a warm water bath (40-50°C) that facilitated the removal of any wrinkles and air bubbles produced during sectioning. The paraffin embedded sections of lung tissue were then collected on to a pre-coated glass microscope slide. The slides used were coated in poly-L-lysine to improve adhesion of sections. The samples were then left to bind to the slides on a hot plate for 15-30 minutes, then in an oven at 37-45°C for a minimum of 24 hours.

3.3.1.7 Haematoxylin and Eosin Stain

To evaluate the lung architecture by LM the tissue sections were stained with Haematoxylin and Eosin (H and E); a routine stain chosen for its ability to stain various cellular components of tissue. Haematoxylin is a basic dye that stains nuclear heterochromatin and cytoplasm rich in ribonucleoprotein blue. Eosin is an acid dye that stains cytoplasm, muscle and connective tissue various shades of pink.

The embedding process must be reversed in order to remove the paraffin wax from the tissue and allow water soluble dyes to penetrate the sections. Therefore, before any staining could be done, the slides were "deparaffinized" by running them through xylene followed by series of graded alcohol (100% to 70%). The dewaxed tissue sections were stained with Mayer's haematoxylin for 1.5 minutes. Sections were washed in running tap water for 5 minutes, and then stained with 1% aqueous eosin for 10 minutes. Following a 20 second wash in running tap water, sections were dehydrated once again (increasing strengths of alcohol and subsequently replaced by xylene).

The stained section on a slide must be covered with a glass coverslip to protect the tissue from being scratched, to provide better optical quality for viewing under the LM and to preserve the tissue section for archival purposes. The stained slides were taken through the reverse process that they went

through from paraffin section to water, i.e. series of graded alcohol to xylene), at which the mountant DPX was placed over the section and the coverslip on top of the mountant. The stained sections were then ready to view by LM.

3.3.1.8 Image Analysis

IA software was used to capture digitised light microscopy (LM) images of saline polymer A and bleomycin-treated (positive control) tissue sections. LM images (x100 magnification) were saved as TIFF files and imported into the Leica Q550IW IA System, for image processing. IA was also used for the quantification of the total area of the nuclei (μm^2) that were recorded to give an indication of nuclei numbers, i.e. larger area would indicator more nuclei. Ten TIFF images were captured of random areas over three lung tissue sections at each time point. These images were then used to quantify the number of cells (nuclei area) using the Qwin analysis software.

3.3.1.9 Statistical Analysis

Statistical analyses included Andersson-Darling normality test, two-sample t-test and non-parametric Mann-Whitney test. A two-sample t-test was chosen as an appropriate test due to the data being derived from two independent random samples. This test was used if the data were normally distributed and the variances were equal within each group. If this was not the case, a non-parametric Mann-Whitney test was used. All analyses were performed in Microsoft Minitab 13. Significance was assumed at $p \leq 0.05$.

3.3.2 PROCESSING LUNG TISSUES FOR TEM

3.3.2.1 Instillation

Animals were instilled using the same method as described previously in Chapter 2 (Section 2.3.1). Test animals received a double dose of 0.5 units of bleomycin in 0.5 ml saline. Animals instilled were sacrificed at days 7 and 21 days after the second instillation.

3.3.2.2 Fixation of Lung Tissue

The lungs were excised as detailed in Chapter 2 (Section 2.3.3). The upper right lobe of the lungs was selected for examination by transmission electron microscopy (TEM), as it is the first lobe of the lungs to be challenged by inhaled xenobiotics. The lobe was tied off from the rest of the lungs and rapidly instilled with cold (4°C) glutaraldehyde (3%) fixative. The lobe was then removed and immersed in more fresh fixative for 1 hour at 4°C. This method of fixation preserves the cellular structure of the tissue by cross-linking proteins via their amine groups. The gluteraldehyde fixative was replaced with phosphate buffer and washed overnight (~12 hours).

Tissue processing, sectioning and staining for TEM was carried out by an electron microscopist, Mr Mike Turner, at the School of Biosciences, Cardiff University. A brief overview of these procedures has been outlined below in Sections 3.3.2.3 to 3.3.2.5.

3.3.2.3 Tissue Processing

Once the tissue has been fixed (Section 3.3.2.2), it must be processed into a form in which it can be made suitable for TEM. This was achieved by embedding the fixed lung tissue in a resin (Araldite), that acts as a support matrix for the lung tissue, permitting ultra thin (e.g. 60 to 90 nm) sections to be cut.

Prior to tissue processing, a piece of fixed lung tissue was cut away from the lobe and cut into 1 mm cubed pieces. The tissue cubes were placed into a squat, glass, sample vial that was used to carry the tissues through the various stages of dehydration, post-fixation and resin infiltration. The sample vials are kept on a rotating wheel inside a fume cupboard.

Post-fixation was carried out by osmicating (1% osmium tetroxide in phosphate buffer) for 60 minutes at 4°C. The tissue was then passed through a series of graded alcohols, (30%-90%: 15 minutes in each, then 2 x 100%: 30 minutes each). Once dehydrated, the lung tissue samples were placed into new sample vials and immersed in propylene oxide for 30 minutes. This was

followed by overnight (~12 hours) rotation in a fume cupboard in a 50/50 mix of propylene oxide and Araldite CY212. During this time the propylene oxide dissipated leaving only the Araldite. The following day the tissue was infiltrated with Araldite for eight hours.

Finally, the tissue samples were embedded in Araldite. This process involved placing one cube of tissue into a plastic/disposable, embedding capsule and topping up the capsule with fresh Araldite. The capsule was then placed into a resin oven and polymerised at 60°C for 48 hours.

3.3.2.4 Sectioning

Following resin polymerisation, the capsule was cut away from the resin/tissue block using a razor blade. Excess resin was trimmed from the blocks until the tissue was exposed. Semi-thin survey sections (2 µm) were taken using a glass knife and mounted onto glass slides, and the tissue stained with toluidine blue; the stain helps to reveal cellular architecture. Appropriate areas for ultra-thin sectioning were identified from the semi-thin sections and the blocks trimmed accordingly. The resin blocks were sectioned to 60-90nm on an LKB 3 Ultramicrotome using a diamond knife. Sections were expanded on a water trough and collected onto clean 200-mesh, 3.05 mm copper grids.

3.3.2.5 Counter Staining

Prior to visualisation of the tissue sections via TEM, heavy metal staining or "counter staining" was required to help resolve the ultrastructure of the lung tissue. Counter staining was achieved by using Reynold's lead citrate and 2% aqueous uranyl acetate. These heavy metal stains are general purpose and not very specific. Uranyl acetate stains membranous structures and structures containing nucleic acids. The lead in lead citrate binds to RNA-containing structures and hydroxyl groups of carbohydrates.

Droplets of each stain were placed in rows on the sterile side of parafilm and the grids were floated section side down on a given drop. Sections were stained for 10 minutes with uranyl acetate, followed by staining with Reynolds

lead citrate for five minutes. Finally, the grids were washed by transferring over 3 drops of filtered de-ionised water. The grids were allowed to air dry at room temperature in filter paper-lined Petri dishes prior to viewing in the TEM.

The sections were imaged using a JEOL 1210 TEM at an acceleration voltage of 80 KeV.

3.4 RESULTS

3.4.1 GROSS MORPHOLOGY OF THE LUNGS

Morphological changes such as lung enlargement and discolouration of the surface of the lungs can provide a subjective indication of inflammation or lipoproteinosis (Lee and Richards, 2004). Saline-instilled lungs showed no morphological changes after a single or double instillation. However, in the polymer A-instilled lungs 7 days post-single and post-double instillation revealed areas of yellow/brown discolouration suggesting possible inflammation of the lungs. By day 28 after a single instillation, the polymer-treated lungs appeared not to be different to the saline-treated lungs, while 28 days after the double instilled lungs, there were still areas of discolouration.

3.4.2 GROSS MORPHOLOGY AND CHANGES IN LYMPH NODES

The thoracic lymph nodes that were excised from sacrificed animal were collected and photographed digitally (Figure 3.1). The sizes of the lymph nodes were measured using an IA system. Lymph nodes collected and sized by IA from the saline-treated animals did not appear to be enlarged at any of the time points used in the study (Figure 3.2). Instillation of polymer A caused the lymph nodes to increase in size, a 2.2-fold increase in lymph node size 7 days after a single instillation and a 2.3-fold increase 7 days after a double instillation was quantified by IA (Figure 3.2). The size of the lymph nodes had returned to approximately control levels (1.2-fold increase) by day 28 suggesting recovery of the inflammatory response (Figure 3.2).

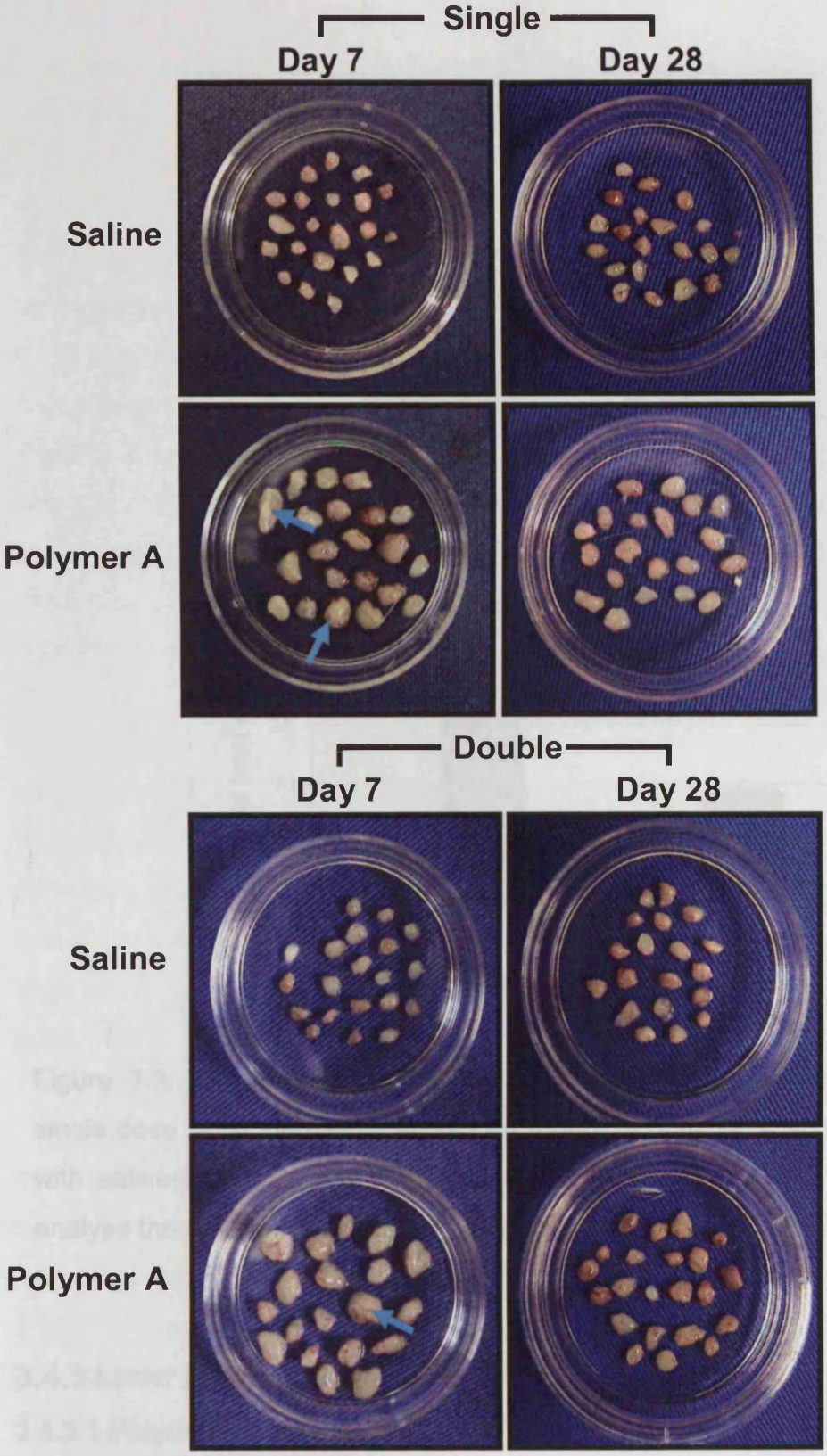

Figure 3.1: Photographs of the lymph nodes after an instillation of either a single or double instillation of saline or 9 mg/ml of polymer A. Blue arrows indicates examples of enlarged lymph nodes. Quantitative analysis of the lymph nodes size was used as an indicator of injury and recovery.

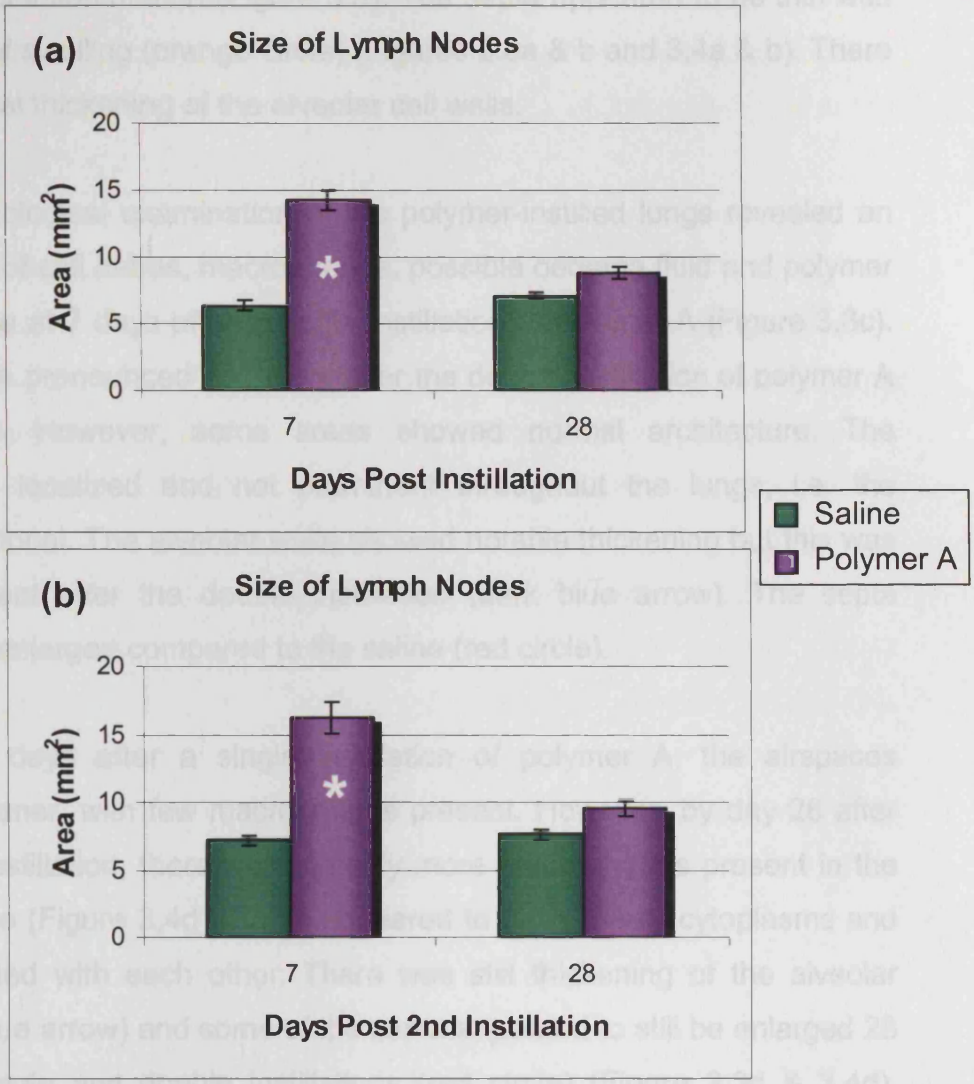

Figure 3.2: The changes in the sizes of lymph nodes collected from a single dose (a) or double dose (b) of 9 mg/ml of polymer A and compared with saline-instilled animals. A two-tailed T-test was used to statistically analyse the data. (mean±SEM, * = significantly different $p \leq 0.05$) (n=6).

3.4.3 LIGHT MICROSCOPY

3.4.3.1 Polymer A Lung Sections

Sections of lungs from saline and polymer A-treated animals were stained with Hematoxylin and Eosin (H & E). At all time points, for both single and double instillations of saline, the lungs exhibited normal architecture with clean alveolar spaces (light green arrow), thin alveolar walls (light blue arrow) and

no evidence of inflammation (Figure 3.3). The septa appeared to be thin with no evidence of swelling (orange circle) (Figures 3.3a & b and 3.4a & b). There was some focal thickening of the alveolar cell walls.

The histopathological examination of the polymer-instilled lungs revealed an accumulation of cell debris, macrophages, possible oedema fluid and polymer in the airspace at 7 days after a single instillation of polymer A (Figure 3.3c). This was more pronounced at 7 days after the double instillation of polymer A (Figure 3.4c). However, some areas showed normal architecture. The damage was localized and not prominent throughout the lungs, i.e. the damage was focal. The alveolar walls showed notable thickening but this was more prominent after the double instillation (dark blue arrow). The septa appear to be enlarged compared to the saline (red circle).

Twenty-eight days after a single instillation of polymer A, the airspaces appeared cleaner, with few macrophages present. However, by day 28 after the second instillation, there were notably more macrophages present in the alveolar space (Figure 3.4d). Some appeared to have foamy cytoplasms and had aggregated with each other. There was still thickening of the alveolar walls (dark blue arrow) and some of the septa appeared to still be enlarged 28 days after single and double instillations (red circle) (Figure 3.3d & 3.4d). There was no histological evidence of PMNs infiltration at any time point.

3.4.3.2 Bleomycin Lung Sections

Bleomycin sections from a double instillation were used to compare with polymer A sections. No pathological alterations were found in the lungs from saline-instilled rats. The saline-instilled lungs appeared to have normal architecture with clean alveolar spaces, thin alveolar walls and normal septa. There was sporadic thickening of the alveolar wall (Figure 3.5a & b).

Seven days following the double instillation of bleomycin, there was some accumulation of cell debris and AMs in the alveolar airspace but no evidence of oedema fluid. There was focalized thickening of the interstitial space (dark blue arrow) and slight enlargement of septa (red circle) (Figure 3.5c).

However, as seen with polymer A instillations, there were areas of the lungs that showed normal architecture. By day 22 the alveolar spaces were clear, septa appeared normal but there was still evidence of interstitial thickening (dark blue arrow) (Figure 3.5d).

3.4.3.3 Quantitative Histopathology

Analysis of the area occupied by nuclei with a given tissue area for polymer A-instilled versus saline controls (Figure 3.6) and bleomycin-treated lungs (Figure 3.7) revealed significant differences. In the saline-treated lungs the area occupied by nuclei was on average 1.1 μm^2. The area occupied by nuclei in the polymer A sections were characterised by a 3.5-fold increase at day 7 and a 2.5-fold increase at day 28 in the single-instillation model and in the double instillation model a 2.1-fold increase at day 7 and a 2.6-fold increase at day 28 compared to the saline control sections. When the bleomycin-treated model was compared with the sections from the polymer A model there was a 2.1-fold increase at day 7 and 3.9-fold increase at day 22 in the area occupied by the nuclei (Figure 3.7).

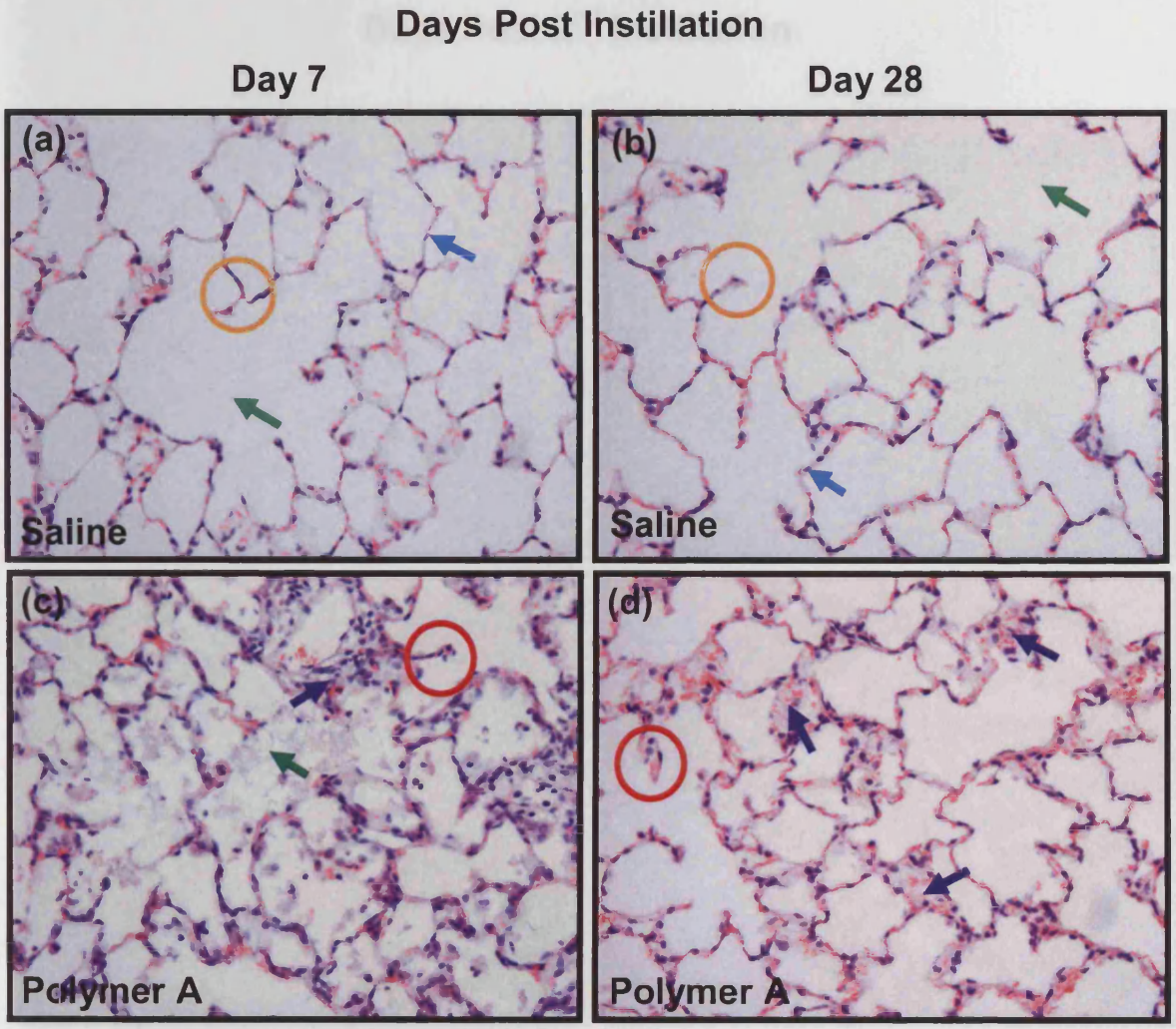

Figure 3.3: Representative LM images of the lungs after a single instillation of either saline or 9 mg/ml polymer A (n=3). Sections have been stained with H&E. Alveoli air spaces indicated with green arrows, interstitial walls indicated with blue arrows and septa are highlighted by circles.

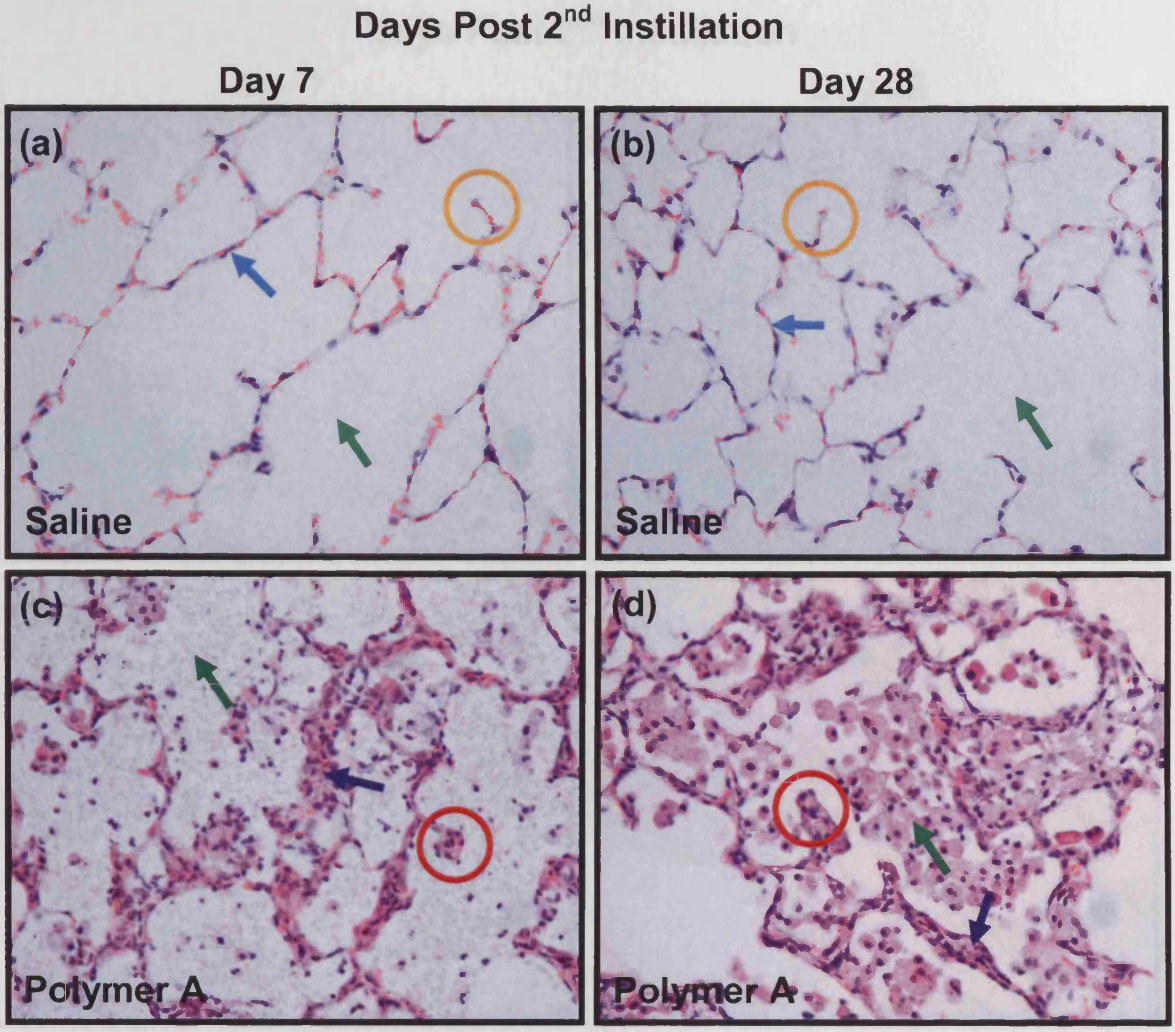

Figure 3.4: Representative LM images of the lungs after a double instillation of either saline or 9 mg/ml of polymer A (n=3). Sections have been stained with H&E. Alveoli air spaces indicated with green arrows, interstitial walls indicated with blue arrows and septa are highlighted by circles.

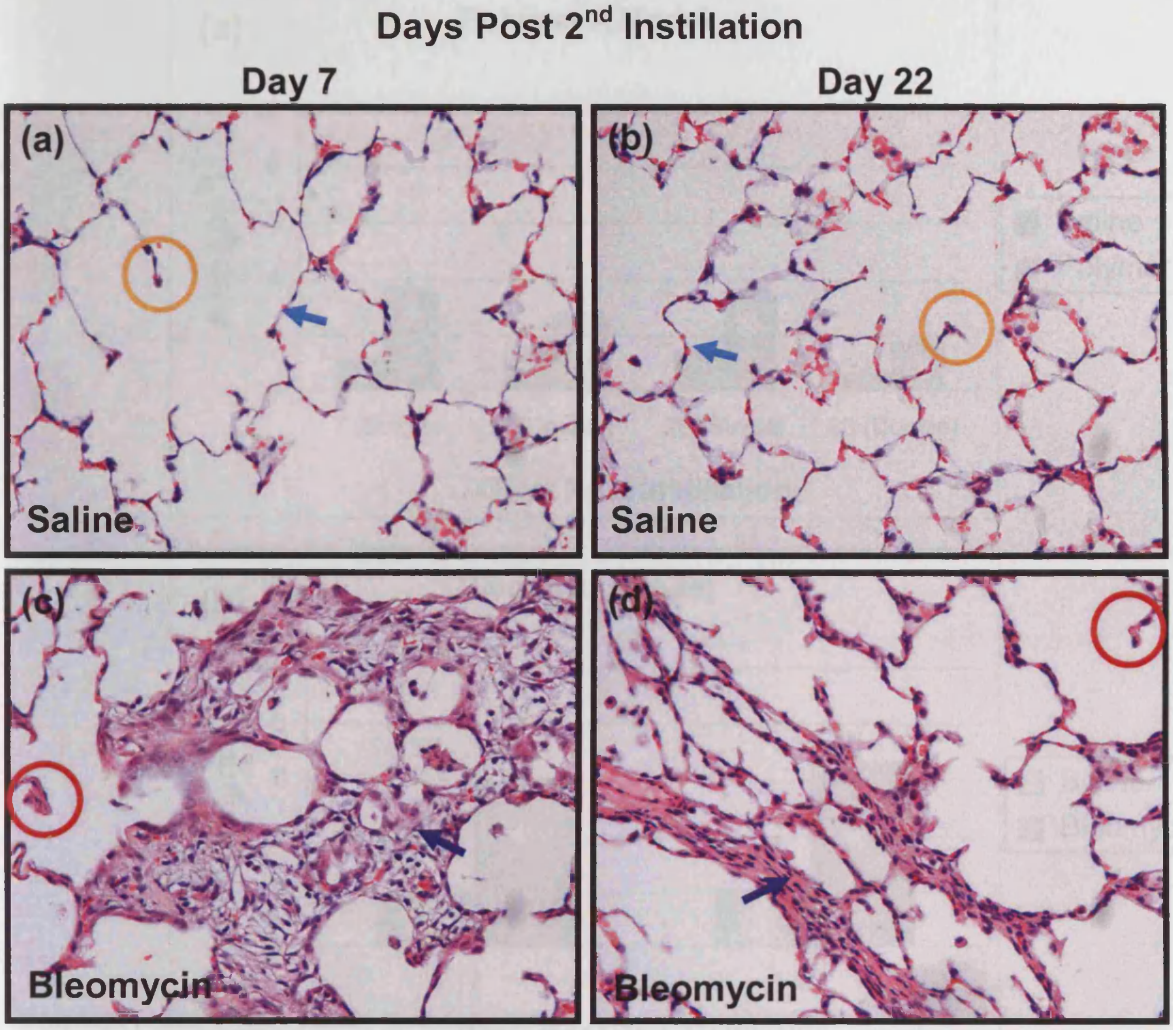

Figure 3.5: Representative LM images of the lungs after a double instillation of either saline or Bleomycin (n=3). Sections have been stained with H&E. Interstitial walls indicated with blue arrows and septa are highlighted by circles.

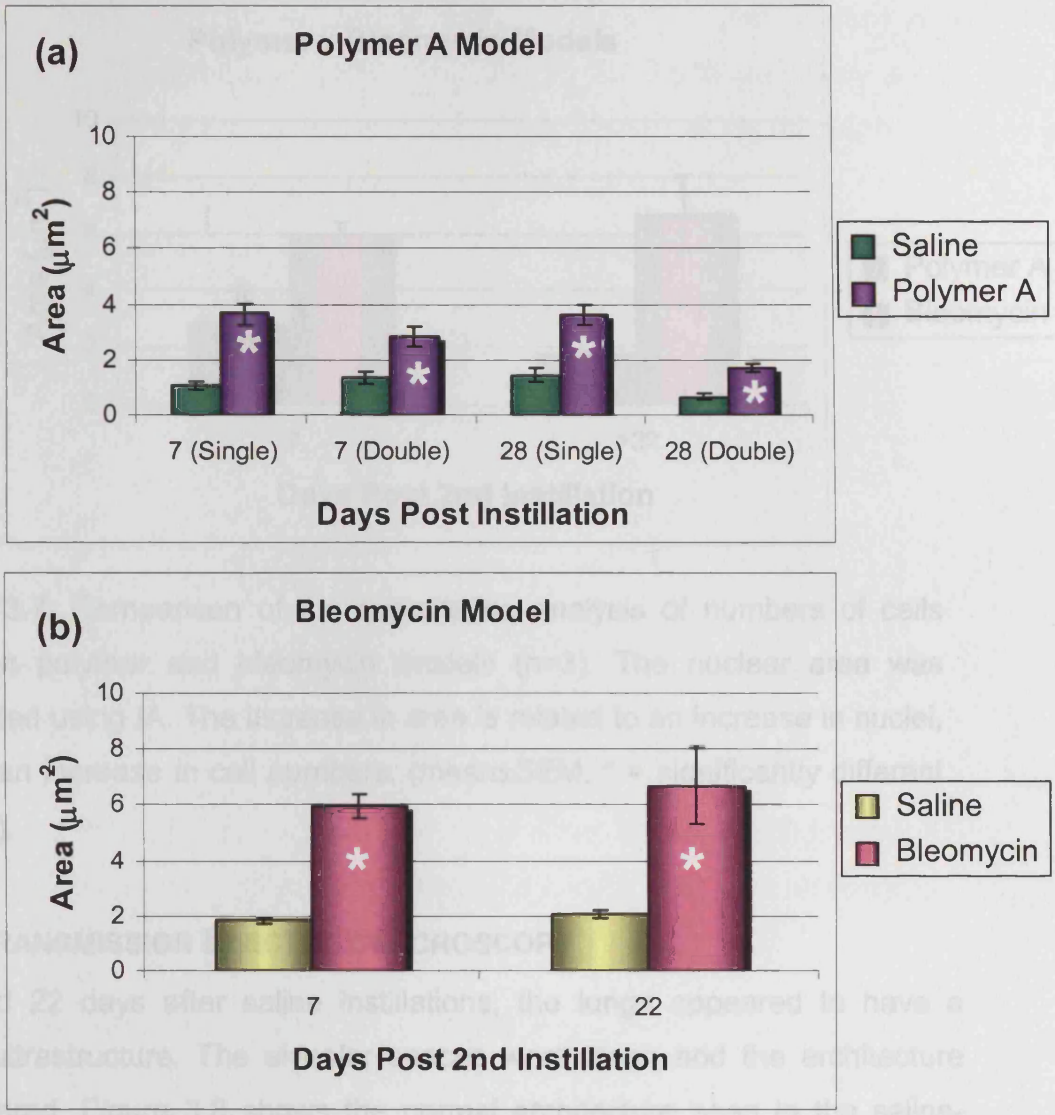

Figure 3.6: Quantitative analysis of numbers of cells. The nuclei area was calculated using an image analysis system and recorded (n=3). The increase in area is related to an increase in nuclei, hence an increase in cell numbers. (mean±SEM, * = significantly different $p \leq 0.05$).

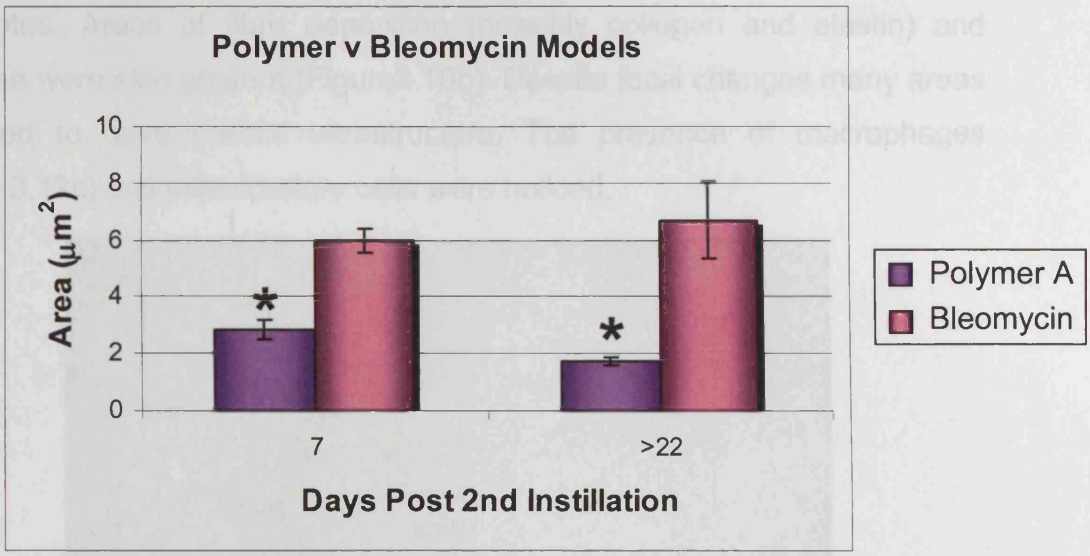

Figure 3.7: Comparison of the quantitative analysis of numbers of cells between polymer and bleomycin models (n=3). The nuclear area was calculated using IA. The increase in area is related to an increase in nuclei, hence an increase in cell numbers. (mean±SEM, * = significantly different $p \leq 0.05$).

3.4.4 TRANSMISSION ELECTRON MICROSCOPY

At 7 and 22 days after saline instillations, the lungs appeared to have a normal ultrastructure. The alveolar spaces were clean and the architecture was ordered. Figure 3.8 shows the normal architecture seen in the saline-instilled lungs. The type I pneumocytes and endothelial cells appeared thin (Figure 3.8 & 3.9a); septa appeared to be undamaged with typical connective tissue fibres present at the edge of the septa. Elastin fibres were visible at the outer edge and an extensive network of collagen fibres (Figure 3.10a). However, occasional blebs and fibres were seen in minor areas at both time points. The type II pneumocytes appeared round and mainly located in the corners of the alveoli (Figure 3.11a). Occasional AMs were seen in the alveolar spaces (Figure 3.12a).

Seven days after the bleomycin-treatment blebbing, and caveolae (Figure 3.9b) were seen and there were focal areas where fibres were deposited. The

septa appeared to be enlarged and widespread thickening of the interstitium was noted. Areas of fibre deposition (possibly collagen and elastin) and caveolae were also present (Figure3.10b). Despite focal changes many areas appeared to have normal ultrastructure. The presence of macrophages (Figure 3.12c) and inflammatory cells were noticed.

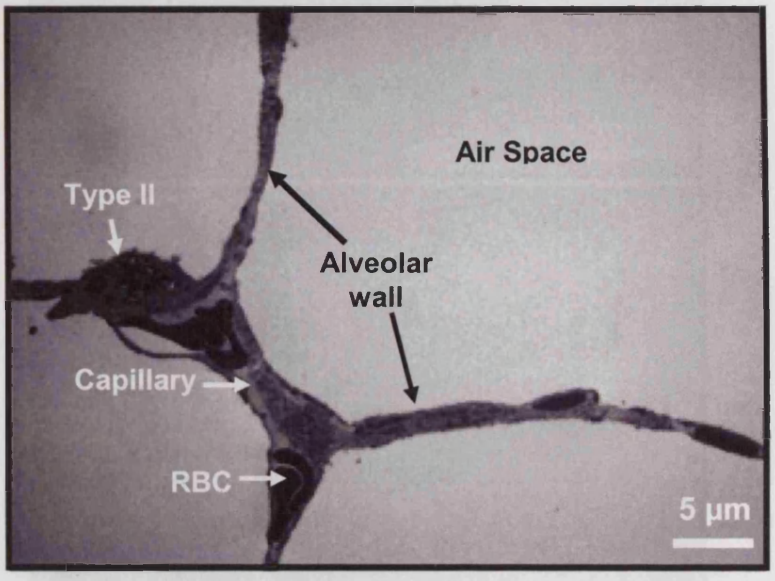

Figure 3.8: Representative TEM images of from saline instilled lungs 7 days after the second instillation, illustrating a normal alveolar unit showing thin alveolar wall and clean airspaces (n=3).

The lungs architecture became disorganised and infiltration of inflammatory cells were seen (Figure 3.9b and 3.13). Type II pneumocytes appeared to be cubodial (Figure 3.11b) and flattened (Figure 3.11c). Some type II cells appeared to have an increase number of lamella bodies in their cytoplasm some of the lamellar bodies appeared to be empty. An increase number of AMs were seen in the airspaces (Figure 3.12b) and foamy macrophages were first observed (Figure 3.12c).

By day 22, there was a reduced sign of lung injury, but there were still large areas of thickening and fibre deposition. Furthermore, there was still debris in the alveolar spaces and foamy macrophages were present.

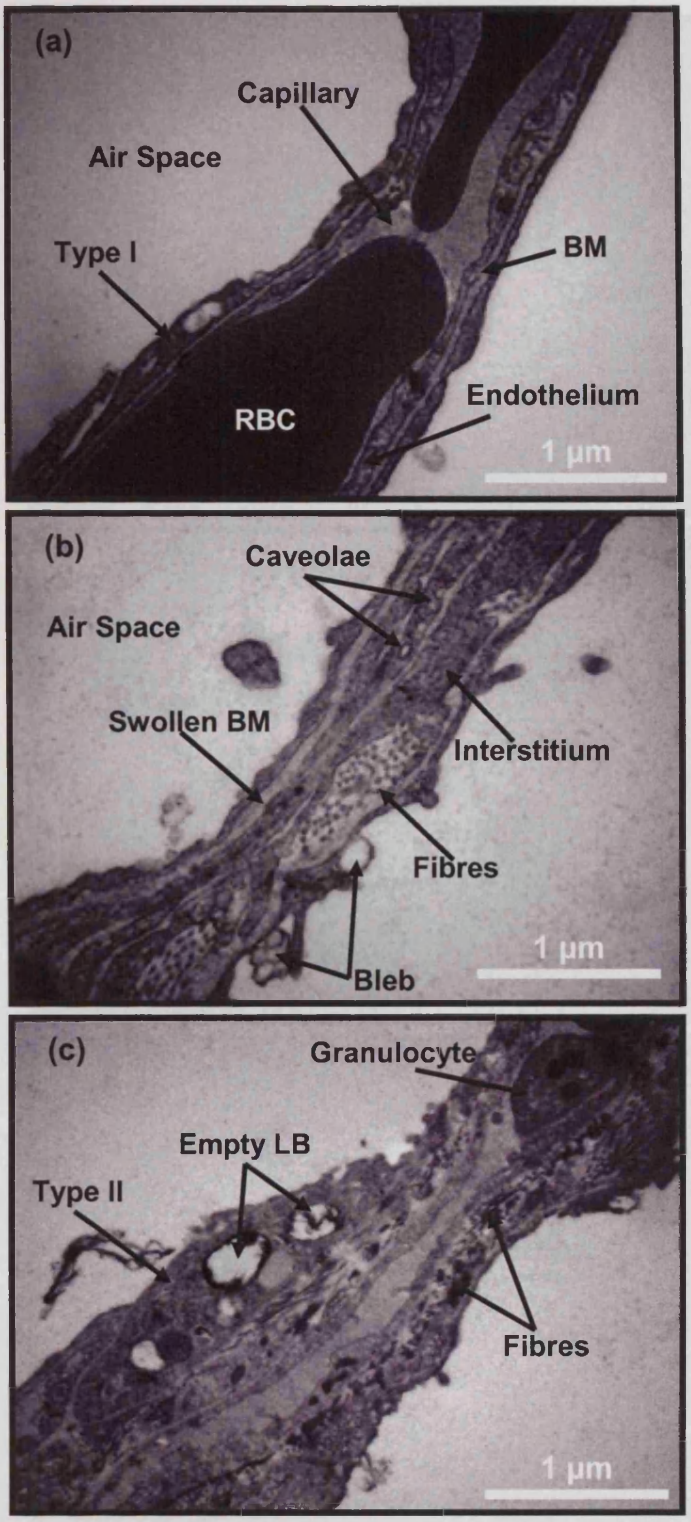

Figure 3.9: Representative TEM images from saline-instilled (normal) (a) and bleomycin-instilled (damaged) (b & c) lungs (n=3). (a) Alveolar wall showing normal lung architecture, thin endothelium and epithelium, (b) alveolar wall 7 days after bleomycin-instillation, shows early signs of damage including thickening of interstitium, blebbing and formation of caveolae, (c) alveolar wall 22 days after bleomycin-instillation, shows signs of severe damage including disorganised architecture, cellular infiltration, flattened type II pneumocytes (type II) with empty lamella bodies (LB) and deposition of fibres. (BM- basement membrane, RBC- red blood cell, type I- type I pneumocytes).

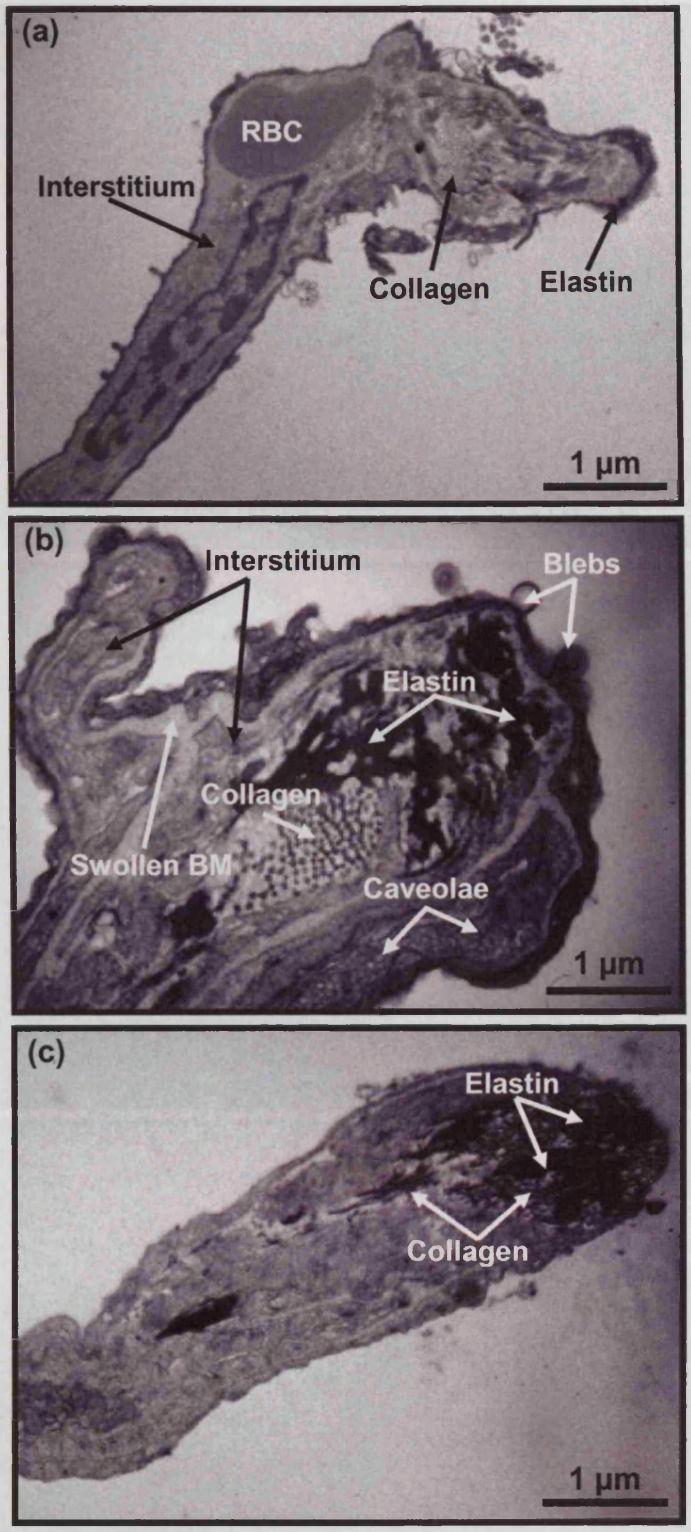

Figure 3.10: Representative TEM images from saline-instilled (normal) (a) and bleomycin-instilled (damaged) (b & c) lungs (n=3). (a) Normal alveolar septa 7 days after saline-instillation, shows normal architecture with connective tissue fibres present at edge of alveolar septa, (b) alveolar septa 7 days after bleomycin-instillation, shows signs of thickening of interstitium, fibre deposition and caveolae and (c) alveolar septa 22 days after bleomycin-instillation, still showing signs of

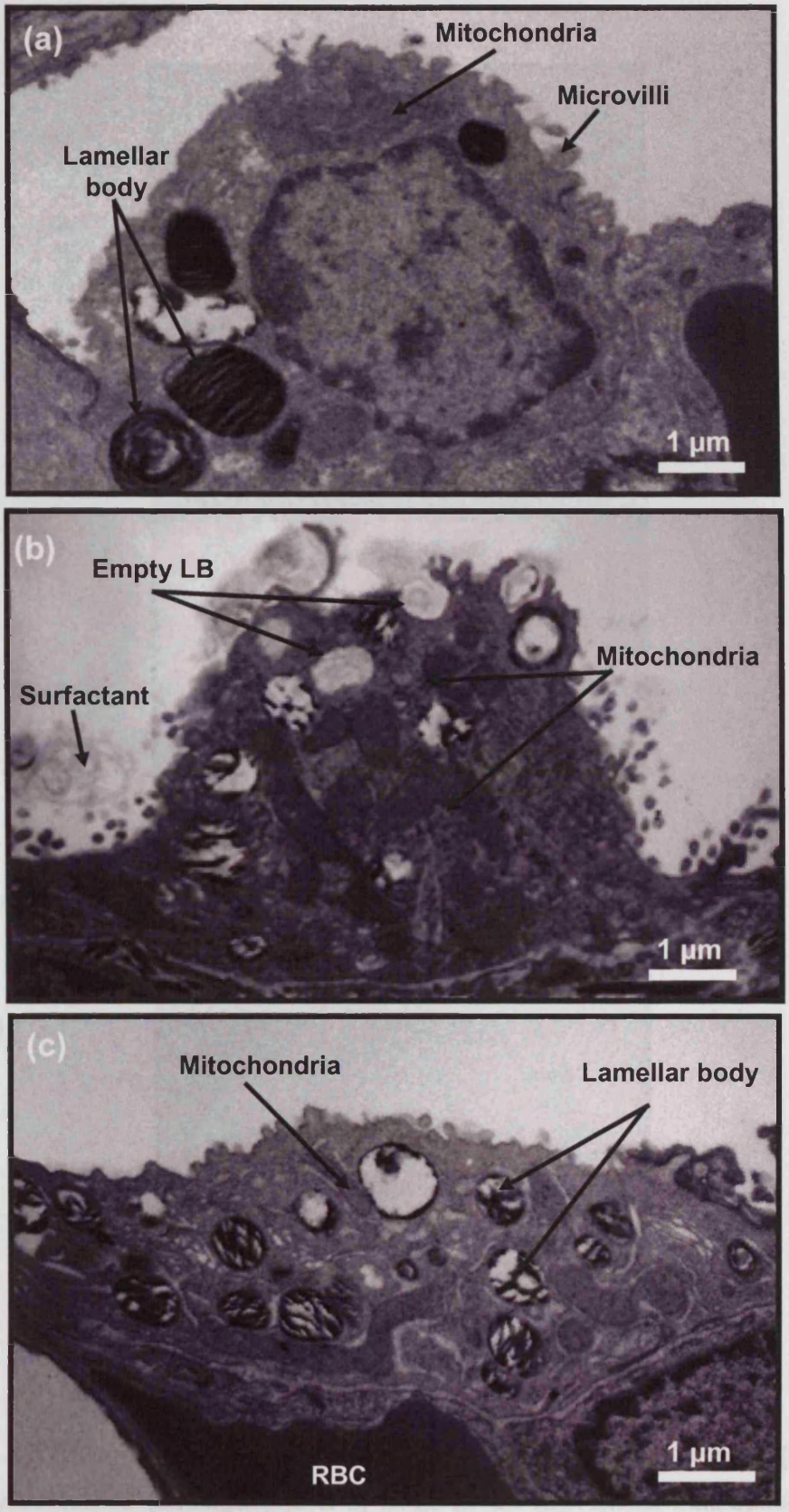

Figure 3.11: Representative TEM images of either normal (saline-instilled) (a) or damaged (bleomycin-instilled) (b & c) lungs (n=3). Images show (a) normal type II cell, (b) cuboidal type II pneumocytes 7 days after bleomycin-instillation and (c) flattened type II pneumocytes 7 days after bleomycin-instillation. (LB – lamellae bodies, RBC- red blood cell).

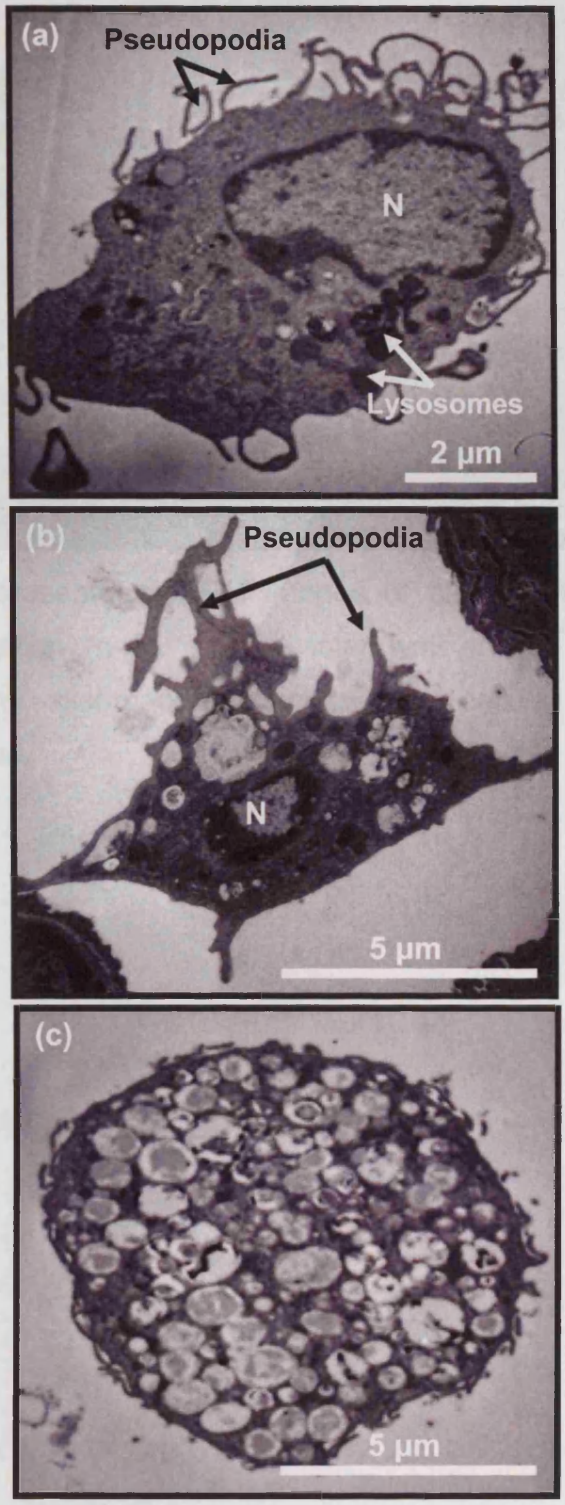

Figure 3.12: Representative TEM images from saline-instilled (normal) (a) and bleomycin-instilled (damaged) (b & c) lungs (n=3). (a) Normal macrophage, (b) activated macrophage 7 days after bleomycin-instillation showing signs of phagocytosed material and (c) foamy macrophage 7 days after bleomycin-

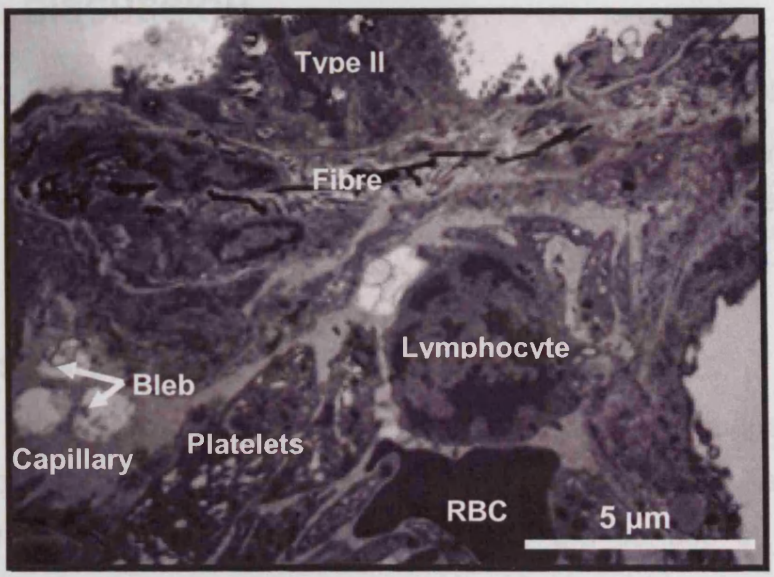

Figure 3.13: Representative TEM images of bleomycin-treated lungs 7 days after instillation (n=3). The alveolar wall shows signs of severe damage including disorganised architecture, cellular infiltration and deposition of fibres.

3.5 DISCUSSION

A histological investigation was performed in order to compliment the toxicological investigations described in Chapter 2. This study provided information on cellular and ultrastructural changes that accompanied the lung damage.

3.5.1 GROSS MORPHOLOGY OF LUNGS AND LYMPH NODES

The gross morphology of the lungs following exposure suggested lung damage induced by inflammation as denoted by the lungs discoloration. However, these observations were restricted to the surface of the lungs. Hence, histological investigations were employed using LM to investigate the underlying cellular and interstitial pathology. Particles instilled into the lungs are translocated by AMs to the thoracic lymph nodes (Adamson and Prieditis 1998, Seaton and Cherrie, 1998) and once deposited, bioreactive particles cause the lymph nodes to enlarge (Lee and Richards, 2004). This could explain some of the enlargement seen in the lymph nodes collected from the polymer-instilled rats.

3.5.2 LIGHT MICROSCOPY

The light microscopy results complemented those previously observed in the toxicology investigations (Chapter 2). Focalised injury and cellular infiltration (e.g. cell membrane, plasma products and AMs) was seen 7 days after a single instillation of polymer A. The injury progressively deteriorated 7 days after a double instillation of the polymer. This subsequent degeneration reflects either inflammatory-mediated damage or direct toxic effect of the polymer on the epithelium cells. Histopathological observations were accompanied and dominated by oedematous fluid in the alveolar space

Twenty eight days after the single instillation there were a few signs of cellular infiltration (AMs and PMNs) and normal lung architecture was present. However, by day 28 after a double polymer instillation, the presence of oedema fluid had diminished but the presence of inflammatory cells (predominantly AMs) persisted in the alveoli; indicating an abatement of

pulmonary inflammation with residual alveolar clearance and repair. The large number of AMs may be due to the presence of residual polymer or cell debris in the airspace that requires clearance. At 28 days post instillation some areas of alveolar cell wall still appeared to be thickened. This is probably due to type II pneumocyte differentiation as a means to replace damaged type I pneumocytes and restore the integrity of the alveolar epithelium.

When comparing the results of the toxicology studies reported in Chapter 2, the histopathological data yield conflicting results. The toxicology data revealed no distinct increase in the levels of protein or free cells after a double dose of polymer A. However, the observed pathological effects suggested that this was not the case. This discrepancy between the toxicology and the histology data could be due to the failure of the lungs to lavage properly before toxicological analysis.

Carthew *et al.* (2006), used polymer A as a positive control in a 13 week instillation study. Chronic inflammation and granuloma formation was associated with the instillation. Focal changes, mainly within the alveolar spaces, were characterised by aggregated AMs with foamy cytoplasms. Changes within the interstitium were seen along with hypertrophic and hyperplasic type II pneumocytes (Carthew *et al.,* 2006). Similarly, aggregated and foamy AMs were observed in the present study, along with interstitial changes; changes in type II pneumocytes could not be characterised. Unlike the present investigation, the Carthew *et al.* study showed no indication of oedema fluid in the alveolar space that was most likely due to the time scale of their study, since any oedematous fluid would have abated by 13- weeks, as it is an early response to lung injury.

An established bleomycin model of drug induced pulmonary oedema and inflammation (Balharry, 2005) was used to compare with the injury caused by polymer A. In a manner similar to the polymer model, substantial changes to the lung architecture following the instillation of bleomycin were observed. There was extensive thickening of the alveolar cell walls and presence of a small amount of debris in the alveolar airspace. Unlike the polymer A model

at day 28, 22 days after the second bleomycin instillation the alveolar airspaces were clean with little evidence of intra-alveolar oedema but there was still extensive thickening of the alveolar wall. Upon comparison between the two models, nuclear area was significantly higher at both time points in the bleomycin model, indicating an increase in the number of cells. This suggests that there could be additional regeneration of the epithelium. At the later time point, the bleomycin lungs still appeared to be different to the saline-treated lungs, which could suggest that the injury may not be reversible. Longer term studies using bleomycin can lead to the development of fibrosis where type II pneumocytes proliferation is followed by abnormal differentiation of the epithelium (Adamson, 1984).

3.5.3 TEM

TEM was used to assess the damage, at the ultrastructural level, caused by instilling bleomycin. There was minimal focal damage observed after the instillation of saline that could be attributed to experimental stress caused by the instillation procedure; the damage is thought to be transient (Brown and White, 1997).

The earliest changes caused by the bleomycin instillations were observed in the type I pneumocytes and endothelial cells. Blebs and caveolae were seen prominently at 7 days but sporadically at 22 days and act as an indicator for damage. Type I pneumocytes are sensitive to toxic agents because of the relatively large surface area and attenuated cytoplasm (Miller and Hook, 1990). Few blebs and caveolae were noted in the saline-instilled lungs, thus their presence in the bleomycin-treated lungs may be due to the toxicity of the bleomycin.

As with the LM results, there was little evidence of intra-alveolar oedema in the bleomycin instilled samples and any occurrence seemed to be sporadic. Previous bleomycin studies have noted interstitial oedema fluid (Adamson, 1984; Aso *et al.*, 1976).

The lungs are a resilient organ and a variety of mechanisms exist to repair any cellular/tissue damage. The TEM investigations revealed various stages of repair were taking place in tissue exposed to bleomycin. The process of repair starts with the replacement of damaged type I pneumocytes. It is commonly believed that type I pneumocytes are incapable of dividing (Weibel, 1974). It is still widely accepted that type II pneumocytes are stem cells of the alveolar epithelium; after normal turnover and lung injury type II pneumocytes will divide and differentiate into type I pneumocytes (type II pneumocyte hyperplasia) (Bingle *et al.*, 1990; Miller and Hook, 1990). The new type II pneumocytes become flattened. The flattened type II cells will then lose lamellar bodies and develop into type I pneumocytes to restore normal architecture (Miller and Hook, 1990). This was clearly seen 7 days after instillation of bleomycin. This suggests that the lungs were attempting to repair the damage cause by the instillation of bleomycin. However, without inclusion of longer time points it is not known whether type II pneumocytes proliferation would have been followed by abnormal differentiation of the epithelium which could possibly lead to fibrosis (Adamson, 1984).

Apart from hyperplasia, type II pneumocytes can also become hypertrophic after exposure to toxic substances. This is characterised by an increase in size and/or number of lamellar bodies located in the cytoplasm of the type II pneumocytes (Miller and Hook, 1990). Bleomycin has been shown to be directly toxic to type II pneumocytes (Karam *et al.*, 1995). Aso *et al.* (1976) reported that hypertrophic type II pneumocytes in rats, which had been given bleomycin, contained an increase in the number of lamellar bodies. In this study, type II pneumocytes had an increase number of lamellar bodies 7 and 22 days after bleomycin-instillation. Several type II pneumocytes appeared to have empty lamellar bodies which could contribute to increase protein level since lamellar bodies store surfactant. Further studies looking at polymer A instilled lungs using TEM would provide additional information relating to the type of damage at the LM level and allow further comparisons to be made with the bleomycin model.

3.6 CONCLUSION

The typical pattern of injury, incurred following bleomycin-treatment is well characterised and was established in the model used in this study. The sequences of events maybe summarised as follows; type I pneumocytes damage; interstitial oedema; inflammatory cell influx; type II pneumocyte hyperplasia and hypertrophy. The main difference seen in the polymer A model was the observation of intra-alveolar oedema instead of interstitial oedema. Without a TEM investigation on polymer-treated sections, there is no evidence of type II pneumocyte hyperplasia and hypertrophy. From comparisons between the two models at LM level bleomycin appears to cause more potent effects in the lungs.

CHAPTER 4

OPTIMISATION OF 2D SDS PAGE FOR BAL FLUID

4.1 INTRODUCTION

The two-dimensional sodium dodecyl sulphate polyacrylamide gel electrophoresis (2D SDS PAGE) technique separates proteins according to charge (isoelectric point (pI)) and size (molecular weight (MW)). Isoelectric focusing is performed in a pH gradient. Due to the amphoteric nature of proteins (i.e. can be either acidic or basic depending on the pH) they become protonated or deprotonated depending on the pH environment. The net charge of a protein is the sum of all the negative and positive charges of the amino acid side chains. Each protein has a pI that is the pH value where the net charge is zero.

Isoelectric focusing is performed by placing a protein mixture on a gel strip that contains an immobilized pH gradient (buffered acrylamide derivatives called 'immobiline' that are co-polymerized within the gel matrix) developed by Bjellqvist *et al.* (1982). These strips are commercially available, and thus, aid reproducibility. When an electric field is applied the proteins start to migrate towards the oppositely charged electrode. When it reaches its pI the protein no longer has a net charge so stops migrating. If the proteins drift away they will gain a net charge and the electric field will cause them to migrate back to their pI and therefore, focusing the proteins.

The second step to this technique involves SDS PAGE, a procedure introduced by Shapiro *et al.* (1959). Before the second dimension the focused proteins are equilibrated with a SDS buffer that transforms them into SDS-protein complexes to initiate unfolding. SDS forms a complex with the proteins in a ratio of approximately 1.4 g SDS/g of protein. The SDS masks the charge of the protein and forms an anionic complex that has a net negative charge proportional to the mass of the protein. Hence, when an electric field is applied, proteins will migrate towards the anode. This separation allows the molecular weight of the proteins to be estimated. The proteins disulfide bonds are also disrupted and this induces further unfolding of molecules. The bonds formed between two adjacent cysteine residues can only be cleaved by a reducing thio reagent such as dithiothreitol (DTT); the reduced cysteine

residues are then protected from reforming the bonds by a subsequent alkylation with iodoacetamide.

Sample preparation is a key stage for good quality results using the 2D SDS PAGE techniques (Rabilloud, 1999; Macri *et al.,* 2000; Molloy, 2000). It is essential that there is no loss or modification of proteins from the sample. In order to avoid this, treatment of the sample should be kept to a minimum, samples should always be kept on ice during any treatment and the sample preparation time should be kept as short as possible (Westermeir and Navan, 2002).

An effective sample preparation procedure will include five critical steps (Fichmann and Westermeier, 1999);

1. **Solubilize proteins** – Chaotropic agents, detergents, reducing agents, buffers and ampholytes are used to solubilize the proteins.

2. **Prevent protein aggregation and loss of solubility during isoelectric focusing** – Urea and thiourea are the most common chaotropic agents. They disrupt hydrogen bonds and prevent unwanted aggregations or formations of secondary structures that affects protein mobility. The detergent, 3[(3-Cholamidopropyl) dimethylammonio]-propanesulfonic acid (CHAPS), is added to disrupt hydrophobic interactions and increase the solubility of proteins at their pI. CHAPS is a zwitterionic detergent and allow proteins to migrate according to their own charge. DTT is the common reducing agent that is used to disrupt disulfide bonds, that is important for analysis of proteins as single subunits (Rabilloud, 1999).

3. **Prevent protein modification** – To prevent protein modification samples have to be kept on ice at all times and repeated thawing must be avoided (Fichmann and Westermeier, 1999).

4. **Remove or digest nucleic acids and other interfering molecules** – Protein precipitation followed by resuspension in sample solution should be employed to remove contaminates such as salts, detergents, nucleic acids and lipids from the sample that would interfere with protein separation (Amersham, 2002).

5. **Prevent artifactual oxidation** – Iodoacetamide is used to prevent reoxidation during the electrophoresis; reoxidation can result in spot streaking and other artefacts. (Amersham, 2002).

Another consideration for the optimisation of 2D SDS PAGE is to determine which system, in this case, Multiphor II or Hoefer Dalt, produce the best separation and most reproducible 2D gels. Finally, there was also a choice of detection methods: (1) Silver stain and, (2) SYPRO Ruby Stain.

Optimisation is an important process, as there is no single method or standard protocol for sample preparation that can be universally applied to all samples analysed by 2D SDS PAGE (Görg *et al.*, 2004). The optimised 2D SDS PAGE technique will be utilised to investigate the proteins in BAL fluid samples collected from the models described in Chapter 2, with the aim of identifying any alterations between saline control and polymer-treated lungs.

4.2 MATERIALS AND STOCK SOLUTIONS

4.2.1 MATERIALS

Amersham Biosciences, Bucks, UK.

2-D Clean-Up Kit (80-6484-51) – Containing Co-precipitant, Precipitant, Washer Additive and Washer Buffer.

3[(3-Cholamidopropyl)dimethlammonio]-propanesulfonic Acid (17-1314-01)

Ammonium Persulfate (APS) (17-1311-01)

Application Piece (80-1129-46)

Bromophenol Blue (17-1329-01)

Dithiothreitol (17-1318-02)

ExcelGel Gradient XL 12-14 (17-1236-01)

ExcelGel SDS Buffer Strips (Cathodic and Anodic) (17-1342-01)

Glycerol (17-1325-01)

HiTrap Blue Column (17-0412-01)

ImageScanner (18-1170-84)

Immobiline™ DryStrip Cover Fluid (17-1335-01)

Immobiline™ DryStrip Gels pH3-10, 18 cm (17-1234-01)

Iodoacetamide (RPN6302)

IPG Buffer pH 3-10 (17-6000-87)

PlusOne™ Silver Staining Kit, Protein (17-1150-01) – Contains EDTA-Na_2, Formaldehyde, Glutaraldehyde, Silver Nitrate, Sodium Acetate, Sodium Carbonate, Sodium Thiosulphate

Protease Inhibitor (80-6501-23)

Sodium Dodecyl Sulfate (SDS) (17-1313-01)

Tetramethylethylene Diamine (TEMED) (17-1312-01)

Thiourea (RPN6301)

Tris Base (Tris(hydroxymethyl)-aminoethane) (17-1321-01)

Urea (17-1319-01)

Bio-Rad, Hertfordshire, UK.

Prestained SDS-PAGE standards (161-0318)

SYPRO Ruby stain (170-3138)

Tris-glycine buffer (2l) (161-0771)

Fisher, Loughborough, UK.

Dialysis Membrane Spectra/Por ® MWCO: 6 000- 8 000 Daltons (BIO-200-030A)

Genomic Solutions, Huntington, UK.

Duracryl Solution (0080-0085)

Investigator™ Silver Stain Kit (0080-0183) – Containing Developer (Sodium Thiosulfate, Potassium Carbonate), Fixative Solution 1, Fixative solution 2 (Potassium Tetrathionate, Sodium Acetate), Formaldehyde, Glutaraldehyde, Silver Nitrate Solution (Silver nitrate), Stop Solution (Tris).

Millipore, USA.

Microcon Centrifugal Filter Device YM-50 (42423)

Sigma, UK.

Agarose (A-9539)

Sodium Phosphate (342483)

Sodium Chloride (S-3014)

Tris-Hydrochloride (HCl) (T-3038)

4.2.2 STOCK SOLUTIONS

Dalt Gels (Amersham Biosciences, Bucks, UK).

Displacing Solution	-	Tris-HCl (pH8.8, 25 % w/v)
		Glycerol (50 % w/v)
		Bromophenol Blue
		Deionised Water (25 % w/v)
Acrylamide Solution	-	Duracyl
		SDS (10 %)
		APS (10 %)

TEMED (10 %)
Deionised Water

Sealing Solution - Tris-Glycine Buffer
Agarose

Equilibration (Amersham, UK).

SDS Equilibration Buffer - Tris-HCl (50 mM, pH 8.8)
Urea (6 M)
Glycerol (30 % w/v)
SDS (2 % w/v)
Bromophenol Blue

HiTrap Blue Columns (Amersham, UK).

Binding Buffer (pH 7) - Sodium Phosphate Buffer (20 mM)
Elusion Buffer (pH 7) - Sodium Phosphate (20 mM)
NaCl (2 M)

PlusOne™ Silver Staining Kit, Protein (Silver staining for Multiphor Gels) (Amersham, UK).

Fixative Solution - Ethanol (40 %)
Acetic Acid (10 %)
Deionised Water

Sensitising Solution - Ethanol (30 %)
Sodium Acetate (6.8 %)
Sodium Thiosulphate (0.2 %)
Glutardialdehyde (0.125 %)
Deionised Water

Silver Nitrate Solution - Silver Nitrate (0.25 %)
Formaldehyde (0.015 %)
Deionised Water

Developer Solution	-	Sodium Carbonate (2.5 %)
		Formaldehyde (0.0074 %)
		Deionised Water
Stop Solution	-	EDTA-Na_2 (1.46 %)
		Deionised Water

Sample Preparation.

Rehydration Solution	-	Urea (8 M)
		CHAPS (2 % w/v)
		IPG Buffer (2 %)
		Bromophenol Blue
		DTT (7 mg/2.5ml) prior to use
Protein Lysis Solution	-	Urea (8 M)
		Thiourea (1 M)
		CHAPS (4 % w/v)
		Tris Base (40 mM)
		DTT (50 mM)
		IPG Buffer pH3-10
		Protease Inhibitor

Silver Staining Solutions (Investigator Kit) (Genomic Solutions, UK).

Fixative Solution 1	-	Ethanol (40 %)
		Acetic Acid (10 %)
		Deionised Water
Fixative solution 2	-	Ethanol (30 %)
		Potassium Tetrathionate (8 mM)
		Sodium Acetate (829 mM)
		Glutaraldehyde (0.5 %)
		Deionised Water
Silver Nitrate Solution	-	Silver nitrate (11.7 mM)

Formaldehyde (0.009 %)
Deionised Water

Developer Solution - Sodium Thiosulfate (63 mM)
Potassium Carbonate (0.2 M)
Formaldehyde (0.005 %)
Deionised Water

Stop Solution - Tris (0.4 M)
Acetic Acid (2 %)
Deionised Water

SYPRO Ruby Staining Solutions

SYPRO Fixative Solution - Methanol (40 %)
Acetic Acid (1 %)

SYPRO Wash Solution - Methanol (10 %)
Acetic Acid (6 %)

4.3 METHODS

4.3.1 SAMPLE PREPARATION

4.3.1.1 Dialysis and Freeze Drying

BAL fluid has a high salt content due to the NaCl vehicle solution used to lavage the lungs. Salt interferes with the isoelectric focusing step of the electrophoretic process by accumulating at both ends of the DryStrip gels. This results in streaking on the gel because the proteins in these areas cannot focus properly.

BAL fluid samples (10 ml) were placed in pre-soaked dialysis bags that were then placed in beakers containing 5 litres of distilled water. The beakers were placed on mixers in a cold room for 24 hours. The water was changed every hour for the first 8 hours. Following dialysis, samples were frozen before being placed in the freeze drier for 24 hours or until dry. Dried samples could then be rehydrated to the desired concentration using lysis solution.

4.3.1.2 Albumin Removal– HiTrap Blue Column

HiTrap Blue columns were used for the removal of albumin from BAL samples. Albumin was removed from samples, as it is the most abundant protein present and could possibly mask minor proteins. HiTrap Blue columns were washed out and equilibrated with binding buffer (5-10 column volumes). BAL samples were then centrifuged for 5 minutes (7,500 x *g*) before they were applied to the column (0.5-1 ml/min). The column was then washed with binding buffer (5-10 column volumes) until no effluent material appeared and then eluted with elution buffer (5-10 column volumes).

4.3.1.3 2D Clean Up Kit

Precipitant solution (300 µl) (2D Clean Up Kit, Amersham Biosciences, UK) was added to an eppendorf tube with the reconstituted BAL fluid sample (100 µl) (Section 4.3.1.1), mixed by vortexing before being incubated on ice (15 minutes). Co-precipitant (300 µl) was then added, mixed by vortexing and the mixture centrifuged for 5 minutes (12,000 x *g*). The supernatant was removed

with a pipette and the pellet was then incubated on ice (5 minutes) with co-precipitant (40 µl), before being centrifuged for 5 minutes (12,000 x *g*). The wash was then removed with a pipette and discarded. The pellet was partially dispersed in distilled (25 µl) water by vortexing before the wash buffer (1 ml) and the wash additive (5 µl) were added and then the pellet was fully dispersed. The sample was incubated (-20°C, 30 minutes, vortexed 20 seconds every 10 minutes) before being centrifuged for 5 minutes (12,000 x *g*). The supernatant was then discarded and the pellet was allowed to dry before being resuspended in rehydration solution.

4.3.1.4 Acetone Precipitation

Ice cold acetone (2 ml) was added into an eppendorf tube with reconstituted BAL sample (500 µl) and the proteins were allowed to precipitate (-20°C, 2 hours). The sample was then centrifuged (13,000 x *g*, 10 minutes). The acetone was decanted off and discarded. The pellet was dried in air (5 minutes) before it was resuspended in rehydration solution.

4.3.1.5 Pre-fractionation

Due to the complexity of the 2D gel profile pre-fractionation was employed to reduce the numbers of proteins on each gel. The Microcon^{TM} sample reservoir was inserted into the vial. Reconstituted BAL fluid sample (500 µl) (Section 4.3.1.1) was pipetted on to the sample reservoir. The assembly was centrifuged (13,000 x *g*, 12 minutes). The filtrate in the vial was collected for separation and contained proteins below the 50 kDa molecular weight limit. The sample reservoir was placed upside down in new vial and centrifuged (1000 x *g*, 3 minutes). The retentate was stored for separation and contained protein with molecular weight above 50 kDa.

4.3.1.6 Protein Concentration – The Bradford Assay

The concentration of protein in the BAL samples was determined using the Bradford Assay (Chapter 2; Section 2.3.6).

4.3.2 FIRST DIMENSION– ISOELECTRIC FOCUSING

4.3.2.1 Sample loading

Prepared BAL fluid samples were either loaded at the rehydration step – in-gel rehydration (Section 4.3.2.2) or during isoelectic focusing – sample cup loading (Section 4.3.2.3).

4.3.2.2 Immobiline™ DryStrip Gel Rehydration

The rehydration solution (350 µl), that contained the prepared BAL fluid sample (in-gel rehydration), was pipetted into the slots within the reswelling cassette (Section 4.2.3). The protective covers were removed from the DryStrip Gels (Section 4.2.3). The DryStrip gels were placed gel side down into the slots of the reswelling cassettes and were covered with Immobiline™ DryStrip Cover Fluid to minimise evaporation of the rehydration solution and subsequent urea crystallisation. DryStrip gels were rehydrated overnight at room temperature. Following rehydration they could be stored at –80°C for up to 4 weeks (See Appendix 1 for diagrammatic depiction of this process).

4.3.2.3 Isoelectric Focusing

The Immobiline™ DryStrip Kit was set up on the Multiphor™ II Electrophoresis Unit and was filled with Immobiline™ DryStrip Cover Fluid. Isoelectric focusing (IEF) electrode strips (11 cm) were soaked in distilled water (0.5 ml) and excess water was removed. DryStrip Gels were rinsed with deionised water and drained on filter paper briefly before being transferred to the DryStrip aligner in the Immobiline DryStrip tray. The moistened IEF electrode strips were placed across the cathodic and anodic ends of the DryStrip gels, partially touching the gel. The electrodes were then aligned and fitted over the electrode strips. Sample cups were fitted and Immobiline™ DryStrip Cover Fluid was poured into the tray to completely cover the strips. The appropriate samples were loaded into the cups. The temperature of the MultiTemp III Thermostatic circulator was set at 20°C and the DryStrip gels were run (Phase 1: 500 V, 2 mA, 5 W, 1 minutes; Phase 2: 3500 V, 2 mA, 5 W, 1hours 30 minutes; Phase 3 3500 V, 2 mA, 5 W, 5 hours 20 minutes).

Following isoelectric focusing, the DryStrip gels could be stored at –80°C for up to 4 weeks (See Appendix 2 for diagrammatic depiction of this process).

4.3.3 SECOND DIMENSION– SDS-PAGE ELECTROPHORESIS

4.3.3.1 Multiphor II System (Flatbed system)

The DryStrip gels were first equilibrated in DTT and SDS equilibration buffers (10 ml, 15 minutes) and followed by iodoacetamide and SDS equilibration buffers (10 ml, 15 minutes). The MultiTemp III Thermostatic circulator was set at 15°C. The Multiphor™ II precast gel was placed onto the Multiphor™ II Electrophoresis Unit with Immobiline™ DryStrip Cover Fluid between them, thus ensuring there were no air bubbles. The cathodic and anodic buffer strips were placed on the gel and partially covering it. The DryStrip gel was placed face down on the gel parallel to the cathodic buffer strip and application pieces were placed under both ends. A third application strip was used to load the molecular weight markers (5 µl). The IEF holder was placed onto the electrophoresis unit and run in two steps (Phase 1: 1000 V, 40 mA, 40 W, 45 minutes; Phase 2: 1000 V, 40 mA, 40 W 2 hours 40 minutes). After Phase 1, the IPG gel and application pieces were removed and replaced by the cathodic buffer strip (See Appendix 3 for diagrammatic depiction of this process).

4.3.3.2 Hoefer Dalt System (Vertical system)

The Dalt casting chamber was cleaned with water and wiped dried and placed on a level surface. Glass beads were placed into the feeding channel and then the caster was filled with the appropriate number of separators, blocks and glass cassettes. Acrylamide gel solution was added slowly (~750 ml) to prevent the introduction of bubbles, and then followed by displacing solution (50 ml). The gel was immediately overlaid with water (~1 ml/gel) to prevent evaporation. The 12 gels were allowed to set for an hour (See Appendix 4 for diagrammatic depiction of this process).

The gel tank was filled with Tris-glycine buffer (2 L) and water (5 L) 2 hours before the start of the electrophoresis run and the water bath was then set to 10°C and Dalt pump turned on. The DryStrip gels were equilibrated firstly in

SDS equilibration buffer with DTT (10 mg/10 ml, 15 minutes) and secondly in SDS equilibration buffer with iodoacetamide (25 mg/10 ml, 15 minutes). The DryStrip Gels were then placed into the glass cassette to ensure that the gel surfaces touched without any air bubbles being introduced. Molecular weight markers (8 µl) were applied to an application piece. Agarose sealing solution was then applied to the application piece before it was placed on the gel. This solution was also used to cover the DryStrip gel and allowed to solidify (5 minutes). The gel cassettes were loaded into the gel tank and run overnight (100 V) (See Appendix 5 for diagrammatic depiction of this process).

The new DALT*six* systems allow precast gels to be used. This improves the reproducibility between gels.

4.3.4 STAINING

4.3.4.1 Silver Staining Multiphor II Gels

PlusOne™ Silver Staining Kit was used to stain the precast gels. A typical gel was stained as follows. A gel was placed in a staining tray on a shaker with fixing solution (30 minutes). The fixing solution was decanted off and replaced by sensitizing solution (30 minutes). The sensitizing solution was decanted off and the gel was washed three times in distilled water. The silver solution was added (20 minutes) and then removed prior to the gel being washed three times in distilled water. The developer solution was then added (5 minutes; preliminary experiments showed 5 minutes was the optimum staining time), removed and replaced with stop solution (10 minutes). The stop solution was removed and the gel was washed three times with distilled water. A preserving solution was added before the gels were imaged using the Amersham ImageScanner.

4.3.4.2 Silver Staining for Dalt Gels

Investigator™ Silver Staining Kit was used to stain the Dalt gels. The gels were typical stained as follows. Gels were carefully removed from the glass cassettes prior to being exposed to Fixative 1 solution (1 hour) before being placed in Fixative 2 solution overnight (~ 12 hours). Gels were then washed in deionised water six times before being placed in a silver nitrate solution (45

minutes). Each gel was washed individually in deionised water before being placed separately in the Developer solution (9 minutes). The gels were then placed in Stop solution (10 minutes) and then imaged using the Amersham ImageScanner.

4.3.4.3 SYPRO Staining of Proteins for Dalt Gels

Gels were carefully removed from the glass cassettes before being placed in SYPRO fixative solution (1 hour). They were then placed in the SYPRO Ruby stain overnight (~12 hours) and then washed once in SYPRO wash solution (1 hour). Gels were visualised using a Typhoon 8600.

4.4 RESULTS

4.4.1 PRELIMINARY GELS

The preliminary optimization experiments for BAL fluid revealed two inherent problems, (1) salt interference with protein separation and (2) generation of adequate protein concentrations to visualise spots on gels. When unprepared BAL fluid sample was focused during the first step of the technique, there was interference observed by the bromophenol blue band stopping and not migrating to the anode. This suggested that there was too much salt in the sample. Hence, the first stage of the optimisation process required the removal of the salt from the BAL samples, this was achieved by dialysis. A molecular weight cut off of 6,000 – 8,000 Da was used to insure minimal loss of protein. A Bradford assay on the sample before and after dialysis showed minimal loss of protein. Dialysed samples showed improved isoelectric focusing. The separation by SDS-PAGE and visualisation using silver stain produced a gel that had few spots; this indicated low protein concentration in the sample. Therefore the dialysis step was followed by the freeze drying of the BAL fluid in order to concentrate the lavage proteins. After freeze drying, the proteins needed to be reconstituted in lysis solution. The differences in protein concentration before and after freeze drying are shown in Table 4.1.

Sample	Before Freeze Drying (mg/ml)	After Freeze Drying (mg/ml)
Saline Day 7	$0.060 \pm 2.89 \times 10^{3}$	0.366±0.058
Polymer Day 7	0.270±0.012	0.433±0.091

Table 4.1: Example of protein concentration of BAL fluid before and after freeze drying (n=3).

Following dialysis and reconstitution of BAL fluid samples there were substantially more spots visualised on the gels. Figures 4.1 (a - d) and 4.2 (a & b) demonstrate 2D gels that have undergone dialysis and freeze drying steps. The next stage was to determine the optimal concentrations of BAL

proteins required for loading. A number of 2D gels were run using different concentration of proteins (20, 50, 75 and 100 µg) (Figure 4.1). Two dimensional (2D) gels with 20 µg of protein (Figure 4.1a) showed very few spots, while gels with 75 and 100 µg showed significantly more spots but some proteins were overloaded, as denoted by the black smear (Figure 4.1c and d). Gels loaded with 50 µg of protein showed more spots than 20 µg gel, but there was still a notable decrease in the number of spots compared to the 75 and 100 µg. The gels run on both the Multiphor II and the Hoefer Dalt system exhibited poor spot separation with horizontal and vertical streaking. Therefore, further sample preparation steps were required to improve spot clarity and to reduce streaking on the 2D gels.

During the preliminary experiments the two loading techniques, in-gel rehydration and sample cup loading were compared. Problems occurred such as leaking of sample and cover fluid with sample cup loading. Therefore, in-gel rehydration was the preferred method for loading.

The preliminary experiment also allowed the reproducibility of the 2D gels to be investigated. The BAL fluid sample loaded on the four concentration gels were from the same animal (Figure 4.1).

4.4.2 2D CLEAN-UP KIT VERSES ACETONE PRECIPITATION

In order to improve protein spot clarity and reduce/remove spot streaking, the Amersham '2D Clean-Up Kit' and acetone precipitation was employed. These two techniques were first tested on BAL fluid from healthy rat lungs (i.e. not treated with saline or polymer). The resulting 2D gels are shown in Figure 4.2. The samples were run on both the Multiphor II and the Hoefer Dalt systems and silver staining was used to visualise any spots. The 2D gels optimised using the Amersham 2D Clean-Up kit produced cleaner gels (Figure 4.2e & f), with less interference and considerably more spots when compared to acetone precipitated samples (Figure 4.2c & d) and the control samples (Figure 4.2a & b).

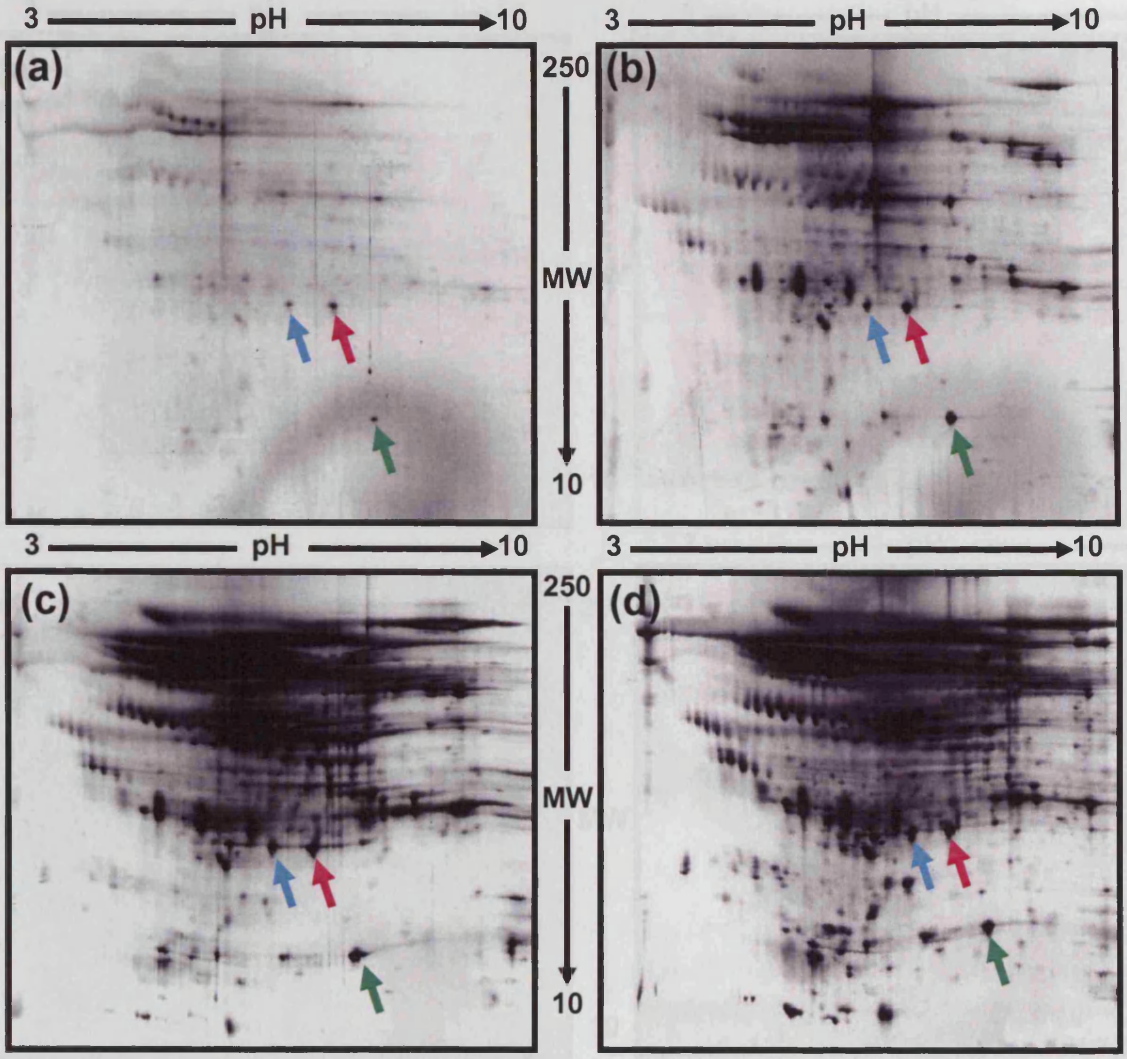

Figure 4.1: Representative 2D gels run on the Multiphor II system (n=4). The gels were loaded with (a) 20 µg, (b) 50 µg, (c) 75 µg and, 100 µg (d) of BAL fluid protein. All samples were desalted and freeze dried. Spots were detected on the 2D gels with silver stain. Examples of the same spots detected between the 2D gels are highlighted by colour-coordinated arrows.

4.4.3 MULTIPHOR SYSTEM VERSES HOEFER DALT SYSTEM

Initially there were two systems available for producing 2D gels (1) the Multiphor II system and (2) the Hoefer Dalt system. The same sample was run on each system to compare differences in the gels (Figure 4.2). Considerably more spots were visualised on the gels run on the Multiphor II system.

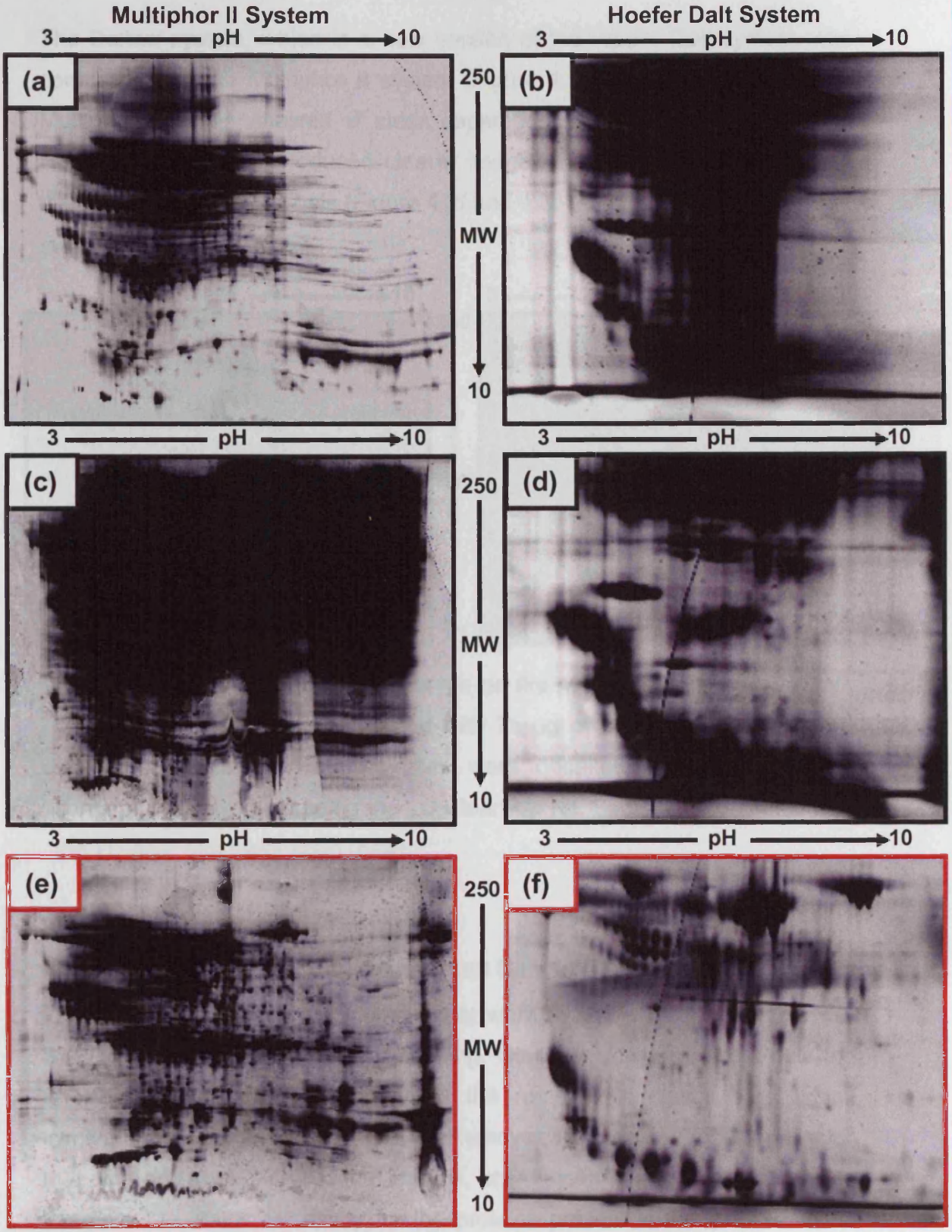

Figure 4.2: Representative 2D gels run using both the Multiphor II and the Hoefer Dalt systems (n=4). G was loaded with 100 µg of BAL fluid protein. All samples were desalted and freeze dried. Spots detect with silver stain. Samples loaded on gels a & b went through no further treatment. The remaining samp underwent acetone precipitation (c & d) and clean up kit (e & f). The red box highlight the optimial gels.

The Dalt*six* system, which is a new version of the Hoefer Dalt system, was compared with the Multiphor II system (Figure 4.3). The 2D gel run on the Multiphor II again showed a clear separation with more spots detected. However, the Dalt*six* produced clearer images that were more reproducible than the Hoefer Dalt 2D gels (Figure 4.2f and 4.3b).

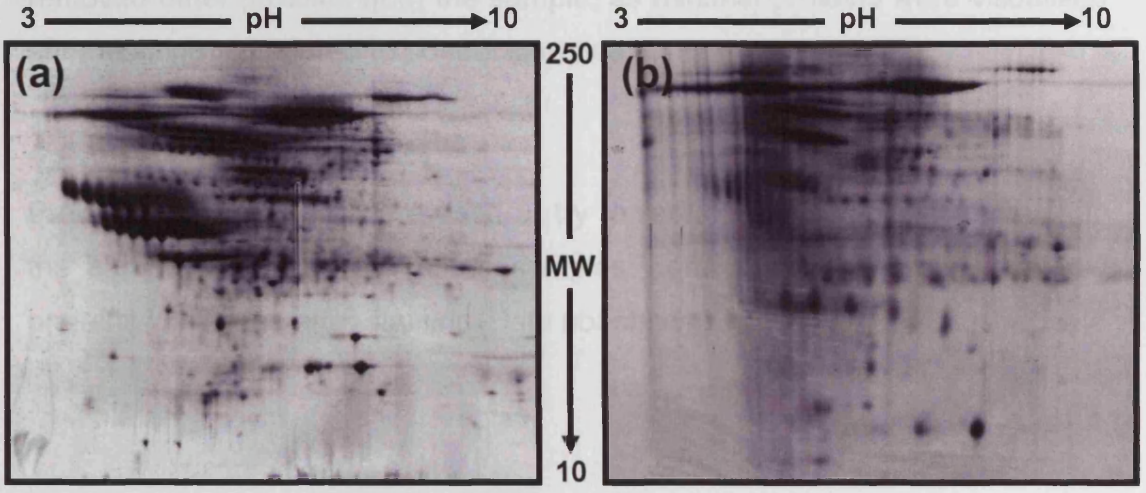

Figure 4.3: Representative 2D gels run on the Multiphor II (a) and Dalt*six* systems (b). Each gel was loaded with 75 µg of BAL fluid protein from saline-treated lungs. Both samples were desalted, freeze dried and contaminants removed using the 2D Clean-Up Kit. Spots were detected on the 2D gels with silver stain (n=4).

4.4.4 SYPRO RUBY STAINING VERSES SILVER STAINING

There were two staining techniques that were available for the 2D gels, i.e. SYPRO ruby staining and silver staining. However, for the precast gels the SYPRO staining procedure required the removal of plastic back which involved special equipment (e.g. Film Remover, Amersham Biosciences, UK) that was not available. For that reason, only Hoefer Dalt gels were used to compare the stains sensitivity for the proteins present in the BAL samples. SYPRO ruby stain can only be used on gels run on the Dalt system. The gels run on the Dalt system stained with either SYPRO ruby or silver stains are illustrated in Figure 4.4. The results suggested that more spots could be

visualised with the silver staining technique when compared to the SYPRO ruby staining technique.

4.4.5 ALBUMIN REMOVAL (HITRAP)

HiTrap columns were used to remove albumin from the BAL fluid samples. The results from the preliminary experiments revealed that the columns removed other proteins from the sample, as minimal proteins were visualised after staining, compared to control samples (Data not shown).

4.4.6 PRE-FRACTIONATION

Pre-fractionation filters were used to try to reduce the number of proteins in the samples. When fractionated samples were separated there were few proteins visualised after staining (Data not shown).

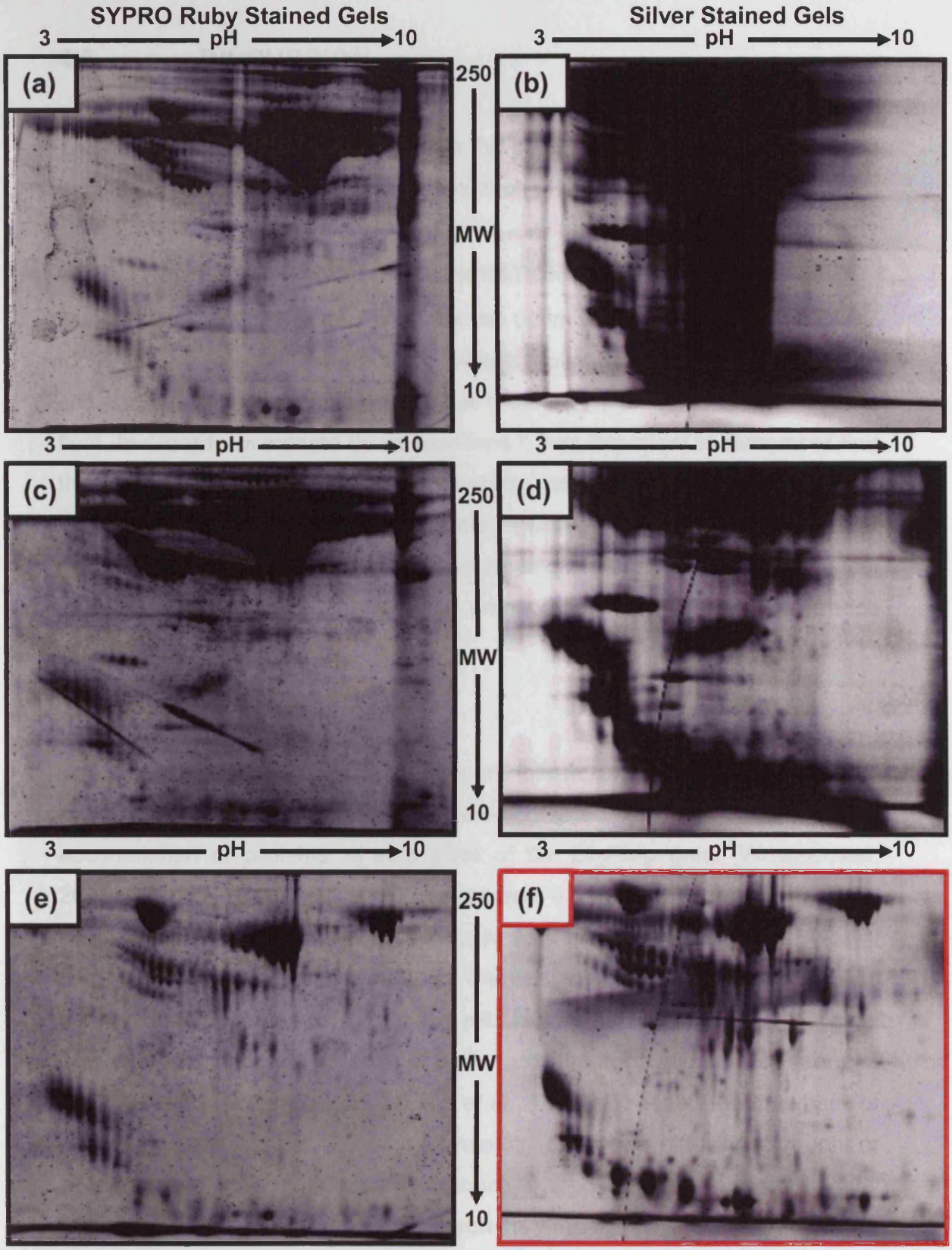

Figure 4.4: Representative 2D gels run using the Hoefer Dalt system (n=4). Each gel was loaded with 100 µg of BAL fluid protein. All samples were desalted and freeze dried. Spots were detected by either SYPRO Ruby stain (a,c & e) or with silver stain (b, d & f). Samples on gels a & b went through no further treatment. The remaining samples underwent acetone precipitation (c & d) and clean up kit (e & f). The red box highlight the optimial gels.

4.5 DISCUSSION

The aim of this study was to optimise the sample preparation and proteomic technique, 2D SDS PAGE, for the separation of proteins in BAL fluid samples.

4.5.1 TROUBLESHOOTING FOR OPTIMISATION OF 2D GELS

During the preliminary experiments for the optimisation of the 2D SDS PAGE for BAL fluid, two critical problems were encountered: (1) interference from salt and other contaminants and (2) low protein concentration in isolated BAL fluid. In order to overcome these problems it was important to remember that the key criterion to carrying out proteomic analysis is that there must be minimal loss or modification to the proteins and as such, it is imperative that only the necessary sample preparation steps are performed. In this instance, in addition to the necessary sample preparation steps, dialysis and freeze drying steps were used.

4.5.1.1 Dialysis

Salt contamination is the most frequent cause of insufficient focusing of protein spots interfering with the isoelectric focusing step, resulting in the accumulation of proteins at both ends of the DryStrip gels. (Westermeier, 2001). For this reason, salt was removed from the sample. A common method used in proteomics is dialysis, as salts have a much lower molecular weight than the proteins (Rabilloud, 1996). Dialysis was found to be an efficient method for removing salt producing satisfactory and reproducible 2D gels. This was also the case for Lenz *et al.* for both the separation of dog (Lenz *et al.*, 1990) and human BAL fluid (Lenz *et al.*, 1993). However, the drawback of this technique can be a loss of proteins, either by diffusing through or adsorption onto the membrane (Rabilloud, 2002). However, a Bradford assay of the dialysis water determined that proteins were not being lost from the BAL fluid samples.

Other researchers have successfully used different methods to remove salt; (1) precipitation with trichloroacetic acid (TCA) or organic solvents (e.g. cold

acetone) (Rabilloud, 1996; Wattiez *et al.*, 1999; Görg *et al.*, 2004), (2) spin dialysis (Görg *et al.*, 2004), (3) ion-exchange chromatography (Sabounchi-Schütt *et al.*, 2001) and (4) gel filtration (Lindahl *et al.*, 1995). Plymoth *et al.* (2003) compared some of these methods for the removal of salt from BAL fluid samples. TCA precipitation was found to impair 2D gels with 40 % loss of protein, gel filtration decreased streaking but results were difficult to reproduce and only small volumes could be processed through the columns. Dialysis resulted in sample dilution but since the next stage was to concentrate the sample this did not matter. In contrast, Plymoth *et al.* (2003) observed a 50 % improvement in 2D gel resolution after removing salt by dialysis. Hence, in this study, dialysis was chosen as it provided an efficient method for removing salt from the whole sample in one batch without introducing any contaminates.

4.5.1.2 Freeze Drying

Since the protein concentration in dialysed BAL fluid was outside the limits of detection, a method of concentration was required. The method of choice was freeze drying or lyophilization, which is a procedure that removes water from a sample by sublimation (Carrasquillo *et al.,* 2000). A number of other researchers used lyophilization to concentrate BAL fluid (Lindahl *et al.*, 1999; Magi *et al.*, 2002; He, 2003; Sabounchi-Schütt *et al.*, 2003).

4.5.1.3 Albumin Removal

Albumin was removed from some samples, as it is the most abundant protein present and could possibly be hindering the detection of other protein with similar pI and molecular weights. Plymoth *et al.* (2003) used anti-Human Serum Albumin (HSA) columns to remove albumin from BAL fluid. They found that the removal of albumin changed the 2D gel profile, allowing them to detect protein spots that had been previously been hidden. Albumin caused these proteins to be co-precipitated and trapped in the 1^{st} dimension rather than hidden by the albumin spots. These workers also found that some other proteins were adsorbed non-specifically to the column. The HiTrap method used to remove the albumin in this study produced disappointing results, as the HiTrap seemed to have removed the majority of the other proteins present. This also seemed to be the case for Lenz *et al.* (1993) who believed

detection was impaired and identification of scarce proteins in BAL fluid was hindered by abundant proteins like albumin, transferrin, α1-antitrypsin and immunoglobulins A and G. They tried removing albumin by binding to Affigel-Blue but found unsatisfactory results because other protein spots were lost. Consequently, in the present study, the focus turned to cleaning up the whole sample.

4.5.1.4 Streaking

Some gels exhibited horizontal and vertical streaking that could have been caused by a variety of factors. Horizontal streaks are primarily due to insufficient solubility of particular proteins during the isoelectric focusing step, possibly caused by excess liquid that was not absorbed by the strip, overloading, sample solubility problems, non-protein contamination (e.g. nucleic acids adhering to proteins) and incomplete focusing (Garfin, 2000; Görg *et al.*, 2000). The 2D gels that were run for optimisation were loaded with 100 µg of protein and therefore some of the horizontal streaking may have been due to overloading of the protein.

Non-protein impurities in samples can interfere with protein separation in 2D gels and therefore have to be removed prior to their separation. Lipids that would be present in high concentration from surfactant in BAL fluid can cause a problem, as they reduce the solubility of many proteins, and can also affect both the pI and molecular weight. Two methods were employed to remove contaminants from the samples, the 2D Clean-Up Kit and acetone precipitation. The 2D Clean-Up Kit was found to be the most robust in removing the contamination from the sample and producing a clearer image. This kit works by quantitatively precipitating proteins while leaving behind the interfering substances such as salt, lipids, phenols and nucleic acids. The recovered proteins are later resuspended in rehydration solution and ready for the rehydration step (Amersham Biosciences, 2002). Less horizontal streaking was found in the 2D gels from the samples that had been treated with the 2D Clean-Up Kit. Acetone is a component of the precipitant and co-precipitant solutions, the improvement in the resolution maybe due to the other components in these solutions aiding precipitation compared to acetone

alone. The method involves multiple steps including a wash that would remove components of the precipitant and co-precipitant solutions that may also improve the resolution of the 2D gels.

In contrast to horizontal streaking, vertical streaking normally relates to a problem with the SDS PAGE separation, including loss of protein solubility at their pI, dust contamination and incorrect placement of the DryStrip (Garfin, 2000). It can also be the result of salt fronts, protein aggregates and incomplete focusing (Görg *et al.*, 2000). Thus, removal of salt and other contaminants is crucial for clean separations and hence, the need for the 2D Clean-Up Kit step.

4.5.1.5 Pre-fractionation

The 2D gels from the pre-fractionated samples produced disappointing results. The results are probably explained by protein retention to the filter and resulting in the dramatic loss of proteins. Therefore, pre-fractionation was not a viable sample preparation method.

4.5.2 STAINING

The 2D gels need to be stained in order to visualise the spots. The important properties for a proteomic stain are: (1) sensitivity (low detection limit); (2) linear dynamic range (for quantitative accuracy); (3) reproducibility and (4) compatibility with mass spectrometry (MS). Unfortunately, to date no staining method meets all of these requirements (Görg *et al.*, 2004). For 2D gels run on the Hoefer Dalt system there was two specific stains available, (1) silver stain and (2) SYPRO Ruby stain.

4.5.2.1 Silver staining

Silver staining of proteins separated on polyacrylamide gels were first introduced in 1979 by Switzer *et al.* (1979). Silver binds to the amino acid side chains, primarily the sulfhydryl and carboxyl groups of proteins. Since then numerous methods have been used. The silver staining technique is a multi-step procedure that requires stopping the reaction at a given time point in

order to prevent over-development. This can cause problems in the reproducibility of gels (Patton, 2002). Another drawback of silver staining is that certain classes of proteins such as calcium-binding proteins and glycoproteins stain poorly. Silver staining can detect proteins down to 0.1 ng and is 100 times more sensitive than Coomassie Brilliant Blue (Patton, 2001). The silver staining techniques have to omit glutaraldehyde, as this interferes with the MS step. For MS analysis it is important to obtain a complete trypsin digestion of the protein sample. Glutaraldehyde modifies lysine residues and prevents complete trypsin digestion (Rabilloud, 1990).

Due to its high sensitivity, silver staining is ideal for the detection of trace components in protein samples and the analysis of protein samples available in limited quantity. The detection limit is as low as 0.1 ng of protein per spot. There are several drawbacks such as poor reproducibility, limited dynamic range, certain proteins stain poorly or not at all and, the procedure is labour intensive (Görg *et al.*, 2000).

4.5.2.2 SYPRO Staining

SYPRO ruby dye is an endpoint stain, and thus, staining times are not critical and staining can be performed overnight without over-developing the gels. The stain does not interfere with subsequent MS. It detects lysine, arginine and histidine residues, and as such, relies upon the basic composition for protein detection (Lopez *et al.,* 2000). SYPRO ruby is a non-covalent stain with a detection limit of 1-2 ng of protein, it shows little protein-to-protein variation. In addition, it does not modify the proteins (Görg, 2000; Lopez *et al.*, 2000).

In this study, the silver staining technique was found to detect more spots on the Dalt gels compared to the SYPRO ruby stained gels. This was not expected, as SYPRO ruby dye, on side-by-side comparison, has been reported to visualise 20% more protein compared with silver staining (minus glutaraldehyde) (Patton, 2002). Görg *et al.* (2000) found similar but not identical patterns when comparing SYPRO ruby and silver stained gels. The

difference in protein profiles could be explained by the nature of proteins present in BAL fluid.

The differences in the detection levels (Silver stain - 0.1 ng; SYPRO - 1 ng) could explain the discrepancy in the profiles, abundant proteins stained well with both stains while the smaller, scarce proteins were only detected by silver staining. The type of proteins present in BAL fluid may also help explain the variations; SYPRO ruby detects lysine, arginine and histidine residues on the proteins that are all basic and hydrophilic residues, while silver stain binds primarily to the sulfhydryl and carboxyl groups of proteins.

Another consideration is the cost, SYPRO ruby is expensive compared to silver stain. It also requires a fluorescent scanner to visualise gels because the spots are not visible by eye; spot picking needs to be done by a spotcutter.

Noël-Georis *et al.* (2002) believed silver staining is the best method for detecting BAL fluid proteins on 2D gels. Silver stain is also the method of choice for a number of other researchers investigating BAL fluid (Lindahl *et al.*, 1995; Wattiez *et al.*, 2000; von Bredow *et al.*, 2001; Magi *et al.*, 2002; He, 2003; Sabounchi-Schütt *et al.*, 2003). Since quantitation of protein spots was not desired only their absence/presence, silver staining was the method of choice for the visualisation of proteins in this study.

4.5.3 MULTIPHOR II SYSTEM VERSES HOEFER DALT SYSTEM

The comparison between the Multiphor II and the Hoefer Dalt systems found that more spots were visualised on gels run on the Multiphor II system. This is a flatbed system that only allows 1 gel to be run at a time. The advantage here is that precious and expensive BAL samples are not rapidly depleted during the optimisation of the experimental work. In contrast, an advantage of the Hoefer Dalt system is that 10 gels can be run simultaneously under the same environmental conditions, thus helping with the productivity and the reproducibility of the gels. Since the reproducibility of gels is vital for

comparisons between samples, any variability that could be introduced by casting gels should be minimised. The Multiphor system allows precast gels to be used but gels need to be cast for Hoefer Dalt system. The Hoefer Dalt system was also not reliable to run at the required voltage overnight; possibly due to the age of the electrodes/equipment. The Dalt*six* is a new version of the Hoefer Dalt system. As its name suggests it has the capability of running 6 gels simultaneously. Precast gels were also compatible with the new system.

Spot resolution was increased in the Multiphor II gels compared to Dalt gels this could be explained because the Multiphor II gels are thinner (0.5 mm) than the Dalt gels (1 mm). This allows higher voltages to be applied resulting in less protein diffusion because there is a shorter running time. (Görg *et al.*, 2000)

Another explanation for differences observed between the flatbed and vertical systems was transferring of the proteins from IPG strips to SDS PAGE gels. In the Multiphor II systems, the IPG strips are laid with the gel side down, directly onto the gel surface. Whilst with both of the Dalt systems the cassettes were filled with 2-3 ml of agarose solution before the IPG strips were inserted and positioned in contact with the upper edge of the SDS gel. Therefore, less surface area is in contact with the SDS PAGE gels and could potentially lead to proteins not entering the gel.

Another advantage in using precast gels is that they are attached to a plastic support that prevents alterations in gel size (shrinkage due to organic solvents or expansion upon rehydration with aqueous solvents) during the staining procedure (Görg *et al.*, 2000).

The reproducibility was found to be greatly improved with silver stain but fewer spots were detected with silver stain. Consequently, this made the Multiphor II system the preferred equipment to use for the proteomic experiments with the valuable BAL fluid samples collected from the polymer models (Chapter 2).

4.6 CONCLUSION

To summarise, the optimal sample preparation procedure for 2D SDS PAGE of BAL fluid involved three steps:

(1) Dialysis – salt removal.

(2) Freeze drying – concentrate BAL lavage proteins.

(3) 2D Clean-Up Kit – removes contaminants by selective precipitation.

Seventy five micrograms of BAL fluid was found to be the optimal concentration to be loaded on the 2D gels and run on the Multiphor II system. The protein spots were best detected by the silver staining. Following the determination of the optimal sample preparation steps, these procedures will now be used to perform proteomic analysis on BAL fluid samples from rats treated with polymer A (Chapter 5). In order to increase reproducibility, each sample preparation step was performed on all samples that were going to be compared at the same time to reduce any changes due to environmental differences/alterations.

CHAPTER 5:
2D SDS PAGE FOR POLYMER A AND BLEOMYCIN MODELS

5.1 INTRODUCTION

Two-dimensional Sodium Dodecyl Sulphate Polyacrylamide Gel Electrophoresis (2D SDS PAGE) was employed in the present study to investigate differences in protein translation during the development of pulmonary oedema and inflammation. A model for polymer A-induced injury in the rat lungs was characterised using conventional toxicology (Chapter 2) and histological analysis (Chapter 3). These investigations showed that polymer A produced different biological endpoints relating to both dose (single or double) and time. In order to examine protein profiles in broncho-alveolar lavage (BAL) fluid collected from the lungs of animals exhibiting oedema and inflammation, proteomic technology was applied. Optimisation of the 2D SDS PAGE technique for BAL fluid was first undertaken (Chapter 4). To summarise, the optimal sample preparation procedure for 2D SDS PAGE of BAL fluid involved the following steps:

(1) Dialysis – salt removal

(2) Freeze drying – concentrate BAL lavage proteins

(3) 2D Clean-Up Kit – removes contaminants

(4) 75 µg of BAL fluid – optimal concentration loaded on the 2D gel

(5) Multiphor II system – employed to separate proteins

(6) Silver stain – detected protein spots on 2D gels.

A model of mild oedema resulted from a single polymer A instillation into the rat lungs. This model was used to identify changes in protein profiles during the peak of lung injury (7 days post-single instillation). The changes in protein profiles of lung repair mechanisms were also investigated (28 days post-single instillation). Following a double polymer A instillation, a model of persistent oedema developed. The same time point was selected to profile any protein changes.

Finally, the protein profiles of BAL fluid collected from a bleomycin-induced model of lung injury was used for comparison, since there were no other proteomic models that had been established using polymer A or similar synthetic resin polymers.

5.2 MATERIALS AND STOCK SOLUTIONS

5.2.1 MATERIALS

All materials required to carry out the proteomic procedure are detailed in Chapter 4 (Section 4.2.1). In addition, the following materials were required for the present research:

Dionex (UK) Ltd, Surrey, UK.

PepMap C18 Column

Matrix Science Ltd, London UK.

MASCOT Software

Micromass UK Ltd, Manchester, UK.

MassLynx 3.5

NanoESI Q-Tof Mass Spectrometer

NonLinear Dynamics Ltd, Newcastle, UK.

Phoretix 2D Expression Software

Promega UK Ltd, Southampton, UK.

Trypsin (Sequencing Grade) (V5111)

Waters Ltd, Hertford, UK.

Capillary Liquid Chromatography

5.2.2 STOCK SOLUTIONS

The stock solutions required to carry out the proteomic procedure are detailed in Chapter 4 (Section 4.2.2).

5.3 METHODS

5.3.1 SAMPLES

BAL fluid samples were collected from polymer A-instilled and bleomycin-instilled rat lungs (Chapter 2). Saline-instilled rats were used as control samples.

5.3.2 SAMPLE PREPARATION AND 2D SDS PAGE

The optimal sample preparation comprised of dialysis (Chapter 4; Section 4.3.1.1), freeze drying (Chapter 4; Section 4.3.1.1) and 2D Clean Up (Chapter 4; Section 4.3.1.3). The 2D SDS PAGE was carried out as described in Chapter 4 (Sections 4.3.2 and 4.3.3). The gels were then silver stained (Chapter 4; Section 4.3.4.2) before being imaged using the Amersham ImageScanner.

5.3.3 IMAGE ANALYSIS

Gel analysis was performed using Phoretix 2D Expression software. In this study, we were interested in the absence of spots in a given gel when compared with another gel, in order to find protein markers, and simplify the analysis procedure. Therefore differences in protein abundance between the gel sets were not analysed as part of this work (Dr Ian Brewis (2005) Personal Communication). The spots selected for picking had to be clearly defined (i.e. not merged with any adjacent spots). Spots had to appear on 75% of the gels in the set.

5.3.4 IN-GEL PROTEIN DIGESTION

In-gel protein digestion and tandem mass spectrometry (MS/MS) was carried out by Mr Peter Ashton at the School of Chemical Science, The University of Birmingham, UK. A brief overview of these procedures has been outlined below.

In-gel trypsin digestion of manually excised protein spots was performed using an automated 96-well plate protocol plate modified from Shevchenko *et al.* (1996). The key steps (1-16) are briefly outlined as follows:

(1) Dehydration with acetonitrile (100% 80 µl, 5 minutes)

(2) De-stained with potassium ferricyanide (30 mM) and sodium thiosulfate, pentahydrate (100 mM); (50 µl per spot, 15 minutes shaking occasionally)

(3) Washed (2-3 times) in with ammonium bicarbonate (25 mM; 50 µl) and the supernatant removed

(4) Acetonitrile was added (100% 50 µl, 15 minutes) and the supernatant removed

(5) Rehydration in ammonium bicarbonate (25 mM, 50 µl, 10 minutes) and supernatant was removed

(6) Acetonitrile was added (100% 50 µl, 15 minutes) and the samples were dried to completeness in an oven (60 ºC, 30-45 minutes)

(7) Dithiothreitol (10 mM) in ammonium bicarbonate (25 mM) was added (25 µl, 56 ºC for 1 hour) and the sample was cooled to room temperature before the supernatant was removed

(8) Iodoacetamide (55 mM) in ammonium bicarbonate (25 mM) was added (25 µl, 45 minutes at room temperature in the dark)

(9) Supernatant was removed and the gel plugs washed with ammonium bicarbonate (25 mM, 25 µl, 10 minutes)

(10) Supernatant was removed and acetonitrile added (100% 50 µl, 15 minutes)

(11) Supernatant was removed and the plugs were rehydrated with ammonium bicarbonate (25 mM, 50 µl, 10 minutes)

(12) Following further dehydration in acetonitrile (100% 50 µl, 15 minutes) and removal of the supernatant, the spots were dried to completion in an oven (60 ºC, 30-45 minutes).

(13) Sequencing grade modified trypsin was prepared (as described by the manufacturer) and made to a final concentration of 6.25 ng/µl in ammonium bicarbonate (50 mM). This trypsin solution was added to the gel spots (10µl on ice until the gel had fully rehydrated).

(14) Once fully rehydrated (approximately 20 minutes), the plug was covered with ammonium bicarbonate (25 mM, 10 µl) incubated at 37ºC overnight.

(15) The supernatant that surrounded the gel plug was removed and placed in a well in a clean plate and dried to completion in an oven (60 °C for 1 hour)
(16) The remaining peptides were then resuspended in 1% (v/v) formic acid (6 µl) for MS/MS.

5.3.5 TANDEM MASS SPECTROMETRY

MS/MS was performed on the samples. The peptides in a given sample (5 µl) were separated by capillary liquid chromatography and a PepMap C18 column (75 µm i.d. x 15 cm) before being analysed using a nanoESI Q-Tof mass spectrometer. Following MS/MS the raw data were processed using MassLynx 3.5 to produce a single peak-list (pkl-files).

5.3.6 MASCOT SEARCH

MASCOT is a powerful search engine which uses mass spectrometry data to identify proteins from primary sequence databases. The resulting pkl-files from the MS/MS were compared with the NCBI non-identical protein sequence database (NCBInr) using the MASCOT search software. Identifications were made by comparing the experimentally generated data with theoretical data calculated for each database entry. The rationale is to retrieve proteins that would produce the same set of data if digested and analysed in the same manner as the protein in the study. MASCOT provides a list of candidate proteins that most closely match the input data and the candidate proteins are ranked using a scoring system. Figure 5.1 illustrates a typical result report obtained from the software. At the top of the page there are a few lines to identify the search: title, date, user name, etc. Following the header was an overview list of significant hits and a histogram of the score distribution for the top matches. In this particular example, scores greater than 46 were reported to be significant. This is, the chance of a random match getting a score of 46 is $p<0.05$. The next section of the report contained tabular summary of the matching proteins. For each protein, the accession number, the protein molecular mass and the overall score were given. This was followed by a table summarising the matched peptides (Figure 5.2). By

following the hyperlinks from the main report page, more detailed reports were available.

In MASCOT, the score for an MS/MS match is based on the absolute probability (P) that the observed match between the experimental data and the database sequence is a random event. The reported score is -10Log(P). The expectant value is the number of times you could expect to get this score or better by chance. It can be derived directly from the score and the threshold (set at $p < 0.05$). A completely random match has an expectation value of 1 or more. The better the match, the smaller the expectation value.

Following matching of a peptide to a protein, the quality of the raw MS/MS data were validated (required the presence of good quality y-ion data). Finally, each of the peptides was used to BLAST search to confirm the protein identified by MASCOT was the only relevant match in the non-redundant protein database for a particular peptide sequence (Kinter and Sherman, 2000).

MASCOT SEARCH RESULTS

User : Martina Hicks
Email : hicksm@cardiff.ac.uk
Search title : Polymer A Spot A6
MS data file : D:\Martina\IB131205A6.pkl
Database : NCBInr 20060122 (3229171 sequences; 1108386787 residues)
Taxonomy : Mammalia (mammals) (445426 sequences)
Timestamp : 23 Jan 2006 at 14:31:26 GMT
Significant hits:

gi|7331218	keratin 1 [Homo sapiens]
gi|28317	unnamed protein product [Homo sapiens]
gi|71051822	Unknown (protein for MGC:116262) [Rattus norvegicus]
gi|13638435	Calgranulin A (Migration inhibitory factor-related protein 8) (MRP-8) (p8)
gi|435476	cytokeratin 9 [Homo sapiens]
gi|136429	Trypsin precursor
gi|76617900	PREDICTED: similar to keratin 4 isoform 2 [Bos taurus]
gi|186685	keratin type 16
gi|55638143	PREDICTED: similar to keratin 1B [Pan troglodytes]
gi|73965955	PREDICTED: similar to keratin 20 [Canis familiaris]

Probability Based Mowse Score

Ions score is -10*Log(P), where P is the probability that the observed match is a random event.
Individual ions scores > 46 indicate identity or extensive homology ($p<0.05$).
Protein scores are derived from ions scores as a non-probabilistic basis for ranking protein hits

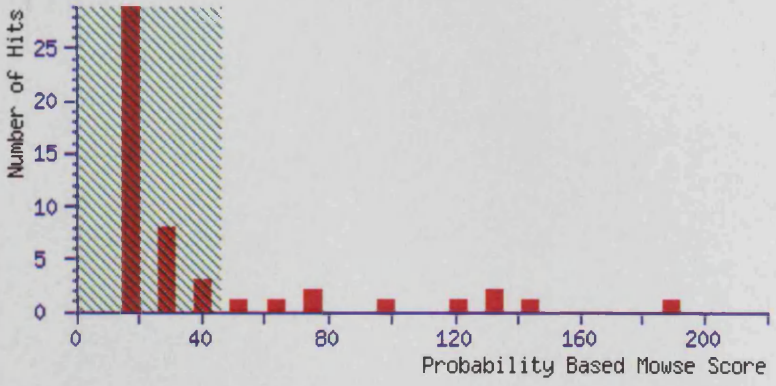

Figure 5.1: Example of the main result report from an MS/MS ion search of peptides from an in-gel tryptic digest of a protein against the NCBInr database.

Calgranulin A (Migration inhibitory factor-related protein 8) (MRP-8) (p8)

Query	Observed	Mr(expt)	Mr(calc)	Delta	Miss	Score	Expect	Rank	Peptide
82	791.3849	1580.755	1580.732	0.022	0	94	9.2e-07	1	K.MVTTECPQFVQNK.N
90	602.9816	1805.923	1805.931	-0.008	0	41	0.17	1	K.ALSNVIEVYHNYSGIK.G

Figure 5.2: Example of the summary section of the MASCOT report contains a tabular summary of the matching proteins (In this example: calgranulin A).

5.4 RESULTS

5.4.1 POLYMER A MODEL: 2D SDS PAGE

A representative set of saline control and polymer A-treated 2D gels are shown for each time point (day 7 (single) - Figure 5.3, day 28 (single) - Figure 5.4, day 7 (double) - Figure 5.5 and day 28 (double) - Figure 5.6). These sets of gels were run on the Multiphor II system. There was considerable spot interference on the polymer A gel from the day 7 samples when compared to the saline control gel for both the single and double-instillation models. By day 28 there is less interference present.

The interference was too vast on the day 7 (single) gel set for the 2D Expression IA software to analyse (Figure 5.3). IA found no differences in the day 28 gels from the single-instillation model (Figure 5.4). However, differences and similarities between the gels from the double instillation could be detected following normalization of the gels (Figure 5.5 and 5.6).

5.4.2 POLYMER A MODEL: MS/MS

Selected proteins were excised for subsequent identification by MS/MS. Spots had to appear on 75% of the gels to be chosen for MS/MS analysis. The proteins identified by MS/MS and subsequent MASCOT search are shown in Table 5.1.

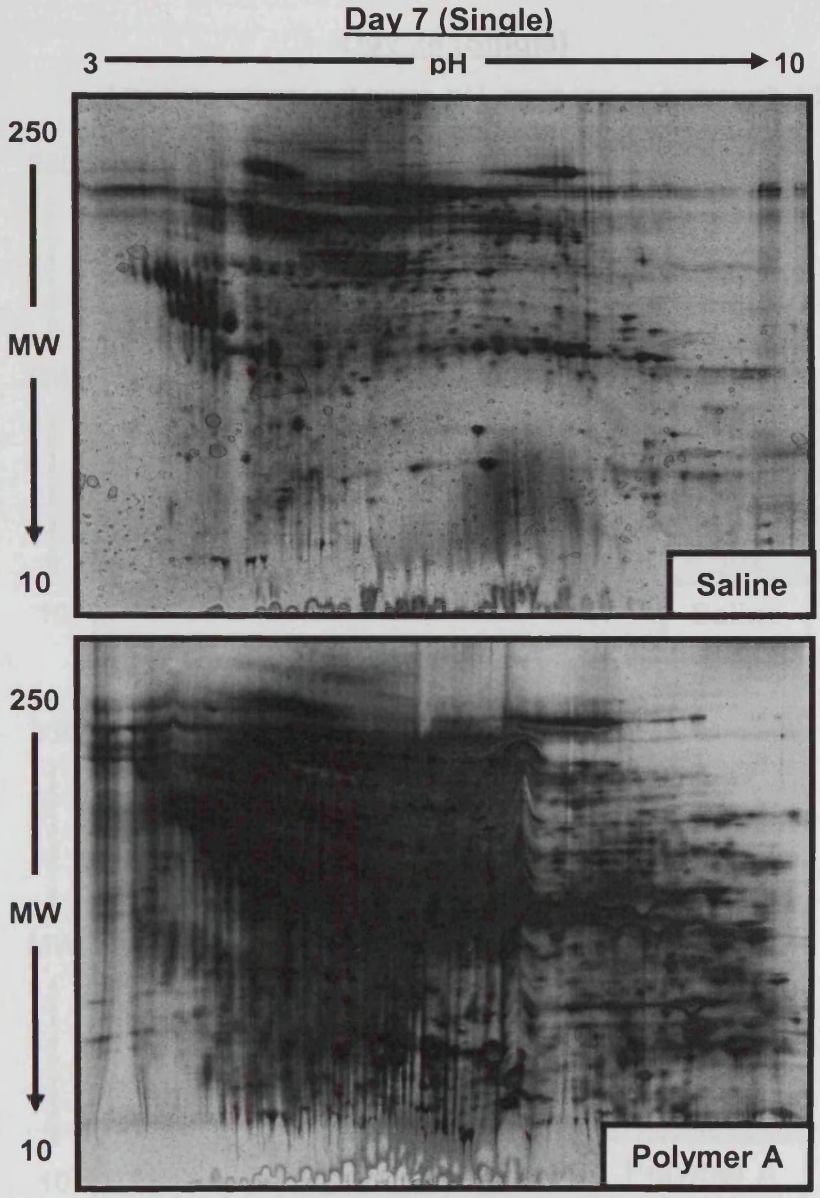

Figure 5.3: A representative set of 2D-gels from the day 7 saline control and polymer A-treated single-instilled samples. Seventy five micrograms of protein was loaded on to each gel and gels were run on the Multiphor II system. Spots were detected using silver stain. Due to the level of interference on the polymer gels the 2D Expression Software was unable to analysis them.

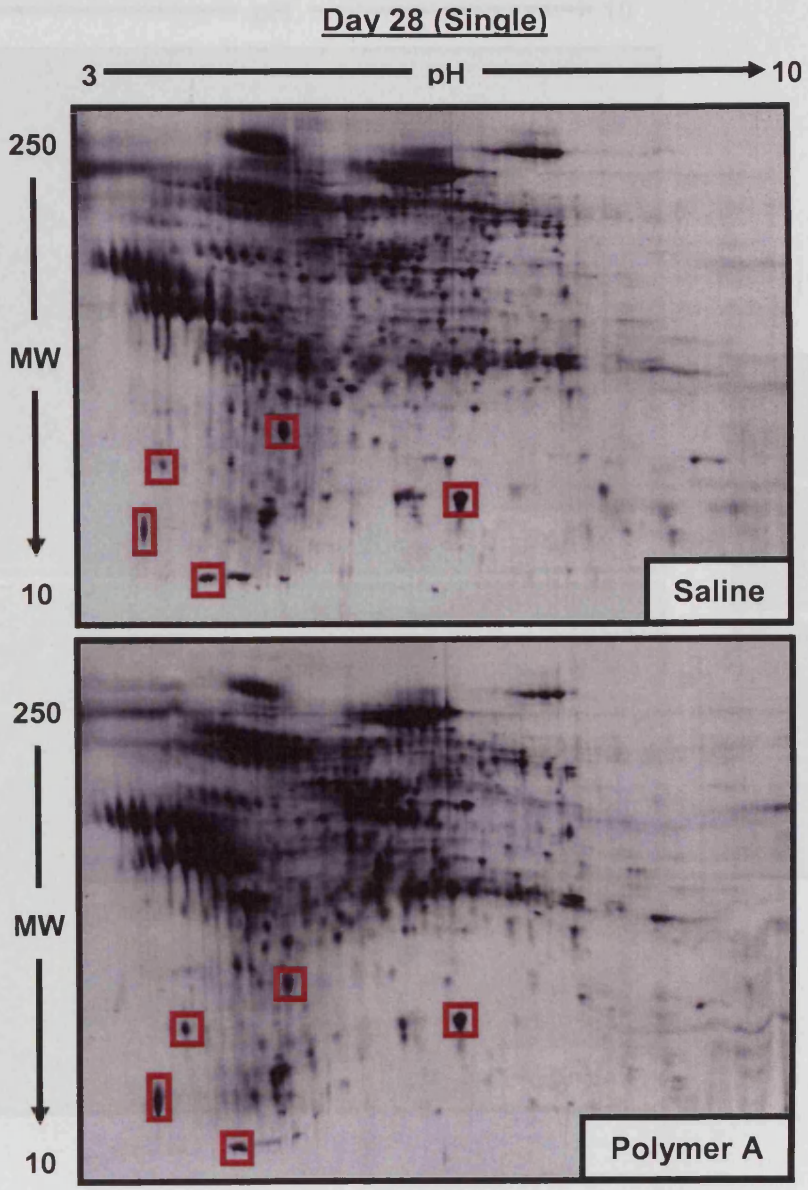

Figure 5.4: A representative set of 2D-gels from the day 28 saline control and polymer A-treated single-instilled samples. Seventy five micrograms of protein was loaded on to each gel and gels were run on the Multiphor II system. Spots were detected using silver stain. The red boxes are reference spots found on both gels. The 2D Expression Software could not find any differences between the gel sets.

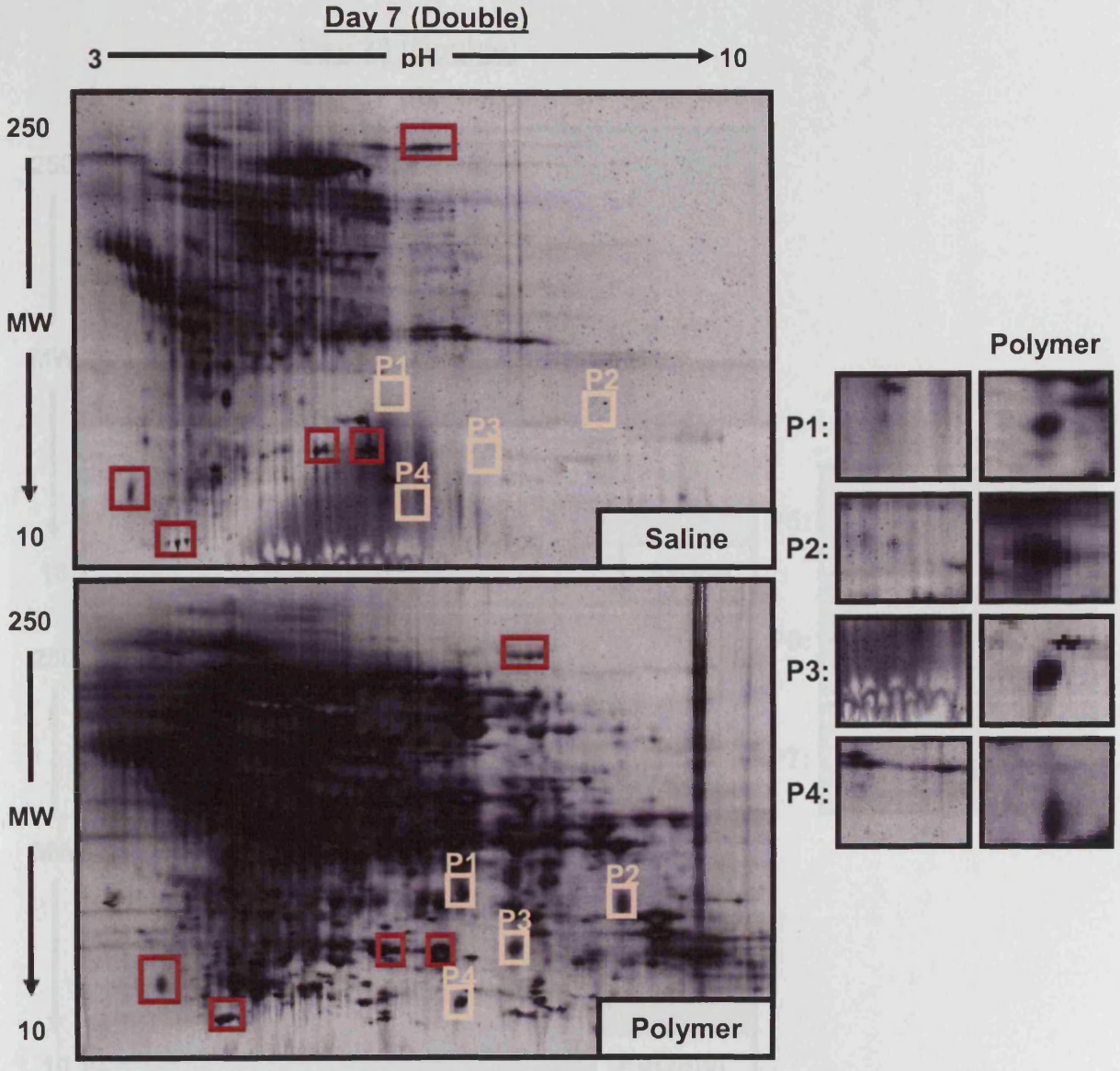

Figure 5.5: A representative set of 2D-gels from the day 7 saline control and polymer A-treated double-instilled samples. Seventy five micrograms of protein was loaded on to each gel and gels were run on the Multiphor II system. Spots were detected using silver stain. The red boxes are reference spots found on both gels. The peach boxes (P1-P4) are spots selected for MS/MS analysis. The selected spots are shown enlarged on the right-hand side of the gel images.

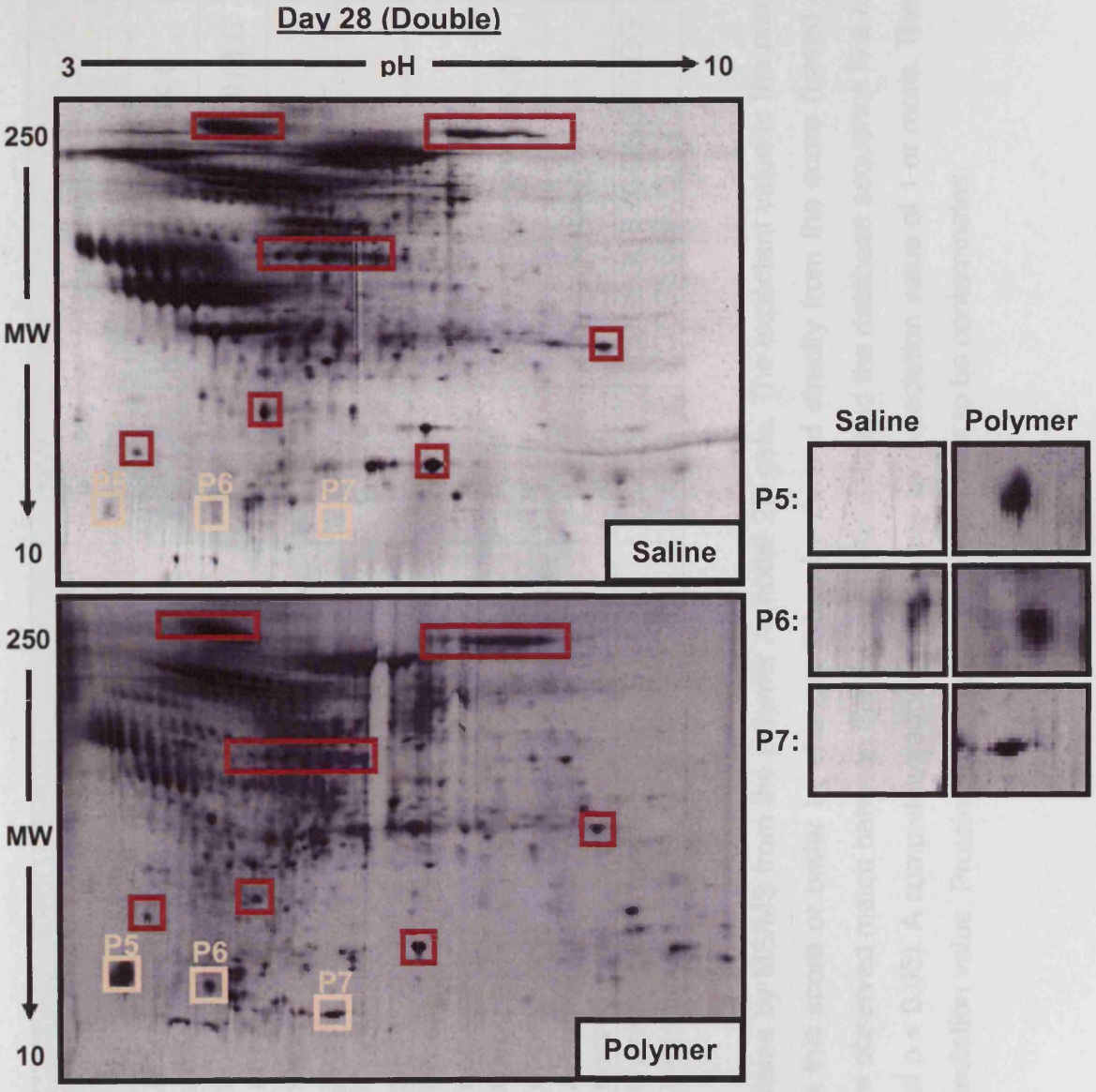

Figure 5.6: A representative set of 2D-gels from the day 28 saline control and polymer A-treated double-instilled samples. Seventy five micrograms of protein was loaded on to each gel and gels were run on the Multiphor II system. Spots were detected using silver stain. The red boxes are reference spots found on both gels. The peach boxes (P5-P6) are spots selected for MS/MS analysis. The selected spots are shown enlarged on the right-hand side of the gel images.

Spot No	Accession No (NCBInr)	Name	Expectation Value	MW (Daltons) and pI	Peptide
P1	gi|19705431	**Albumin [Rattus norvegicus]**	1.2e-05	70670 6.09	K.TCVADENAENCDK.S
P1	gi16758014	**Hemopexin [Rattus norvegicus]**	0.0024	52000 7.58	R.CNADPGLSALLSDHR.G
P2	gi|71390	Keratin high-sulfur matrix protein IIIB2	0.00019	11131 6.28	R.TGPATTICSSDK.F
P3	gi|435476	Cytokeratin 9 [Homo sapiens]	0.7	62320 5.19	K.STMQELNSR.L
P4	gi|6981424	**Prosaposin [Rattus norvegicus]**	0.00047	62908 5.13	K.LVTDIQTAVR.T
P5	gi|13638435	**Calgranulin A [Rattus norvegicus]**	9.2e-07	10289 5.68	K.MVTTECPQFVQNK.N
P6	gi|19705431	**Albumin [Rattus norvegicus]**	0.65	70670 6.09	K.KYEATLEK.C
P7	gi|435476	Cytokeratin 9 [Homo sapiens]	0.00048	62320 5.19	R.GGSGGSYGGGGSGGG YGGGSGSR.G

Table 5.1: Identification of proteins by MS/MS from the polymer A model 2D gels. The expectant value is the number of times you could expect to get this score or better by chance. It can be derived directly from the score (based on the absolute probability (P) that the observed match between the experimental data and the database sequence is a random event) and the threshold (set at $p < 0.05$). A completely random match has an expectation value of 1 or more. The better the match, the smaller the expectation value. Proteins in bolds are considered not to be contaminates.

5.4.3 BLEOMYCIN MODEL: 2D SDS PAGE

A representative set of saline control and bleomycin treated 2D-gels are shown in Figure 5.7 (day 7) and 5.8 (day 22). Unlike the polymer gels, there was no spot interference. These sets of gels were run on the Dalt*six* system to increase productivity. Differences and similarities between the gels could be detected following normalization of the gels (Figure 5.7 and 5.8).

5.4.4 BLEOMYCIN MODEL: MS/MS

Selected proteins were excised for subsequent identification by MS/MS. The raw data collected from the MS/MS was interpreted using the MASOT search software. The proteins identified by MS/MS and subsequent MASCOT search are shown in Table 5.2.

.

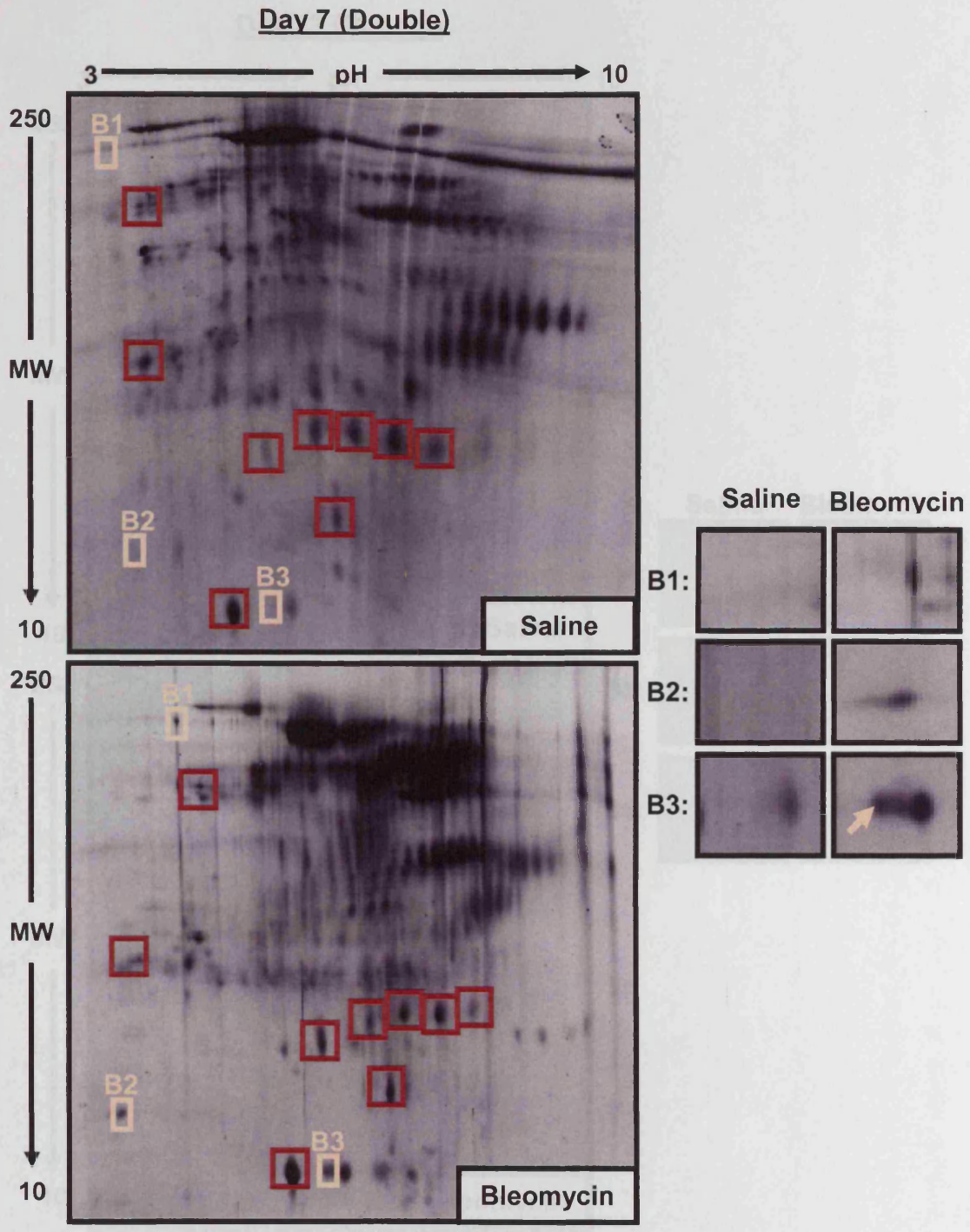

Figure 5.7: A representative set of 2D-gels from the day 7 saline control and bleomycin-treated double-instilled samples. Seventy five micrograms of protein was loaded on to each gel and gels were run on the Dalt*six* system. Spots were detected using silver stain. The red boxes are reference spots found on both gels. The peach boxes (B1-B3) are spots selected for MS/MS analysis. The selected spots are shown enlarged on the right-hand side of the gel images.

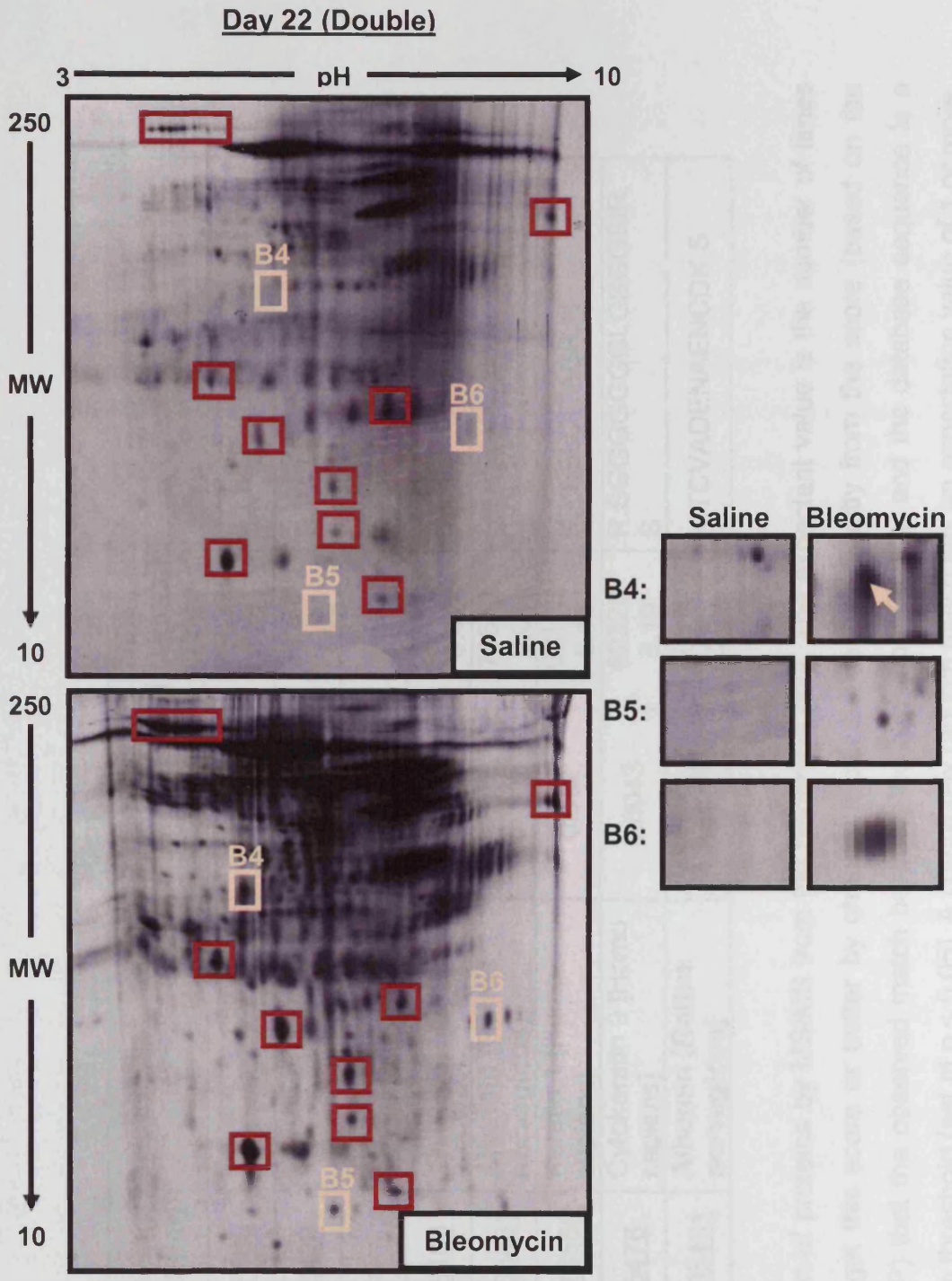

Figure 5.8: A representative set of 2D-gels from the day 22 saline control and bleomycin-treated double-instilled samples. Seventy five micrograms of protein was loaded on to each gel and gels were run on the Dalt*six* system. Spots were detected using silver stain. The red boxes are reference spots found on both gels. The peach boxes (B4-B6) are spots selected for MS/MS analysis. The selected spots are shown enlarged on the right-hand side of the gel images.

Spot No	Accession No (NCBInr)	Name	Expectation Value	MW (Daltons) and pI	Peptide
B1	gi|136406	Cationic trypsin precursor	0.014	26837 8.42	K.LSSPATLNSR.V
B2	gi|136429	Trypsin precursor	0.085	25078 7.00	R.VATVSLPR.S
B3	n/a	Insufficient concentration	n/a	n/a	n/a
B4	gi|136406	Cationic trypsin precursor	0.025	26837 8.42	K.LSSPATLNSR.V
B5	gi|19705431	**Albumin [Rattus norvegicus]**	0.00024	70670 6.09	K.APQVSTPTLVEAAR.N
B6	gi|17318569	Keratin 1 [Homo sapiens]	0.032	66198 8.16	K.YEELQITAGR.H
B7	gi|435476	Cytokeratin 9 [Homo sapiens]	0.0043	62320 5.19	R.SGGGGGGGLGSGGSIR.S
B8	gi|19705431	**Albumin [Rattus norvegicus]**	2.4e-08	70670 6.09	K.TCVADENAENCDK.S

Table 5.2 Identification of proteins by MS/MS from the bleomycin gels. The expectant value is the number of times you could expect to get this score or better by chance. It can be derived directly from the score (based on the absolute probability (P) that the observed match between the experimental data and the database sequence is a random event) and the threshold (set at $p < 0.05$). A completely random match has an expectation value of 1 or more. The better the match, the smaller the expectation value.Proteins in bolds are considered not to be contaminates.

5.5 DISCUSSION

The aim of this study was to profile proteins from BAL fluid samples collected from saline and polymer-instilled rat lung injury models and to analyse the differences in these profiles. The ultimate objective was to identify potential BAL protein markers, using mass spectrometry, for different severities of lung injury and repair, that could potentially be used for early clinical diagnosis, thus replacing the current clinical tests such as chest radiographs and blood gas monitoring. The current tests only describe the situation relatively late after the initial cellular disturbance so there is a considerable interest in detecting early phases of lung injury.

5.5.1 OVERVIEW OF TECHNICAL PROBLEMS

5.5.1.1 Sample

Proteomics has proven to be a powerful tool for identifying early changes at the protein level in a variety of disease states (Kvasnicka, 2002). 2D SDS PAGE is the most widely used method for analysing proteins in a complex mixture (Berkelman and Stenstedt, 1998). The major problem to overcome in the analysis of the polymer gels was the spot interference observed in the day 7 gels for both the single and double models. This interference was not present on any of the bleomycin gels, and as such, was probably caused by the presence of the synthetic resin polymers in the BAL samples. A possible reason why the polymer is not removed during the sample preparation stages could be that the polymer binds to/coats the proteins or form aggregates with the proteins in the BAL fluid. Unfortunately, any attempt to remove the polymer would also result in the loss of sample proteins, and hence, cause a subsequent change in the BAL proteomic profile. Consequently, with the level of interference present and the use of silver stain, it was difficult to analyse the gels comprehensively. As an attempt to improve these gels, they were run using a lower sample protein concentration (50 µg) and using the Dalt*six* gel system. However, this did not improve the gel clarity. Therefore the original sets of gels (run on the Multiphor II System) had to be used for further analysis using the 2D Expression software.

An alternative to removing the interference/polymers may be to change the stain. A change to a fluorescent stain such as one of the SYPRO stains, may improve the spot resolution on the gels. However, during the optimisation experiments (Chapter 4), it was determined that SYPRO ruby stain did not detect as many spots as the silver stain. Therefore, as a compromise in the detection sensitivity under these circumstances, the use of the SYPRO ruby stain may be the best answer to this problem. Furthermore, the use of SYPRO stains would require the plastic backing to be removed from the gels; a complicated procedure involving special equipment (e.g. Film Remover, Amersham Biosciences, UK) that was not available during this research project. Finally, by removing the backing, the gels could be prone to breaking which makes their IA difficult. A further setback in changing the stain is that this would not overcome any binding of the proteins by the polymer.

Another possible way to overcome an interfering substance such as poorly soluble resin polymers could be the use of different IPG strips (e.g. non-linear or smaller pH ranges). In these investigations, the polymer was mainly in the lower, acidic pH range, and the use of IPG strips pH 6-9 or 6-11 would focus in on that part of the gel away from the interference. This could reduce the complexity of the gels, thereby improving the IA. IPG strips with narrow intervals with only one or two pH units are also available which allows very high protein loads and provokes excellent spot resolution. This could also simplify the analysis, as theoretically, there would be fewer spots on each of the gels. However, these require adequate amounts of samples to run enough gels to cover the pH areas of interest. In the present study, the BAL samples were of limited supply.

Adequate sample quantity was found to be another problem with the running of the 2D gels. Since all animal experiments had to be completed in the first year and a half of the study (due to the Home Office licence expiring), there was a limited amount of BAL fluid sample available and it was not possible to repeat any animal experiments to acquire more samples. Consequently, only a limited number of gels could be run.

5.5.1.2 Equipment

The greatest challenge to the 2D SDS PAGE, MS and bioinformatics approach is the complex nature of cellular proteomes. The general proteins that are visualised by conventional staining methods are normally high abundance proteins. Low abundance proteins, which are not normally detected by conventional staining, include regulatory proteins, receptors and other proteins that play a key role in cellular processes. Besides low abundance proteins, alkaline and hydrophobic proteins are generally not observed on 2D gels under standard conditions.

Despite these challenges, 2D SDS PAGE coupled with MS and bioinformatics tools, was employed in this study. Due to the extensive use of proteomic research in industry and academia, it was hoped that comparisons could be made with other studies using BAL fluid. In terms of equipment and personnel, 2D based technology is well-suited to an academic setting. Access to MS and bioinformatics resources can usually be obtained through fee-for-service facilities. Alternative proteomic methodologies rely on cutting-edge, high-cost MS instrumentation (e.g. FT-ICR mass spectrometer can cost over $1m). Another bonus with the 2D SDS PAGE techniques is that proteins stored within dried 2D gels can be identified after several years (Beranova-Giorgianni, 2003). Therefore, allowing further research to be done on the data from the present study in the future.

The gels that could be analysed in this study produced disappointing results, with only a few of the spots returning with possible protein identities. MS/MS using a nanoESI Q-Tof mass spectrometer has currently been found to be more accurate than MALDI instruments, but MS/MS is more susceptible to protein contamination. Contamination is a common problem with the 2D SDS PAGE technique, and one that was encountered in the present study. Contaminants are derived from skin and hair (e.g. keratin) and from the trypsin digestion stage of sample preparation. In this investigation, the source of such contamination could have happened at any stage from the collection of BAL fluid to the MS/MS analysis of the spots. Therefore, the use of added

precautions such as reducing the amount of handling of samples and the 2D gels may improve the results.

Accurate quantitative analysis with silver stained gels is compromised by the narrow dynamic range of the stain and by the fact that different proteins have different staining characteristic. Time and financial constraints only allowed a limited number of spots to be analysed via MS/MS. MS analysis of silver stained gels also has a number of drawbacks for example, silver stain detects proteins down to the femtomole level, and consequently, the quantity of protein in a silver stain spot is usually low. The amount of sample available for analysis is further reduced through losses that occur during the preparation of peptide digests (Westermeier and Naven, 2002). Thus, MS data from digests of silver stained proteins may contain only a few peptide signals, which may not be enough for unambiguous protein identification. Moreover, the reduced peptide signal renders the analysis susceptible to interference from contaminants; a possible scenario explaining the level of contaminants identified in this study. The only other alternative currently available is MALDI-ToF, which is also known to have serious problems with contamination, especially keratin, and has been deemed to be less accurate than MS/MS (Lieber, 2002).

5.5.2 PROTEINS IDENTIFIED BY PROTEOMICS

In total, 13 protein spots were picked and sent for MS/MS analysis (plus negative control for each gel). Despite the above mentioned problems, the MS/MS analysis did identify some interesting proteins. Albumin was identified as spots on gels from both polymer A and bleomycin models of lung injury. The most interesting proteins, prosaposin and calgranulin A, were identified on the polymer A model (double) at day 28.

5.5.2.1 Albumin

Out of the 13 protein spots picked, 4 spots were identified as a fragment of albumin. Each of the spots related to one or more different peptides. Albumin is the most abundant protein in the blood, where it acts as a carrier protein

(Peters, 1996). It is a large-molecular-weight protein that does not cross the alveolar capillary membrane rapidly. It is found in the lung and other extracellular spaces at a reduced concentration compared to the blood. The concentration of albumin in BAL fluid has been found to be higher in patients with pulmonary sarcoidosis (Kriegova *et al.,* 2006) and interstitial lung disease (Ward *et al.,* 1997). Albumin and immunoglobulin G (IgG) have been found to be present in pulmonary oedema fluid in concentrations that are 75–95% of plasma levels in lung injury pulmonary oedema (Hastings *et al.,* 2004).

Albumin concentration in BAL fluid has been proposed as a marker of increased permeability of the alveolar space in inflammation (Baughman, 1997). In the bleomycin gels, 2 out of the 6 spots, were identified as albumin; the other 4 spots all returned as contaminates. Its presence in the injured lungs of rats may be the result of chronic leakage due to increased vascular permeability.

5.5.2.2 Hemopexin

For one of the spots (Spot No - P1 day 7 polymer A (double)) the Mascot search identified it as either albumin or hemopexin. Hemopexin is also a plasma protein and is a haem-binding plasma glycoprotein. After haptoglobin, it provides the second line of defence against haemoglobin-mediated oxidative damage during intravascular hemolysis. Hemopexin, together with haptoglobin and transferrin, form the fourth most abundant group of plasma proteins after albumin, immunoglobulins and the plasma proteases (Delanghe and Langlois, 2001; Baker *et al.,* 2003). Hemopexin is a 60 kDa plasma protein that binds haem non-covalently with the highest known affinity of any haem binding proteins. Hemopexin is mainly synthesised by the hepatic parenchymal cells. Its receptors are mainly expressed in the liver but have also been detected on human T-lymphocytes and PMNs (Delanghe and Langlois, 2001).

Haem is used in a wide variety of biological processes, including respiration and energy transfer (Baker *et al.,* 2003). The major sources of extracellular haem are haemoglobin from ruptured erythocytes, myoglobin and enzymes

with haem prosthetic groups, including peroxidase and cytochrome from damaged tissues or secreted myeloperoxidase from PMNs (Delanghe and Langlois, 2001). The release of haem into extracellular fluids has potentially severe consequences for health, given that haem is highly toxic because of its ability to catalyze free radical formation (Baker *et al.,* 2003). Since there is an elevated level of PMNs at both time points (day 7 and 28) there could be an elevated level of haem in the alveoli. This could be one reason for the presence of hemopexin in the samples. Another source may be from the plasma as proteins are known to cross the alveolar capillary membrane into the alveoli or due to damage in the alveolar wall causing plasma proteins to leak into the alveolar.

These results suggest that the majority of the same proteins are present in both the bleomycin and saline samples. Therefore, it would be interesting to investigate proteins that are increased or decreased in quantity between the two samples. This is, however, difficult when using silver stain as it may give false positives due to possible differences in staining intensities. This could be overcome by using a different type of stain or by having an internal standard to normalise the spot intensities.

5.5.2.3 Calgranulin A

The polymer A gels identified calgranulin A on the day 28 gels. Calgranulin A is also known as S100A8 (Srikrishna *et al.*, 2001) and MRP8 (Sopalla *et al.*, 2002), and is a member of the S100 family, which is the largest group of small acidic calcium binding proteins (Roth *et al.*, 2003). This family of proteins has 13 (Manitz *et al.*, 2003) members and are characterised by two calcium binding sites (Vandal *et al.*, 2003). Calgranulin A belongs to a subgroup of S100 family called myeloid related proteins (MRPs) because their expression is almost completely restricted to cells of myeloid origins, i.e. PMNs and monocytes. Calgranulin B (S100A9) and S100A12 are also members of this subgroup (Rouleau *et al.*, 2003). The MRPs are expressed abundantly in the cytosol of PMNs and at lower levels in monocytes (Rouleau *et al.*, 2003).

The function of calgranulin A and the other MRPs are poorly understood. Calgranulin A is known to exist as a homerdimer but also form heterodimers in the presence of calcium with calgranulin B (Vandal *et al.*, 2003) called calprotectin in response to inflammation (Merkel *et al.*, 2005). This hetermeric complex has been found in sera of patients suffering from cystic fibrosis (Renaud *et al.*, 1994), chronic bronchitis, rheumatoid arthritis (Odink *et al.*, 1987) and crohn's disease (Tamboli *et al.*, 2003); all disorders denoted by chronic inflammation. High serum concentration of MRPs has been found in granulomatous conditions, such as tuberculosis and sarcoidosis (Ryckman *et al.*, 2003). Previous studies using polymer A as a positive control found granulomas present after a 13 week instillation study (Carthew *et al.*, 2006). No granulomas were found in this study but this could be due to the difference in time scale.

Calgranulin A, calgranulin B and the heterodimer they form have been shown to act as potent inducers of PMN chemotaxis and adhesion (Ryckman *et al.*, 2003). When calgranulin A was injected intraperitonally into mice it stimulated an accumulation of PMNs and macrophages within 4 hours (Rouleau *et al.*, 2003). During inflammatory responses, PMNs migrate in a multistep fashion from blood to inflammatory sites where they are involved in immune defence. Chronic inflammation was found after a double instillation of polymer A (Chapter 2). Calgranulin A and B are constitutively expressed in the cytosol of PMNs and constitute 30% of the total cytosolic protein (Ryckman *et al.*, 2003). Therefore, the presence of calgranulin A in this investigation could be directly related to the elevated number of PMNs found in the polymer model as demonstrated by the toxicological data (Chapter 2, Section 2.4.2). Previous studies by other investigators showing its role in recruitment of PMNs and macrophages, could explain their presence in the lungs of the polymer model, as calgranulin A, along with other S100 proteins, are now believed to be a new class of chemotactic factors contributing to PMNs migration to inflammation sites. Calgranulin A and the other MRPs pro-inflammatory properties makes them attractive targets for novel, diagnostic, therapeutic approaches to manipulate the innate immune system in inflammatory disease (Roth *et al.*, 2003).

5.5.2.4 Prosaposin

Prosaposin is a member of the saposin-like protein (SAPLIPs) family which encompasses 235 different lipid-interacting proteins. The SAPLIPs members have diverse functions (Bruhn, 2005) including:

1. **Lipid catabolism** – Saposin A, B, C and D
2. **Regulation of surfactant tension** – SP-B
3. **Antimicrobial activity** – granulysin.

Prosaposin is involved in the regulation of cell proliferation, lipid transfer and apoptosis. It is also the precursor protein for the mature saposins A, B, C and D (Bruhn, 2005). Prosaposin exists in an intracellular form (68 kDa) and an extracellular form (73 kDa). Studies (Kishimoto *et al.*, 1992) suggest that prosaposin is biosynthesised, glycosylated and secreted extracellularly to generate saposins A, B, C and D. Little is known about the function of prosaposin that is an integrated membrane component (Kishimoto *et al.*, 1992). Prosaposin has at least one lipid binding domain and three lysosomal hydrolase domains (O'Brien and Kishimoto, 1991).

Saposin A, C and D appear to stimulate enzyme activities such as galactosidase and sphingomyelinase (Kishimoto *et al.*, 1992). Saposin B acts as a detergent-like protein solubilizing multiple lipid substrates for enzyme hydrolysis, acting mainly on glycolipds as well as sphingomeylin (O'Brien and Kishimoto, 1991). A study of the distribution of saposins and prosaposin in rat tissues revealed a wide distribution. Saposins were the dominant forms in lung, spleen, liver and kidney whereas; prosaposin predominated in plasma (O'Brien and Kishimoto, 1991).

Extensive similarities in the amino acid sequence of prosaposin and saposins with that of the major pulmonary surfactant protein SP-B suggest they may have similar functions (Kishimoto *et al.*, 1992). Similar to saposins, SP-B also binds lipids; SP-B selectively interacts with phosphatidylglycerol (Baatz *et al.*, 1990; Patthy, 1991), and is an essential component of mammalian pulmonary

surfactant. Finally, SP-B, along with SP-C, are important for pulmonary surfactant replacement (Weaver and Conkright, 2001)

Prosaposin was also found to be present in the day 28 polymer sample and not in the saline control samples. In the lungs, it may be involved in lipid binding due to the presence of a lipid binding domain, and may facilitate in surfactant synthesis due to its high lipid composition. It may be there just as a precursor for one of the mature saposins (A, B, C or D). An increase in cell numbers was seen by histology in the polymer A models at day 28 (Chapter 3, Section 3.4.3.3) which partly could be accounted for by cell proliferation. One of prosaposin roles is in the regulation of cell proliferation. Other than the homologies with SP-B, there is no literature on the role of prosaposin or any of the saposins with regard to their role in the lungs. Proteomic studies on human BAL fluid from patients suffering from interstitial lung diseases have shown an elevation of saposin D when compared to healthy control patients (Wattiez *et al.*, 1999; Wattiez *et al.*, 2000).

5.5.3 FUTURE WORK

In order to confirm the proteomic results, an enzyme-linked immunosorbant assay (ELISA) for calgranulin A and prosaposin would have been beneficial. This could provide further evidence for their presence in BAL fluid collected at day 28, following a double instillation of polymer A, and their absence from saline-treated controls. An ELISA on the day 7 double instillation samples would also provide information about whether they were present at this earlier time point. ELISAs on the bleomycin model might help determine whether these proteins were specific to the type of damage observed in the polymer A model. Western blots could also be used to identify the proteins on the different gels from the single polymer A-instillation model and the bleomycin model. Unfortunately, specific equipment is required to perform western blots on 2D gels (e.g. Film Remover, Amersham Biosciences, UK; miniVE Vertical Electrophoresis System, Amersham Biosciences, UK) neither of which were available, nor was time permitted.

5.6 CONCLUSIONS

Despite difficulties with the 2D gels, a number of interesting proteins were detected as being present on the test set of gels and not in the controls. The two most interesting proteins, prosaposin and calgranulin A, were found in the polymer double instillation model at day 28. Prosaposin is a lipid binding protein with homologies to SP-B, while calgranulin A is a calcium-binding protein found in the cytosol of PMNs, and associated with chronic inflammatory diseases. From the results obtained in the present study, 2D SDS PAGE may not be an efficient method for the discovery of biomarkers, especially in complex mixtures such as BAL fluid, and in conjunction with the use of poorly soluble material such as synthetic resin polymers. This is disappointing in view of the fact that human samples of BAL and serum are readily available for screening purposes and the potential detection of early disease onset and/or pulmonary repair following drug treatment.

CHAPTER 6:

IMMUNOHISTOCHEMICAL ANALYSIS OF LUNG SECTIONS

6.1 INTRODUCTION

The discovery of novel proteins provides new opportunities for development of drug therapies and act as potential biomarkers to injury and disease. The localisation of the proteins can also lead to insights about the function of the proteins and mechanisms behind the observed injury/disease.

Secreted and transmembrane proteins have properties that lend themselves to being used as therapeutic agents or targets (Clark *et al.*, 2003), for example the suggested role of IL-6 mediating injury repair responses of airway smooth muscle cells following inflammation in diseases such as asthma and chronic bronchitis (Panettieri, 2002). Cocoacrisp (CC) is a member of the cysteine rich secretory protein (CRISP) family. These are a large group of single chained secretory proteins. The CRISP family of proteins are characterised by exhibiting a high content of cysteine residues (Guo *et al.*, 2005; Osipov *et al.*, 2005; Yamazaki and Morita, 2004). They were first discovered in mammals but they have subsequently been found in some invertebrates, insects and plants (Shikamoto *et al.*, 2005; Yamazaki and Morita, 2004). The function of CC is still being investigated.

From the investigation into the function of CC the presence of the protein was found in developing lungs of bovine embryos, using immunohistochemistry (Kahn (2005) personal communication). Recently, Balharry (2005) found the appearance of elevated levels of CC in lung tissue from a bleomycin induced model of pulmonary oedema. Therefore, it may have the potential to act as a clinical marker for early bleomycin-induced lung injury (Balharry, 2005).

The main characteristic of the CC protein is the presence of two LCCL domains, named because the best characterized proteins that were found to contain this module were Limulus factor C, cochlear protein Coch-5b2 and late gestation lung protein (Lgl1) (Liepinsh *et al.*, 2001). The key functional aspect of this protein is its sensitivity to lipopolysaccharide (LPS) endotoxin. Binding initiates a host defence mechanism, protecting the organism from

infection. It is thought that the LCCL domain may be involved in the binding of LPS (Trexler *et al.*, 2000). Lgl1 which is involved in lung maturation, also contains two LCCL domains. Increased expression of Lgl1 has been shown to coincide with the production of surfactant (Kaplan *et al.*, 1999). Figure 6.1 compares the modular architecture of CC and lgl1 proteins.

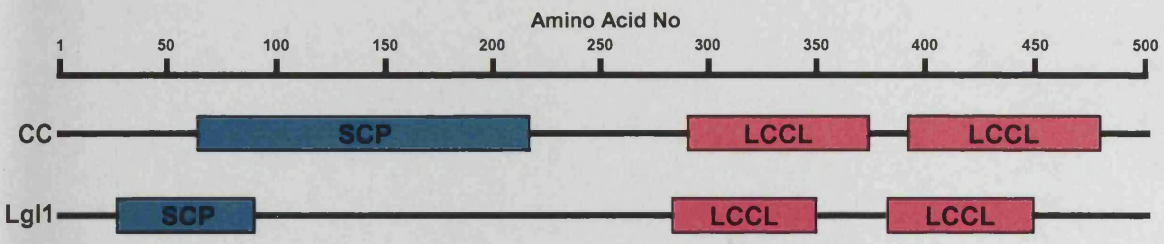

Figure 6.1: Modular architecture of CC and lgl1 proteins. Both proteins contain a secreted cysteine protein (SCP) domain and two LCCL domains. (Adapted from NCBI and Oyewumi *et al.*, 2003)

Pulmonary surfactant is synthesised and secreted by type II pneumocytes and Clara cells. It prevents alveolar collapse by providing a fluid film that lowers surface tension (Khubchandani and Snyder, 2001). In addition, it plays an active role in the pulmonary host defence system. As mentioned in Chapter 1, there are several surfactant specific proteins, (SP-A - D), which are closely associated with surfactant lipid (Goerke, 1998). SP-A is the most abundant surfactant protein in the alveoli (Khubchandani and Snyder, 2001).

SP-A is 34-36 KDa protein that has a role in lowering the surface tension, regulating synthesis of surfactant phospholipids, secretion and recycling. Along with SP-D, SP-A is involved in the innate immune responses in the lung by binding to various pathogens and particles (Khubchandani and Snyder, 2001). The localisation of SP-A using immunohistochemistry has been observed in type II cells in healthy lung section (Ochs *et al.*, 2002; Phelps *et al.*, 2004). It has been reported that in lung sections from patients suffering from lipoproteinosis, intra-alveolar accumulation of SP-A was observed

(Brasch *et al.*, 2004). SP-A localisation was selected to be studied as it is the most abundant of the four surfactant proteins.

The aim of this study was to utilise immunohistochemical techniques to analyse CC and SP-A regulation and localisation in lung sections from the polymer-instilled rat model compared to saline-instilled control model, in order to provide further information about the mechanism of polymer-induced lung injury.

6.2 MATERIALS AND STOCK SOLUTIONS

6.2.1 MATERIALS

BDH, Dorset, UK.

DPX mountant (36029)

In-house Antibody Production, Cardiff University, Cardiff, UK.

Cocoacrisp primary antibody (rabbit)

Control serum pre-bleed (rabbit)

Leica Microsystems Imaging Solution Ltd., Buckinghamshire, UK.

Leica Q550 IW workstation

Leica QWin image analysis software

Sigma-Aldrich, Dorset, UK.

Tris Buffered Saline (T6664)

Tween 20 (P7949)

Santa Cruz, USA.

Surfactant Protein A Antibody (SC-13977)

Vector Laboratories, Peterborough, UK.

Antigen Unmasking Solution (H-3300)

RTU Vectastain Universal Quick Kit (PK-7800)

Vector NovaRed Substrate Kit for Peroxidase (SK-4800)

6.2.2 STOCK SOLUTIONS

Hydrogen Peroxide Solution	-	Hydrogen Peroxide (0.3%)
		Methanol

TBS/Tween	-	Tween 20 (0.1%) Tris Buffered Saline (TBS)
Primary Antibody	-	Primary Antibody (0.05%) Blocking Serum (1.5%) TBS
Serum Control	-	Serum Control Blocking Serum (1.5%) TBS

6.3 METHODS

6.3.1 PROCESSING LUNG TISSUES FOR IMMUNOHISTOCHEMISTRY

Animals were treated with a single or double dose of polymer A, or saline and then sacrificed at 7 and 28 days after dosing, as described in Chapter 2 (Sections 2.3.1-2.3.3). The lungs were inflated and stored in 10% neutral buffered formalin at 4°C for a minimum of 24 hours (Chapter 3; Section 3.3.1.3). After this time, the lungs were processed for paraffin embedding and sectioning (Chapter 3; Section 3.3.1.4-3.3.1.6).

6.3.2 ANTIGEN UNMASKING

Sectioned tissue samples were prepared for the immunoassay by dewaxing with xylene (2 minutes) followed by a series of graded alcohols (100% to 70%; 2 minutes each). After dewaxing, antigen unmasking was carried out on the fixed lung tissue sections. The fixation process leads to cross-linking of the cellular proteins within the tissue to such an extent that the specific antigen binding sites are masked. Unmasking breaks down some of this cross-linking to expose the antigen for immunoassay techniques. The unmasking process was conducted as follows: the antigen unmasking solution was diluted (1 in 100) with distilled water, after which the solution was then heated to boiling point in a microwave. The lung tissue sections were immersed in the boiling solution (2 minutes) prior to washing in tap water (5 minutes).

6.3.3 BLOCKING ENDOGENOUS PEROXIDASE ACTIVITY

To quench peroxidase activity endogenous to the tissue, all the lung tissue sections were immersed in hydrogen peroxide solution (0.3%) for 30 minutes, followed by a wash in tap water (2 minutes).

6.3.4 IMMUNOHISTOCHEMISTRY

The immunoassay was carried out using a RTU Vectastain Universal Quick kit containing prediluted blocking serum (normal horse serum), prediluted biotinylated pan-specific secondary antibody and ready-to-use

streptavidin/peroxidase preformed complex. Tissue sections were washed with TBS/tween solution prior to incubating the sections with blocking serum (10 minutes). The sections were then incubated with the CC primary antibody, the SP-A antibody or serum control at 4°C overnight (~12 hours). The following morning, the sections were washed in TBS (3 x 5 minutes), before the secondary antibody was added. The secondary antibody was incubated for 10 minutes before being washed twice (5 minutes each) with TBS. The streptavidin/peroxidase complex was added to the sections (5 minutes). Another two washes with TBS (5 minutes) were carried out prior to addition of the peroxidase substrate, NovaRed. NovaRed solution was prepared according to the kit instructions and incubated on the sections (15 minutes). Sections were washed in tap water then counter-stained with light green stain (5 minutes). Following a 30 second wash in tap water, slides were dehydrated and fixed using DPX mounting medium.

6.3.5 IMAGE ANALYSIS

Digitised light microscopy (LM) images of saline and polymer A-treated tissue sections were captured. LM images (x200 magnification) were saved as TIFF files and imported into the Leica Q550IW IA System, for image processing (BéruBé *et al.,* 2003).

Image processing involved the adjustment of the background white levels to ensure all the lung tissue and staining was detected in the TIFF images (Figure 6.2a). Once this parameter was established, IA involved the detection of lung tissue that contained the label (shaded blue, Figure 6.2b). The total area (mm^2) of labelled protein in control versus polymer A treated samples was calculated by the computer software. Ten TIFF images were captured of random areas over two lung tissue sections at each time point. The labelled areas of these images were then quantified using Qwin analysis software.

6.3.6 STATISTICAL ANALYSIS

A two-tailed Student's t-test was then applied to the resulting data to determine any statistical differences in the expression of CC across the two time points.

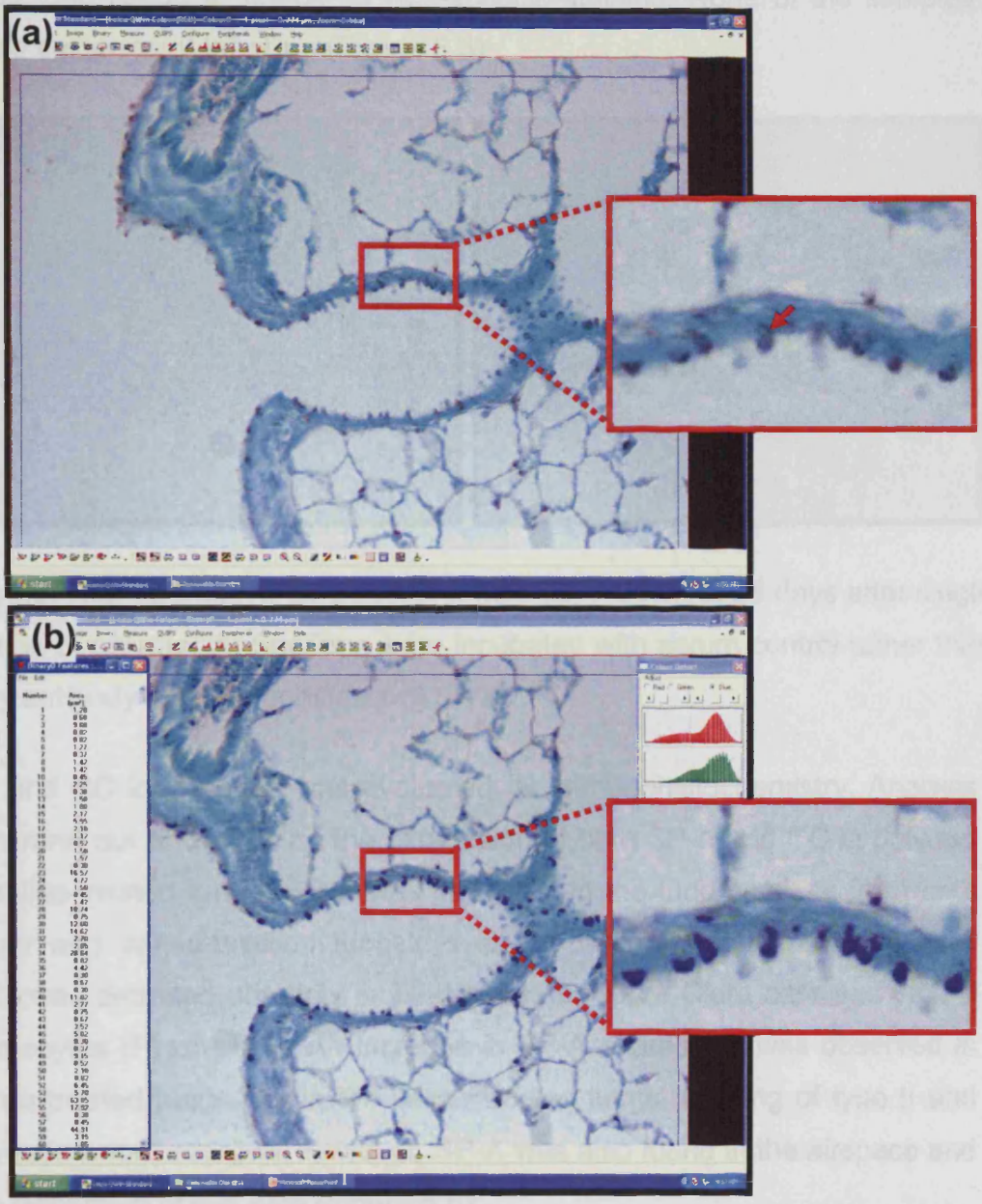

Figure 6.2: Screen prints of digital images of SP-A labelled tissue. (a) Images showing SP-A labelling as a red/brown colour, indicated by arrows; (b) Images converted by the Leica Q550IW Image Analysis System for colour detection, SP-A label coloured blue by software.

6.4 RESULTS

6.4.1 LIGHT MICROSCOPY OF LUNG TISSUE SECTIONS

LM analysis of sections treated with serum control rather than primary antibody was carried out at all time points for both saline and polymer A-instilled lung tissue to check for non-specific staining. None of the samples showed evidence of labelling (Figure 6.3).

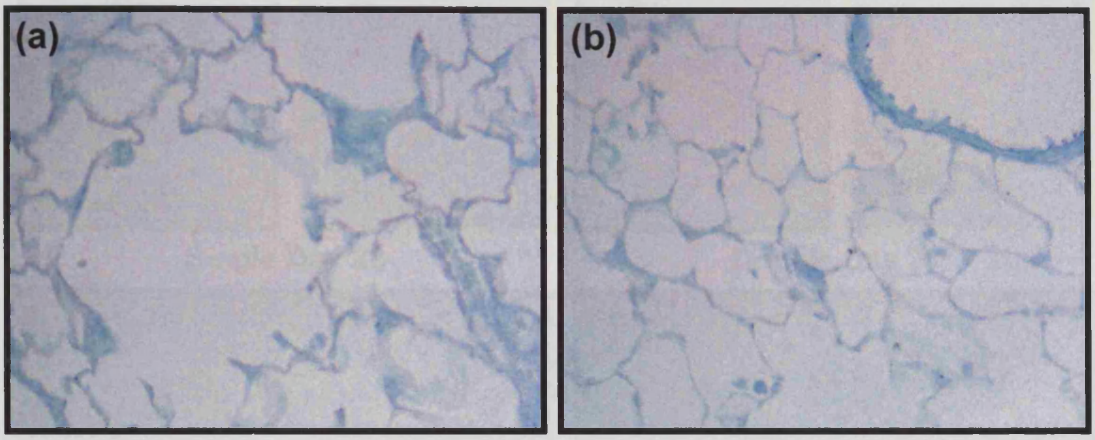

Figure 6.3: Representative lung sections from (a) 7 days (b) 28 days after single instillation of polymer A. Sections were incubated with serum control rather than primary antibody (x200 magnification) (n=3).

SP-A and CC localisation was evaluated by immunohistochemistry. Analysis was carried out to determine the expression of both SP-A and CC in polymer and saline-treated lungs. SP-A was observed in the lung sections from both polymer and saline-instilled lungs. In all the saline-treated samples SP-A protein was detected primarily in what appeared to be Clara cells and type II pneumocytes (Figure 6.4). An increase in SP-A expression was observed in polymer treated lungs. As in the saline treated lungs, staining of type II and Clara cells were recorded. However, SP-A was also found in the airspace and in the cytoplasm of the AMs (Figure 6.5).

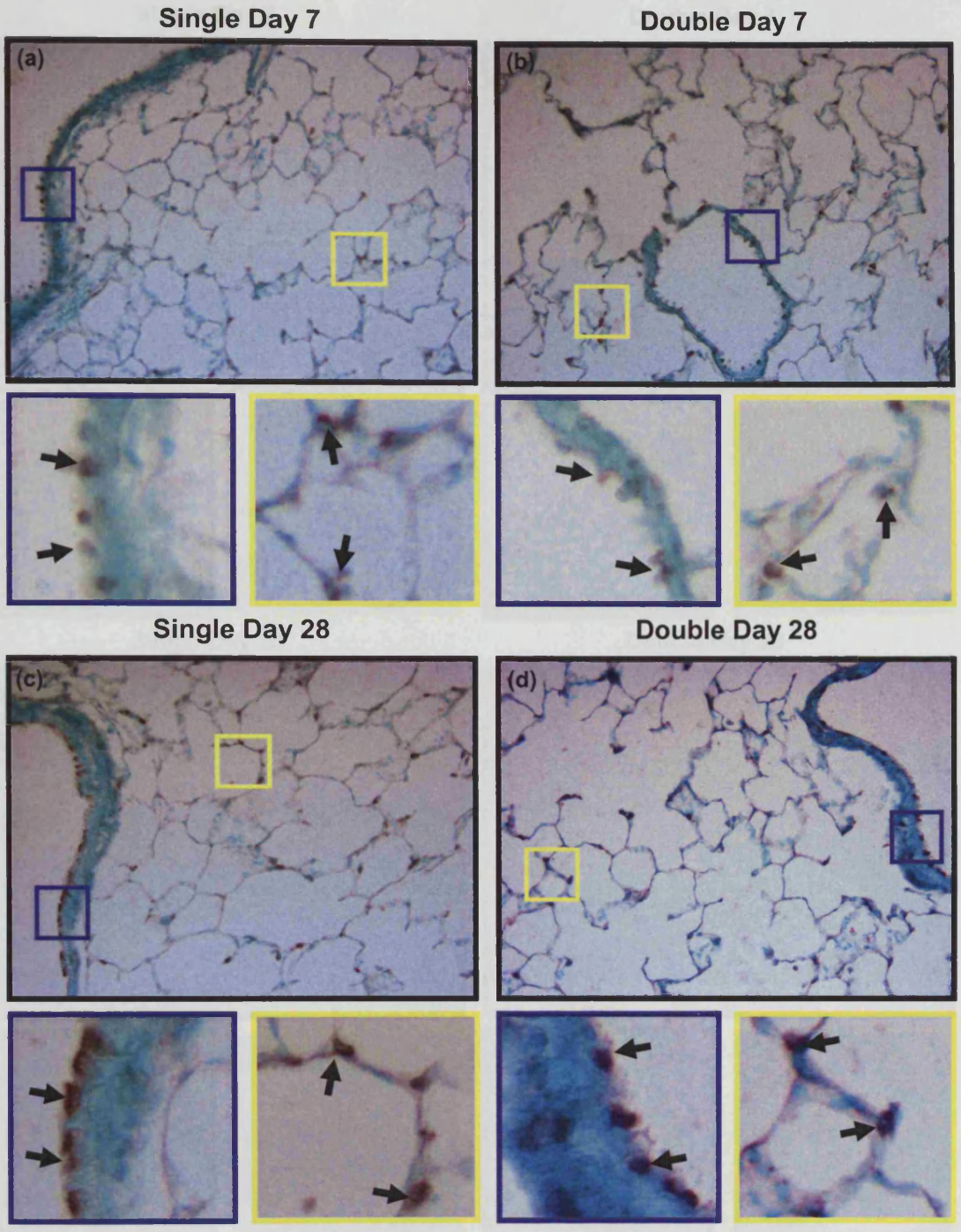

Figure 6.4: Representative SP-A expression in lung tissue from saline-treated animals. SP-A labelling appears red/brown, indicated by arrows; (a) 7 days after single instillation, (b) 7 days after double instillation, (c) 28 days after single instillation and (d) 28 days after double instillation. Blue boxes show stained Clara cells in the airways. Yellow boxes show examples of type II pneumocyte staining. All images in black boxes at x200 magnification. Colour boxes x1000 magnification (n=3).

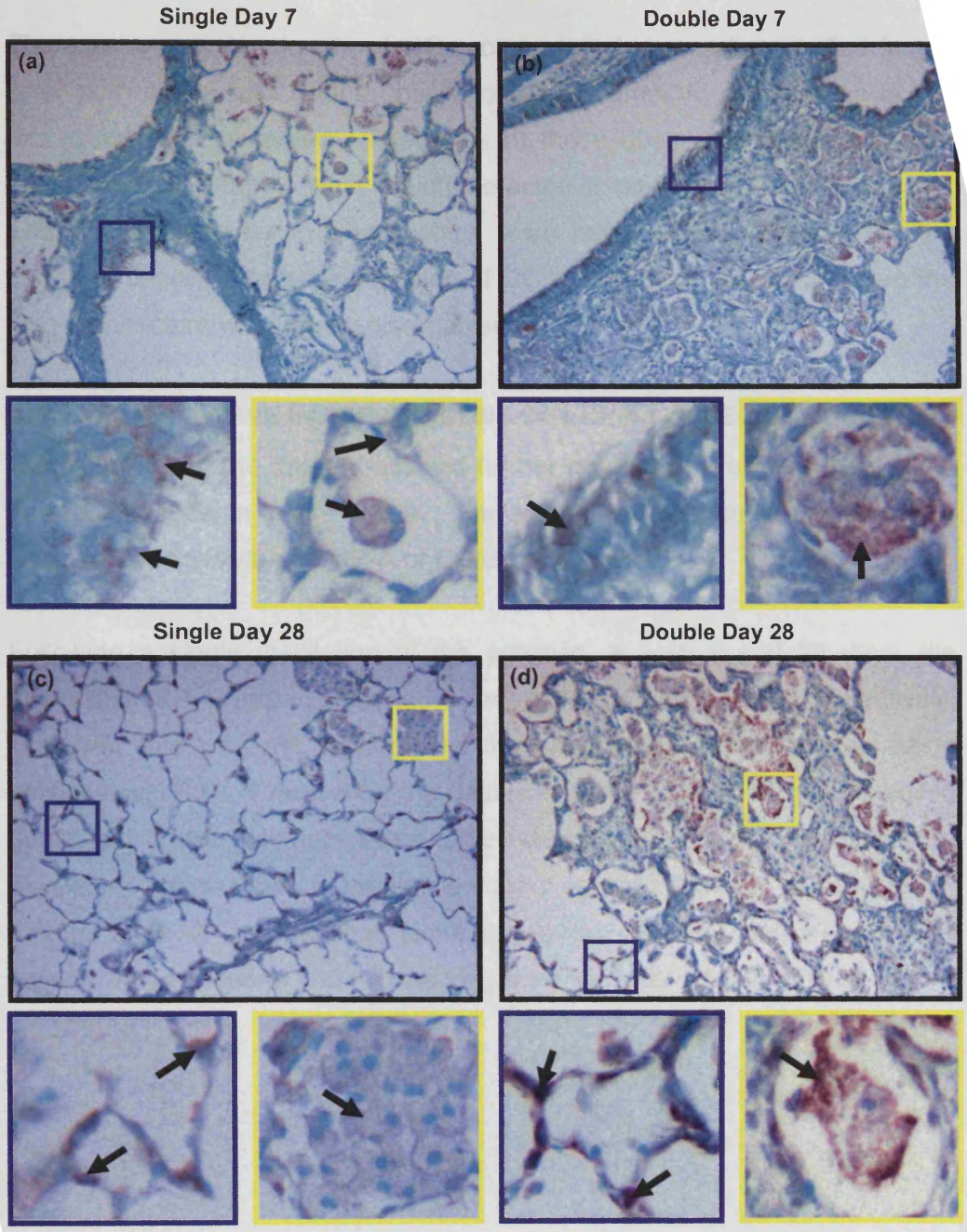

Figure 6.5: Representative SP-A expression in lung tissue after instillation of polymer A. SP-A labelling appears red/brown, indicated by arrows; (a) 7 days after single instillation, (b) 7 days after double instillation, (c) 28 days after single instillation and (d) 28 days after double instillation. Blue boxes show examples of type II pneumocyte staining. Yellow boxes show staining in the airspaces. All images in black boxes at x200 magnification. Colour boxes x1000 magnification (n=3).

There were very low levels of CC protein detected in saline-instilled lungs. After both single and double instillations of polymer A, an increase in CC expression was observed. Examples of these observations are shown in Figure 6.6. CC proteins were mainly detected lining the surface of the tissue. This appeared to be in areas which were more severely affected by the instillate. There was also expression of CC in regions of the tissue where the lung architecture was largely disorganised.

6.4.2 QUANTITATIVE IMAGE ANALYSIS OF LUNG TISSUE SECTIONS

Quantification of the images allowed further non-subjective analysis of SP-A and CC expression in the tissue. The area (mm^2) of protein label detected was used as the value for SP-A or CC expression.

Following a single instillation of the polymer, at both 7 and 28 days, the amount of SP-A expression had increased by 3 and 4-fold, respectively. However, this was not significantly different from that found in the saline sections, whereas, 7 days after the double instillation, the SP-A had increased by 11-fold in the polymer-treated lung tissue sections. This was statistically significantly higher than in the saline control sections ($p \leq 0.05$). By day 28 the amount of SP-A detected had fallen to a 4-fold increase compared with the saline-treated sections and was no longer significantly different (Figure 6.7).

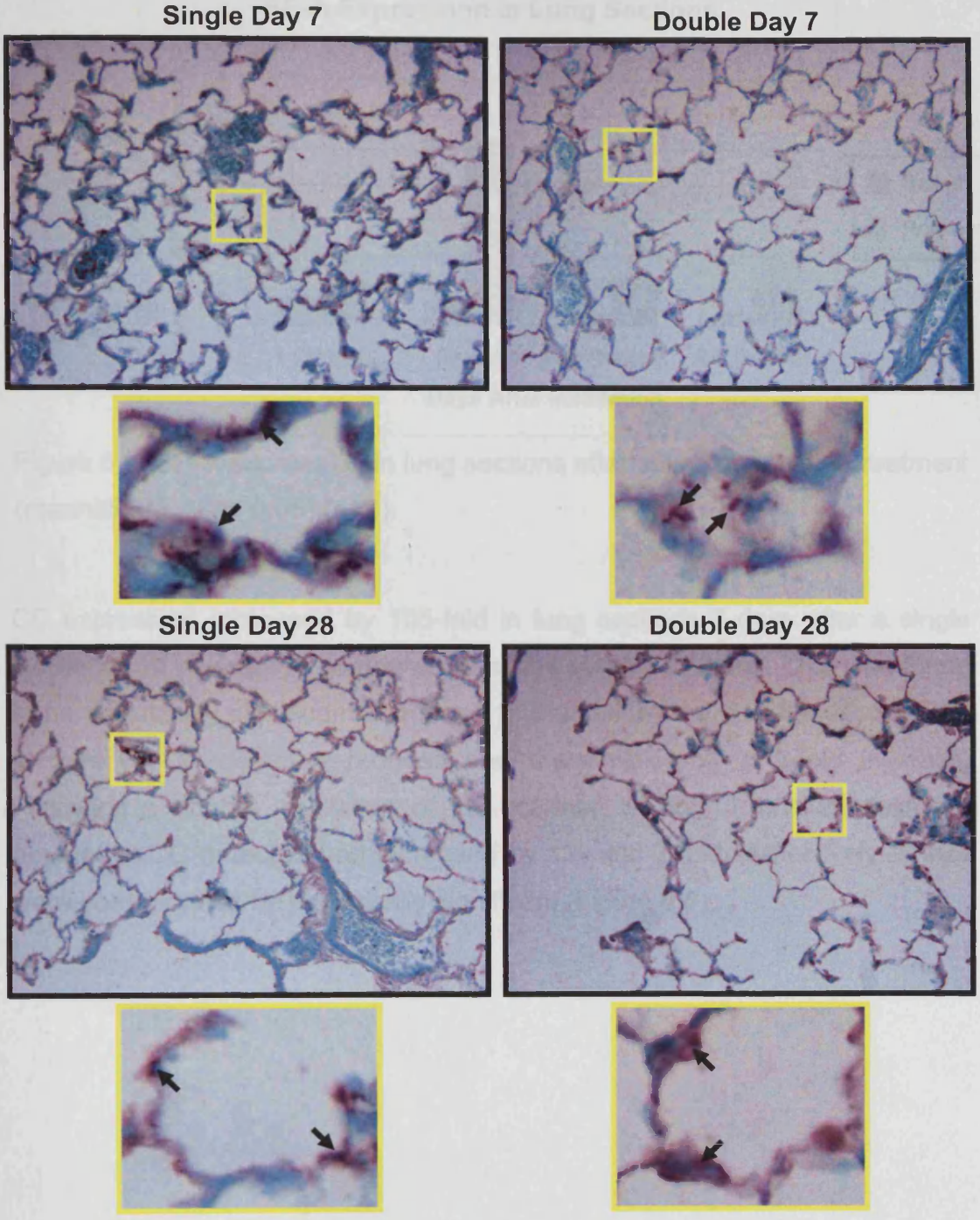

Figure 6.6: Representative CC expression in lung tissue after instillation of polymer A. CC labelling appears red/brown, indicated by arrows; (a) 7 days after single instillation, (b) 7 days after double instillation, (c) 28 days after single instillation and (d) 28 days after double instillation. Yellow boxes show examples of CC staining in the alveolar epithelium (black boxes x200 and yellow boxes x1000 magnification) (n=3).

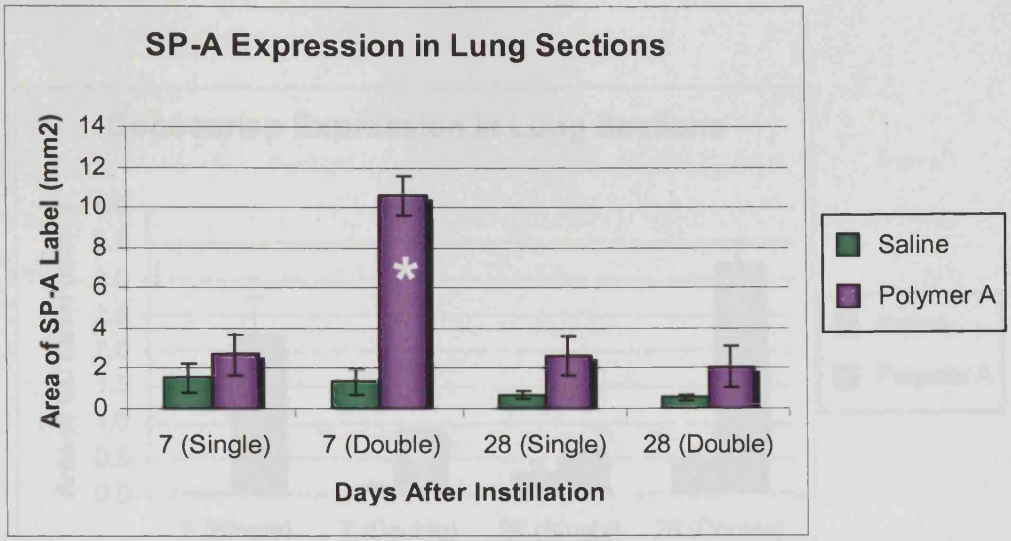

Figure 6.7: SP-A expression in lung sections after saline or polymer treatment (mean±SEM, *=p≤ 0.05) (n=3).

CC expression increased by 105-fold in lung sections 7 days after a single instillation of polymer A compared to saline control sections. This was found to be statistically significant compared to the saline control. After 28 days the amount of CC detected reduced and there was only a 2-fold increase. Following a double instillation of the polymer, at both 7 and 28 days the amount of CC detected had increased by 12- and 7-fold respectively. These were both found to be statistically significant (Figure 6.8).

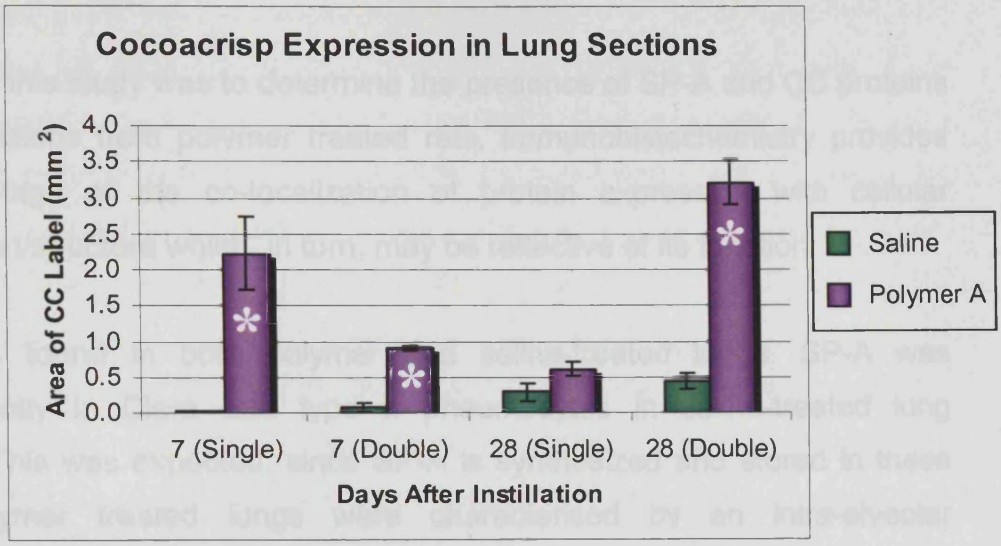

Figure 6.8: CC expression in lung sections after saline or polymer treatment (mean±SEM, *=p≤ 0.05) (n=3).

6.5 DISCUSSION

The aim of this study was to determine the presence of SP-A and CC proteins in lung sections from polymer treated rats. Immunohistochemistry provides the advantage of the co-localization of protein expression with cellular organisation/structure which, in turn, may be reflective of its function.

SP-A was found in both polymer and saline-treated lungs. SP-A was predominantly in Clara and type II pneumocytes in saline-treated lung sections. This was expected, since SP-A is synthesized and stored in these cells. Polymer treated lungs were characterised by an intra-alveolar accumulation of SP-A. SP-A is involved in the innate immune responses in the lung by binding to various pathogens and particles (Khubchandani and Snyder, 2001). Therefore, the current data suggest that the SP-A is binding to the polymer particles in the airspaces. Intracellular SP-A content of AMs is increased in polymer-treated lung sections. This may be due to SP-A activation of AMs or the due to the presence of SP-A in surfactant that is ingested by AMs in the normal course of phagocytosis (Hermans and Bernard, 1999). Furthermore, the AMs would be ingesting polymer particles that may well be coated with the protein. Both toxicological (Chapter 2) and histopathological (Chapter 3) data collected from the instillation models indicated an increase in AMs. Moreover, there was no SP-A antibody signal detected in the serum control samples.

Several investigations by other workers have examined surfactant protein alterations in lung disease. Investigations using enzyme-linked immunosorbant assay (ELISA) to examine SP-A concentration in BAL fluid have shown elevated levels of SP-A in patients suffering from hypersensitive pneumonia, lipoproteinosis, acute lung Injury, sarcoidosis and in asbestos-exposed workers (Gunther *et al.*, 1994; Hamm *et al.*, 1994; Kuroki *et al.*, 1998; Lesur *et al.*, 1996; Cheng *et al.*, 2003). A reduction in SP-A was observed in cystic fibrosis, cigarette smokers and acute respiratory distress syndrome (ARDS) patients (Kuroki *et al.*, 1998; Shijubo *et al.*, 1998; Postle *et*

al., 1999). In order to support the immunohistochemistry data collected, an ELISA would have been beneficial, as the levels of SP-A in BAL fluid and plasma could be determined. However, due to time and money constraints this could not be performed. Elevated levels of SP-A in blood or BAL fluid could have the potential as a biomarker for injury. However since it should be noted that elevated SP-A levels are observed in a number of lung diseases, thus it would not be a specific biomarker for polymer-induced injury.

In this study, CC was found to be expressed at all time points after polymer-instillation. There was also a low level detection in saline-instilled lung sections, i.e. low level expression or non-specific binding. As with the SP-A, there was no signal in serum control samples confirming that the CC expression in the experimental samples were genuine.

Unlike SP-A, the function of CC is unknown. CC has been found to be located on the surface of the lungs, and it has a homology to Lgl1 and other CRISP proteins, suggesting that it is a secreted extracellular protein. If the similarity of CC and Lgl1 persists, then CC (like Lgl1) could be involved in lung defence (Trexler *et al.*, 2000). The response of CC response to lung injury seems to be transient, as significantly higher levels are found after 7 days, in sections from both single and double polymer treatments. There is a return to baseline values 28 days after a single instillation but there is still significant difference at this time point after a double-instillation, suggesting the double instillation is associated with some pretty severe pulmonary changes at 28 days. The levels of CC in bleomycin-treated lungs were also found to be elevated at day 7 after a single instillation. There were no significance differences seen in the double bleomycin instillation samples, suggesting that the type of injury caused by the polymer is different to that found in the bleomycin sections.

Another function of the Lgl1 protein is in the regulation of extracellular matrix (ECM) degradation (Kaplan *et al.*, 1999). The breakdown of the ECM, particularly proteoglycans, leads to increased vascular permeability which is a critical step in the onset of pulmonary oedema (Miserocchi *et al.*, 2001). Similarly, Lgl1 causes trypsin inhibition which can result in reduced ECM

degradation, and hence, reduced oedema. Therefore assuming that CC has a similar role as Lgl1, this could infer that CC may be involved in the regulation of the ECM. CRISPs isolated from snake venom have been reported to function by blocking voltage-gated calcium and/or potassium channels, therefore providing a possible mechanism for CC to resist the development of pulmonary oedema (Yamazaki and Morita, 2004; Guo *et al.*, 2004). Unlike the results found in the bleomycin-treated lungs sections, the location of CC signal was found predominantly on the lung surface and not associated with blood vessels (Balharry, 2005). The detection of an increase level of the CC in blood or BAL fluid samples would increase the prospect that CC could potentially be used as a biomarker for polymer-induce injury or in the subsequent repair of damaged tissue.

6.6 CONCLUSION

To summarize, SP-A and CC have been found to be upregulated in the polymer A model indicating that they play a role in lung defence following exposure to polymer particles. Increased levels of CC and SP-A in the BAL and blood could provide a potential clinical marker for induced lung injury.

CHAPTER 7

GENERAL DISCUSSION

7.1 OVERVIEW

The primary aim of this study was to identify biomarkers for pulmonary oedema, inflammation and epithelial repair. This was achieved by using an animal model (rat) of lung injury to develop a better understanding of the protein alterations in the disease state.

The inhalation of poorly soluble particles (PSPs) such as synthetic resin polymers causes a spectrum of morphological, biochemical and molecular changes in the rat lungs (Mossman, 2000). These include inflammation, acute and chronic epithelial cell damage, epithelial changes including hyperplasia, metaplasia and neoplasia, alveolitis, granuloma formation and alterations in interstitial cell populations that may lead to interstitial fibrosis (Mossman, 2000). The relatively high molecular weight and poor aqueous solubility of the synthetic polymers make them ideal for commercial use in aerosolized formulations (e.g. hairspray, deodorant). However, these characteristics may render them bio-persistent in the lung environment and cause lung overload. In this study, a single and double intratracheal instillation of the polymers was employed. This was expected to induce a model of lung inflammation, oedema and the progressive destruction of normal lung architecture, as a means to characterise any protein alterations that occurred during these injurious events.

An important objective was to use conventional toxicological and histological approaches to characterise the injury/repair model and to evaluate the severity of lung injury. Once this had been accomplished, the principal aim was achieved by applying proteomics to evaluate the protein changes in broncho-alveolar lavage (BAL) fluid during various stages of lung injury.

Proteomics has proven to be a powerful tool for identifying early changes at the protein level in a variety of disease states (Görg *et al.*, 2004). Using two-dimensional sodium dodecyl sulphate polyacrylamide gel electrophoresis (2D SDS PAGE), combined with tandem mass spectrometry (MS/MS) to analyse

BAL fluid proteins, it was possible to identify markers for pulmonary damage and repair.

The first hypothesis for this study was that polymer-induced lung injury caused the same damage as bleomycin-induced lung injury. However, this was not the case, as both the toxicological and histopathological studies indicated significant differences in the manifestation of lung damage. In the former, changes were observed for the lung to body weight, surface protein concentration and LFC values, and in the latter, intra-alveolar oedema prevailed, rather than the expected interstitial oedema, in the polymer model (Chapters 2 and 3). These differences may have arisen due to the two substances having dissimilar time courses for peak injury or different mechanisms of toxicity in the lungs. Bleomycin-induced lung injury is a well characterised model of direct fibrotic injury (Aso *et al.*, 1976; Starcher *et al.*, 1978; Thrall *et al.*, 1979; Catravas *et al.*, 1983; Balharry *et al.*, 2005), and the differences seen in the lung generated by the polymer implied that the polymer generated a distinct model of lung injury. Comparisons with other lung models, in particular other PSPs, could provide further information about the type of mechanism involved. Titanium dioxide, carbon black and diesel particulate are all classed as PSPs. They have been used by several research groups to induce lung injury (Cullen *et al.,* 2000; Donaldson, 2000; Mossman, 2000; Borm *et al.*, 2004). PSPs have been found to cause pulmonary inflammation (as seen in the polymer model) which leads to proliferation and tissue remodelling that can progress towards fibrosis and neoplasic lesions. It has been hypothesised that the damage is caused by reactive oxygen species (ROS) and reactive nitrogen species (RNS) (Borm *et al.,* 2004; Knaapen *et al.,* 2004). These oxidants can be derived from the oxidant-generating properties of particles themselves, which are mostly determined by the physicochemical characteristics of the particle surface, and the ability of particles to stimulate cellular oxidant generation. Cellular ROS/RNS can be generated by various mechanisms, including mitochondrial activation or activation of NAD(P)H-oxidase enzymes (Knaapen *et al.,* 2004). Another hypothesis for the lung injury caused is that there is an overload of the lungs' clearance mechanism. Indeed, enlarged, aggregated and possibly foamy

macrophages were observed in the polymer model, and may be indicative of lung overload (Cullen *et al.,* 2000; Oberdorster, 2002; Borm *et al.,* 2004; Elder *et al.,* 2005).

The second hypothesis was that polymer and bleomycin-induced lung injury caused protein changes in BAL fluid which can be identified using proteomic techniques. The toxicological data showed for both the polymer and the bleomycin models that there was a significant increase in surface protein collected from the lungs compared to the saline controls. Proteomics was used to analyse the difference in protein profiles in the models compared to saline controls. The proteomic technique 2D SDS PAGE was employed due to its extensive use for proteomic separation of BAL fluid proteins on a gel by other researchers, enabling possible comparisons to be made between different studies (Lindahl *et al.,* 1998; Wattiez *et al.*, 2000; Bredow *et al.*, 2001; Wang *et al.,* 2005). In light of the second hypothesis, the proteomic technique, 2D SDS PAGE did not separate the protein mixtures adequately to allow comprehensive image analysis and further identification of protein spots of interest with the polymer model. This was an unexpected development since other pulmonary research groups have used successfully 2D SDS PAGE, coupled with MS, to analyse BAL fluid. For example, Lindahl *et al.* (1998), observed levels of IgA, ceruloplasmin and the pro form of apolipoprotein A-1 to be lower in smokers BAL fluid when compared to non-smokers. Von Bredow *et al.* (2001), reported reduced amounts of SP-A in the BAL fluid of cystic fibrosis patients when compared to healthy controls, while Wattiez *et al.* (2000), found an accumulation of SP-A in patients suffering from idiopathic pulmonary fibrosis. Sabounchi-Schütt *et al.* (2003), used 2D SDS PAGE to find increased levels of Clara cell protein, heat shock 27 kd protein 1 and $ß_2$-microglobulin in BAL fluid collected from patients suffering from sarcoidosis.

It should be noted that all the BAL fluid samples used in the aforementioned studies were collected from human patients and not animal models. In the few animal studies that have been conducted, altered expression patterns in BAL protein profiles were distinquished (e.g. Zhao *et al.,* 2006; Signor *et al.,* 2004).

Zhao *et al.* (2005), used normal and asthmatic mice models to investigate changes in BAL fluid and found a significant increase in lungkine, a family of chitinases, gob-5 and surfactant protein-D. Signor *et al.* (2004), studied the protein content of BAL fluid in rats following an allergen and an endotoxin challenge. They discovered an increase in T-kininogen I and II, α-1-antitrypsin, calgranulin A, fetuin A and B, and haptoglobin, in both models when compared to controls, and a decrease in Clara cell 10 kDa secretory protein and SP-B. The reason for the disappointing results obtained from the polymer model was thought to be due to 'interference' caused by the polymer particles that remained suspended in the BAL fluid. This line of reasoning was made more evident by the lack of 'interference' observed in the 'particle-free', bleomycin model.

In terms of equipment and personnel, the 2D based technology was well suited to the academic setting. Advantages of this technique were that it provides a hard copy record of separation, there was good resolution of proteins, it gave information on MW and pI and post-translational modifications could be detected. 2D SDS PAGE was a relatively inexpensive technique when compared to some of the other mass spectrometry based techniques.

The limitations to the 2D SDS PAGE technique were three-fold. Firstly, only a restricted subset of proteins was amenable to 2D SDS PAGE (e.g. membrane and very basic proteins were not represented). Therefore, potential proteins of interest may have been missed as they were not resolved on the 2D gels. Secondly, 2D SDS PAGE was a laborious method where analysis and quantification of low abundant proteins (<150kDa) was technically difficult. A more high throughput and sensitive technique such as protein chips (Chen *et al.,* 2003), could increase the number of proteins identified, and hence, produce a large number of potential biomarkers. Thirdly, protein spot/gel analysis was limited by elaborate image analysis routines, derived from commercial software packages, which have not been standardized at the academic research level. A more automated and user friendly software package could not only speed up the analysis of 2D gels but could also lead

to more protein spots of interest being recognized and identified by MS analysis.

In the study, 2D SDS PAGE identified a smaller number of changes than expected (i.e. absence/presence) between polymer and control profiles. One interpretation would be that rather than new proteins being translated, the increase in surface protein concentration was more likely due to the up/down regulations of proteins. Therefore, it would have been interesting to analyse these differences as well. However, due to the use of silver staining to detect proteins, this would be difficult due to limited dynamic range (Görg *et al.*, 2000). Using 2D SDS PAGE based proteomics, differences between the reference and altered states were measured by quantifying the ratios of spot intensities between independent 2D gels. Unfortunately, spot recognition and quantification was time-consuming and not particularly accurate, even if computer-assisted (Mann, 1999). A more accurate technique for quantitative proteomics would be isotope-coded affinity tags (ICAT) (Gygi *et al.,* 1999). Rather than relying on 2-D PAGE separation and subsequent image analysis of proteins immobilized within gels, ICAT utilizes isotopic tags which covalently bind to cysteines within a protein. These tags would be nearly identical but exist in a light or heavy isotopic form. For example, one can label a normal sample with the light reagent and a diseased sample with the heavy reagent. When bound to the same peptide, a concrete mass change of exactly eight mass units would be evident when analyzed by mass spectrometry. Protein tagging would then be followed by separation and identification of proteins within these complex mixtures by liquid chromatography and mass spectrometry (Gygi *et al.,* 1999; Han *et al.,* 2001).

The strength of this technique lies in its ability to allow quantification and identification within a single analysis. It also can be applied to samples from any source, as it does not require metabolic labeling. Weaknesses include the frequent need for extensive sample fractionation before MS/MS analysis can proceed. Also, since the procedure targets cysteine residues, certain proteins and peptides will be missed – in particular those that undergo post-translational modifications (Gygi *et al.,* 1999; Han *et al.,* 2001)

7.2 CONCLUSIONS

In conclusion, the proteomic analysis of the polymer A model has provided new potential markers for pulmonary oedema and inflammation. The many findings from this study include:

- The use of toxicology and histology was demonstrated as an appropriate technique for characterising and quantifying a model of pulmonary injury

- The optimisation of 2D SDS PAGE for analysis of BAL fluid

- Implementation of 2D SDS PAGE to separate BAL fluid proteins to aid the search for biomarkers

- Prosaposin and calgranulin A identified using proteomics as potential protein markers in the polymer A model. The presence of these proteins in blood renders them potential clinical tools

- Cocoacrisp protein and surfactant protein A were also identified, using immunohistochemistry, as possible biomarkers for polymer A-induced pulmonary injury. The presence of these proteins in BAL and blood render them potential clinical tools.

7.3 ULTIMATE OBJECTIVE

Presently, most clinical tests for lung injury are based on changes in pulmonary function (Jones and McAteer, 1990). Chest radiographs and blood gas monitoring will only describe the situation relatively late after the initial cellular disturbance (Jones and McAteer, 1990; Hansen-Flaschen, 1995). Hence, there is now considerable interest in detecting early phases of lung injury to aid in diagnoses and treatment. Identification of biomarkers for lung injury in BAL fluid could provide the ground work for a clinical test. Ultimately,

a specific biomarker in blood could provide a more efficient test, as blood can be collected quickly and without the need of anaesthetics. The use of such a non invasive clinical evaluation could become routine in hospitals to test for severity, time point and type of lung injury, as well as for screening and differentiation of benign versus malignant disease, differential histology and defining prognosis. A clinical test could also provide information about the patient's response to current drugs or treatment, this information could provide an indication to the clinician to whether the patient is on the right course of treatment. Another application could be 'in the field' to assess priority of care for victims following exposure to high risk material. The test could ideally provide information relating to type of injury and its severity to enable physicians to treat only exposed patients, i.e. triage.

The two different models, i.e. polymer and bleomycin, provided different protein profiles to each other and to the control. Toxicological and histopathological investigations showed that the two models caused a different type of lung injury. Therefore, the protein markers identified can be said to be injury-type specific, where bleomycin-induced fibrosis, and the resin polymers initiated pulmonary oedema. A library of such biomarkers would now be required to further identify and categorize different types of injury; ideally incorporated into one simple clinical test for pulmonary damage.

The discovery of cocoacrisp (CC) and surfactant protein A (SP-A) expression in oedematous tissue may represent the best biomarkers uncovered by this study. Cocoacrisp may be linked to surfactant production, extracellular matrix remodelling and the blocking of ion channels. One of the most significant elements of this discovery was that CC was detected on the surface of the lungs, this finding may prove fruitful in the possible development of a diagnostic tool for blood or BAL samples. SP-A is a known marker for lipoproteinosis, hypersensitive pneumonia, acute lung injury, sarcoidosis and in asbestos-exposed workers (Gunther *et al.,* 1994; Hamm *et al.,* 1994; Lesur *et al.*, 1996; Kuroki *et al.*, 1998; Cheng *et al.*, 2003). It has also been detected in BAL fluid and blood and is specifically made in the lungs, and thus, may represent a good biomarker for lung injury. Finally, these proteins may

potentially form the basis of a diagnostic assay used to determine expose and harm in the respiratory epithelia to aerial xenobiotics and/or provide a target for drug therapy.

7.4 FUTURE WORK

2D SDS PAGE

2D SDS PAGE technology, on which most proteome profiling is based currently, is limited in various ways, particularly in the difficulty of finding and quantitatively estimating low abundance proteins. The major drawback in this study was the image analysis software used to detect changes in the profile and the subsequent tandem mass spectrometry analysis used to identify spots of interest. To overcome image analysis problems, 2-D Fluorescence Difference Gel Electrophoresis (2-D DIGE) technology (Amersham Biosciences, UK) could be employed. 2-D DIGE is a method that labels protein samples with fluorescent dyes before 2-D electrophoresis, enabling accurate analysis of differences in protein abundance between samples. It is possible to separate up to three different samples within the same 2-D gel. This permits the inclusion of up to two samples (i.e. control and test) and an internal standard in every gel. The internal standard is prepared by mixing together equal amounts of each sample in the experiment and including this mixture on every gel within an experimental series. Normalization of the internal standard across gels allows the ratio of relative abundance of the same protein in different samples to be compared directly (Hoffert *et al.,* 2004; Shen *et al.,* 2004).

At the present time, protein arrays are poised to become a central proteomics technology (Shen *et al.,* 2006). The use of protein arrays would eliminate the need to separate proteins on gels. In the microarray or chip format, detection of proteins and monitoring their expression levels can be carried out with minimum use of materials, while generating large amounts of data (Shen *et al.,* 2006). As with the 2D-DIGE technology, reference and test samples can be labelled with fluorescent dyes, and then incubated on a chip of arrayed

antibodies. Increased or decreased protein expression is then assessed using a scanner and up- or down-regulated proteins can be identified from the ratios of the two dyes. There are a number of important technical challenges and bottlenecks in protein array technologies, including the problems of obtaining global, functional protein expression for array construction, coupling proteins to the surface of the array, the sensitivity and dynamic range of detection systems, standardisation and data storage (Chen *et al.,* 2003; Shen *et al.,* 2006).

PROTEIN MARKERS

Further investigations into the function of CC, whether it is present in BAL, and whether it can be detected in blood are important. Cocoacrisp is potentially a very good marker for early oedema and research into its role in the development or resistance to oedema could prove informative. Immunohistochemistry may provide the localization of the prosaposin and calgranulin A proteins identified by the proteomic analysis in lung tissue sections that may provide further information on their role in lung injury. Western blots for SP-A and CC could also be used to investigate their presence in BAL fluid samples, whereas ELISA (enzyme-linked immunosorbant assay) could be used to determine the presence of all the proteins in blood samples. Finally, selective immunohistochemistry and ELISA using proteins from candidate genes identified in other investigations have the potential to be used in the discovery of protein biomarkers for lung injury and disease without the need to separate proteins on a gel.

BRONCHO-ALVEOLAR LAVAGE

The collection of BAL fluid samples from humans is a difficult procedure that requires a qualified clinician. The problems related to the BAL procedure, such as hypoxemia and hypotension, are often directly linked to the effects of general anaesthesia. Due to the risks involved, it is particularly difficulty to obtain normal control samples. For that reason, it would be preferable to identify changes in specific proteins present in the blood, an easy component to collect from humans, to act as a clinical marker. The proteins identified in

this study were not specific to the lungs, and their alterations in blood might be observed. The final limitation in this study was the amount of BAL fluid samples available due to the small number of animal experiments carried out. To overcome this, a cell model such as *in vitro* models of human respiratory epithelia (e.g. MatTek Corp., USA), could be used to replace the need for more animals. This would also reduce differences seen within species, since rats have been found to respond to low-toxicity dusts with more inflammation, proliferation and metaplasia than other species (Donaldson, 2000).

REFERENCES

Abbott, A. (1999). The promise of proteomics. *Nature* **402**(703), pp. 715-720.

Adamson, I. Y. and Bakowska, J. (1999). Relationship of keratinocyte growth factor and hepatocyte growth factor levels in rat lung lavage fluid to epithelial cell regeneration after bleomycin. *American Journal of Pathology* **155**(3), pp. 949-954.

Adamson, I. Y. and Prieditis, H. (1998). Silica deposition in the lung during epithelial injury potentiates fibrosis and increases particle translocation to lymph nodes. *Experimental Lung Research* **24**(3), pp. 293-306.

Adamson, I. Y. R. (1984). Drug-Induced Pulmonary Fibrosis. *Environmental Health Perspectives* **55**, pp. 25-36.

Alberti, A., Luisetti, M., Braschi, A., Rodi, G., Iotti, G., Sella, D., Poletti, V., Benori, V. and Baritussio, A. (1996). Bronchoalveolar lavage fluid composition in alveolar proteinosis. Early changes after therapeutic lavage. *American Journal of Respiratory and Critical Care Medicine* **154**(3 Pt 1), pp. 817-820.

Amersham Biosciences. (2002). *www.amershambiosciences.com* Amersham Biosciences.

Aso, Y., Yoneda, K. and Kikkawa, Y. (1976). Morphologic and biochemical study of pulmonary changes induced by bleomycin in mice. *Laboratory Investigation* **35**(6), pp. 558-568.

Baatz, J. E., Elledge, B. and Whitsett, J. A. (1990). Surfactant protein SP-B induces ordering at the surface of model membrane bilayers. *Biochemistry* **29**(28), pp. 6714-6720.

Baker, H. M., Anderson, B. F. and Baker, E. N. (2003). Dealing with iron: common structural principles in proteins that transport iron and heme. *Proceedings of the National Academy of Science of the United States of America* **100**(7), pp. 3579-3583.

Balazs, G., Noma, S., Khan, A., Eacobacci, T. and Herman, P. G. (1994). Bleomycin-induced Fibrosis in Pigs: Evaluation with CT. *Radiology* **191**, pp. 269-272.

Balharry, D. (2005). *Gene Profiling of Lung Toxicity.* University of Cardiff.

Balharry, D., Oreffo, V. and Richards, R. (2005). Use of toxicogenomics for identifying genetic markers of pulmonary oedema. *Toxicology and Applied Pharmacology* **204**(2), pp. 101-108.

Baughman, R. P. (1997). The uncertainties of bronchoalveolar lavage. *European Respiratory Journal* **10**(9), pp. 1940-1942.

Bell, D. Y. and Hook, G. E. (1979). Pulmonary alveolar proteinosis: analysis of airway and alveolar proteins. *American Review of Respiratory Disease* **119**(6), pp. 979-990.

Beranova-Giorgianni, S. (2003). Proteome analysis by two-dimensional gel electrophoresis and mass spectrometry: strengths and limitations. *Trends In Analytical Chemistry* **22**(5), pp. 273-281.

Berg, I., Schluter, T. and Gercken, G. (1993). Increase of bovine alveolar macrophage superoxide anion and hydrogen peroxide release by dusts of different origin. *Journal of Toxicology and Enviromental Health* **39**(3), pp. 341-354.

Berkelman, T. and Stenstedt, T. (1998). *2-D Electrophoresis. Principles and Methods* Amersham Biosciences.

Berman, J. S., Beer, D. J., Theodore, A. C., Kornfeld, H., Bernardo, J. and Center, D. M. (1990). Lymphocyte recruitment to the lung. *American Review of Respiratory Disease* **142**(1), pp. 238-257.

Bermudez, E., Mangum, J. B., Asgharian, B. and Wong, B. A. (2002). Long Term Pulmonary Responses of Thress Laboratory Rodent Species to Subchronic Inhalation of Pigmentary Titanium Dioxide Particles. *Toxicological Sciences* **70**, pp. 86-97.

BéruBé, K. A., Sexton, K., Jones, T. P. and Richards, R. J. (2003). Quantitative Image Analysis of Urban Airborne Particulate Matter. *Proceedings - Royal Microscopical Society* **38**(1), pp. 3-12.

Bingle, L., Bull, T. B., Fox, B., Guz, A., Richards, R. J. and Tetley, T. D. (1990). Type II pneumocytes in mixed cell culture of human lung: a light and electron microscopic study. *Environmental Health Perspectives* **85**, pp. 71-80.

Bishop, A. E. (2004). Pulmonary epithelial stem cells. *Cell Proliferation* **37**(1), pp. 89-96.

Bjellqvist, B., Ek, K., Righetti, P. G., Gianazza, E., Gorg, A., Westermeier, R. and Postel, W. (1982). Isoelectric focusing in immobilized pH gradients: principle, methodology and some applications. *Journal of Biochemical and Biophysical Methods* **6**(4), pp. 317-339.

Borm, P. J., Schins, R. P. and Albrecht, C. (2004). Inhaled particles and lung cancer, part B: paradigms and risk assessment. *International Journal of Cancer* **110**(1), pp. 3-14.

Bracco, D. and Favre, J. B. (1998). Pulmonary injury after ski wax inhalation exposure. *Annals of Emergency Medicine* **32**(5), pp. 616-619.

Bradford, M. M. (1976). A rapid and sensitive method for the quantitation of microgram quantities of protein utilizing the principle of protein-dye binding. *Analytical Chemistry* **72**, pp. 248-254.

Brasch, F., Birzele, J., Ochs, M., Guttentag, S. H., Schoch, O. D., Boehler, A., Beers, M. F., Muller, K. M., Hawgood, S. and Johnen, G. (2004). Surfactant proteins in pulmonary alveolar proteinosis in adults. *European Respiratory Journal* **24**(3), pp. 426-435.

Brown, R. F., Drawbaugh, R. B. and Marrs, T. C. (1988). An investigation of possible models for the production of progressive pulmonary fibrosis in the rat. The effects of repeated intratracheal instillation of bleomycin. *Toxicology* **51**(1), pp. 101-110.

Brown, R. F. and White, D. E. (1997). Ultrastructure of rat lung following inhalation of ricin aerosol. *International Journal of Experimental Pathology* **78**(4), pp. 267-276.

Bruhn, H. (2005). A short guided tour through functional and structural features of saposin-like proteins. *Biochemical Journal* **389**(Pt 2), pp. 249-257.

Carrasquillo, K. G., Sanchez, C. and Greibenow, K. (2000). Relationship between conformational stability and ltophilization-induced structural changes in chymotrypsin. *Biotechnology and Applied Biochemistry* **31**, pp. 41-53.

Carthew, P. (2006). Personnel Communication. Safety and Environmental Assurance Centre, Unilever R&D, Colworth, Colworth House, Sharnbrook, Bedford, MK44 1LQ

.

Carthew, P., Fletcher, S., White, A., Harries, H. and Weber, K. (2006). Transcriptomic and Histopathology changes in rat lung after intratracheal instillation of polymers. *Inhalation Toxicology* **18**(4), pp. 221-245.

Carthew, P., Griffiths, H., Keech, S. and Hartop, P. (2002). Safety assessment for hair-spray resins: risk assessment based on rodent inhalation studies. *Inhalation Toxicology* **14**(4), pp. 401-416.

Catravas, J. D., Lazo, J. S., Dobuler, K. J., Mills, L. R. and Gillis, C. N. (1983). Pulmonary Endothelial Dysfunction in the Presence or Absence of Interstitial Injury Induced by Intratracheally Injected Bleomycin in Rabbits. *American Review of Respiratory Disease* **128**, pp. 740-746.

Chen, G. Y., Uttamchandani, M., Lue, R. Y., Lesaicherrea, M. L. and Yao, S. Q.. (2003). Array-Based Technologies and their Applications in Proteomics. *Current Topics in Medicinal Chemistry,* **3** (6), pp. 705-724

Cheng, I. W., Ware, L. B., Greene, K. E., Nuckton, T. J., Eisner, M. D. and Matthay, M. A. (2003). Prognostic value of surfactant proteins A and D in patients with acute lung injury. *Critical Care Medicine* **31**(1), pp. 20-27.

Chilvers, M. A. and O'Callaghan, C. (2000). Local mucociliary defence mechanisms. *Paediatric Respiratory Reviews* **1**(1), pp. 27-34.

Clark, H. F., Gurney, A. L., Abaya, E., Baker, K., Baldwin, D., Brush, J., Chen, J., Chow, B., Chui, C., Crowley, C., Currell, B., Deuel, B., Dowd, P., Eaton, D., Foster, J., Grimaldi, C., Gu, Q., Hass, P. E., Heldens, S., Huang, A., Kim, H. S., Klimowski, L., Jin, Y., Johnson, S., Lee, J., Lewis, L., Liao, D., Mark, M., Robbie, E., Sanchez, C., Schoenfeld, J., Seshagiri, S., Simmons, L., Singh, J., Smith, V., Stinson, J., Vagts, A., Vandlen, R., Watanabe, C., Wieand, D., Woods, K., Xie, M. H., Yansura, D., Yi, S., Yu, G., Yuan, J., Zhang, M., Zhang, Z., Goddard, A., Wood, W. I., Godowski, P. and Gray, A. (2003). The secreted protein discovery initiative (SPDI), a large-scale effort to identify novel human secreted and transmembrane proteins: a bioinformatics assessment. *Genome Research* **13**(10), pp. 2265-2270.

Creuwels, L. A. J. M., Golde, L. M. G. v. and Haagsman, H. P. (1997). The Pulmonary Surfactant System: Biochemical and Clinical Aspects. *Lung* **175**, pp. 1-39.

Cullen, R. T., Tran, C. L., Buchanan, D., Davis, J. M., Searl, A., Jones, A. D. and Donaldson, K. (2000). Inhalation of poorly soluble particles. I. Differences in inflammatory response and clearance during exposure. *Inhalation Toxicology* **12**(12), pp. 1089-1111.

Davis, G. S., Holmes, C. E., Pfeiffer, L. M. and Hemenway, D. R. (2001). Lymphocytes, lymphokines, and silicosis. *Journal of Environmental Pathology Toxicology and Oncology* **20 Suppl 1**, pp. 53-65.

Dehler, M., Zessin, E., Bartsch, P. and Mairbaurl, H. (2006). Hypoxia causes permeability oedema in the constant-pressure perfused rat lung. *European Respiratory Journal* **27**(3), pp. 600-606.

Delanghe, J. R. and Langlois, M. R. (2001). Hemopexin: a review of biological aspects and the role in laboratory medicine. *Clinica Chimica Acta* **312**(1-2), pp. 13-23.

Donaldson, K. (2000). Nonneoplastic lung responses induced in experimental animals by exposure to poorly soluble nonfibrous particles. *Inhalation Toxicology* **12**(1-2), pp. 121-139.

Doyle, I. R., Davidson, K. G., Barr, H. A., Nicholas, T. E., Payne, K. and Pfitzner, J. (1998). Quantity and structure of surfactant proteins vary among patients with alveolar proteinosis. *American Journal of Respiratory and Critical Care Medicine* **157**(2), pp. 658-664.

Driscoll, K. E., Costa, D. L., Hatch, G., Henderson, R., Oberdorster, G., Salem, H. and Schlesinger, R. B. (2000). Intratracheal instillation as an exposure technique for the evaluation of respiratory tract toxicity: uses and limitations. *Toxicological Sciences* **55**(1), pp. 24-35.

Elder, A., Gelein, R., Finkelstein, J. N., Driscoll, K. E., Harkema, J. and Oberdorster, G. (2005). Effects of subchronically inhaled carbon black in three species. I. Retention kinetics, lung inflammation, and histopathology. *Toxicological Sciences* **88**(2), pp. 614-629.

Ezaki, T., Baluk, P., Thurston, G., La Barbara, A., Woo, C. and McDonald, D. M. (2001). Time course of endothelial cell proliferation and microvascular remodeling in chronic inflammation. *American Journal of Pathology* **158**(6), pp. 2043-2055.

Ferin, J. (1994). Pulmonary retention and clearance of particles. *Toxicology Letters* **72**, pp. 121-125.

Fichmann, J. and Westermeier, R. (1999). 2D Protein Gel Electrophoresis. In: Link, A.J. ed. *Methods in Molecular Biology, Vol 112: 2d Proteome Analysis Protocols*. Humana Press Inc.

Fiorentino, D. F., Zlotnik, A., Mosmann, T. R., Howard, M. and O'Garra, A. (1991). IL-10 inhibits cytokine production by activated macrophages. *Journal of Immunology* **147**(11), pp. 3815-3822.

Foster, W. M. (2002). Mucociliary transport and cough in humans. *Pulmonary Pharmacology & Therapeutics* **15**(3), pp. 277-282.

Frampton, M. W. (2001). Systemic and cardiovascular effects of airway injury and inflammation: ultrafine particle exposure in humans. *Environmental Health Perspectives* **109 Suppl 4**, pp. 529-532.

Friedetzky, A., Garn, H., Kirchner, A. and Gemsa, D. (1998). Histopathological changes in enlarged thoracic lymph nodes during the development of silicosis in rats. *Immunobiology* **199**(1), pp. 119-132.

Furuichi, Y. and Birkhed, D. (1999). Retention of fluoride/triclosan in plaque following different modes of administration. *Journal of Clinical Periodontology* **26**(1), pp. 14-18.

Gamazo (2004). Efficacy of a vaccine against Salmonella enteritidis based on Gantrez nanoparticles as adjuvant and delivery system. *European Society of Clinical Microbiology and Infectious Diseases* **902**, p. 1205.

Garfin, D., Heerdt, L., Castle, L., Dale, E., Harbers, A., Sadownick, B., Strong, W., Whitman, C. and Zhu, M. (2000). *2-D Electrophoresis for Proteomics A Methods and Product Manual. www.biorad.com* www.biorad.com.

Goerke, J. (1998). Pulmonary surfactant: functions and molecular composition. *Biochimica et Biophysica Acta* **1408**(2-3), pp. 79-89.

Gordon, S. B. and Read, R. C. (2002). Macrophage defences against respiratory tract infections. *British Medical Bulletin* **61**, pp. 45-61.

Görg, A., Obermaier, C., Boguth, G., Harder, A., Scheibe, B., Wildgruber, R. and Weiss, W. (2000). The current state of two-dimensional electrophorsis with immobilized pH gradients. *Electrophoresis* **21**, pp. 1037-1053.

Görg, A., Weiss, W. and Dunn, M. J. (2004). Current two-dimensional electrophoresis technology for proteomics. *Proteomics* **4**, pp. 3665-3685.

Grattendick, K., Stuart, R., Roberts, E. and Lincoln, J. (2002). Alveolar Macrophage Activation by Myeloperoxidase. A Model for Exacerbation of Lung Inflammation. *American Journal of Respiratory Cell and Molecular Biology* **26**, pp. 716-722.

Gunther, A., Kalinowski, M., Elssner, A. and Seeger, W. (1994). Clot-embedded natural surfactant: kinetics of fibrinolysis and surface activity. *American Journal of Physiology* **267**(5 Pt 1), pp. L618-624.

Guo, M., Teng, M., Niu, L., Liu, Q., Huang, Q. and Hao, Q. (2005). Crystal structure of the cysteine-rich secretory protein stecrisp reveals that the cysteine-rich domain has a K+ channel inhibitor-like fold. *Journal of Biological Chemistry* **280**(13), pp. 12405-12412.

Gygi, S. P., Rist, B., Gerber, S. A., Turecek, F., Gelb, M. H., and Aebersold, R. (1999). Quantitative analysis of complex protein mixtures using isotope-coded affinity tags. *Nature Biotechnology* **17, pp.** 994-999.

Hagimoto, N., Kuwano, K., Miyazaki, H., Kunitake, R., Fujita, M., Kawasaki, M., Kaneko, Y. and Hara, N. (1997). Induction of apoptosis and pulmonary fibrosis in mice in response to ligation of Fas antigen. *American Journal of Respiratory Cell and Molecular Biology* **17**(3), pp. 272-278.

Hamm, H., Luhrs, J., Guzman y Rotaeche, J., Costabel, U., Fabel, H. and Bartsch, W. (1994). Elevated surfactant protein A in bronchoalveolar lavage fluids from sarcoidosis and hypersensitivity pneumonitis patients. *Chest* **106**(6), pp. 1766-1770.

Han, D. K., Eng, J., Zhou, H. and Aebersold, R. (2001). Quantitative profiling of differentiation-induced microsomal proteins using isotope-coded affinity tags and mass spectrometry. *Nature Biotechnology*, **19** pp. 946-951.

Hansen-Flaschen, J. (1995). Cardiogenic and Noncardiogenic Pulmonary Edema. In: Grippi, M. ed. *Pulmonary Pathophysiology.* Philadelphia J.B. Lippincott Company.

Hastings, R. H., Folkesson, H. G. and Matthay, M. A. (2004). Mechanisms of alveolar protein clearance in the intact lung. *Am J Physiol Lung Cell Mol Physiol* **286**(4), pp. L679-689.

Hay, J., Shahzeidi, S. and Laurent, G. (1991). Mechanisms of bleomycin-induced lung damage. *Archives of Toxicology* **65**(2), pp. 81-94.

He, C. (2003). Proteomic analysis of human bronchoalveolar lavage fluid: expression profiling of surfactant-associated protein A isomer derived from human pulmonary alveolar proteinosis using immunoaffinity detection. *Proteomics* **3**, pp. 87-94.

Henderson, R. F., Driscoll, K. E., Harkema, J. R., Lindenschmidt, R. C., Chang, I. Y., Maples, K. R. and Barr, E. B. (1995). A comparison of the inflammatory response of the lung to inhaled versus instilled particles in F344 rats. *Fundamental and Applied Toxicology* **24**(2), pp. 183-197.

Hermans, C. and Bernard, A. (1999). Lung epithelium-specific proteins: characteristics and potential applications as markers. *American Journal of Respiratory and Critical Care Medicine* **159**(2), pp. 646-678.

Hermans, C., Dong, P., Robin, M., Jadoul, M., Bernard, A., Bersten, A. D. and Doyle, I. R. (2003). Determinants of serum levels of surfactant proteins A and B and Clara cell protein CC16. *Biomarkers* **8**(6), pp. 461-471.

Hicks, G. H. (2000). *Cardiopulmonary Anatomy and Physiology.* W.B. Saunders Company.

Hirsch, J., Hansen, K. C., Burlingame, A. L. and Matthay, M. A. (2004). Proteomics: current techniques and potential applications to lung disease. *American Journal of Physiology-Lung Cellular and Molecular Physiology* **287**(1), pp. L1-23.

Hoffert, J. D., van Balkom B. W. M., Chou C-L. and Knepper M. A. (2003). Application of difference gel electrophoresis to the identification of inner medullary collecting duct proteins. *American Journal of Physiology Renal Physiology* **286**, pp F170-F179.

Hook, G. E. (1991). Alveolar proteinosis and phospholipidoses of the lungs. *Toxicologic Pathology* **19**(4 Pt 1), pp. 482-513.

Housley, D. G., Berube, K. A., Jones, T. P., Anderson, S., Pooley, F. D. and Richards, R. J. (2002). Pulmonary epithelial response in the rat lung to instilled Montserrat respirable dust and their major mineral components. *Occupational and Environmental Medicine* **59**, pp. 466-472.

Shen, J., Person, M. D., Zhu, J., Abbruzzese, J. L. and Li, D. (2006). Microarray: A Versatile Platform for High-Throughput Functional Proteomics. *Combinatorial Chemistry & High Throughput Screening*, **9** (3), pp. 203-212

Hunter, T. C., Andon, N. L., Koller, A., III, J. R. Y. and Haynes, P. A. (2002). The Functional Proteomics Toolbox: Methods and Application. *Journal of Chromatography B* **782**, pp. 165 - 181.

Irache, J. M., Huici, M., Konecny, M., Espuelas, S., Campanero, M. A. and Arbos, P. (2005). Bioadhesive Properties of Gantrez Nanoparticles. *Molecules* **10**, pp. 126-145.

Iyer, R., Hamilton, R. F., Li, L. and Holian, A. (1996). Silica-induced apoptosis mediated via scavenger receptor in human alveolar macrophages. *Toxicology and Applied Pharmacology* **141**(1), pp. 84-92.

Izbicki, G., Segel, M. J., Christensen, T. G., Conner, M. W. and Breuer, R. (2002). Time course of bleomycin-induced lung fibrosis. *International Journal of Experimental Pathology* **83**(3), pp. 111-119.

Jeffery, P. K. (2000). Pathological Spectrum of Airway Inflammation. In: Page, C.P. et al. eds. *Cellular Mechanisms in Airways Inflammation* Birkhauser Verlag.

Jeffries, A. and Turley, A. (1999). *Crash Course. Respiratory System.* Second Edition ed. Mosby.

Johansson, J. (1998). Structure and properties of surfactant protein C. *Biochimica et Biophysica Acta (BBA) - Molecular Basis of Disease* **1408**(2-3), pp. 161-172.

Johansson, J. and Curstedt, T. (1997). Molecular structures and interactions of pulmonary surfactant components. *European Journal Biochemistry* **244**(3), pp. 675-693.

Johnson, M. D., Widdicombe, J. H., Allen, L., Barbry, P. and Dobbs, L. G. (2002). Alveolar epithelial type I cells contain transport proteins and transport sodium, supporting an active role for type I cells in regulation of lung liquid homeostasis. *Proceedings of the National Academy of Science of the United States of America* **99**(4), pp. 1966-1971.

Jones, J. G. and McAteer, E. M. (1990). The quantitative evaluation of acute lung injury. *Clinical Physics and Physiological Measurement* **11 Suppl A**, pp. 127-131.

Kagawa, J. (2002). Health effects of diesel exhaust emissions--a mixture of air pollutants of worldwide concern. *Toxicology* **181-182**, pp. 349-353.

Kaminski, N., Allard, J. D., Pittet, J. F., Zuo, F., Griffiths, M. J., Morris, D., Huang, X., Sheppard, D. and Heller, R. A. (2000). Global analysis of gene expression in pulmonary fibrosis reveals distinct programs regulating lung inflammation and fibrosis. *Proceedings of the National Academy of Science of the United States of America* **97**(4), pp. 1778-1783.

Kaplan, F., Ledoux, P., Kassamali, F. Q., Gagnon, S., Post, M., Koehler, D., Deimling, J. and Sweezey, N. B. (1999). A novel developmentally regulated gene in lung mesenchyme: homology to a tumor-derived trypsin inhibitor. *American Journal of Physiology* **276**(6 Pt 1), pp. L1027-1036.

Karam, H., Hurbain-Kosmath, I. and Housset, B. (1995). Direct toxic effect of bleomycin on alveolar type 2 cells. *Toxicology Letters* **76**(2), pp. 155-163.

Kennedy, S. (2001). Proteomic profiling from human samples: the body fluid alternative. *Toxicology Letters* **120**, pp. 379 - 384.

Khubchandani, K. R. and Snyder, J. M. (2001). Surfactant protein A (SP-A): the alveolus and beyond. *Faseb Journal* **15**(1), pp. 59-69.

Kim, K. I., Kim, C. W., Lee, M. K., Lee, K. S., Park, C. K., Choi, S. J. and Kim, J. G. (2001). Imaging of occupational lung disease. *Radiographics* **21**(6), pp. 1371-1391.

Kinter, M. and Sherman, N. (2000). *Protein Sequencing and Identification Using Tandem Mass Spectrometry*. New York: John Wiley.

Kishimoto, Y., Hiraiwa, M. and O'Brien, J. S. (1992). Saposins: structure, function, distribution, and molecular genetics. *Journal of Lipid Research* **33**(9), pp. 1255-1267.

Klose, J. (1975). Protein Mapping by Combined Isoelectric Focusing and Electrophoresis of Mouse Tissues. *Humangenetik* **26**(3), pp. 231-243.

Knaapen, A. M., Borm, P. J. A., Albrecht, C. and Schins, R. P. F. (2004). Inhaled particles and lung cancer. Part A: Mechanisms. *International Journal of Cancer* **109**(6), pp. 799-809.

Kodavanti, U. P., Jackson, M. C., Ledbetter, A. D., Richards, J. R., Gardner, S. Y., Watkinson, W. P., Campen, M. J. and Costa, D. L. (1999). Lung injury from intratracheal and inhalation exposures to residual oil fly ash in a rat model of monocrotaline-induced pulmonary hypertension. *Journal of Toxicology and Enviromental Health A* **57**(8), pp. 543-563.

Kreda, S. M., Gynn, M. C., Fenstermacher, D. A., Boucher, R. C. and Gabriel, S. E. (2001). Expression and localization of epithelial aquaporins in the adult human lung. *American Journal of Respiratory Cell and Molecular Biology* **24**(3), pp. 224-234.

Kriegova, E., Melle, C., Kolek, V., Hutyrova, B., Mrazek, F., Bleul, A., du Bois, R. M., von Eggeling, F. and Petrek, M. (2006). Protein Profiles of Bronchoalveolar Lavage Fluid from Patients with Pulmonary Sarcoidosis. *American Journal of Respiratory and Critical Care Medicine* **173** pp. 1145-1154.

Kuempel, E. D., O'Flaherty, E. J., Stayner, L. T., Smith, R. J., Green, F. H. and Vallyathan, V. (2001). A biomathematical model of particle clearance and retention in the lungs of coal miners. *Regulatory Toxicology and Pharmacology* **34**(1), pp. 69-87.

Kuroki, Y., Takahashi, H., Chiba, H. and Akino, T. (1998). Surfactant proteins A and D: disease markers. *Biochimica et Biophysica Acta* **1408**(2-3), pp. 334-345.

Kvasnicka, F. (2003). Proteomics: General Strategies and Application to Nutritionally Relevant Proteins. *Journal of Chromatography B* **787**(1), pp. 77-89

Larsen, G. L. and Holt, P. G. (2000). The Concept of Airway Inflammation. *American Journal of Respiratory and Critical Care Medicine* **162**, pp. S2-S6.

Lazo, J. S. and Humphreys, C. J. (1983). Lack of metabolism as the biochemical basis of bleomycin-induced pulmonary toxicity. *Proceedings of the National Academy of Science of the United States of America* **80**(10), pp. 3064-3068.

Lee, S. H. and Richards, R. J. (2004). Montserrat volcanic ash induces lymph node granuloma and delayed lung inflammation. *Toxicology* **195**(2-3), pp. 155-165.

Lehnert, B. E., Valdez, Y. E. and Stewart, C. C. (1986). Translocation of particles to the tracheobronchial lymph nodes after lung deposition: kinetics and particle-cell relationships. *Experimental Lung Research* **10**(3), pp. 245-266.

Lenz, A. G., Meyer, B., Costabel, U. and Maier, K. (1993). Bronchoalveolar lavage fluid proteins in human lung disease: analysis by two-dimensional electrophoresis. *Electrophoresis* **14**(3), pp. 242-244.

Lenz, A. G., Meyer, B., Weber, H. and Maier, K. (1990). Two-dimensional electrophoresis of dog bronchoalveolar lavage fluid proteins. *Electrophoresis* **11**(6), pp. 510-513.

Lesur, O., Bernard, A. M. and Begin, R. O. (1996). Clara cell protein (CC-16) and surfactant-associated protein A (SP-A) in asbestos-exposed workers. *Chest* **109**(2), pp. 467-474.

Lewis, R. W., Harwood, J. L. and Richards, R. J. (1987). The fate of instilled pulmonary surfactant in normal and quartz-treated rats. *Biochemical Journal* **243**(3), pp. 679-685.

Liebler, D. C. (2002). *Introduction to Proteomics Tools for the New Biology.* Humana Press Inc.

Liepinsh, E., Trexler, M., Kaikkonen, A., Weigelt, J., Banyai, L., Patthy, L. and Otting, G. (2001). NMR structure of the LCCL domain and implications for DFNA9 deafness disorder. *EMBO Journal* **20**(19), pp. 5347-5353.

Lindahl, M., Stahlbom, B., Svartz, J. and Tagesson, C. (1998). Protein patterns of human nasal and bronchoalveolar lavage fluids analyzed with two dimensional gel electrophoresis. *Electrophoresis* **19**, pp. 3222-3229.

Lindahl, M., Stahlbom, B. and Tagesson, C. (1995). Two dimensional gel electrophoresis of nasal and bronchoalveolar lavage fluids after occupational exposure. *Electrophoresis* **16**, pp. 1199-1204.

Lindahl, M., Svartz, J. and Tagesson, C. (1999). Demonstration of different forms of the anti-inflammatory proteins lipocortin-1 and Clara cell protein-16 in human nasal and bronchoalveolar lavage fluids. *Electrophoresis* **20**, pp. 881-890.

Lohmann-Matthes, M.-L., Steinmuller, C. and Franke-Ullmann, G. (1994). Pulmonary Macrophages. *European Respiratory Journal* **7**, pp. 1678-1689.

Lopez, M., Berggren, K., Chernokalskaya, E., Lazarev, A., Robinson, M. and Patton, W. F. (2000). A Comparison of Silver Staining and SYPRO Ruby Protein Gel Stain with Respect to Protein Detection in Two-Dimensional Gels and identification by Pepide Mass Profiling. *Electrophoresis* **21**, pp. 3673-3683.

Lum, H. and Malik, A. B. (1994). Regulation of vascular endothelial barrier function. *American Journal of Physiology* **267**(3 Pt 1), pp. L223-241.

Lynn, W. S., Bhattacharya, S. N., Passerro, M. P. and Tye, R. (1974). Composition and Function of Pulmonary Surfactant. *Annals of the New York Academy of Sciences* **221**, pp. 209-211.

MacNee, W. and Donaldson, K. (2003). Mechanism of Lung Injury caused by PM10 and ultrafine particles with special reference to COPD. *European Respiratory Journal* **21**(Suppl.40), pp. 47s-51s.

Macri, J., McGee, B., Thomas, J. N., Du, P., Stevenson, T. I., Kilby, G. W. and Rapundalo, S. T. (2000). Cardiac sarcoplasmic reticulum and sarcolemmal proteins separated by two-dimensional electrophoresis: surfactant effects on membrane solubilization. *Electrophoresis* **21**(9), pp. 1685-1693.

Magi, B., Bini, L., Perari, M. G., Fossi, A., Sanchez, J.-C., Hochstrasser, D., Paesano, S., Raggiaschi, R., Santucci, A., Pallini, V. and Rottoli, P. (2002). Bronchoalveolar lavage fluid protein composition in patients with sarcoidosis and idiopathic pulmonary fibrosis: A two-dimensional electrophoretic study. *Electrophoresis* **23**(19), pp. 3434-3444.

Manitz, M. P., Horst, B., Seeliger, S., Strey, A., Skryabin, B. V., Gunzer, M., Frings, W., Schonlau, F., Roth, J., Sorg, C. and Nacken, W. (2003). Loss of S100A9 (MRP14) results in reduced interleukin-8-induced CD11b surface expression, a polarized microfilament system, and diminished responsiveness to chemoattractants in vitro. *Molecular and Cellular Biology* **23**(3), pp. 1034-1043.

Mann, M. (1999). Quantitative Proteomics. *Nature Biotechnology* 17, pp. 944-955.

Merkel, D., Rist, W., Seither, P., Weith, A. and Lenter, M. C. (2005). Proteomic study of human bronchoalveolar lavage fluids from smokers with chronic obstructive pulmonary disease by combining surface-enhanced laser desorption/ionization-mass spectrometry profiling with mass spectrometric protein identification. *Proteomics* **5**(11), pp. 2972-2980.

Miller, B. E. and Hook, G. E. (1990). Hypertrophy and hyperplasia of alveolar type II cells in response to silica and other pulmonary toxicants. *Environmental Health Perspectives* **85**, pp. 15-23.

Miserocchi, G., Negrini, D., Passi, A. and De Luca, G. (2001). Development of lung edema: interstitial fluid dynamics and molecular structure. *News in Physiological Sciences* **16**, pp. 66-71.

Molloy, M. P. (2000). Two-dimensional electrophoresis of membrane proteins using immobilized pH gradients. *Analytical Biochemistry* **280**(1), pp. 1-10.

Moore, S. A., Strieter, R. M., Rolfe, M. W., Standiford, T. J., Burdick, M. D. and Kunkel, S. L. (1992). Expression and regulation of human alveolar macrophage-derived interleukin-1 receptor antagonist. *American Journal of Respiratory Cell and Molecular Biology* **6**(6), pp. 569-575.

Mossman, B. T. (2000). Mechanisms of action of poorly soluble particulates in overload-related lung pathology. *Inhalation Toxicology* **12**(1-2), pp. 141-148.

Murphy, S. A., Bérubé, K. A., Pooleya, F. D. and Richards, R. J. (1998). The response of lung epithelium to well characterised fine particles. *Life Sciences* **62**(19), pp. 1789-1799.

Murphy, T. J., Thurston, G., Ezaki, T. and McDonald, D. M. (1999). Endothelial cell heterogeneity in venules of mouse airways induced by polarized inflammatory stimulus. *American Journal of Pathology* **155**(1), pp. 93-103.

Noel-Georis, I., Bernard, A., Falmagne, P. and Wattiez, R. (2002). Database of bronchoalveolar lavage fluid proteins. *Journal of Chromatography B* **771**, pp. 221-236.

Oberdorster, G. (1995). Lung Particle Overload: Implications for Occupational Exposure to Particles. *Regulatory Toxicology and Pharmacology* **27**, pp. 123-135.

Oberdorster, G. (2000). Determinants of the pathogenicity of man-made vitreous fibers (MMVF). *International Archives of Occupational and Environmental Health* **73 Suppl**, pp. S60-68.

Oberdorster, G. (2002). Toxicokinetics and effects of fibrous and nonfibrous particles. *Inhalation Toxicology* **14**(1), pp. 29-56.

Oberdorster, G., Ferin, J., Gelein, R., Soderholm, S. C. and Finkelstein, J. (1992). Role of the alveolar macrophage in lung injury: studies with ultrafine particles. *Environmental Health Perspectives* **97**, pp. 193-199.

O'Brien, J. S. and Kishimoto, Y. (1991). Saposin proteins: structure, function, and role in human lysosomal storage disorders. *Faseb Journal* **5**(3), pp. 301-308.

Ochs, M., Johnen, G., Muller, K. M., Wahlers, T., Hawgood, S., Richter, J. and Brasch, F. (2002). Intracellular and intraalveolar localization of surfactant protein A (SP-A) in the parenchymal region of the human lung. *American Journal of Respiratory Cell and Molecular Biology* **26**(1), pp. 91-98.

Odink, K., Cerletti, N., Bruggen, J., Clerc, R. G., Tarcsay, L., Zwadlo, G., Gerhards, G., Schlegel, R. and Sorg, C. (1987). Two calcium-binding proteins in infiltrate macrophages of rheumatoid arthritis. *Nature* **330**(6143), pp. 80-82.

O'Farrell, P. H. (1975). High Resolution Two-Dimensional Electrophoresis of Proteins. *The Journal of Biological Chemistry* **250**(10), pp. 4007-4021.

Osipov, A. V., Levashov, M. Y., Tsetlin, V. I. and Utkin, Y. N. (2005). Cobra venom contains a pool of cysteine-rich secretory proteins. *Biochemical and Biophysical Research Communications* **328**(1), pp. 177-182.

Oyewumi, L., Kaplan, F. and Sweezey, N. B. (2003). Lgl1, a mesenchymal modulator of early lung branching morphogenesis, is a secreted glycoprotein imported by late gestation lung epithelial cells. *Biochemical Journal* **376**(Pt 1), pp. 61-69.

Panettieri, R. A., Jr. (2002). Airway smooth muscle: an immunomodulatory cell. *Journal of Allergy and Clinical Immunology* **110**(6 Suppl), pp. S269-274.

Patthy, L. (1991). Homology of the precursor of pulmonary surfactant-associated protein SP-B with prosaposin and sulfated glycoprotein 1. *Journal of Biological Chemistry* **266**(10), pp. 6035-6037.

Patton, P. F. (2001). *Detecting proteins in polyacrylamide gels and on electroblot membranes*. BIOS Scientific Publishers Ltd.

Patton, W. F. (2002). Detection technologies in proteome analysis. *Journal of Chromatography B* **771**, pp. 3-31.

Peters, T. (1996). *All about albumin, biochemistry, genetics, and medical applications* New York: Academic Press.

Phelps, D. S., Umstead, T. M., Mejia, M., Carrillo, G., Pardo, A. and Selman, M. (2004). Increased surfactant protein-A levels in patients with newly diagnosed idiopathic pulmonary fibrosis. *Chest* **125**(2), pp. 617-625.

Pison, U., Herold, R. and Schurch, S. (1996). The pulmonary surfactant system: biological functions, components, physicochemical properties and alterations during lung disease. *Colloids and Surfaces A: Physiochemical and Engineering Aspects* **114**, pp. 165-184.

Plymoth, A., Lofdahl, C. G., Ekberg-Jansson, A., Dahlback, M., Lindberg, H., Fehniger, T. E. and Marko-Varga, G. (2003). Human bronchoalveolar lavage: biofluid analysis with special emphasis on sample preparation. *Proteomics* **3**(6), pp. 962-972.

Postle, A. D., Mander, A., Reid, K. B., Wang, J. Y., Wright, S. M., Moustaki, M. and Warner, J. O. (1999). Deficient hydrophilic lung surfactant proteins A and D with normal surfactant phospholipid molecular species in cystic fibrosis. *American Journal of Respiratory Cell and Molecular Biology* **20**(1), pp. 90-98.

Prescott, G. J., Cohen, G. R., Elton, R. A., Fowkes, F. G. and Agius, R. M. (1998). Urban air pollution and cardiopulmonary ill health: a 14.5 year time series study. *Occupational and Environmental Medicine* **55**(10), pp. 697-704.

Rabilloud, T. (1990). Mechanisms of Protein Silver Staining in Polyacrylamide Gels: A 10-year Synthesis. *Electrophoresis* **11**, pp. 785-794.

Rabilloud, T. (1996). Solubilization of proteins for electrophoretic analysis. *Electrophoresis* **15**(5), pp. 813-829.

Rabilloud, T. (1999). Silver Staining of 2-D Electrophoresis Gels. *Methods In Molecular Biology* **112**, pp. 297-305.

Rabilloud, T. (2002). Two-dimensional gel electrophoresis in proteomics: old, old fashioned, but it still climbs up the mountains. *Proteomics* **2**(1), pp. 3-10.

Renaud, W., Merten, M. and Figarella, C. (1994). Increased coexpression of CFTR and S100 calcium binding proteins MRP8 and MRP14 mRNAs in cystic fibrosis human tracheal gland cells. *Biochemical and Biophysical Research Communications* **201**(3), pp. 1518-1525.

Reynolds, H., Fulmer, J. D., Kazmierowskil, J. A., Roberts, W. C., Frank, M. M. and Crystal, R. G. (1977). Analysis of Cellular and Protein Content of Broncho-Alveolar Lavage Fluid from Patients with Idiopathic Pulmonary Fibrosis and Chronic Hypersensitivity Pneumonitis. *The Journal of Clinical Investigation* **59**(165-175).

Reynolds, H. Y. and Newball, H. H. (1974). Analysis of proteins and respiratory cells obtained from human lungs by bronchial lavage. *Journal of Laboratory and Clinical Medicine* **84**(4), pp. 559-573.

Reynolds, L. J., McElroy, M. and Richards, R. J. (1999). Density and substrata are important in lung type II cell transdifferentiation in vitro. *International Journal of Biochemistry & Cell Biology* **31**(9), pp. 951-960.

Reynolds, L. J. and Richards, R. J. (2001). Can toxicogenomics provide information on the bioreactivity of diesel exhaust particles. *Toxicology* **165**, pp. 145-152.

Richards, R. J., Atkins, J., Marrs, T. C., Brown, R. F. and Masek, L. (1989). The biochemical and pathological changes produced by the intratracheal instillation of certain components of zinc-hexachloroethane smoke. *Toxicology* **54**(1), pp. 79-88.

Richards, R. J. and Curtis, C. G. (1984). Biochemical and Cellular Mechanisms of Dust Induced Lung Fibrosis. *Environmental Health Perspectives* **55**, pp. 393-416.

Richards, R. J., Masek, L. C. and Brown, R. F. (1991). Biochemical and cellular mechanisms of pulmonary fibrosis. *Toxicologic Pathology* **19**(4 Pt 1), pp. 526-539.

Richardson, D. L., Pepper, D. S. and Kay, A. B. (1976). Chemotaxis for human monocytes by fibrinogen-derived peptides. *British Journal of Haematology* **32**(4), pp. 507-513.

Richardson, P. S. and Peatfield, A. C. (1981). Reflexes concerned in the defence of the lungs. *Bulletin Europeen de Physiopathologie Respiratorie-Clinical Respiratory Physiology* **17**(6), pp. 979-1012.

Rosen, S. H., Castleman, B. and Liebow, A. A. (1958). Pulmonary Alveolar Proteinosis. *The New England Medical Journal of Medicine* **258**(23), pp. 1123-1142.

Roth, J., Vogl, T., Sorg, C. and Sunderkotter, C. (2003). Phagocyte-specific S100 proteins: a novel group of proinflammatory molecules. *Trends In Immunology* **24**(4), pp. 155-158.

Rouleau, P., Vandal, K., Ryckman, C., Poubelle, P. E., Boivin, A., Talbot, M. and Tessier, P. A. (2003). The calcium-binding protein S100A12 induces neutrophil adhesion, migration, and release from bone marrow in mouse at concentrations similar to those found in human inflammatory arthritis. *Clinical Immunology* **107**(1), pp. 46-54.

Ryckman, C., Vandal, K., Rouleau, P., Talbot, M. and Tessier, P. A. (2003). Proinflammatory activities of S100: proteins S100A8, S100A9, and S100A8/A9 induce neutrophil chemotaxis and adhesion. *Journal of Immunology* **170**(6), pp. 3233-3242.

Sabounchi-Schutt, F., Astrom, J., Eklund, A., Grunewald, J. and Bjellqvist, B. (2001). Detection and identification of human bronchoalveolar lavage proteins using narrow-range immobilized pH gradient DryStrip and the paper bridge sample application method. *Electrophoresis* **22**, pp. 1851-1860.

Sabounchi-Schutt, F., Astrom, J., Hellman, U. and Grunewald, J. (2003). Changes in bronchoalveolar lavage fluid proteins in sarcoidosis: a proteomics approach. *European Respiratory Journal* **21**, pp. 414-420.

Sartori, C. and Matthay, M. A. (2002). Alveolar epithelial fluid transport in acute lung injury: new insights. *European Respiratory Journal* **20**(5), pp. 1299-1313.

Savill, J. S., Wyllie, A., Henson, J., Walport, M., Henson, P. and Haslett, C. (1989). Macrophage phagocytosis of aging neutrophils in inflammation: programmed cell death in the neutrophil lead to its recognition by macrophages. *J. Clinical Investigation* **83** pp. 865-875.

Seaton, A. and Cherrie, J. W. (1998). Quartz exposures and severe silicosis: a role for the hilar nodes. *Occupational and Environmental Medicine* **55**(6), pp. 383-386.

Sendo, F., Tsuchida, H., Takeda, Y., Gon, S., Takei, H., Kato, T., Hachiya, O. and Watanabe, H. (1996). Regulation of neutrophil apoptosis--its biological significance in inflammation and the immune response. Human Cell **9**(3) pp. 215-222

Seymour, J. F. and Presneill, J. J. (2002). Pulmonary Alveolar Proteinosis. *American Journal of Respiratory and Critical Care Medicine* **166**, pp. 215-235.

Shah, P. L., Hansell, H., Lawson, P. R., Reid, K. B. M. and Morgan, C. (2000). Pulmonary alveolar proteinosis: clinical aspects and current concepts on pathogenesis. *Thorax* **55**, pp. 67-77.

Shapiro, S. E., Konstantinov, A. A., Zelenskaia, M. I. and Chapovskaia, L. G. (1959). [Electrophoretic investigation of blood proteins in typhoid and paratyphoid fevers treated by synthomycin.]. *Zhurnal Mikrobiologii Epidemiologii Immunibiologii* **30**(4), pp. 66-70.

Shen, A. S., Haslett, C., Feldsien, D. C., Henson, P. M. and Cherniack, R. M. (1988). The intensity of chronic lung inflammation and fibrosis after bleomycin is directly related to the severity of acute injury. *American Review of Respiratory Disease* **137**(3), pp. 564-571.

Shen J., Person M.D., Zhu J., Abbruzzese J.L. and Li D. (2004). Protein expression profiles in pancreatic adenocarcinoma compared with normal pancreatic tissue and tissue affected by pancreatitis as detected by two-dimensional gel electrophoresis and mass spectrometry. *Cancer Research* **64**, pp *9018-9026.*

Shevchenko, A., Wilm, M., Vorm, O. and Mann, M. (1996). Mass spectrometric sequencing of proteins silver-stained polyacrylamide gels. *Analytical Chemistry* **68**(5), pp. 850-858.

Shijubo, N., Honda, Y., Itoh, Y., Yamaguchi, T., Kuroki, Y., Akino, T., Kawai, T. and Abe, S. (1998). BAL surfactant protein A and Clara cell 10-kDa protein levels in healthy subjects. *Lung* **176**(4), pp. 257-265.

Shikamoto, Y., Suto, K., Yamazaki, Y., Morita, T. and Mizuno, H. (2005). Crystal structure of a CRISP family Ca2+ -channel blocker derived from snake venom. *Journal of Molecular Biology* **350**(4), pp. 735-743.

Sopalla, C., Leukert, N., Sorg, C. and Kerkhoff, C. (2002). Evidence for the involvement of the unique C-tail of S100A9 in the binding of arachidonic acid to the heterocomplex S100A8/A9. *Bioliological Chemistry* **383**(12), pp. 1895-1905.

Srikrishna, G., Panneerselvam, K., Westphal, V., Abraham, V., Varki, A. and Freeze, H. H. (2001). Two proteins modulating transendothelial migration of leukocytes recognize novel carboxylated glycans on endothelial cells. *Journal of Immunology* **166**(7), pp. 4678-4688.

Starcher, B. C., Kuhn, C. and Overton, J. E. (1978). Increased Elastin and Collagen Content in the Lungs of Hamster Receiving an Intratracheal Injection of Bleomycin. *American Review of Respiratory Disease* **117**, pp. 299-305.

Switzer, R. C., 3rd, Merril, C. R. and Shifrin, S. (1979). A highly sensitive silver stain for detecting proteins and peptides in polyacrylamide gels. *Analytical Biochemistry* **98**(1), pp. 231-237.

Tamboli, C. P., Richard, F. and Colombel, J. F. (2003). Fecal calprotectin in Crohn's disease: new family ties. *Gastroenterology* **124**(7), pp. 1972-1974.

Telford, I. R. and Bridgeman, C. F. (1995). *Respiratory System* Harper Collins College Publishers.

Thrall, R. S., McCormick, J. R., McReynolds, R. A. and Ward, P. A. (1979). Bleomycin-Induced Pulmonary Fibrosis in the Rat. *American Journal of Pathology* **95**, pp. 117-130.

Tran, C. L., Buchanan, D., Cullen, R. T., Searl, A., Jones, A. D. and Donaldson, K. (2000). Inhalation of poorly soluble particles. II. Influence Of particle surface area on inflammation and clearance. *Inhalation Toxicology* **12**(12), pp. 1113-1126.

Trapnell, B. C., Whitsett, J. A. and Nakata, K. (2003). Pulmonary Alveolar Proteinosis. *The New England Medical Journal of Medicine* **349**, pp. 2527-2539.

Trexler, M., Banyai, L. and Patthy, L. (2000). The LCCL module. *European Journal Biochemistry* **267**(18), pp. 5751-5757.

van Eeden, S. F., Tan, W. C., Suwa, T., Mukae, H., Terashima, T., Fujii, T., Qui, D., Vincent, R. and Hogg, J. C. (2001). Cytokines involved in the systemic inflammatory response induced by exposure to particulate matter air pollutants (PM(10)). *American Journal of Respiratory and Critical Care Medicine* **164**(5), pp. 826-830.

Vandal, K., Rouleau, P., Boivin, A., Ryckman, C., Talbot, M. and Tessier, P. A. (2003). Blockade of S100A8 and S100A9 suppresses neutrophil migration in response to lipopolysaccharide. *Journal of Immunology* **171**(5), pp. 2602-2609.

von Bredow, C., Birrer, P. and Griese, M. (2001). Surfactant protein A and other bronchoalveolar lavage fluid proteins are altered in cystic fibrosis. *European Respiratory Journal* **17**(4), pp. 716-722.

Wang, M., Xiao, G. G., Li, N., Xie, Y., Loo, J. A. and Nel, A. E. (2005). Use of a fluorescent phosphoprotein dye to characterize oxidative stress-induced signaling pathway components in macrophage and epithelial cultures exposed to diesel exhaust particle chemicals. *Electrophoresis* **26**(11), pp. 2092-2108.

Wanner, A., Salathe, M. and O'Riordan, T. G. (1996). Mucociliary clearance in the airways. *American Journal of Respiratory and Critical Care Medicine* **154**(6 Pt 1), pp. 1868-1902.

Ward, C., Fenwick, J., Booth, H. and Walters, E. H. (1997). Albumin is not suitable as a marker of bronchoalveolar lavage dilution in interstitial lung disease. *European Respiratory Journal* **10**(9), pp. 2029-2033.

Wattiez, R. and Falmagne, P. (2005). Proteomics of bronchoalveolar lavage fluid. *Journal of Chromatography B* **815**, pp. 169-178.

Wattiez, R., Hermans, C., Bernard, A., Lesur, O. and Falmagne, P. (1999). Human bronchoalveolar lavage fluid: two-dimensional gel electrophoresis, amino acid microsequencing and identification of major proteins. *Electrophoresis* **20**(7), pp. 1634-1645.

Wattiez, R., Hermans, C., Cruyt, C., Bernard, A. and Falmagne, P. (2000). Human bronchoalveolar lavage fluid protein two-dimensional database: Study of intersititial lung diseases. *Electrophoresis* **21**, pp. 2703-2712.

Weaver, T. E. and Conkright, J. J. (2001). Function of surfactant proteins B and C. *Annu Rev Physiol* **63**, pp. 555-578.

Weibel, E. R. (1974). A note on differentiation and divisibility of alveolar epithelial cells. *Chest* **65**, pp. Suppl:19S-21S.

West, J. B. (1992). *Pulmonary Pathophysiology - The Essentials.* Baltimore: Williams and Wilkins.

West, J. B. (2003). *Pulmonary Pathophysiology. The Essentials.* Sixth ed. Lippincott Williams and Wilkins.

Westermeier, R. (2001). *Electrophoresis in Practice*. Wiley-VCH.

Westermeier, R. and Naven, T. (2002). *Proteomics in Practice. A Laboratory Manual of Proteome Analysis*. Wiley-VCH.

Wolfensohn, S. and Lloyd, M. (1998). Practical Use of Distress Scoring Systems in the Application of Humane Endpoints. .*Handbook of Laboratory Animal Management and Welfare.* Oxford: Blackwell Science, pp. 48-53.

Yamazaki, Y. and Morita, T. (2004). Structure and function of snake venom cysteine-rich secretory proteins. *Toxicon* **44**(3), pp. 227-231.

Zhao, J., Zhu , H., Wong, C. H., Leung, K. Y. and Wong W. S. F. (2005). Increased lungkine and chitinase levels in allergic airway inflammation: A proteomics approach. *Proteomics* **5**(11) pp. 2799 - 2807

APPENDIX

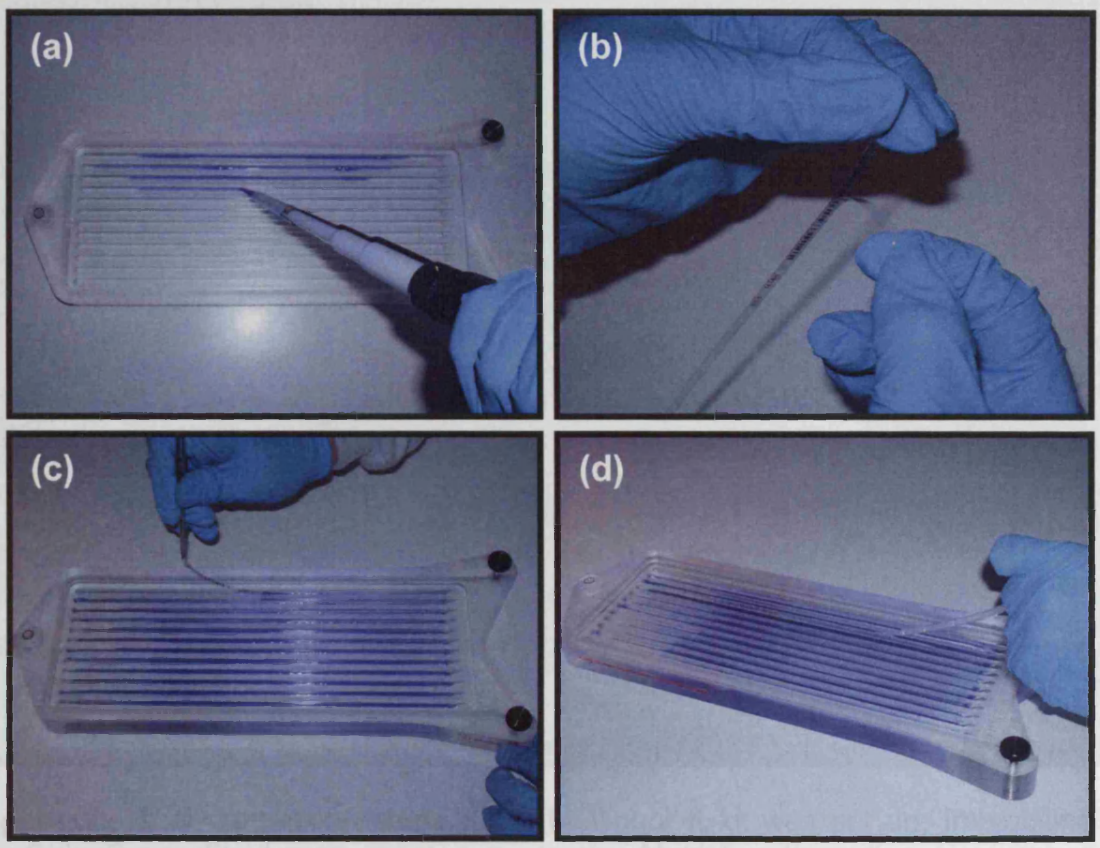

Appendix 1: Photographs of the different steps involved in the rehydration stage of the 2D SDS PAGE technique. (a) Loading the rehydration solution, (b) removing the protective cover from DryStrip Gel, (c) loading DryStrip gels and (d) covering DryStrip gels with Immobiline™ DryStrip Cover Fluid.

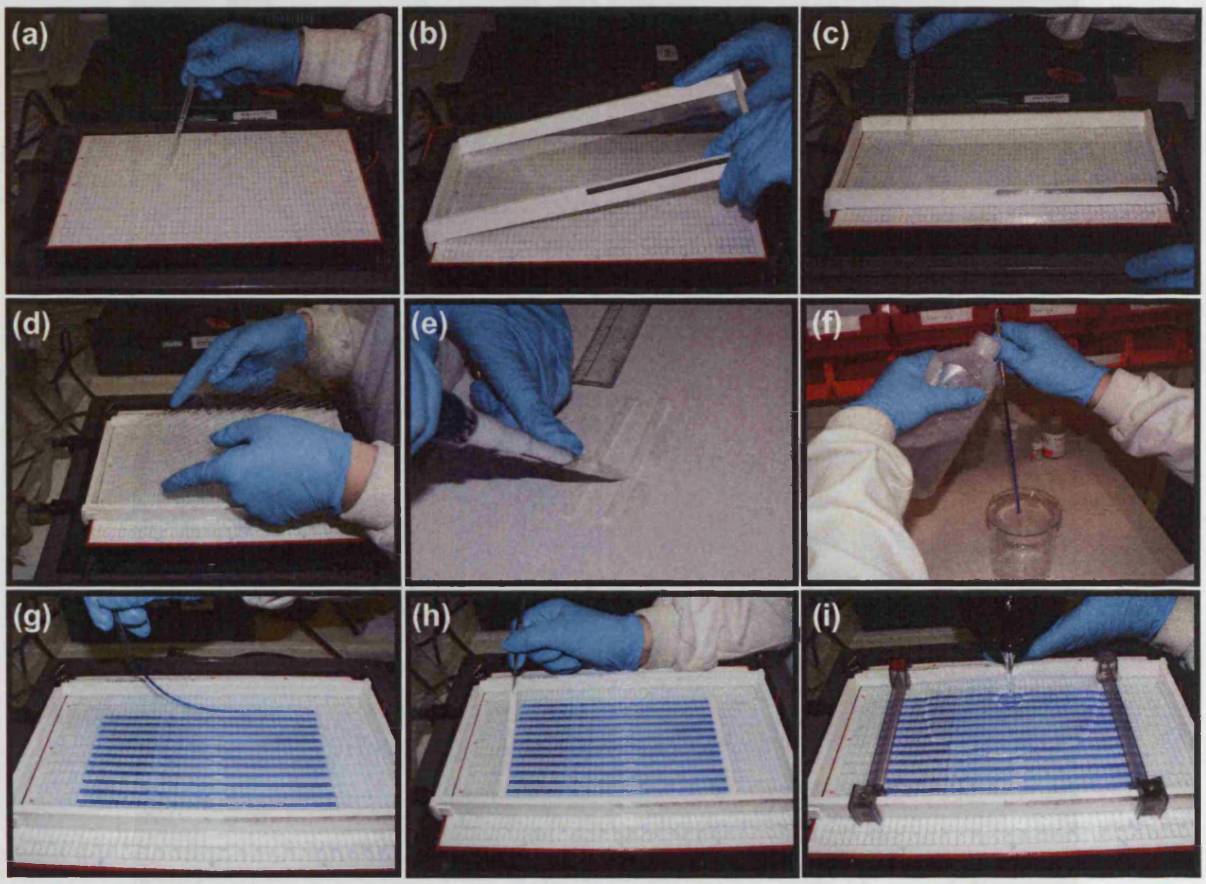

Appendix 2: 1st dimension steps. The Multiphor II kit was set up; Immobiline™ DryStrip Cover Fluid was pipetted on to the Multiphor II cooling plate (a), the Immobiline™ DryStrip tray was positioned on to the cooling plate and connected to the unit (b), Immobiline™ DryStrip Cover Fluid was pipetted on to the Immobiline™ DryStrip tray (c) and the DryStrip aligner was placed into the tray (d). The IEF electrode strips soaked in distilled water (e). The IPG strips were washed with distilled water (f) and drained on filter paper before being transferred to the Immobiline DryStrip tray (g). The moistened IEF electrode strips were placed across the ends of the DryStrip Gels, partially touching the gel (h). The electrodes were fitted over the electrode strips and Immobiline™ DryStrip Cover Fluid was poured into the tray to completely cover the strips (i).

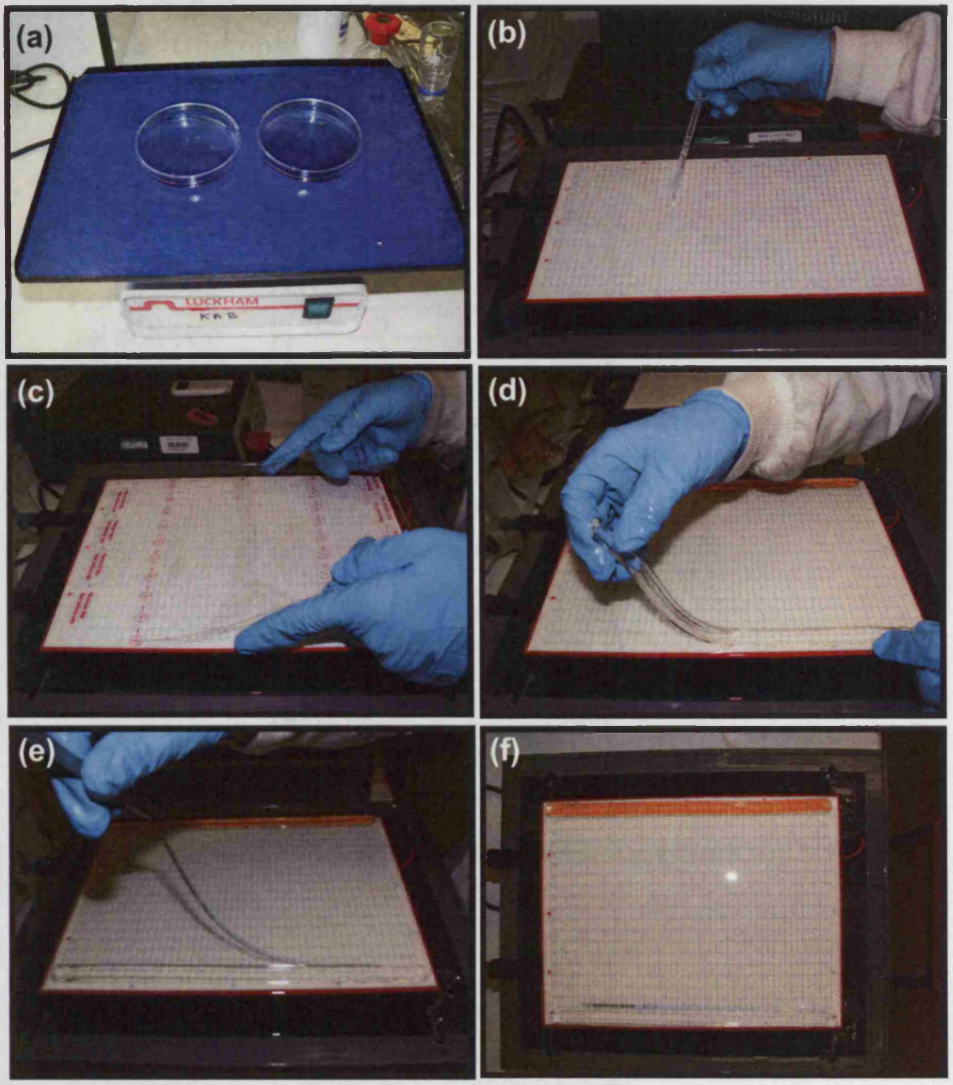

Appendix 3: 2nd Dimension steps. The IPG strips are first equilibrated in DTT and SDS equilibration buffer followed by iodoacetamide and SDS equilibration buffer (a). Immobiline™ DryStrip Cover Fluid (b) was placed between the Multiphor™ II precast gel and the Multiphor™ II Electrophoresis Unit (c). The cathodic (clear) and anodic (orange) buffer strips were placed on the gel partially covering the gel (d) and the Drytrip Gels was placed face-down on the gel parallel to the cathodic buffer strip (e-f).

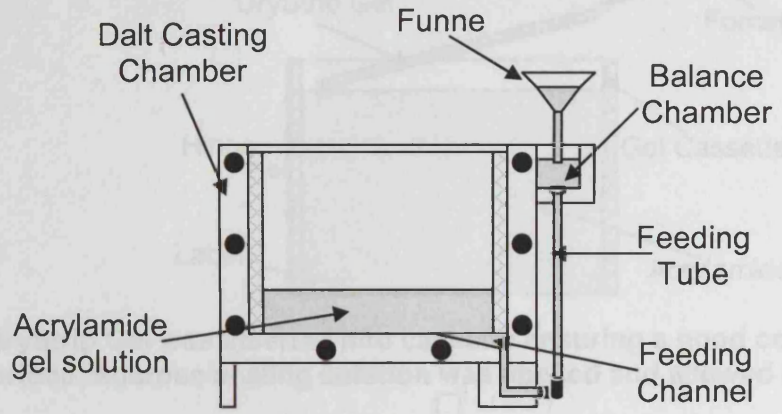

Acrylamide gel solution was added slowly

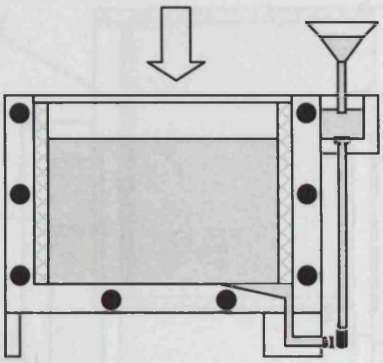

Acrylamide gel solution added until 2 cm from top.

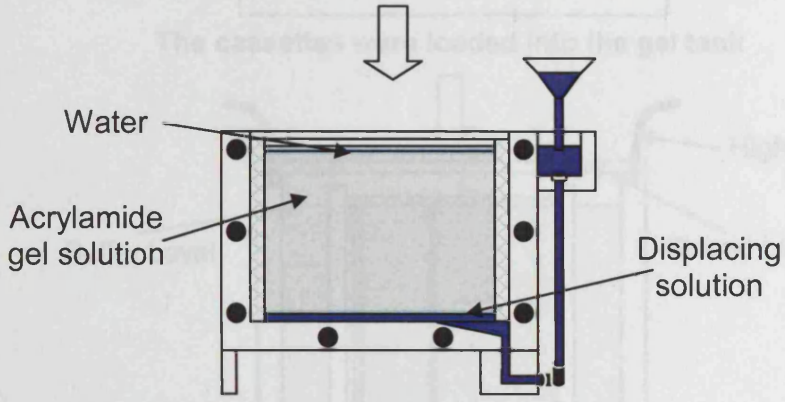

Displacing solution was added to prevent acrylamide gel solution solidifying in feeding tube and channel. Water was overlaid to prevent evaporation.

Appendix 4: Diagram of the Dalt casting chamber.

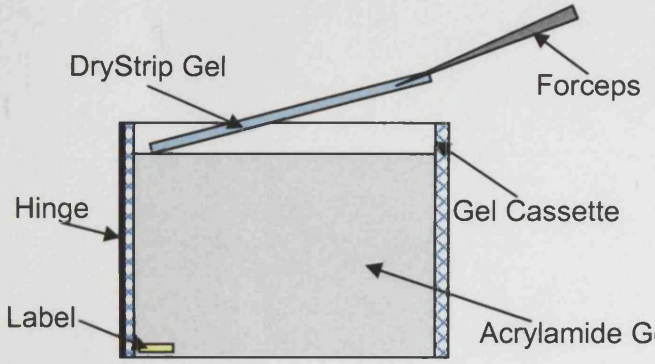

The DryStrip Gel was inserted into cassette ensuring a good contact with gel surface. Agarose sealing solution was applied and allowed to solidify.

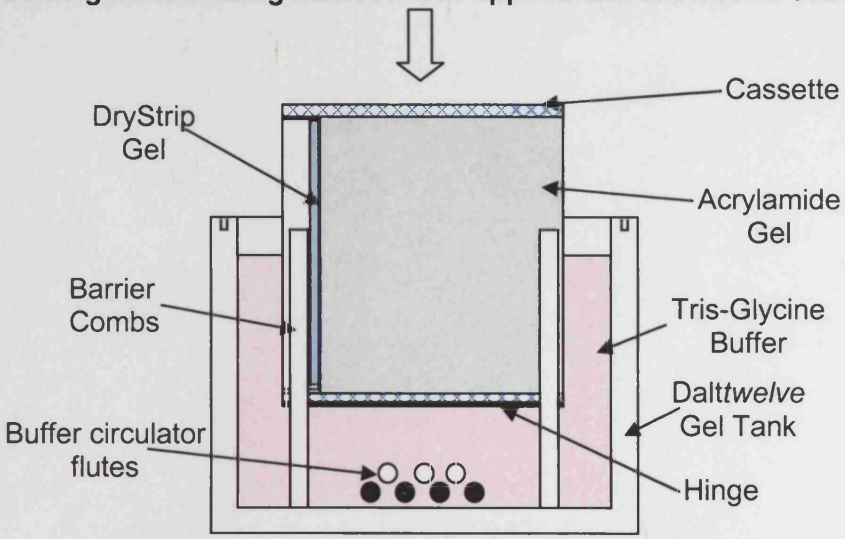

The cassettes were loaded into the gel tank

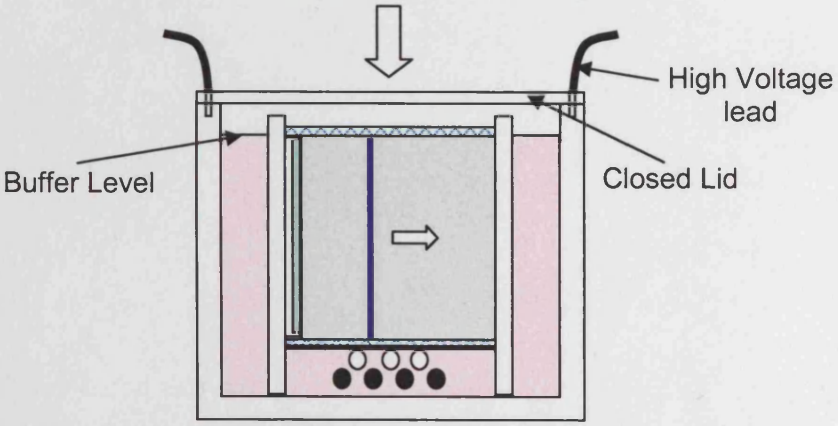

The gels were run overnight at 100V

Appendix 5: Flow diagram showing the loading of DryStrip Gels, loading of the gel cassettes and running of the Dalt*twelve* system.